

**Variation of wheat yields
as a consequence
of soil and meteorological variability**

Dissertation
zur Erlangung des
Doktorgrades der Naturwissenschaften (Dr. rer. nat.)

der
Naturwissenschaftlichen Fakultät III
Agrar- und Ernährungswissenschaften, Geowissenschaften und Informatik
der Martin-Luther-Universität Halle-Wittenberg

vorgelegt von
Herrn Eric Bönecke

Verteidigt am: 13.05.2024

Referees:
Prof. Dr. Hans-Jörg Vogel
Prof. Dr. Dr. Kurt-Christian Kersebaum

„Ich stehe auf der Grenze von Hier und Dort, und fast kommt es mir vor, als ob beides dasselbe wäre.“

Wilhelm Busch

(Analogous translation: "I stand on the line between here and there, and it almost seems to me that both are the same.")

Acknowledgement

This dissertation would not have been possible without the long breath of many people who have been extremely supportive in my work over the past years.

Firstly, I would like to express my sincere gratitude to my supervisors and mentors Dr. Uwe Franko, Prof. Dr. Hartmut Stützel and Dr. Jörg Rühlmann for their continuous support of all my studies and research. Combined, they define of who I am today and the way I approach my research. Under Uwe Franko I learnt all necessary skills to solve many modelling problems. Mr. Stützel taught me to think out of my bubble and broadened my knowledge in agronomy and wheat research. Jörg Rühlmann contributes with an endless pool of interesting ideas and showed me how to think around the corner. Thanks for all the pushes, the patience, and foremost in the believe of my progress. They all broadened my understanding and left a lasting impact on my perspective and provided the space I need(ed) to develop. I know, it's not always easy waiting for my results. Thank you.

Furthermore, I am grateful for the collaborations with numerous scientists across various research fields and research groups whom I worked together with. Their contributions have been invaluable in making my research successful. On behalf of the many, I would like to express my sincere appreciation to Dr. Ralf Gründling and Dr. Tsu Wei Chen as they have outstandingly contributed to my growth, development and persistence.

The majority of my work involved computational processing and analysis of data, which was collected from many sources or existing experiments I haven't done. I would therefore like to express my sincere appreciation to all the individuals who contribute to the advancement of science, including those who have directly supported my research. My honest gratitude goes out to the gardeners, laboratory staff, practitioners, trainees, research assistants, and others who have played integral roles in my journey.

Throughout my time at the Environmental Research Centre (UFZ), the Leibniz University Hannover (LUH), and the Leibniz Institute of Vegetable and Ornamental Crops (IGZ), I have been fortunate to receive support from various institutions, including the Federal Office for Agriculture and Food (BLE), the Federal Ministry of Education and Research (BMBF), the German Research Foundation (DFG), and the agricultural European Innovation Partnership (EIP-AGRI) program, which is backed by the innovation bank of the federal state of Brandenburg (ILB). I am truly grateful to all the taxpayers and officials who have generously contributed and continue to contribute to the progress of research in Germany.

I am immensely grateful to my parents, Steffi and Frank-Peter, who likely never imagined having an academically inclined child who would forge its own unique path towards becoming a self-assured individual. Despite enduring my "know-it-all" attitudes, they never doubted my journey and provided unwavering support, ensuring that I always had a safe haven to turn back to in times of need.

Finally, I want to express my most genuine gratitude to my dear friend, Ramona Reck, who, despite battling a serious illness, continues to strive towards her aspirations. Throughout my growth and professional journey, you have been a constant source of support, always cheering me on. Your strength and resilience are truly remarkable, and I am forever grateful for your presence in my life.

Synopsis

A continuing global population growth requires a continuing increase in food production. However, food security can be significantly affected by spatial and temporal variations in crop yields. Even on soils of a very good nutrient and water storage capacity and a seemingly uniform distribution, a small-scale variability of yields is observed. This variability is even more evident at regions of even higher spatial heterogeneity. Moreover, crop yield productivity varies not only from year to year due to the ambient meteorological conditions, but also over decades. Strikingly, the yield increment of many important crops - as seen since the 1960s due to the agricultural intensification - slowed down remarkably during the last decades in Germany. This may be in conjunction with climatic changes and increasing occurrence of climate extremes. This trend is seen also for wheat yields, however, as wheat is the most produced cereal in Germany, the productivity level should be at least maintained if not improved. At the same time, long-term uniform fertilization of arable land led to excessive nutrient levels as well as high environmental nutrient contamination risks, such as nitrate pollution of drinking water, eutrophication of water bodies or greenhouse gas emissions. Hence, the production should take into account a sustainable nutrient management.

To analyse and address the yield variability at different spatial and temporal scales, the present thesis is separated into two main parts with wheat as the main crop focused on. The first part mainly focuses on the causes of wheat yield variation and comprises two studies that analysis the effects of climatic changes on wheat yield variation in different regions of Germany and the effects of seasonal varying soil water availability on the within-field wheat yield variation. Thereafter, the second main part addresses a site-adapted nutrient management that considers the small-scale causes of the yield variation.

The key objectives of the first study in the first part of the thesis were therefore (I) to determine the magnitude of relevant climatic changes on wheat yields in Germany, and (II) to detect whether sites divided into classes of lower and higher yield potential were affected differently. The latter objective was also tested on sites of different soil types (from loamy sands to clayey silts).

As multiple environmental and agronomic factors affect crop yields, a statistical meta-analysis was conducted to estimate the impact of individual environmental and agronomic factors. Therefore, a large database of wheat yields from nitrogen fertilization experiments of nearly 60 years over Germany were collected as well as the environmental conditions at the experimental sites and normal trend analyses conducted in the first place. However, since the nitrogen experiments differ in their spatial and temporal extent, mixed effect models were applied to address this imbalance and

simultaneously disentangle the multitude of influencing factors. To identify the magnitude of the individual influencing factors on crop yields – and foremost the climatic factors, computing of the coefficient of determination (R^2) for generalized linear mixed models was employed.

The results of study revealed that changes of the climatic conditions in interaction with different site and soil conditions had a stronger pronounced impact on the yield variance of wheat than, for instance, breeding. Sites of lower yield potential or of sandy soils already had an incipient yield levelling in the mid to late 1980s showing annual variations of yield between 4-12 t ha⁻¹. Yield variation at these sites were in particular negatively influenced by detrimental weather conditions, e.g., number of heat stress days above 27°C during the generative phase with up to 30% impact. Contrary, at sites with higher yield potential, wheat yields have been constantly increasing over time. However, indications of yield levelling are also seen on sites of loamy to clayey soils for the last years. The analysis additionally revealed a shift of 13- and 17-days towards earlier in the year during the observation period for sowing and harvesting dates, respectively.

It can be concluded that wheat production was continuously adjusting to climatic changes with regard to both genetic and management modifications. However, in the light of continuous climatic changes, it might be particularly necessary to employ systematically all measures to support stable wheat production in Germany. As such, earlier sowing in combination with ‘early’ wheat genotypes might be a suitable strategy to deal with increasing drought stress. Furthermore, small-scale site adapted management strategies, in particular at sites with lower yield potential, could reduce the risk of drought induced yield losses.

To investigate then the causes of wheat yield variations at a site of relatively homogeneous top soil conditions, the second study of the first part of this thesis was conducted on a field east of the Harz Mountain in Germany. This region predominantly consists of chernozem soil developed over loess and is low in precipitation amounts having a negative to equalized climatic water balance. The top soil therefore has a very high nutrient and water storage capacity and is – according to its aeolian origin – relatively homogeneously distributed over the area.

The main research goals of this study were (i) to detect the small-scale soil structures to model the water dynamics in this loess-area and (ii) to determine and evaluate the time when the water availability effected the wheat yield variability the most. Therefore, a process-oriented soil model was applied on a 4x4 m soil texture map to account for the distribution of the soil physical properties and employed for a crop rotation of 7 years (including 4 years of wheat cultivation) under consideration of daily weather data. The soil texture map was derived from apparent electrical resistivity measurements by calibration with lab-analysed soil texture data. The hydrological

properties were derived from pedotransfer functions. The small-scale yield variability was evaluated and interpreted by applying linear and quantile regression analysis.

It was found that the above-mentioned small-scale yield variability was noticeably influenced by the amount of available water within the whole rooting zone during the grain filling phase in a comparatively dry year. The coefficient of determination (R^2) increased from <0.01 to 0.14 and 0.18 when the wheat yield variability of the chosen year was correlated with the amount of available water within 0-30 cm, 0-100 cm and 0-170 cm, respectively. Attained yields had a maximum of about 7 t ha^{-1} for available soil water contents between 350 and 420 mm. Below 350 mm available soil water, maximum wheat yields decreased down to around 5 t ha^{-1} at 250 mm available soil water.

In this second study it was successfully shown how soil process modelling can combine daily weather conditions and crop yield history with sensor-based soil texture maps that provide sufficient subsoil information. Hence, this technique combination is suitable for decision support systems – also on loess-developed chernozem soils with relatively homogeneous top soil conditions in relatively dry regions.

As the yield productivity of crops is decisively co-determined by the soil's capacity to supply crops with the necessary nutrients (often described as soil fertility), the final part of this thesis demonstrates how small-scale soil property differences can be considered in a fertilization decision support system. Exemplarily shown for liming, which is a key management to maintain or improve the soil's fertility and consequently crop productivity, the study was conducted in the Oder River valley - an area of high within-field yield variation caused by the very heterogeneous soils developed on fluvial and morainic substrates.

Therefore, the main research goals were (i) to create high-resolution maps of the liming relevant soil parameters and (ii) to apply a lime recommendation algorithm adapted to this data basis and (iii) to compare the results of this novel decision support system with a field uniform lime recommendation based on conventional data acquisition. To obtain high-resolution maps, geophysical recordings from two different soil sensor platforms were calibrated with lab-analysed reference soil samples. Sub-area specific lime recommendations were subsequently derived from a continuous, stepless algorithm, which was developed from the well-recommended but conventionally class-based VDLUFA system to fit the high-resolution soil maps.

The lime recommendation assessment based on this sensor and algorithm combination showed the best performance under the highest possible resolution of the underlying soil parameter maps. The sensor calibration with lab analysed reference soils showed a distinct five-soil group

differentiation after reclassification of the derived clay, silt and sand fractions, while conventional soil assessment maps only determined three out of the five soil groups. If lime recommendations are based on wrong field uniform soil texture allocations, 63% of the selected field would be over-fertilized by approximately 12 t of lime, 6% would receive approximately 6 t too little lime and only 31% would be adequately limed. Hence, high-resolution soil maps exhibited the small-scale spatial patterns and spatial interrelations between the target variables and therefore suit as input data to determine fertilizer recommendations as required for a sustainable agriculture.

In summary, this thesis highlights the significant impact of changing climatic conditions and of the soil heterogeneity on crop yield variations. The sensitivity of the yield productivity to past climatic conditions, particularly the influence of increasing temperatures, underlines the need for adaptation strategies in agricultural practices. It was found that sites of higher yield potential are less susceptible to adverse weather effects. However, knowing the distribution and availability of the soil water also explained yield variability at sites of relatively good soil conditions in a comparatively dryer year as such conditions might become more frequent in the future.

Moreover, through a site-specific fertilization adapted to the sensitivity of high-resolution data, fertilization may improve the soil fertility to the needs of a sustainable agriculture. Therefore, a transition towards a sustainable agriculture including small-scale soil maps in combination with smart decision systems is recommended. This could be extended to other nutrients in particular the nitrogen, which is a crucial factor in an environmentally friendly crop production to reduce losses through leaching or volatilization.

Zusammenfassung

Ein anhaltendes Wachstum der Weltbevölkerung erfordert eine kontinuierliche Steigerung der Nahrungsmittelproduktion. Die Ernährungssicherheit kann jedoch erheblich durch räumliche und zeitliche Schwankungen von Ernteerträgen beeinträchtigt werden. Selbst auf landwirtschaftlichen Flächen mit Böden sehr guter Nährstoff- und Wasserspeicherkapazität und einer scheinbar einheitlichen Verteilung in der Fläche, ist eine kleinräumige Variabilität von Weizenerträgen zu beobachten. Diese Variabilität ist in Regionen mit größerer räumlicher Bodenheterogenität noch mal deutlicher ausgeprägt. Außerdem schwankt die Ertragsproduktivität von Kulturpflanzen nicht nur von Jahr zu Jahr durch die meteorologischen Bedingungen während einer Vegetationsperiode, sondern auch grundlegend im Laufe von Jahrzehnten. Auffallend ist, dass sich der Ertragszuwachs für viele wichtige Anbaukulturen, darunter auch Weizen, in den letzten Jahrzehnten in Deutschland deutlich verlangsamt hat. Dies könnte mit den klimatischen Veränderungen und dem zunehmenden Auftreten von Klimaextremen zusammenhängen. Da Weizen jedoch das meistproduzierte Getreide ist in Deutschland, sollte das Produktivitätsniveau zumindest gehalten, wenn nicht sogar verbessert werden. Gleichzeitig führte die langjährige und gleichmäßige Düngung von Ackerflächen zu überhöhten Nährstoffgehalten sowie zu hohen Umweltbelastungsrisiken durch Nährstoffe, wie z.B. Nitratbelastung des Trinkwassers, Eutrophierung von Gewässern oder Treibhausgasemissionen. Daher sollte bei der Produktion auf ein nachhaltiges Nährstoffmanagement geachtet werden.

Um die Variabilität des Weizens in unterschiedlicher räumlicher und zeitlicher Auflösung zu analysieren, ist die vorliegende Arbeit in zwei Hauptteile gegliedert. Der erste Teil befasst sich hauptsächlich mit den Ursachen der Weizenertragsschwankungen und umfasst zwei Studien, die zum einen die Auswirkungen klimatischer Veränderungen auf die Weizenertragsschwankungen in verschiedenen Regionen Deutschlands als auch die Auswirkungen der Bodenwasserverfügbarkeit auf die kleinräumigen Weizenertragsschwankungen untersuchen. Der zweite Hauptteil befasst sich dann mit einem standortangepassten Nährstoffmanagement, das die kleinräumigen Ursachen der Ertragsschwankungen berücksichtigt.

Die übergeordneten Ziele der ersten Studie im Teil I der Arbeit waren (i) die Bestimmung des Ausmaßes relevanter klimatischer Veränderungen auf die Weizenerträge in Deutschland und (ii) die Feststellung, ob Standorte mit geringerem und höherem Ertragspotenzial unterschiedlich betroffen sind. Dies wurde auch an Standorten mit unterschiedlichen Bodentypen (von lehmigen Sanden bis zu tonigen Schluffen) getestet.

Da Ernteerträge von vielen Umwelt- und agronomische Faktoren beeinflusst sind, wurde eine statistische Meta-Analyse durchgeführt, um die Auswirkungen einzelner Umwelt- und agronomischer Faktoren abzuschätzen. Dazu wurden Weizenertragsdaten von Stickstoffdüngungsversuchen aus fast 60 Jahren in Deutschland sowie Umweltbedingungen an den Versuchsstandorten zusammengetragen und zuerst normale Trendanalysen durchgeführt. Da die Stickstoffversuche jedoch in ihrer räumlichen und zeitlichen Ausdehnung variieren und der Datensatz somit nicht ausreichend ausbalanciert ist, wurden außerdem statistische Mischmodelle zur Entflechtung der einzelnen Einflussfaktoren verwendet. Um das Ausmaß der einzelnen Einflussfaktoren - vor allem der klimatischen Faktoren - auf die Ernteerträge zu ermitteln, wurde das Bestimmtheitsmaßes (R^2) für lineare Mischmodelle berechnet.

Die Ergebnisse der Studie zeigten, dass Veränderungen der klimatischen Bedingungen in Wechselwirkung mit unterschiedlichen Standort- und Bodenbedingungen einen stärkeren Einfluss auf die Ertragsentwicklung von Weizen haben als beispielsweise die Züchtung. Auf Standorten mit geringerem Ertragspotenzial und sandigeren Böden setzte bereits Mitte bis Ende der 1980er Jahre eine Nivellierung des Ertrages ein mit Ertragsschwankungen zwischen 4-12 t ha⁻¹. Die Ertragsschwankungen auf diesen Standorten wurden vor allem durch ungünstige Witterungsbedingungen negativ beeinflusst. So machten z.B. die Anzahl der Hitzestress-Tage mit Temperaturen über 27 °C während der generativen Phase bis zu 30 % der Ertragsschwankungen aus. An Standorten mit höherem Ertragspotenzial sind die Weizenerträge dagegen im Laufe der Zeit kontinuierlich gestiegen. Allerdings sind auch auf Standorten mit lehmigeren und tonreicheren Böden Anzeichen einer Ertragsnivellierung zu erkennen. Außerdem ergab die Analyse, dass sich die Aussaat- und Erntetermine im Beobachtungszeitraum um 13 bzw. 17 Tage in Richtung früher im Jahr verschoben haben.

Daraus lässt sich insgesamt schließen, dass sich die Weizenproduktion sowohl in Bezug auf genetische als auch auf Bewirtschaftungsänderungen kontinuierlich an die klimatischen Veränderungen angepasst hat. Angesichts andauernder klimatischer Veränderungen ist es jedoch notwendig alle Maßnahmen zu ergreifen, die eine Stabilisierung der Weizenproduktion in Deutschland unterstützen. So könnte eine frühere Aussaat in Kombination mit "frühen" Weizengenotypen eine geeignete Strategie sein, um dem zunehmenden Trockenstress zu begegnen. Darüber hinaus sollten kleinräumige, standortangepasste Bewirtschaftungsstrategien, insbesondere an Standorten mit geringerem Ertragspotenzial, das Risiko trockenheitsbedingter Ertragsverluste verringern.

Um nun die Ursachen für die Ertragsschwankungen von Weizen an einem Standort mit relativ homogenen Oberbodenbedingungen zu untersuchen, wurde die zweite Studie des ersten Teils dieser Arbeit auf einem Feld östlich des Harzes in Deutschland durchgeführt. Diese Region besteht überwiegend aus Tschernosem-Böden, die sich über Löß entwickelt haben. Sie ist außerdem niederschlagsarm und weist eine negative bis ausgeglichene klimatische Wasserbilanz auf. Der Oberboden hat daher eine sehr hohe Nährstoff- und Wasserspeicherkapazität und ist - entsprechend seinem äolischen Ursprung - relativ homogen über die Fläche verteilt.

Die Hauptziele dieser Studie waren (i) die Erfassung der kleinräumigen Bodenstrukturen zur Modellierung der Wasserdynamik in diesem Lößgebiet und (ii) die Bestimmung und Bewertung des Zeitpunktes, zu dem sich die Wasserverfügbarkeit am stärksten auf die Ertragsvariabilität des Weizens auswirkt. Zu diesem Zweck wurde ein prozessorientiertes Bodenmodell auf eine Bodentexturkarte mit 4x4 m Auflösung, um die Verteilung der physikalischen Bodeneigenschaften zu berücksichtigen, aufgesetzt und Modellierungen des Wasserhaushalts für eine Fruchtfolge von insgesamt 7 Jahren (inklusive 4 Jahre Weizenanbau) unter Verwendung täglicher Wetterdaten durchgeführt. Die Bodentexturkarte wurde aus Messungen des scheinbaren elektrischen Widerstands durch Kalibrierung mit laboranalytischen Bodentexturdaten abgeleitet und hydrologischen Eigenschaften mittels Pedotransferfunktionen. Die kleinräumige Ertragsvariabilität wurde mittels linearer und Quantilregressionen bewertet und interpretiert.

Es zeigte sich, dass die kleinräumige Ertragsvariabilität in einem vergleichsweise trockenen Jahr während der Kornfüllungsphase deutlich von der Menge des verfügbaren Wassers innerhalb der gesamten Wurzelzone beeinflusst wurde. Das Bestimmtheitsmaß (R^2) der Korrelation der Ertragsvariabilität mit den Mengen des verfügbaren Wassers in 0-30 cm, 0-100 cm bzw. 0-170 cm des gewählten Jahres stiegen von $<0,01$ auf 0,14 bzw. 0,18 an. Die erzielten Erträge erreichten ein Maximum von etwa 7 t ha^{-1} bei verfügbaren Bodenwassergehalten zwischen 350 und 420 mm. Unterhalb von 350 mm verfügbarem Bodenwasser sanken die maximalen Weizenenerträge bis auf etwa 5 t ha^{-1} bei 250 mm verfügbarem Bodenwasser.

In dieser zweiten Studie wurde erfolgreich gezeigt, wie die Modellierung von Bodenprozessen in Kombination von Wetterbedingungen, Ertragshistorie und sensorbasierten Bodentexturkarten, kleinräumige Schwankungen innerhalb eines Feldes sichtbar macht. Daher eignet sich diese Technikombination für Entscheidungsunterstützungssysteme - auch auf lössgeprägten Tschernosem-Standorten mit relativ homogenem Oberboden und relativ trockenen Regionen.

Da die Ertragsproduktivität Pflanzen entscheidend von der Fähigkeit des Bodens die notwendigen Nährstoffe bereitzustellen (auch Bodenfruchtbarkeit genannt) mitbestimmt wird, soll

im letzten Teil dieser Arbeit gezeigt werden, wie die kleinräumigen Bodeneigenschaftsunterschiede in einem Düngungsentscheidungssystem berücksichtigt werden können. Die Studie wurde im Oderbruch durchgeführt, eine Region, die durch räumlich stark schwankende Erträge aufgrund der sehr heterogenen Böden, die sich auf fluviatilen und Moränen Substraten entwickelt haben, gekennzeichnet ist.

Die wichtigsten Forschungsziele dieser Studie waren (i) die Erstellung präziser Karten der für die Kalkung relevanten Bodenparameter, (ii) die Anwendung eines an diese Datenbasis angepassten Kalkempfehlungsalgorithmus und (iii) der Vergleich der Ergebnisse dieses neuartigen Entscheidungsunterstützungssystems mit einer schlageinheitlichen Kalkempfehlung auf der Grundlage konventioneller Datenerfassung. Um hochauflösende Karten zu erhalten, wurden geophysikalische Aufnahmen von zwei verschiedenen Bodensensorplattformen mit laboranalytischen Referenzbodenproben kalibriert. Anschließend wurden teilflächenspezifische Kalkempfehlungen aus einem kontinuierlichen, stufenlosen Algorithmus abgeleitet, der aus dem bewährten, aber konventionell klassenbasierten VDLUFA-System zur Anpassung an die hochauflösenden Bodenkarten entwickelt wurde.

Die auf dieser Kombination aus Sensor und Algorithmus basierende Bewertung der Kalkempfehlungen zeigte die beste Leistung bei der höchstmöglichen Auflösung der zugrunde liegenden Bodenparameterkarten. Die Sensorkalibrierung mit laboranalytisch untersuchten Referenzproben zeigte nach der Rückklassifizierung der abgeleiteten Ton-, Schluff- und Sandfraktionen eine deutliche Differenzierung in fünf Bodengruppen, während die herkömmliche Bodenschätzkarte nur drei der fünf Bodengruppen ermittelte. Wenn Kalkempfehlungen auf falschen schlageinheitlichen Bodentexturzuordnungen beruhen, würden 63 % des ausgewählten Feldes um ca. 12 t Kalk überdüngt werden, 6 % würden ca. 6 t zu wenig Kalk erhalten und nur 31 % wären ausreichend gekalkt. Hochaufgelöste Bodenkarten zeigten also die kleinräumigen Muster und Zusammenhänge zwischen den Zielvariablen auf und eignen sich daher als Eingangsdaten zur Ermittlung von Düngeempfehlungen, wie sie für eine nachhaltige Landwirtschaft erforderlich sind.

Zusammenfassend lässt sich sagen, dass diese Doktorarbeit die Auswirkungen der sich ändernden klimatischen Bedingungen als auch der Bodenheterogenität auf die Schwankungen der Ernteerträge auf verschiedenen Ebenen aufzeigt. Die Schwankungen der Ertragsproduktivität durch sich verändernde klimatische Bedingungen, insbesondere der Einfluss steigender Temperaturen, unterstreicht die Notwendigkeit von Anpassungsstrategien in der landwirtschaftlichen Praxis. Es wurde außerdem aufgezeigt, dass Standorte mit einem höheren Ertragspotenzial weniger anfällig für ungünstige Witterungseinflüsse sind, aber auch, dass die Bodenwasserverfügbarkeit die

Ertragsschwankungen an Standorten mit relativ guten Bodenbedingungen in einem vergleichsweise trockenen Jahr erklärt.

Außerdem kann durch eine standortspezifische Düngung auf Basis hochauflösender Daten, die Bodenfruchtbarkeit verbessert werden. Damit wird den Erfordernissen einer nachhaltigen Landwirtschaft Rechnung getragen. Dies sollte auf andere Nährstoffe ausgeweitet werden, insbesondere auf die Stickstoffdüngung, die ein entscheidende Größe für eine umweltfreundliche Pflanzenproduktion ist, um Verluste durch Auswaschung oder Verflüchtigung zu verringern.

Content

Acknowledgement	iii
Synopsis	v
Zusammenfassung	ix
Content	xiv
List of figures	xvi
List of tables	xxii
List of abbreviations	xxv
General introduction	1
Growing population and food demand.....	1
Constraints of land expansion.....	2
Adverse effects of intense farming practices on the environment	3
Impact of changing climate conditions on crop yields.....	5
Site adapted nutrient management - a solution for sustainable agriculture	6
Soil quality and fertility	7
Analysing spatiotemporal yield variation	8
Selected approaches to analyse yield variation	8
Considerations at different spatiotemporal scales	12
Thesis outline and research objectives	15
Thesis overview	18
Clarification of contribution	20
Part I – Causes of a spatiotemporal yield variability	21
Decoupling of impact factors reveals the response of German winter wheat yields to climatic changes	22
Abstract	23
Introduction	24
Materials and Methods.....	26
Results	38
Discussion.....	60
References.....	63
Supporting Material	68

Determining the within-field yield variability from seasonally changing soil conditions.....	88
Abstract	89
Introduction	90
Materials and Methods.....	93
Results and discussion.....	99
Conclusion	106
References.....	107
Part II – Small-scale adapted nutrient management	114
Guidelines for precise lime management based on high-resolution soil pH, texture and SOM maps generated from proximal soil sensing data	115
Abstract	116
Introduction	117
Materials and Methods.....	121
Results and discussion.....	132
Outlook.....	144
Conclusions	144
References.....	146
Thesis synthesis	153
General discussion	153
Result summary.....	156
Overall conclusions	157
Outlook.....	159
References.....	159
Affidavit	xxvi
Curriculum Vitae	xxvii

List of figures

Figure 1: Wheat yield development in Germany and agronomic advancements since the 1950s (Oerke, 2006). 2

Figure 2: Trends of the global food production (a), the nitrogen (N) fertilizer use (b) and land surface used for agricultural crop production since the 1960s (Tilman, 1999)..... 2

Figure 3: Depiction of the nitrogen (N) budget in crop production and the resulting N components (ammonia (NH₃), nitrogen oxides (NO_x), nitrous oxide (N₂O), dinitrogen gas (N₂), ammonium (NH₄⁺), nitrate (NO₃⁻), dissolved organic nitrogen (DON), and particulate organic nitrogen (PON)) released into the environment (orange arrows) and N recycling within the soil (shown in the grey box) (Zhang et al., 2015). The Nitrogen Use Efficiency (NUE) is defined as the ratio of the output (green arrow) to the agricultural inputs (blue arrows), i.e., $NUE = N_{yield}/N_{input}$ (Moll et al., 1982). 4

Figure 4: A simplified scheme of the interactive water and nutrient dynamics within the soil-crop system, as used in process-oriented agro-ecosystem models (Kersebaum and Wallor, 2023) based on the meteorological inputs. 12

Figure 5: Scales at which research questions are addressed in agricultural systems including the different types of users and decisions and policies of interest (Jones et al., 2017). 13

Figure 6: Data processing scheme from raw data to final data analysis. Crop, phenological, climatic, agro-climatic, and site-specific data were collected in the first place and analysed for their trends. All data was combined into a data set from which individual agro-climatic variables were decoupled from all other influential factors using statistical mixed-effect models. Finally, the intensity of each variable was estimated by computing the coefficient of determination (R^2) for generalized linear mixed models as introduced by Piepho (2019) ... 27

Figure 7 Examples for the yield response curves to nitrogen fertilizer level and derived maximum yields and corresponding nitrogen values of three fertilization experiments. The green crosses mark the maximum achievable winter wheat yields as derived from a quadratic linear function and its corresponding nitrogen level..... 29

Figure 8 Development stages (black vertical bars), phases (coloured), and reference values according to the plant developmental BBCH-scale (Meier 1997) similar to the Zadoks scale (Zadoks et al. 1974) for winter wheat along the whole vegetation period..... 31

Figure 9: Grain yield development (as dry matter content) of winter wheat and nitrogen fertilization dosages across the study sites in Germany between 1949 and 2016. (a), Overall grain yield development. Data points refer to the derived experimental values (Exp. dat.) as described in Methods and to mean values of the Federal Statistical Office of Germany (Fed. Stat. Off.) The blue line visualizes the development of the official statistical data and the brown line shows the yield development of the experimental data. (b), Development of nitrogen fertilization dosages. (c), Yield development of sites with yield potential lower than 70 points. (d), Yield development of sites with a yield potential of more than 70 points. The yield potential classification of the sites is based on the Muencheberg Soil Quality Rating (Mueller et al. 2010) (MSQR, Methods)..... 38

Figure 10: Estimated phenology trends of winter wheat across the study sites between 1951 and 2015. (a), Average days of sowing, harvest, and the actual crop phenological stages (emergence, begin of stem elongation, heading, and hard dough) after the 1st of September. Average duration (b) and thermal duration (c) of the entire growing season (GS) divided into the generative phase (GP) and vegetative phase (VP). The latter comprises the leaf development phase (LP) and the stem elongation phase (SP). Inverse triangles indicate trend changes. 41

Figure 11: Climate trends within phenological growth phases of winter wheat across the study sites in Germany. Trends are shown for the growing season (GS), vegetative phase (VP), leaf development phase (LP), generative phase (GP), and stem elongation phase (SP). (a), Mean temperature between 1951 and 2014. (b), Precipitation between 1951 and 2014. (c), Wheat specific potential evapotranspiration between 1951 and 2006. (d), Wheat-specific climatic water balance between 1951 and 2006 43

Figure 12: Proportions of variance explained by the main influential factors (genotype, location, and time) and their interactions in German long-term yield data. Results indicate a relative strong variance of all factors that changes along the timeline (time effect) except those caused by altering genotypes, which were relatively low. Moderate variabilities were only found for the location effect and the location × time interaction. Other interaction effects were rather low with no effect for the genotype × time interaction 46

Figure 13: Effect of selected agro-climatic variables on winter wheat yield development. Each break represents an agro-climatic variable and the stretches of the coloured areas shows their influence in percentages, described as ‘coefficient of determination for mixed effect-models’ (Method). Low yield potential sites refer to sites with quality points between 0 and less than 70, while high yield potential sites refer to quality points between 70 and 100. The

classification is based on the Muencheberg Soil Quality Rating (Mueller et al. 2010) (MSQR, Methods). Tmean is the average temperature (°C), Tmax is the maximum temperature (°C), HS27n is defined as the number of heat stress days above 27°C, HS31n is defined as the number of heat stress days above 31°C, GRmean is the average global radiation (W m⁻²), Psum is the total precipitation amount (mm), HR20sum is the total amount of precipitation of days with minimum 20 mm precipitation (mm), ETPmean is the average winter wheat specific potential evapotranspiration (mm), and CWBsum is the wheat-specific climatic water balance (mm). All climate variables are related to wheat-specific growth stages: the entire growing season (GS), the vegetative phase (VP), the generative phase (GP), the leaf developmental phase (LP), and the shooting phase (SP) (Method). The mathematical symbol '+' describes a positive relationship to yield development and the '-' a negative relationship (Fehler! Verweisquelle konnte nicht gefunden werden.)..... 47

Figure 14: Grain yield evolution of winter wheat at sites with different heat stress conditions during the generative growth phase at sites with (a) low (0-70 quality points) and (b) high (70-100 quality points) yield potential (classified based on the Muencheberg Soil Quality Rating (Mueller et al. 2010) (MSQR, Methods). The different colours depict the number of heat stress days during generative phase for each single site-year (points) and trend (lines) at the sites with the lowest (green lines (a) & (b)) and highest (red line (a); orange line (b)) number of heat stress days. 59

Figure 15: Grain yield development of winter wheat across the study sites in Germany between 1949 and 2016. Soil types are presented according to German soil classification(Ad-hoc-AG Boden 2005) (Method). a, Overall trend for soils classified as light soils (Methods). b, Overall trend for soils classified as heavy soils. 73

Figure 16: Fertilization development under different soil and site conditions across the study sites between 1958 and 2015. Soil types are presented according to German soil classification(Ad-hoc-AG Boden 2005) and the soil yield potential according to the Muencheberg Soil Quality Rating(Mueller et al. 2010) (MSQR, see Methods). The black trend lines refer to fitted functions. a, Overall trend for soils classified as light soils. b, Overall trend for soils classified as heavy soils. c, Trends for sites with relatively low soil yield potential. d, Trends for sites with relatively high soil yield potential..... 73

Figure 17: Sowing date trends across the study sites as decadal change and dependent on latitude for each site analysed in this study. Three asterisks define significance at the 0.1% level. 74

Figure 18: Climate trends across the study sites in Germany between 1951 and 2006. a, Mean annual temperature between. b, Mean annual precipitation height between. c, Mean annual potential evapotranspiration between. d, Mean annual climatic water balance between.. 74

Figure 19: Development of adverse weather conditions during phenological phases of winter wheat across the study sites. Trends are shown for the growing season (GS), vegetative phase (VP), leaf development and tillering phase (LP), generative phase (GP), and stem elongation and booting phase (SBP). a, Maximum temperature between 1951 and 2006. b, minimum temperature between 1951 and 2006. c, Mean frequency of days with negative climatic water balance (CWB) between 1951 and 2006. d, Global radiation sum between 1983 and 2015 75

Figure 20: Development of occurring heat stress events (cumulative days with Tmax > 31 °C) during the stem elongation phase across all sites with a soil yield potential below 70 quality points 75

Figure 21: Spatial distribution of the locations in this study and their long term (1977-2006) climate and soil conditions. a, Mean annual temperature (MAT). b, Mean annual precipitation (MAP). c, Mean annual climatic water balance (MCWB). d, Soil types after reference (Ad-hoc-AG Boden 2005) 87

Figure 22: Left: annual precipitation sums of the modelling period (2009-2015); right: monthly average temperature and precipitation sum in 2011..... 93

Figure 23: Sketch (a) and photo (b) of the Geophilus system. The electrodes are arranged as an equatorial dipole-dipole-array with a dipole length of 1 m. The dipole spacing ranges from 0.5 to 2.5 m 94

Figure 24: Sampling points in the study field taken in 2012 based on the topographic features (left, elevation map measured by the Geophilus system) and the sampling points taken in 2014 based on the min-max range of the Geophilus ERa recordings (here, channel 4 on a logarithmic scale) (right) 96

Figure 25: Soil texture distribution of the upper soil horizons (crosses), the intermediate loess layer (squares) and the lowermost substrate (triangles) following the German soil classification system (Ad-hoc AG Boden 2005) 100

Figure 26: Comparison of the soil texture heterogeneities of the selected study field from the German soil survey map, with the soil units representing the soil texture values from a representative soil profile and averaged values of a 50 x 50 m survey grid at a 1 m soil depth (left), and the soil texture class distribution map derived from the linear regression model at a 4 x 4 m resolution for the different soil depths (right) according to the German soil classification system (Ad-hoc AG Boden 2005).....	104
Figure 27: Winter wheat yield variability in 2011 (left) and the calculated soil water content at 0-1.7 m soil depths from 01.06.-10.06.2011 (right) with a 36 x 36 m resolution	105
Figure 28: Winter wheat yields and the corresponding regression (dashed) and boundary lines (solid) in relation to the soil water content (0-1.7 m). The formula and R^2 for the regression function are shown.	106
Figure 29: Flow chart visualizing the workflow from the proximal soil sensing to the calculation of the final lime requirement/application maps	121
Figure 30: Applied soil sensing platforms: (a) The non-commercially available Geophilus system with 7 rolling electrode pairs (1) and a γ probe (2), (b) the commercially available Veris mobile sensor platform (Veris MSP) by VERIS Technologies with the ERA instrument (3), (c) the Soil pH Manager™ (water tank (4), soil sampler (5) and pH electrodes (6)) and (d) the OpticMapper (opening coulter (7) and optical module between depth-sensing side wheels (8)).....	122
Figure 31: Spatial resolution of the proximal soil sensor measurements of the Geophilus system (a), the Soil pH Manager (b) and the OpticMapper (c) and the sampled soil reference points (black triangles) and yield pattern (d) in the test field (KL60)	125
Figure 32: Semivariogram analysis of the sensor point data for ordinary kriging analysis of the field KL60: Electrical resistivity (a), Gamma (b), Elevation (c), Electrical conductivity (d), pH (e), Red (f) and Infrared (g) (Model parameters found in Table 18). Dashed lines (red) represent the spatial separation distance up to which point pairs are included in the semivariance estimates.....	132
Figure 33: Mapping results from the sensors available in this study: (a) electrical resistivity (ERA, first channel of the Geophilus system, 0-0.25 m), (b) γ -activity (0-0.3 m), (c) calculated soil moisture index, SWI (dimensionless), (d) digital elevation model, (e) pH, (f) electrical conductivity (ECa-shallow of the Veris MSP; median depth 0.12 m), (g) red (dimensionless, from the Optic mapper of the Veris MSP), (h) infrared (IR, dimensionless) and (i) IR/Red ratio (dimensionless).....	134

Figure 34: Calibration model qualities for the predicted soil parameters pH (a), soil organic matter (SOM) (b), clay (c), silt (d) and sand (e).....	136
Figure 35: Predicted clay content (left), silt content (middle) and sand content (right) from the Geophilus sensor platform.....	137
Figure 36: Geophilus mapped soil texture classes (derived from the German KA5 soil texture classification (Eckelmann et al. 2005)) Ss: pure sand; St2: slightly loamy sand; St3: medium clayey sand; Sl4: highly sandy loam; Ls4: highly sandy loam; Lts: clayey sandy loam (a), the MSP-mapped pH values (b) and SOM content (c) and the lime supply level at 2 x 2 m resolution.....	138
Figure 37: Final CaO requirements calculated at 2 x 2 m resolution (a) and aggregated for potential lime spreader working widths of 18 x 18 m (b) and 36 x 36 m (c) aligned in the management direction.....	141
Figure 38: Distribution of the over-, adequately and under-fertilized areas with uniform LRs (estimates for soil groups 1 (a), 2 (b) and 3 (c) in the VDLUFA classification) compared with the example estimated variable LR for 18 x 18 m management units.....	143

List of tables

Table 1: Regression coefficients of winter wheat yield (t DM ha⁻¹) and nitrogen fertilization (kg N ha⁻¹) trends estimated by segmented regression line analysis and simple linear models (equation 4-7). Heavy soils refer to loams and clayey silts and light soils to sandy loams and loamy sands (Methods). Low yield potential soils are soils with MSQR below 70 points and high yield potential soils with MSQR above 70 points (Methods). SE describes the standard error of the fitted parameter. 39

Table 2: Regression coefficients of the linear and segmented regression analysis of the phenological beginning (days after Sep 1st) and duration (d) of winter wheat development 42

Table 3 Regression coefficients for the linear and segmented trends of climatic factors during phenological phases of winter wheat. P values refer to the slope coefficient..... 44

Table 4 Estimated explained variance (%) of the agro-climatic variables (units in parentheses) on winter wheat yield development between 1958 and 2006 across the study sites in Germany. All explained variances are estimated after accounting for the genetic and non-genetic time trends. Low yield potential sites refer to sites with quality points between 0 and less than 70, while high yield potential sites refer to quality points between 70 and 100. (Methods) 49

Table 5 Coefficient estimates of the fixed effects (genotype, time, and selected agro-climatic variables as found in Fig. 4) in the mixed-effect models on the yield development over time. SE denotes the standard error, DF the degree of freedom, n the number of observations, and p the significance of the estimates of each model. Values in parentheses describe the trend of the appropriately selected agro-climatic variable adjusted by its trend over time (Methods). Low yield potential sites refer to sites with quality points between 0 and less than 70, while high yield potential sites refer to quality points between 70 and 100. (Methods) 52

Table 6 Selected stations with hourly measured air humidity values..... 70

Table 7 Regression coefficients of the relationship between the saturation deficit of the minimum and mean air humidity. Coefficients were estimated for each direction, month, and period as listed in Table 6 and the linear regression functions forced through 0% deficit (Methods). The root mean square error (RMSE) was calculated between observed and estimated minimum air humidity values 71

Table 8 Estimated explained variance of the agro-climatic variables (units in parentheses) on winter wheat yield development between 1958 and 2006 across the study sites in Germany after removing the effect of soil yield potential or the soil type. All explained variances are estimated after already accounting for the genetic and non-genetic time trends	76
Table 9 Estimated explained variance of the agro-climatic variables (units in parentheses) on winter wheat yield development between 1958 and 2006 across the study sites that are characterised through soil yield potential lower than 70 quality points and after removing the effect of soil yield potential or the soil type. All explained variances are estimated after accounting for the genetic and non-genetic time trends. Additionally, the effect of the soil type was removed in second model	78
Table 10 Estimated explained variance of the agro-climatic variables (units in parentheses) on winter wheat yield development between 1958 and 2006 across the study sites that are characterised through soil yield potential greater 70 quality points and after removing the effect of soil yield potential or the soil type. All explained variances are estimated after accounting for the genetic and non-genetic time trends. Additionally, the effect of the soil type was removed in second model	80
Table 11 Estimated explained variance of the agro-climatic variables (units in parentheses) on winter wheat yield development between 1958 and 2006 across the study sites that are characterised through light soils. All explained variances are estimated after accounting for the genetic and non-genetic time trends. Additionally, the effect of the soil yield potential was removed in second model	82
Table 12: Estimated explained variance (%) of the agro-climatic variables (units in parentheses) on winter wheat yield development between 1958 and 2006 across the study sites that are characterised through heavy soils. All explained variances are estimated after accounting for the genetic and non-genetic time trends. Additionally, the effect of the soil yield potential was removed in second model.....	85
Table 13: Descriptive statistics of the sample data from the study site, where OC is the organic carbon content, SD is the standard deviation, CV%, is the percentage of coefficient of variation and the sample size is n.	101
Table 14 Regression parameters (intercept and factor), the mean residual standard error (σ) after cross validation and the coefficient of determination (R^2) of the linear model between the variable ER (Ohm m), used as a proxy, and the clay and sand contents at each depth.	102

Table 15: Estimated soil texture classes (German soil classification system), the class mean values for the clay, silt and sand contents and their areal distributions (ha) within each layer.....	103
Table 16: Soil pH and lime requirement from the VDLUFA guidelines (von Wulffen et al. 2008)	130
Table 17: Content ranges (kg kg^{-1}) of the VDLUFA soil texture groups	130
Table 18: Parameters of the semivariogram models of the on-the-go sensor data	133
Table 19: Overview of the laboratory results for the soil properties measured in this study	135
Table 20: Validation results and descriptive statistics for the predicted soil properties from the (uni- and multi-variate) linear models	137
Table 21: Areal percentages of the VDLUFA lime supply levels (A, B, C, D, E, description in Table 1) at the spatial resolutions of potential lime spreader working widths (18 x 18 m and 36 x 36)	139
Table 22: Summary statistics for the final lime requirements at the three different map resolutions	140
Table 23: Comparison between the variable and uniform liming approach for all possible VDLUFA soil groups with data aggregation to 18 x 18 m	143

List of abbreviations

Ca	Calcium
CANDY	CArbon and Nitrogen Dynamics
CaO	Calcium oxide
CV%	Coefficient of variation
CWB	Climatic water balance
dGNSS	differential Global Navigation Satellite System
DM	Dry matter
DWD	Deutscher Wetter Dienst (German Weather Service)
ECa	Apparent electrical conductivity
ERT	Electrical resistivity tomography
ERa	Apparent electrical resistivity
FAO	Food and Agricultural Organisation
GIS	Geoinformation system
IR	Infra-red
KA5	Kartieranleitung 5 (soil mapping guidance)
LR	Lime requirement
M	Model
MLR	Multi-variate linear regression
MSP	Multi sensor platform
MSQR	Muencheberg Soil Quality Rating
NIR	Near infra-red
PA	Precision agriculture
PET/ETP	Potential evapotranspiration
PF	Precision farming
pH	Power of hydrogen
PSD	Particle size distribution
PTF	Pedotransfer function
RMSE	Root mean square error
SOC	Soil organic carbon
SOM	Soil organic matter
ULR	Univariate linear Regression
Vis-NIR	Visible near infra-red
VRL	Variable-rate liming
YOR	Year of release
WW	Winter wheat

General introduction

Growing population and food demand

Currently, the global population stands at around 8 billion and is projected to reach about 11 billion by 2100, according to estimates by the United Nations' World Population Prospects (United Nations, 2019). By the middle of the 21st century, when the global population is expected to reach about 9 billion, the demand for food is anticipated to double compared to the beginning of this century (Evans, 2009; Godfray et al., 2010). However, to meet the nutritional needs of the growing population this would require a similar achievement in crop production as witnessed during the second half of the 20th century (Foley et al., 2011; Pellegrini and Fernández, 2018). Between 1960 and 2000, the world's population doubled to about 6 billion, while at the same time yields of the world's most important crops, maize, wheat, and rice increased three-fold from about 640 million Mg to 1800 million Mg (Calderini and Slafer, 1998; "FAO," 2023). It is expected that these crops remain the major sources of nutrition for people and for animal fodder in the future and therefore playing a crucial role in food security (Curtis and Halford, 2014; Shiferaw et al., 2013). In temperate regions, wheat (*Triticaceae*) is the dominant crop that contributes to essential amino acids, minerals, vitamins and fibres with the European Union being the biggest wheat producer (Curtis and Halford, 2014).

The significant increase in crop yields during the 20th century, particularly in favourable agro-climatic regions, can be explained by a multitude of factors such as breeding advancements, improvements in management practices, the nitrogen fertilizer production, adoption of new technologies or selection/rotation of cultivated crops (Foley et al., 2011; Pellegrini and Fernández, 2018; Villoria, 2019). For instance, the combination of plant breeding, optimal sowing timing, soil cultivation methods, precise fertilizer application, coordinated use of plant growth regulators, and the application of broad-spectrum fungicides against key diseases has resulted in a significant and constant growth in wheat yields in Germany (Figure 1) (Oerke, 2006). A major first step was done in developing high-yielding crop varieties that responded positively to improved fertilization techniques (Fischer and Edmeades, 2010; McLaren, 2000). These cultivars also became more resistant to rust diseases, shorter in height to avoid lodging, while improving the nitrogen and water utilization (Gervois et al., 2008; Pinstруп-Andersen, 2000). Adaptations such as reduced growth duration and focusing on tolerances against abiotic stresses also increased yields for instance of winter wheat even in unfavourable regions (Blum and Jordan, 1985; Witcombe et al., 2007).

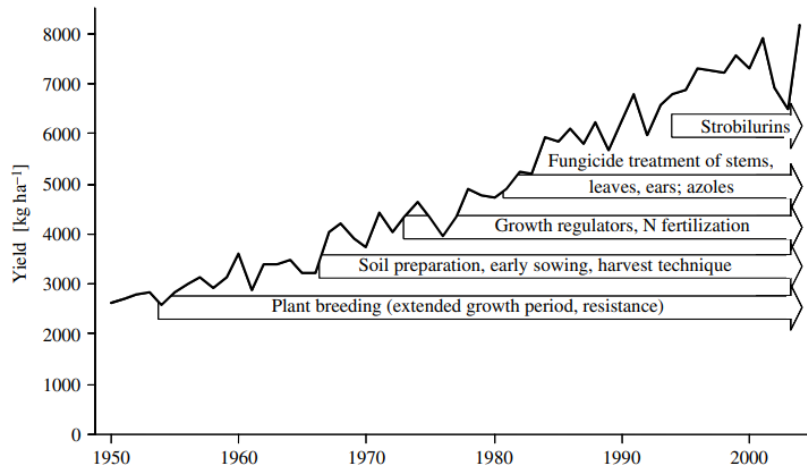


Figure 1: Wheat yield development in Germany and agronomic advancements since the 1950s (Oerke, 2006).

Besides the genetic improvements, the global increase in crop yields were accompanied by a seven-fold increase in the use of nitrogen fertilizer (Figure 2a and b) (Tilman, 1999). In Europe, the amount of nitrogen used in agriculture increased nearly five-fold until the late 1980s, reaching around 34 million tons, while in Germany the amount more than doubled to approximately 2.4 million tons at the same time (“FAO,” 2023). Over the past 30 years, these amounts decreased to around 20 million tons in Europe and to around 1.2 million tons per year in Germany. In addition, there has been a significant global increase by a factor of 15-20 in crop protection by the usage of pesticides (Pinstrup-Andersen, 2000).

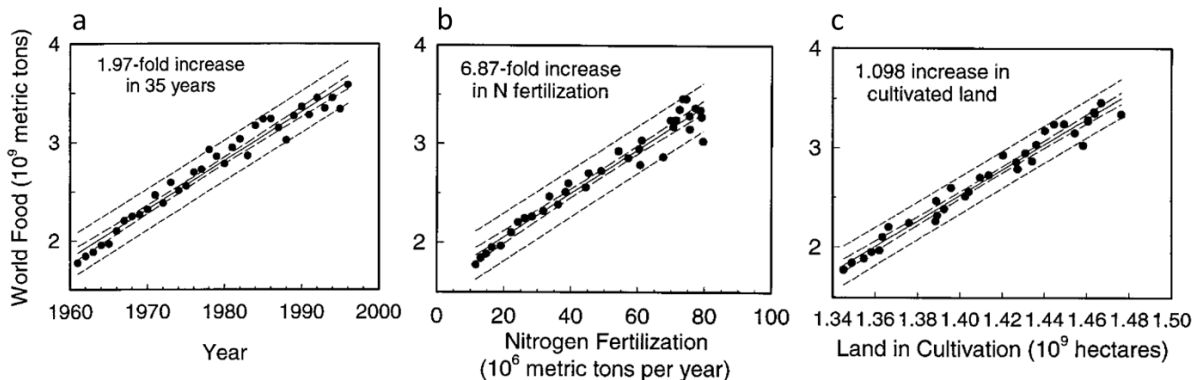


Figure 2: Trends of the global food production (a), the nitrogen (N) fertilizer use (b) and land surface used for agricultural crop production since the 1960s (Tilman, 1999).

Constraints of land expansion

Without the global improvements during the 20th century, the world food production could not have been increased by the documented rate and more natural ecosystems would have been needed to be converted to arable land (Evenson and Gollin, 2003; Tilman, 1999). Interestingly, the total amount of crop land converted to arable land globally only increased by about 10% during that time

(Figure 2c) (Tilman, 1999). After the year 2000, the area of arable land remained relatively stable over Europe, accounting for about one quarter of the continent's surface, with only a marginal increase of less than 1% (EUROSTAT, 2023; Potapov et al., 2022). Contrary in Germany, agricultural land decreased from 58% to 52% between 1950 and 2012 (Gömann and Weingarten, 2018). This decline was mainly caused by the growth of settlement, industrial and transport areas. Around a century ago, these areas made up less than 5% of Germany's territory, grew to 7% by 1950 reaching more than 15% by 2018 (DESTATIS, 2019; Niedertscheider et al., 2014). However, development patterns vary regionally, with e.g., greater infrastructure developments between larger cities and municipalities (Bieling et al., 2013). Additionally, soil degradation continued to increase significantly in the past decade and current regulatory policies of the European Union proclaim that this trend may persist (Louwagie et al., 2011; Paleari, 2017). It is expected that arable land in the European Union may decrease by about 4% in 2050, creating the likelihood that more food will need to be produced from at least the same, if not less, amount of land (Balmford et al., 2005; Grass et al., 2019). As a consequence, constraints on cultivating new cropland in the future may create more pressure on food production, and coupled with the challenges of climate change can exacerbate the global food crisis (Aksoy et al., 2017; Sundström et al., 2014).

Adverse effects of intense farming practices on the environment

Although, the intensification of food production played a significant role in increasing yields in the recent decades, all agricultural management practices itself (e.g., tillage, crop selection, fertilization, irrigation, drainage, harvesting, weed and pest control) affect the environment negatively both directly and indirectly (Glæsner et al., 2014; Smith et al., 2016; Stoate et al., 2009). All inadequate practices and decisions are consequently recognized as primary drivers of soil degradation such as compaction, contamination, erosion, but also the loss of biodiversity or various ecosystem services, which includes carbon sequestration, water regulation, food production, and crop's fibre quality (Kanianska, 2016; McKenzie and Williams, 2015; Phalan et al., 2011; Quinton et al., 2010; Sundström et al., 2014). Hence, under current management practices, soil degradation generates considerable challenges to soil health and exacerbate the increasing need to enhance food production to meet the demands of a growing global population (Evans, 2009; Paleari, 2017).

As mentioned above, the use of nitrogen increased substantially as it is a crucial nutrient for crop productivity (Pellegrini and Fernández, 2018; Tilman, 1999). However, excessive fertilization and manuring lead to environmental degradation and adverse effects on ecosystems, e.g., the emission of harmful nitrogen structures to the atmosphere (e.g., NH_3 or N_2O) (Figure 3), but also to run-off and leaching to surface and groundwater bodies (e.g., NO_3^- or DON) (Spiertz, 2009; Von Blottnitz et al.,

2006; Zhang et al., 2015). Numerous studies conducted worldwide have consistently demonstrated that conventional field and farm management activities such as excessive application of fertilizers, improper application of manure or slurry, and inadequate soil management resulted in a significant contribution to soil erosion, surface runoff and of nitrate loads into rivers and lakes (Bechmann et al., 2009; Follett and Hatfield, 2001; Rashmi et al., 2022; Shepherd and Chambers, 2007; Wang et al., 2023). The agriculture sector itself is responsible for one-third of the global greenhouse gas emissions, mainly caused by deforestation, rice production and livestock emissions of methane and due to nitrogen fertilization (Chen et al., 2020; Cheng et al., 2022; Mosier, 2001; Portmann et al., 2022; Shepherd and Chambers, 2007).

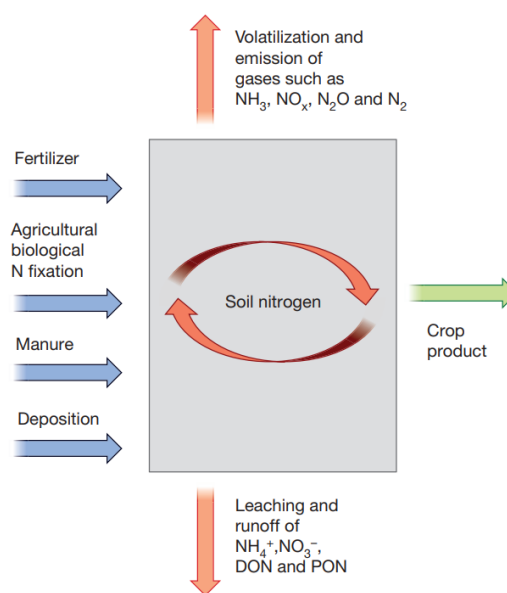


Figure 3: Depiction of the nitrogen (N) budget in crop production and the resulting N components (ammonia (NH₃), nitrogen oxides (NO_x), nitrous oxide (N₂O), dinitrogen gas (N₂), ammonium (NH₄⁺), nitrate (NO₃⁻), dissolved organic nitrogen (DON), and particulate organic nitrogen (PON)) released into the environment (orange arrows) and N recycling within the soil (shown in the grey box) (Zhang et al., 2015). The Nitrogen Use Efficiency (NUE) is defined as the ratio of the output (green arrow) to the agricultural inputs (blue arrows), i.e., $NUE = N_{yield}/N_{input}$ (Moll et al., 1982).

Environmental problems caused by nitrogen were found to be mainly induced due to crop yield prices overweight fertilizer costs by far leading to over applications in systems with focusing only on yield improvements (Finger, 2012; Reijnders, 2003). Rajsic and Weersink, 2008 have shown that the farmer's cost of over-application is lower compared to the cost of under-application. The loss of nitrogen is strongly related to the crop's nitrogen use-efficiency and is therefore a central focus in both intensively managed agricultural systems and scientific research (Spiertz, 2009; Zhang et al., 2015). Moreover, mining and manufacturing processes involved in producing fertilizers pose significant environmental risks, as they release harmful chemicals such as ammonia, fluorine, sulphur oxides, nitrogen oxides, acid mists, fertilizer dust, and harmful radiation into the air, water, and soil

(Aziz et al., 2015; Ju et al., 2007). On that note, the global nitrogen use was already found to exceed its global limits according to the theory of planetary boundaries at the beginning of the 2010s (de Vries et al., 2013; Rockström et al., 2009). Therefore, de Vries et al., 2013 suggested that both the benefits and adverse impacts of nitrogen and the spatial variability should be considered when nitrogen-related impacts are assessed, i.e., avoiding adverse effects on water, air, and soils, and ensuring sufficient food production for the global population.

Impact of changing climate conditions on crop yields

Towards the end of the previous century, yield stagnation – including winter wheat yields – became crucial for several main wheat exporting countries including the United States, Australia, Argentina, and Canada as well as regions such as the European Union, Central Asia or Eastern Europe (Brisson et al., 2010; Calderini and Slafer, 1998). Albeit internal crop-physiological constraints, how the crop physiology responds to climatic changes, especially during critical growth stages and phases, is among the major research objects (Porter and Semenov, 2005; White and Hoogenboom, 2010). With wheat being a major cereal crop produced in Europe and Germany, the biomass production of wheat, is heavily influenced by the agro-climatic conditions experienced during the specific growing season at a given location (Trnka et al., 2014). For instance, changes in soil water availability caused by reduced precipitation can impact soil evaporation and plant transpiration, leading to e.g., a shortened crop growth period (Kang et al., 2009). Also, solar radiation and the absorption of thermal energy are particularly important in regulating photosynthetic processes, where carbon, nitrogen, and other elements are incorporated into plant tissues using light energy from the sun (Lambers and Oliveira, 2019).

Of major concern are increasing temperatures as they have a significant impact on global wheat production (Asseng et al., 2017, 2015; Supit et al., 2010). Temperature changes alone shown significant negative impacts on crop production for various regions in Europe (Webber et al., 2018). As the frequency of years with temperatures exceeding critical thresholds rises, crop damage is likely to increase particularly in the latter half of this century, resulting in drastic reductions in yields (Challinor et al., 2014; Wang et al., 2018). A study by Trnka et al., 2019 projected that without climate change mitigations, up to 60% of the major wheat-growing areas will experience simultaneous water scarcity events by the end of the century. Even with climate change mitigation, negative effects will be still two-fold between 2041 and 2070 compared to the current conditions (Trnka et al., 2019). Therefore, drought stress remains a main driver of reductions in winter wheat yields particularly in low-yielding years even if groundwater-affected sites showed a lower vulnerability to increasing droughts and even if elevated CO₂ concentration in the atmosphere are

thought to partly compensate for yield losses (Kersebaum and Nendel, 2014; Webber et al., 2018). Hence, an increase in severe drought events due to a continuing global warming is to be expected having negative impacts on rain-fed crops like winter wheat (Webber et al., 2018).

Site adapted nutrient management - a solution for sustainable agriculture

Farmers and researchers have long recognized that crop yields are not uniformly distributed across fields even when climate and agricultural practices are uniform over many years (Cochran, 1939; Fisher and Russell, 1925; Jaynes and Colvin, 1997; Warrick and Gardner, 1983). Certain areas in the field consistently produce higher or lower yield than the field average, while other areas may show fluctuations in yields from year to year (Jaynes and Colvin, 1997; O. Chung et al., 2002). Despite the long-standing awareness of these within-field variations, most fields have been traditionally treated as uniform entities and managed uniformly, i.e., cultivation practices and input levels have been the same across the entire field (Stafford, 2000).

In order to meet the increasing global demand for food while minimize the impact of agricultural activities on the environment, it is necessary to change the way of how crops are produced and pursue a sustainable intensification of the agronomic productivity (Reddy, 2016; Spiertz and Ewert, 2009). Moreover, as the availability of land for crop production continues to shrink, it is increasingly important to maximize food production per unit of land in a sustainable manner and minimize the harm to the environment (Schiefer et al., 2016). Therefore, sustainable systems aim to reduce of the use of non-renewable inputs and minimizing harm to the environment and ecosystem services making best use of the space available (Gomiero et al., 2011; Pretty, 2007).

Given the environmental challenges mentioned above, changing the homogeneous field management to a resource-saving systems is now more critical than ever (Smith et al., 2016; Stafford, 2000). Therefore, employing variable rate application (VRA) techniques offers promising solutions for farmers seeking to achieve sustainable intensification in food systems (Garnett et al., 2013; Pierce and Nowak, 1999). However, despite the obvious benefits of this so-called precision agriculture (PA) – also known as precision farming (PF) or smart farming (SF) –, the widespread adoption and successful implementation of PA technology is still lagging behind its full potential (Nowak, 2021; Tamirat et al., 2018). Introduction of global navigation satellite system (GNSS) guidance, monitoring systems, and geographical information systems (GIS) since the early 1990s made within-field yield or soil mapping cost-effective and are therefore central elements of PA technologies (Stafford, 2000).

The true potential of PA lies, however, in its ability to acquire soil data, e.g., through soil sensing or sampling techniques at different scales, and utilize this knowledge to provide accurate input recommendations through decision support systems (Zhang et al., 2002). Several studies have demonstrated the economic and ecological advantages of using precision agriculture tools compared to conventional techniques (Silva et al., 2007; Sylvester-Bradley et al., 1999; Takács-György, 2008). However, the adoption time of this data-driven PA technology, which involves recording and responding to soil information, has been relatively slow even in developed countries, with a growth rate of approximately 2% per year (Nowak, 2021; Reichardt et al., 2009). This slow progress is primarily due to the complexity of the technology, the need for high-level expertise, and the requirement for robust private and public infrastructure support (Kutter et al., 2011; Tamirat et al., 2018). Various solutions exist for data collection, integration, and evaluation in PA, but they often lack accessibility and practical understanding. The successful implementation of innovations also depends on their "low complexity," meaning that the innovation can be easily tested and its benefits observed (Graham and Logan, 2004; Rogers, 2010). Unfortunately, PA does not always meet this criterion, making it challenging for widespread adoption and practical application (Nowak, 2021).

Soil quality and fertility

A sustainable crop production requires a healthy and fertile soil, which refers to the soil's well-being and its resilience to environmental changes (Stagnari et al., 2019), e.g., soils rich in organic matter exhibit a higher biodiversity and serve in storing and supplying water, nutrients, regulating temperature, and adsorbing toxins (Brady and Weil, 2008; Turmel et al., 2015). Soil fertility is an indicator closely linked to the crop productivity (Havlin and Heiniger, 2020; Hodges, 2010). A fertile soil is foremost characterized by its ability to provide plants with an adequate supply of essential dissolved minerals, including potassium (K), calcium (Ca), magnesium (Mg), phosphorus (P), and most notably, nitrogen (N) (Hodges, 2010).

Soil health and fertility are closely linked to soil quality, which assesses the suitability of soil for specific uses or functions using specific indicators to determine the actual inherent soil conditions as well as its attributes (e.g., fertility or water storage) affected by soil management (Doran and Parkin, 1994; Vogel et al., 2019). For instance, the soil water holding capacity (WHC) and its spatial variability is significantly affected by the soil organic matter and texture distribution and therefore regulating plant growth, soil drainage and other soil functional attributes (Bordoloi et al., 2019; Meurer et al., 2020). This soil intrinsic potential as well as the general site conditions can be, however, altered by how the soil is managed (Vogel et al., 2019). For instance, a silty loam can yield more than a sandy soil, even if managed poorly. However, yields on sandy soil can be increased as well, if very high

amounts of water and fertilizer would be used even in unfavourable regions. This, however would lead to tremendous pollution of the environment showing a conflict between crop production and soil health. Hence, understanding the soil's inherent states, functions and hazardous threats is crucial for developing and implementing sustainable management practices to ensure both profitable crop yields and a sustainable soil quality, i.e., providing essential ecosystem services such as nutrient regulation and carbon storage (Blanchy et al., 2023; Meurer et al., 2020). Consequently, to enhance soil fertility and promote crop growth, several management practices including site-specific nutrient and water application or the use of decision support systems are crucial in shaping agricultural outcomes (Sarkar et al., 2017; Witt and Dobermann, 2004).

As an example, a suitable pH range for various crops is crucial for maintaining crop productivity (Neina, 2019; Robson, 2012). A study by Kirchmann and Eskilsson, 2010 demonstrated that most crops experienced a significant increase in yield within a soil pH range of 5.5 to 7.2. Notably, raising the pH from 6 to 7 resulted in nearly a twofold increase in yields for winter wheat and spring barley. Even at pH levels above 6.5, cereal yields continued to rise, with an approximate gain of 640 to 1125 kg per 0.5 unit increase in pH. However, once the pH exceeded 7.2, cereal yields started to decline, possibly due to reduced availability of micronutrients for plant uptake (Kirchmann and Eskilsson, 2010). On the other hand, pH values below the optimal range resulted in a decrease in winter wheat and spring barley yields by approximately 10% for every 0.1 unit decrease in pH (Mahler and McDole, 1987). Hence, addressing suitable soil pH ranges is crucial for an optimal crop growth.

Analysing spatiotemporal yield variation

Selected approaches to analyse yield variation

While natural ecosystems already are complex systems, characterized by non-linear behaviours and responses, the complexity in agro-ecosystems increases even further because these systems can be influenced by numerous agronomic factors, which in turn impact yields and strive to achieve their highest possible productivity (Almekinders et al., 1995).

Field experiments and meta-analysis

To answer certain explicit research questions in agriculture, traditional research focuses on field experiments, which can be well controlled (Petersen, 1994). As Yang, 2010 described, within an experimental setup there are two types of factors influencing the results: those that are the actual

treatment factors (and can be seen as fixed effects) and those which are not of direct relevance for answering a certain objective. These factors may cause extraneous variations – also known as the experimental errors. This type of factors can be seen as both fixed or random depending on whether they were involved in the randomization, i.e., had they been part of the randomly selected sampling units (e.g., plants, soil samples or quadrants in pest surveys) or randomization units (e.g., rows, columns, and plots). Typical errors in an experiment occur due to the lack of uniform conditions depending on the availability of land, years, technical material and money (Yang, 2010).

What a single field experiment at a certain location over a short period of time might not reveal due to spatiotemporal constraints might be uncovered by a literature review or a so-called meta-analysis (MA) (Philibert et al., 2012). A meta-analysis is an approach for summarizing or reanalysing results of existing studies by applying statistical relationships between values reported in studies to an explanatory variable capturing all the heterogeneity within and across studies (e.g., differences in value construct measured, populations or methodologies) (Bergstrom and Taylor, 2006). MAs therefore (i) synthesize or “take stock” of the literature on a particular valuation topic; (ii) conduct hypothesis testing to evaluate the impact of explanatory variables on the targeted value, and (iii) support advanced prediction of the estimates across time and space (Bergstrom and Taylor, 2006). As outlined by Bergstrom and Taylor, 2006, MAs should (i) thoroughly describe the procedure used to select papers and the scientific databases, (ii) evaluating the individual data according to their level of precision, (iii) analysing the heterogeneity of the data with mixed effect models because the site-year variability is usually very high, (iv) carrying out sensitivity analysis, and (v) investigate the possibility of the publication bias. Moreover, MA techniques can assess environmental impacts since they can consider the variability between site-year interactions, which is why this approach is used within the first part of this thesis.

Not only field experiments, but all type of direct measurements of environmental variables are most often cost- and labour-intensive and therefore difficult to obtain. Hence, not all research questions may be answered with well-controlled agronomic research designs but a combination of different technologies and methods to predict data gaps (Almekinders et al., 1995; Veldkamp et al., 2001). Modelling in agro-ecosystems therefore helps to investigate specific agronomic and environmental purposes (Jones et al., 2017; Pasquel et al., 2022). Two major model types – statistical and process-based – were used in this thesis.

Statistical modelling

In agricultural context, statistical models employ mathematical relationships between the independent and the target variable – most often crop yields (Pasquel et al., 2022). These models

have the advantage to bridge data gaps and to explain model uncertainties relatively easy, e.g., in the representation of a low coefficient of determination (R^2) between modelled and observed data or larger confidence intervals around the prediction (Lobell and Burke, 2010). Among the many, most common statistical models used for analysing agricultural questions comprises approaches like linear, non-linear or multivariate regressions or mixed-effect modelling (Yang, 2010). As summarized by Pasquel et al., 2022, particularly mixed-effect models have the power and flexibility to avoid consequences of flawed experimental set-ups or unbalanced data collection and overcome unsuitable statistical test and models. However, such models may struggle to predict values accurately in uncertain circumstances as they (i) rely on observed data only, (ii) cannot be used for extrapolation, (iii) transferred to new sites, (iv) are applied beyond their parameterization and development, and (v) are subject to problems of co-linearity between predictor variables (Lobell and Burke, 2010; Pasquel et al., 2022). For instance, Lobell and Ortiz-Monasterio, 2007 and Sheehy et al., 2006 showed that correlations between historical minimum temperature values and wheat yields partially arose due to a negative correlation between solar radiation and the minimum temperature, while Peng et al., 2004 showed a 10% decline of rice yields in the Philippines with each 1°C increase in the average minimum temperature.

Soil mapping and geo-statistical modelling

In order to meet the demand for an intensified but sustainable crop and soil management, it is concluded in general that the nutrient demand should match the necessary supply in time and space (Day et al., 2003; Spiertz, 2009). As many soil physical and chemical properties vary within fields, water is of crucial interest for crop growth and yields and differences in particular of the water availability can lead to varying levels of productivity in different locations within the same field (He et al., 2022; Teuling and Troch, 2005). The available water content in the soil can be considered as a function of the soil texture, therefore, an understanding of soil textural distribution is essential (Godwin and Miller, 2003; Hall et al., 1977).

With spatial data from geo-physical sensors available, both in-situ and remotely recorded, small-scale modelling becomes more and more relevant in agro-ecosystem modelling (Cammarano et al., 2023; Pedersen and Lind, 2017). Proximal soil sensing provides high-resolution measurements of soil properties derived from mobile sensors in the field (Adamchuk et al., 2015; Viscarra Rossel et al., 2010), while remote sensing utilizes satellite or airborne sensors to capture both information about crop and soil properties, e.g., soil moisture, vegetation indices, land cover, and land use (Aplin, 2004; Mulders, 1987; Zribi et al., 2011). If recorded as relatively large data sets of point measurements by e.g., mobile proximal soil sensing, the data needs to be interpolated for appropriate usage in

precision agriculture (Goovaerts, 1999; Oliver and Webster, 1989). This so-called digital soil mapping involves geo-statistical analysis (a combination of statistical analysis and interpolation including spatial patterns) and calibration with lab-analysed soil data to receive comprehensive small-scale soil data (Webster, 2007).

This knowledge helps to understand the spatial patterns of soil properties and their relationships with the environment supporting land management decisions, such as targeted fertilization or erosion control (Lindblom et al., 2017). By optimizing resource utilization and promoting soil fertility, these techniques may contribute to improved agricultural productivity and environmental sustainability (Spiertz and Ewert, 2009).

Process modelling

Process-based models (also referred to as mechanistic models) differ from statistical/empirical models by utilizing mathematical equations that describe biophysical processes, i.e., environmental variables are directly linked between plant, soil, atmosphere, and management to detect short-term impacts of weather conditions during the vegetation period on the yield variability including the soil heterogeneity (Akaka et al., 2023; Wallach et al., 2018). Process models can be customized to answer specific objectives by simplification of the reality representing numerous bio-geochemical and physical transport processes and even work in the absence of any real data as long as the process has been described (Bouman et al., 1996; Pasquel et al., 2022).

In agronomy, such models are often called crop or crop growth models, soil models or agro-ecosystem models. They can support in management decisions (e.g., management practices, fertilization, irrigation, or pesticide use) or assist in policy making (e.g., erosion prediction, chemical leaching, assessing climate impacts, or yield forecast) (Boote et al., 1996). As Kersebaum and Wallor, 2023 pointed out, they can be an appropriate tool to estimate the amount needed for irrigation or fertilization in relation to site-specific yield expectations and optimize the water or nutrient use efficiency. Hence, they are suitable tools for precision agriculture (Cammarano et al., 2023).

As can be seen in Figure 4, the key processes simulated in those models are mainly related to crops (e.g., development, growth, yield, nutrient and water uptake) and/or soils (e.g., mineralization, water and nutrient movements) considering agronomic interactions (e.g., fertilization, irrigation or tillage) (Boote et al., 1996; Kersebaum and Wallor, 2023). The advantage of these models is that they always produce consistent results for a given set of inputs, as they lack random variations within the model and equations and they can be applied on various scales – from the global scale to e.g., assess the impact of climatic changes and down to regional or field scales to support intra-field crop

management (Elliott et al., 2015; Kersebaum and Wallor, 2023; Witing et al., 2023). On the downside, these models are highly complex and require substantial parameterization for the boundary conditions of the system, e.g., the soil and crop conditions or management information and are therefore time consuming to handle with high expert knowledge needed (Boote et al., 1996).

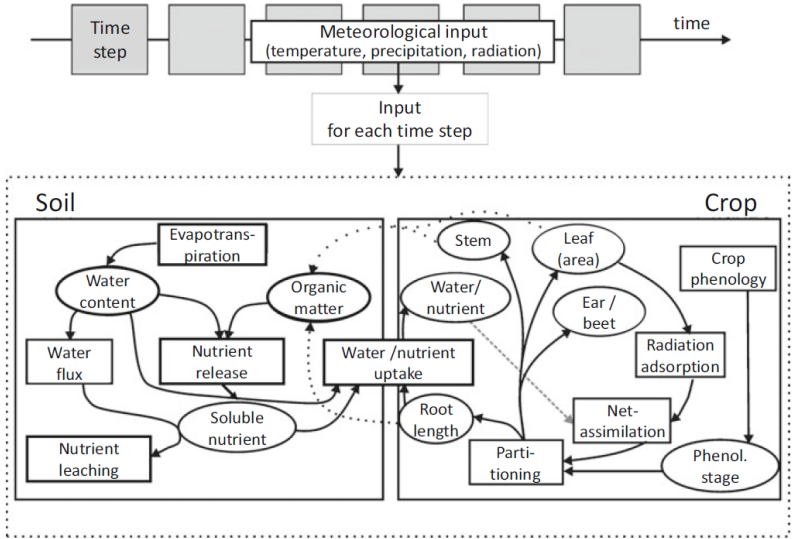


Figure 4: A simplified scheme of the interactive water and nutrient dynamics within the soil-crop system, as used in process-oriented agro-ecosystem models (Kersebaum and Wallor, 2023) based on the meteorological inputs.

Considerations at different spatiotemporal scales

As outlined in the chapters above, various environmental factors, such as weather conditions or soil properties, as well as agronomic decisions, e.g., fertilization, have a significant but impacts of differing magnitude on yields in agro-ecosystems (Almekinders et al., 1995; Veldkamp et al., 2001). Depending on the research question, the consideration of yield variability may therefore vary at different temporal and spatial scales and varying extents, coverage, and resolution of the available data and need to be processed accordingly (Jones et al., 2017; Young, 2006).

Several hierarchical levels related to the impact of spatial variability on crop yields in agro-ecosystems have been identified (Figure 5) (Jones et al., 2017). On one hand, the impact of climate and climatic changes becomes increasingly important the bigger the scale, e.g., from regional, interregional, national, up to the global scale (Brocca et al., 2010; Ewert et al., 2011; Vergni and Todisco, 2011). On the other hand, to establish a sustainable soil and crop management and determine the most effective small-scale management practices, research conducted at scales below the regional level, i.e., the farm or field scale is necessary (Jones et al., 2017; Zhang et al., 2015).

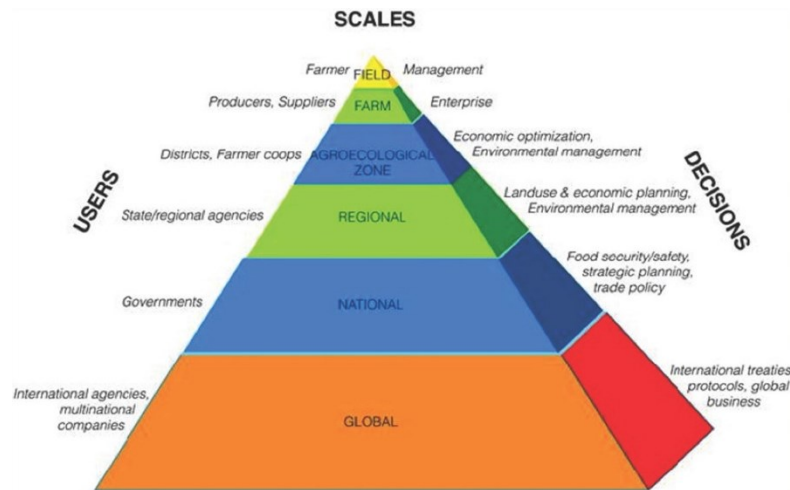


Figure 5: Scales at which research questions are addressed in agricultural systems including the different types of users and decisions and policies of interest (Jones et al., 2017).

It is important to note that the quality and resolution of all spatial and temporal information, regardless of the scale, have a direct impact on modelling results, i.e., influence the accuracy of the models (Hoffmann et al., 2016; Kabat et al., 1997; Kuhnert et al., 2017; Ye et al., 2011). For instance, modelling crop growth on individual agricultural plots, detailed information on management practices, site characteristics, cultivars and the weather is required (Kersebaum et al., 2015). On the other hand, modelling at the landscape or regional scale involves aggregated information, sometimes derived from GIS maps, encompassing soil properties, and long-term weather data from meteorological stations, and region-specific management practices (Hartkamp et al., 1999; Mirschel et al., 2004).

Hence, the lack of reliable and consistent data or data limitations, such as insufficient spatial or temporal coverage, can hinder accurate modelling at smaller as well as on larger scales (Wiesmeier et al., 2019). Also, the aggregation of modelling input data as well as the combination of data from different sources at different spatial and temporal resolutions, can lead to errors and uncertainties when predicting changes in soil properties (Grosz et al., 2017). For instance, as Stockmann et al., 2013 and Wiesmeier et al., 2019 lined out with several publications within their work, soil organic carbon (SOC) stocks are influenced by various biotic and abiotic conditions, which leads to various issues to be focused on at different scales. At field scale, the exact knowledge of the small-scale distribution of the SOC content itself is important for modelling at the field scale, but requires accurate aggregation at larger scales (Wiesmeier et al., 2019). Moreover, Wiesmeier et al., 2019 reviews how this also accounts for all SOC dependent environmental factors that affect either the storage and retain of the SOC (e.g., soil type distinctive inherent properties, such as texture, mineralogy, or drainage), the losses or gains of SOC (e.g., land use and management), or other SOC dynamic influencing environmental factors (e.g., temperature, precipitation, topography, parent

material or soil cover) as they influence the primary productivity, decomposition rates, organic matter stabilization, or the amount and quality of organic inputs to the soil. Hence, all these factors require adequate representation at larger scale, which accounts for the whole small-scale variability.

In addition to their spatial dimensions, agro-ecosystems exhibit significant temporal variability with the various processes operating at varying speeds (Veldkamp et al., 2001). In terms of agricultural productivity, relevant temporal dynamics are either short-term at daily, seasonal, and inter-annual scales, as well as over longer periods encompassing climatic, agronomic, and landscape changes (Vergni and Todisco, 2011). The fastest dynamics occur at the crop level, where physiochemical processes play a dominant role in controlling crop physiology. Short-term processes also become important within the soil-root continuum at the pore space level including dynamics such as root growth, water uptake, faunal activity, gas and nutrient transport or water and temperature-driven phenomena like swelling/shrinking or freeze/thaw cycles (Matzner and Borken, 2008; K. Meurer et al., 2020; Vetterlein and Doussan, 2016). Somewhat slower, but still at relatively fast time scales refer to daily and seasonal dynamics as addressed in the second and third part of this thesis (Dungait et al., 2012). At this scale, adaptation to changing weather conditions to issues like e.g., water scarcity, nutrient deficiencies or plant diseases become crucial for management decisions (Dungait et al., 2012). Finally, inter-annual or decadal changes in e.g., weather condition or the adoption of land management practices can have longer-term effects on crop production or the overall yield level (Shukla et al., 2019; Smith et al., 2016). These effects are mainly addressed in the first part of this thesis.

In particular at the field scale, the focus shifts from the broader concept of "climate" to the specific actual weather conditions affecting crop yields (Ceglar et al., 2016; Hoffmann et al., 2018). The weather conditions during a single vegetation period have a more immediate impact on agricultural operations and decisions such as for strategic or tactical purposes (Jones et al., 2017). As Jones et al., 2017 lined out, strategic purposes aim to support the evaluation of trade-offs among possibly conflicting objectives of decision/policy makers, i.e., to evaluate functional responses in ideally real systems (e.g., end of season grain, biomass yield, or residues in response to a range of nitrogen fertilizer use). Tactical purposes on the other hand help to inform about decisions, such as when to apply pesticides, fertilizer or when to irrigate. They do not represent, however, how to best manage a crop for multiple inputs over the system as a whole, but simply when to perform those predetermined management operations, i.e., when a particular threshold is reached that has been shown before to provide effective management. Moreover, at the local or regional scale, weather limitations may be masked by management practices, making inter-seasonal differences more apparent (Goddard et al., 2010).

Thesis outline and research objectives

The overarching goals of this thesis were (i) to contribute to an improved understanding of the impact of variable soil and changing weather conditions on the variation of crop yields at different spatiotemporal scales and (ii) to show an example of a nutrient management adapted to the small-scale soil differences at a site of high yield variability. As wheat is the most produced cereal in Germany (DESTATIS, 2019), this thesis focuses on the spatiotemporal variability of wheat crops. With that highlighted, the thesis is outlined into two main parts with the general objectives:

Part I - Causes of a spatiotemporal yield variability

Yield productivity differs within fields and over regions as well as between years and over decades. To investigate the spatiotemporal causes of wheat yield variability, Part I of this thesis comprises two studies:

The first study of Part I mainly investigates the impact of changes in climate and weather extremes on the winter wheat yield variation and yield levels at different sites and regions in Germany. This part has been published in *Global Change Biology*:

Bönecke, E., Breitsameter, L., Brüggemann, N., Chen, T.W., Feike, T., Kage, H., Kersebaum, K.C., Piepho, H.P. and Stützel, H., 2020. Decoupling of impact factors reveals the response of German winter wheat yields to climatic changes. *Global Change Biology*, 26(6), pp.3601-3626.

As it is challenging to disentangle the impact of all contributing growth factors on crop yields and to determine the extent and magnitude to which climatic changes contributed to the variation of crop yields, the specific objectives of the first study in the first main part were:

1. to determine the magnitude of the effects of relevant agro-climatic changes on the long-term winter wheat yield development in Germany and
2. to detect whether sites divided into classes of lower and higher yield potential (and different soil types) were affected differently.

The following hypothesis were derived:

- a) Long-term climate changes and increases in weather extremes are having a negative impact on winter wheat yield variation and level.
- b) Yield variation at sites of lower yield potential and sandy conditions are stronger affected by changing meteorological conditions, e.g., increasing temperatures.

The second study of Part I mainly investigates the impact of the small-scale soil differences on the within-field variation of winter wheat yields on a site with seemingly uniform distribution of chernozem soils developed over loess, which have a very good soil nutrient and water storage. This part has been published in Precision Agriculture:

Boenecke, E., Lueck, E., Ruehlmann, J., Gruending, R. and Franko, U., 2018. Determining the within-field yield variability from seasonally changing soil conditions. Precision Agriculture, 19(4), pp.750-769.

As even such relatively homogeneous sites reveal variations in yields, the specific objectives of the second study in the first main part were:

1. to detect the small-scale soil structures on a chernozem soil developed on loess and over old-morainic substrates and to model the soil water dynamics and
2. to determine and evaluate the time when the water availability effected the winter wheat yield variability the most.

The following hypothesis were derived:

- a) The within-field yield variation is mainly characterized by the availability of soil water over the whole rooting zone, i.e., including the water amount below the loess-layer.
- b) The variability is most evident in years with low precipitation during sensitive growth periods.

Part II – Site variable nutrient management

The study in Part II of this thesis mainly demonstrates how the nutrient management can be addressed site-specifically at site of high yield variability that is caused by the soil heterogeneity in a fluvial and morainic influenced landscape. This part consists of one study that has been also published in Precision Agriculture:

Bönecke, E., Meyer, S., Vogel, S., Schröter, I., Gebbers, R., Kling, C., Kramer, E., Lück, K., Nagel, A., Philipp, G. and Gerlach, F., Palme, S., Scheibe, D., Zieger, K., Rühlmann, J., 2021. Guidelines for precise lime management based on high-resolution soil pH, texture and SOM maps generated from proximal soil sensing data. Precision Agriculture, 22(2).

As the yield productivity also is a consequence of the soils capability to provide sufficient nutrient and water, but long-term uniform fertilization of arable land led to excessive nutrient levels as well as high nutrient contamination risk, the specific objectives of the final part of this thesis were:

1. to demonstrate exemplarily for liming, which is a key soil management to maintain or improve the soil's fertility and consequently crop productivity, how small-scale soil property differences can be considered in a fertilization decision support system at sites with high yield variability by
 - i. the creation of precise maps of the liming relevant parameters soil pH, soil organic matter and soil texture derived from different proximal soil sensors and
 - ii. the adaptation of an existing but insufficient fertilization algorithms to the requirements of these modern sensor technologies and
2. to compare the results of this novel decision support system with a field uniform lime recommendation based on conventional data acquisition.

The following hypothesis were derived:

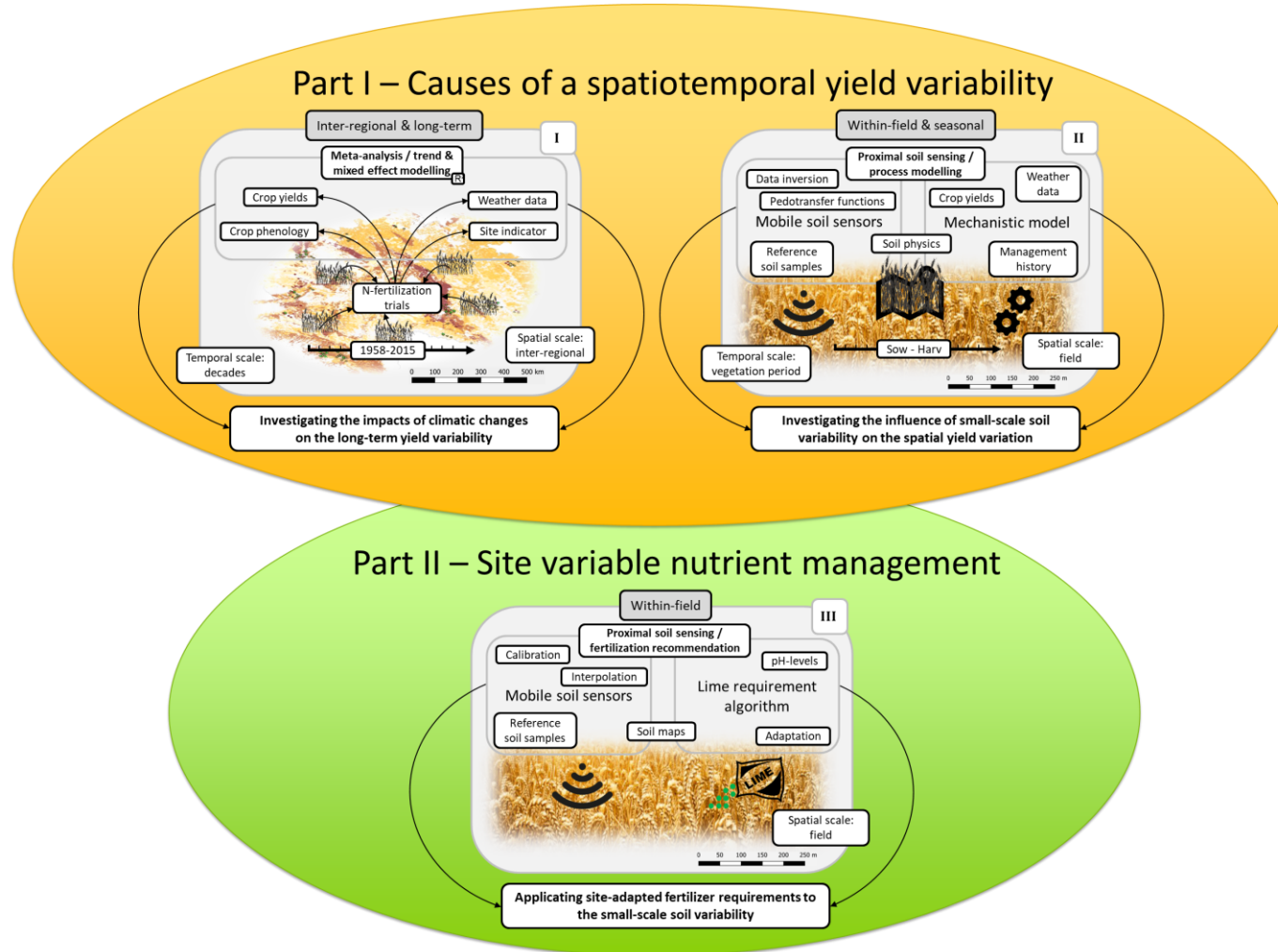
- a) The use of appropriate proximal soil sensors provides an accurate overview of the soil heterogeneity.
- b) The adaptation of the fertilization algorithm to the "stepless" dynamic soil parameters enables the accurate determination of fertilizer requirements.
- c) Accurate knowledge of soil heterogeneity and improved calculation of fertilizer requirements highlights the weaknesses of conventional fertilizer requirement calculation.

Thesis overview

Scales, factors and methods

Study	Scales		Factors				Methods		
	Spatial	Temporal	Soil		Climatic		Genetic	Agronomic	
			static	dynamic	climate	weather			
1	Inter-regional	Decades	X		X	X	X	X	meta-analysis trend-analysis mixed effect modelling soil quality rating
2	Within-field/ /profile	Daily Seasonal Crop rotation	X	X			X	X	proximal soil sensing soil process modelling quantile regression
3	Within-field/sub-area	Fertilization cycle	X	X			X	X	proximal soil sensing geo-statistics fertilization-algorithm

Variation of wheat yields as a consequence of soil and meteorological variability



Clarification of contribution

The publication '[Decoupling of impact factors reveals the response of German winter wheat yields to climatic changes](https://onlinelibrary.wiley.com/doi/10.1111/gcb.15073)' (<https://onlinelibrary.wiley.com/doi/10.1111/gcb.15073>) was fully written by myself and supportively corrected by all co-authors. All authors contributed to the content of the manuscript and discussed the results. Me and Laura Breitsameter collected the data and I carried out the statistical analysis. The main idea was outlined by Hartmut Stützel.

The publication '[Determining the within-field yield variability from seasonally changing soil conditions](https://link.springer.com/article/10.1007/s11119-017-9556-z)' (<https://link.springer.com/article/10.1007/s11119-017-9556-z>) was fully written by me and supportively corrected by all co-authors. All co-authors contributed with their expertise, discussed the results and helped outlining of the manuscript. I was responsible for the data gathering except for the measurements with the Geophilus sensor system, which was done by Jörg Rühlmann and Erika Lück, the data processing and the literature review. The main idea was developed by Uwe Franko.

The publication '[Guidelines for precise lime management based on high-resolution soil pH, texture and SOM maps generated from proximal soil sensing data](https://link.springer.com/article/10.1007/s11119-020-09766-8)' (<https://link.springer.com/article/10.1007/s11119-020-09766-8>) was mainly written and outlined by me. All co-authors supported the process of discussing and correcting the manuscript. Sebastian Vogel and Robin Gebbers contributed to the writing and graphics of the introduction section. Sebastian Vogel, Ingmar Schröter, Jörg Rühlmann and Swen Meyer contributed to the writing of the sensor description section. Sebastian Vogel supported writing the reference sampling section. Jörg Rühlmann contributed writing the lime demand algorithm section. All authors contributed to the data gathering on the field, in the lab, and the literature review. I carried out the data processing and statistical analysis. The main idea was developed by Jörg Rühlmann, Eckart Kramer and Robin Gebbers.

Part I – Causes of a spatiotemporal yield variability

Decoupling of impact factors reveals the response of German winter wheat yields to climatic changes

Eric Bönecke^{1,7}, Laura Breitsameter¹, Nicolas Brüggemann², Tsu-Wei Chen¹, Til Feike³; Henning Kage⁴, Kurt-Christian Kersebaum⁵, Hans-Peter Piepho⁶, Hartmut Stützel¹

¹Institute of Horticultural Production Systems, Leibniz University Hannover, Hannover, Germany.

²Institute of Bio- and Geosciences – Agrosphere (IBG-3), Forschungszentrum Jülich, Jülich, Germany.

³Institute for Strategies and Technology Assessment, Federal Research Centre for Cultivated Plants, Julius Kühn-Institute, Kleinmachnow, Germany.

⁴Institute of Crop Science and Plant Breeding, Christian-Albrechts-University Kiel, Kiel, Germany.

⁵Research Platform "Models & Simulation", Leibniz Centre for Agricultural Landscape Research, Müncheberg, Germany.

⁶Institute of Crop Science, University of Hohenheim, Stuttgart, Germany.

⁷Next-Generation Horticultural Systems, Leibniz-Institute of Vegetable and Ornamental Crops, Grossbeeren, Germany.

Abstract

Yield development of agricultural crops over time is not merely the result of genetic and agronomic factors, but also the outcome of a complex interaction between climatic and site-specific soil conditions. However, the influence of past climatic changes on yield trends remains unclear, particularly under consideration of different soil conditions. In this study, we determine the effects of single agro-meteorological factors on the evolution of German winter wheat yields between 1958 and 2015 from 298 published N-fertilization experiments. For this purpose, we separate climatic from genetic and agronomic yield effects using linear mixed effect models and estimate the climatic influence based on a coefficient of determination for these models. We found earlier occurrence of wheat growth stages, and shortened development phases except for the phase of stem elongation. Agro-meteorological factors are defined as climate covariates related to the growth of winter wheat. Our results indicate a general and strong effect of agro-climatic changes on yield development, in particular due to increasing mean temperatures and heat stress events during the grain-filling period. Except for heat stress days with more than 31°C, yields at sites with higher yield potential were less prone to adverse weather effects than at sites with lower yield potential. Our data furthermore reveal that a potential yield levelling, as found for many West-European countries, predominantly occurred at sites with relatively low yield potential and about one decade earlier (mid-1980s) compared to averaged yield data for the whole of Germany. Interestingly, effects related to high precipitation events were less relevant than temperature related effects and became relevant particularly during the vegetative growth phase. Overall, this study emphasizes the sensitivity of yield productivity to past climatic conditions, under consideration of regional differences, and underlines the necessity of finding adaptation strategies for food production under on-going and expected climate change.

Keywords

Winter wheat · climate change impact · weather extremes · R^2 for mixed effect models · long-term yield development · phenology trend · climate trend · soil yield potential

Introduction

Historical climate change, and first and foremost rising temperatures during the second half of the twentieth century, contributed to profound changes in yield in many major wheat-producing regions globally and in western Europe in particular (Alexander *et al.* 2006; Asseng *et al.* 2014; Frich *et al.* 2002; Lobell *et al.* 2011). For instance, an estimated net loss of 4% in wheat yield, coinciding with increasing temperature and decreasing precipitation between 1980-2008, has been found for France (Lobell *et al.* 2011). Wheat has been found to be very sensitive to high temperatures, and its response to heat stress varies at different phenological stages (Farooq *et al.* 2011; Slafer & Rawson 1994). High temperatures are presumed to be more harmful to grain yield during the reproductive growth phase than during the vegetative phase (Wollenweber *et al.* 2003). Heat stress around anthesis mainly leads to a reduction in photosynthesis rate, increased respiration, accelerated leaf senescence, and enhanced evapotranspiration, which finally results in reduced grain numbers (Porter & Gawith 1999; Reyer *et al.* 2013; Wheeler *et al.* 1996; Wollenweber *et al.* 2003). Exposed to drought stress during reproduction, grain yields of wheat are negatively affected due to a hampered uptake of nutrients, and in combination with a diminished surface cooling (induced by reduced transpiration) crop canopy temperatures increase and lead to further decrease in photosynthetic rates (Mäkinen *et al.* 2018; Porter & Semenov 2005). During stem elongation, water is needed for expansive growth processes that bring up the spike to the top of the canopy through the unfolding leaf, as well as for spike growth and cell expansion, pollen ripening, or grain growth and filling (Farooq *et al.* 2011). With enhanced climate variability during summer across Europe, encompassing a higher risk of heatwaves, droughts and heavy precipitation events, negative impacts on yields are likely to increase (Mäkinen *et al.* 2018; Meehl & Tebaldi 2004; Porter & Semenov 2005).

Besides environmental factors, quality and quantity of grain yields are determined by the crop genetic yield potential and by agronomic measures of crop management that aim to reduce environmental limitations. Despite the ongoing advancement in breeding for higher grain yields since the 1960s, the use of nitrogen fertilizers, irrigation, or pesticides, the steady increase of winter wheat (*Triticum aestivum* L.) yields during the second half of the 20th century has slowed down since the 1990s in several regions of the globe (Brisson *et al.* 2010; Calderini & Slafer 1998; Chen *et al.* 2015; Grassini 2010; Laidig *et al.* 2014). For instance, historical yield records reveal that winter wheat yields almost simultaneously reached a plateau at about 7 to 8.5 t ha⁻¹ in many West European high-yield countries between 1991 and 2000 (Brisson *et al.* 2010; Grassini *et al.* 2013). For Germany, yield data from the National Statistical Office show an increase of winter wheat yields from approximately 3 t ha⁻¹ in 1960 up to 7.5 t ha⁻¹ in the year 1999 (Wiesmeier *et al.* 2015), but thereafter, no further increase has been documented. A number of causes for the stagnation of grain yield have been

discussed. Besides aspects of climatic change (e.g. increasing temperatures, high precipitation events, or drought stress) or the genetic and agronomic progress (expansion of wheat to sites with lower productivity, increasing shares of “second wheat” in crop rotation), socio-economic incentives and/or constraints (e.g. world market price for wheat grain or general production factors; expansion of organic production systems; legal limitations to fertilization; political subsidies, price influences from climate events) were in the focus of research (Brisson *et al.* 2010; Grassini *et al.* 2013; Himanen *et al.* 2013; Laidig *et al.* 2017; Olesen *et al.* 2012; Reidsma *et al.* 2008; Trnka *et al.* 2019).

Many studies only account for the effect of one single impact factor and only take yield data from official statistics that represent annual averages at national or global scale, which result from diverse crop management of a multitude of farmers acting under diverse production conditions (Brisson *et al.* 2010; Calderini & Slafer 1998; Hafner 2003; Lobell & Field 2007; Wiesmeier *et al.* 2015). However, the response of crop yields to climate variability might be enhanced or diminished depending on certain site conditions (Moot *et al.* 1996; Porter & Gawith 1999; Porter & Semenov 2005). As a consequence, national data do not sufficiently consider regional diversity – both environmental and agronomical (Evans 1996; Schlenker 2010; van Ittersum *et al.* 2013). Similarly, studies building on a single experiment or using historical yield and fertilization data from only one location are limited in their explanatory power due to the restricted number of years, locations and used cultivars. Hence, a set-up combining multiple locations over a long period is preferable to compensate for these limitations.

In this study we aim at examining the importance of a range of individual agro-climatic factors affecting winter wheat yields. However, since also other factors affecting yield development changed over time, it is necessary to disentangle the effects of climate change from those of genetic progress, and of all other agronomic factors that changed over time (e.g., socio-economic incentives and constraints). In order to dissect these factors, mixed-effect models were used, which allow attributing yield variability to randomly distributed independent effects. These models serve to analyse data sets – including unbalanced ones – and to dissect various impact factors by means of fixed regression terms and random residuals (Laidig *et al.* 2008; Laidig *et al.* 2017; Mackay *et al.* 2011; Piepho *et al.* 2014). Moreover, statistical models do not depend on field calibration data for many driving variables as required for process-oriented models, and model uncertainties can be assessed in a more transparent way (Lobell & Burke 2010b). Mixed-effect models can further take into account the influence of regional diversity, for instance, regarding soil type and quality. In this study, we make use of historical field trial records found in 34 publications that provide data on winter wheat yields, N-fertilization levels, and cultivars from a total of 298 N-fertilization experiments over a long period of time and with a large geographic spread across Germany. The

amount of nitrogen fertilizer applied is the agronomic factor, which usually has the strongest impact on yield and quality traits and features large regional and inter-annual variation (Whitfield & Smith 1992; Delogu *et al.* 1998; Basso *et al.* 2011). In order to exclude limiting effects of the factor 'N-fertilization', using data from optimum N-fertilization levels has been proven a useful approach (Raun *et al.* 2002; Basso *et al.* 2011). Specifically, experiments with multiple N-levels allow calculating the maximum of the nitrogen supply-yield relationship under standardised and pre-defined conditions.

We analyse the yield development of winter wheat over the last 60 years in Germany based on published data from wheat-nitrogen fertilization experiments. We identify the underlying causes of the observed trends by considering agronomic, genetic, inter-annual, and geographic differences. Based on responses described in the literature, this study considers climatic factors linked to important winter wheat crop growth stages and phases. To estimate the explanatory value of an individual agro-climatic factor, we use a novel approach (Piepho 2019) that compares the total variance estimates between two mixed-effect models – one that includes the climate variable of interest and one that does not, and employs the calculation of a coefficient of determination for such models (Methods). First, we run the analysis over all experiment data across all study sites. In order to understand the impact and specify the significance of soil factors we then split the data into groups of experimental sites differing in yield potential and soil type. Understanding the interactive effects of climatic changes and genetic adaptation (i.e., genetic improvement through plant breeding) on yield productivity development is crucial for developing viable crop adaptation strategies to future climate change.

Materials and Methods

Study design

In order to assess the impact of climatic changes on winter wheat yield development, we applied several processing steps from raw data to final data analysis. As illustrated in Figure 6, we firstly gathered specific crop data including yields, nitrogen fertilization amounts, cultivar choice and year of release. Furthermore, for every experimental site we gathered winter wheat phenology data (i.e., beginning of phenological stages), climatic data, and site-specific soil information including soil type and soil rating (*Ackerzahl*) henceforth called '*soil yield potential*'. In the second stage, we processed the experimental data to derive the optimal nitrogen fertilization amounts and maximum yields. We used the climatic and phenological information to derive crop-specific agro-climatic conditions throughout the observation period. Thirdly, for all time-series data, trend analyses were

performed using simple linear regression models followed by segmented regression analysis. Additionally, linear plateau analyses were carried out for the yield and nitrogen data. Fourthly, we used a data set with all data combined to decouple individual agro-climatic conditions from all other influential crop parameters to finally assess the intensity of these individual factors by computing the coefficient of determination (R^2) for generalized linear mixed models as introduced by Piepho (2019).

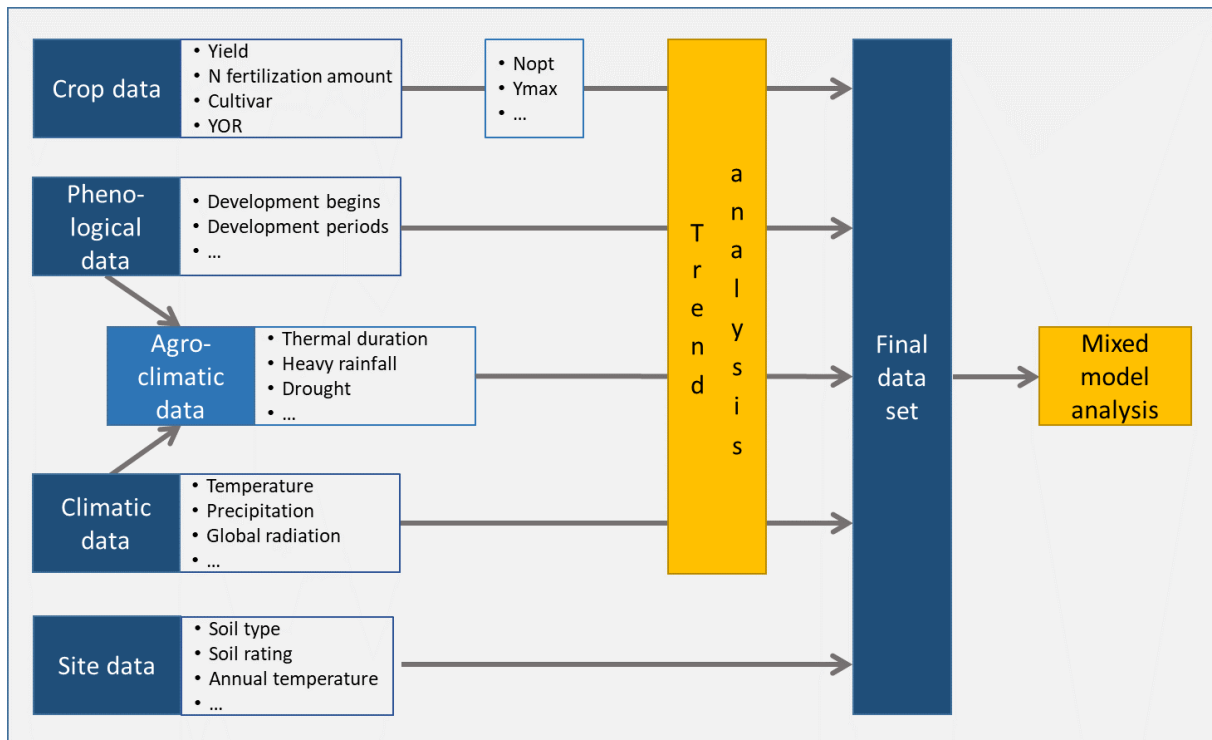


Figure 6: Data processing scheme from raw data to final data analysis. Crop, phenological, climatic, agro-climatic, and site-specific data were collected in the first place and analysed for their trends. All data was combined into a data set from which individual agro-climatic variables were decoupled from all other influential factors using statistical mixed-effect models. Finally, the intensity of each variable was estimated by computing the coefficient of determination (R^2) for generalized linear mixed models as introduced by Piepho (2019)

Dataset compilation

Crop data

Winter wheat field experiment data were gathered from multiple sources including peer-reviewed articles, dissertation theses, habitation theses, conference papers and N-fertilization experiment reports from state authorities. Germany was selected as study region, as it represents a specific breeding region and ensures a sufficient number of well documented experiments. All considered experiments investigated the response of grain yield of one or several cultivars to varied levels of N fertilization (sub-optimal, optimal, supra-optimal). In rainfed experiments with optimal plant protection, grain yields are supposed to be defined by the site-specific soil and climate conditions and limited by the genetic yield potential of the selected cultivar and the applied N rates.

To be included in the study data-set, the following criteria had to be fulfilled by an experiment: at least three levels of total rates of mineral N fertilization (sum of all applications within one growing season) are represented, plant protection excluded biotic stress, and the experiment was not irrigated. Moreover, site- and year-specific grain yields at defined dry matter content (either 86% or 100% dry matter) had to be available for each N-fertilization level. To make data comparable, all analyses were carried out by converting data to 100% dry matter, expressed in tons dry matter per hectare (t DM ha⁻¹). The exact location of each experimental site had to be given. A final dataset was derived from 34 publications comprising 43 individual experimental sites between 1958 and 2015 and a total of 59 individual cultivars (Bönecke *et al.* 2020). The duration of the individual experiments ranged from one to six years. Information about the year of release (YOR) of the corresponding cultivars was retrieved from databases of the Federal Plant Variety Office and from GRIS (Genetic Resources Information System for Wheat and Triticale, CIMMYT).

Calculation of Y_{max} and N_{max}

N-fertilization experiments provide the opportunity to estimate the yield maxima (Y_{max}) for each experiment, which then represent the environmental and agronomic limits in an experimental year and of a region. Y_{max} can then be used to compare the yield variation between different locations and years. To derive potential grain yields under non-N-limited conditions for each experimental year, site and cultivar, data on dry matter grain yield at individual N fertilization levels was used to calculate Y_{max} and the corresponding maximum N fertilization level (N_{max}). Most trials implemented sub-optimal, close to optimal and supra-optimal N-levels in equal quantity steps (e.g. 50, 100, 150 kg N ha⁻¹). We fitted a quadratic yield response function:

$$Y = a + bN + cN^2 \quad (1)$$

to the data of each individual N-fertilization response trial, where N is the applied N-level and Y is the observed yield (Figure 7), using the statistical software R (R Development Core Team 2008). Values of Y_{max} and N_{max} were obtained from the coefficients of these functions by setting their first derivatives to 0 and solving for N :

$$N_{max} = -b/2c \quad (2)$$

$$Y_{max} = a + bN_{max} + cN_{max}^2 \quad (3)$$

where a , b , and c are the model parameters.

When fitting quadratic functions to the trial data, several scenarios need to be considered for interpreting the derived yield as Y_{max} under the given site and climatic conditions: The derived Y_{max} value may lie (i) beyond the highest observed N-level, and (ii) it may be higher or lower than a

measured Y_{\max} value. To deal with these issues, certain thresholds were set: When the derived Y_{\max} was not reached within the observed range of N-levels, an upper threshold was set for acceptance of a study. Specifically, we determined the mean width of the N-level increments. The threshold was computed as the largest N-level tested in the study, plus the mean increment. A study was accepted only if Y_{\max} was estimated to occur at an N-level below that threshold. For instance, in an 80-120-160 kg N ha⁻¹ trial, the mean increment of the N-fertilization levels is 40 kg N ha⁻¹ and when Y_{\max} was estimated at 210 kg N ha⁻¹, the trial was then excluded from the dataset, whereas when Y_{\max} was derived below or equal to 200 kg N ha⁻¹, the trial was included. Moreover, Y_{\max} values below 50 kg N ha⁻¹ were excluded from further analysis and considered as unrealistic under conditions present in Germany. When the derived Y_{\max} value was below the highest yield measured by more than 5%, the measured yield was taken as Y_{\max} . Yet, when the derived Y_{\max} was greater than 5% of the highest measured yield, the derived Y_{\max} was chosen to reflect the maximum yield achievable. In any case, experiments outside these defined thresholds were excluded from the dataset. 11.2% of the data were removed from further analysis due to decreasing yield functions and coefficients of determination below 0.5. Following these plausibility tests, 324 out of 331 individual trials remained within the dataset. The correlations between Y_{\max} and the corresponding N_{\max} , the intercept, and the linear coefficient of the quadratic regression model were 0.51, 0.62, and 0.33, respectively. Correlations between N_{\max} , the intercept, and the slope factors of the quadratic regression model ranged between -0.1 and 0.52.

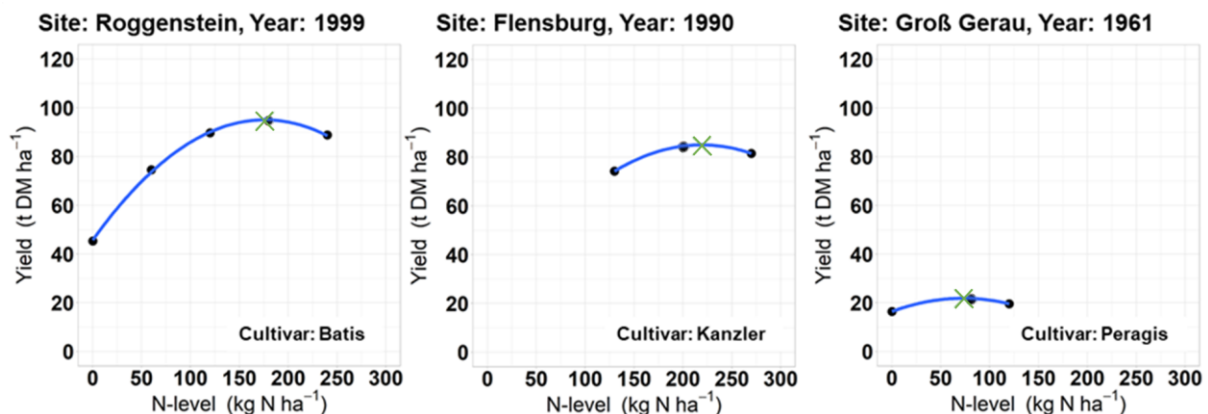


Figure 7 Examples for the yield response curves to nitrogen fertilizer level and derived maximum yields and corresponding nitrogen values of three fertilization experiments. The green crosses mark the maximum achievable winter wheat yields as derived from a quadratic linear function and its corresponding nitrogen level

National yield data

The national average winter wheat yield data was obtained from FAO statistics (<http://www.fao.org>) and from the Federal Statistical Office (German: Statistisches Bundesamt, shortened DESTATIS), Wiesbaden.

Phenological data

None of the publications from which yield data were retrieved provided precise information about phenological stages and phases. Therefore, data on the beginning of the individual phenological stages of winter wheat were retrieved from the phenological observation database on arable cropping systems (ftp://ftp-cdc.dwd.de/pub/CDC/observations_germany/phenology/) from the German Weather Service (Deutscher Wetterdienst, DWD). Phenological dates were recorded from voluntary observers within a radius of 1.5-2 km and not more than 50 m in altitude from the mean altitude of the observation site covering a period from 1951 to 2015 (as at November 2017). Cultivars used in the fertilization experiments may differ from those underlying the phenological records of the DWD. For this study, the beginning of sowing, emergence, stem elongation, heading, hard dough, and harvest were recorded on an annual basis for all sites where experiments were conducted. In order to estimate the start dates of the aforementioned phenological stages, all DWD observation sites within a radius of 30 km of each experiment site were selected using the ArcGIS Desktop software by Esri (version 10.5.1). To eliminate errors and incorrectly recorded single values, data records were processed by an automated selection process. As suggested in Menzel (2003), only observation sites with relatively complete data records of more than 20 or 30 years should be considered as meaningful for reliable predictions because trend analysis strongly depends on the number of years included in the linear regression. In this study, 30 years was set as minimum record length to ensure a certain degree of temporal stability of the resulting trends. Even then, a small uncertainty remained because part of the variation in trends might be caused by differing start and end years. In respect of topography and altitude (m a. s. l.), all stations with more than 50 m difference in altitude from the experimental sites were removed to avoid misinterpretation due to vertical thermal differences and their influence on stage initiation. Mean values and standard deviation for each year of the stage beginning dates were calculated and potential outliers removed when they fell outside the range of the mean value \pm two times the standard deviation as suggested in Siebert & Ewert (2012). After applying the filtering process, the total number of observations obtained for the 43 sites across the study regions was 15238. Moreover, the duration of the whole growing season (GS), the generative phase (GP) and the vegetative phase (VP) was calculated, and in addition VP was subdivided into the leaf development and tillering phase (LP) and the stem elongation and booting phase (SP). As shown in Figure 8, the length of the vegetative phase was defined as the time between emergence and heading and the generative phase as the time between heading and hard dough. The LP and SP were separated by the beginning of the stem elongation.

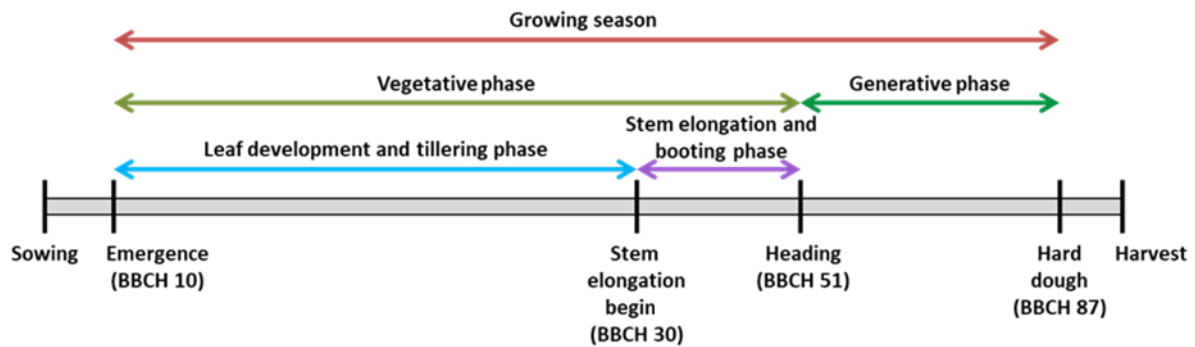


Figure 8 Development stages (black vertical bars), phases (coloured), and reference values according to the plant developmental BBCH-scale (Meier 1997) similar to the Zadoks scale (Zadoks et al. 1974) for winter wheat along the whole vegetation period

Climatic data

As for phenology, high-resolution weather data that allow calculating agro-meteorological variables was scarcely provided within the publications. For this reason and to investigate long-term climate trends for the crop growth phases outlined above at each respective experimental site, we obtained information from several databases providing climate data. The daily mean temperature ($^{\circ}\text{C}$), precipitation (mm) and relative air humidity (%) were obtained from the hydrological raster (HYRAS) data set ($5 \times 5 \text{ km}^2$) of the DWD for the period 1951 to 2015 (Frick *et al.* 2014). The interpolation of the gridded HYRAS dataset is based on a combination of multiple linear regression and inverse distance weights and described in detail in Rauthe *et al.* (2013). Data on minimum and maximum temperature was obtained from the European Climate Assessment & Dataset (ECA&D) database and available for the period 1950 to 2017 (Haylock *et al.* 2008). Data about the surface solar radiation income (global radiation, $\text{W}^{-1} \text{m}^{-2}$) was available for the period 1983 and 2017 (Huld *et al.* 2012) from the Satellite Application Facility on Climate Monitoring (CMSAF) database of the European Organisation for the Exploitation of Meteorological Satellites (EUMETSAT).

Agro-meteorological variables

Obtained climate variables were evaluated for the long-term changes in accordance with the duration of the phenological phases of winter wheat. This was done for individual sites and the overall mean across all study sites. In addition, the long-term trend was estimated for the normal calendar year as well as for the periods of the defined hydrological winter (1st November to 30th April) and summer (1st Mai to 31st October). This was intended to provide information on the weather conditions independent of crop phenology.

Crop and drought parameters

To assess crop-related and site-specific developments during the observation period, additional climatic and hydrological variables were calculated from the available meteorological

datasets. First of all, the thermal duration (TD, °Cd) for each phenological phase was calculated after McMaster & Wilhelm (1997) (formula described in the Supplementary Information). The potential evapotranspiration (ETP, mm) for winter wheat crops was calculated after Haude (1954). The formula and the data processing are described in the Supplementary Information. Moreover, the climatic water balance (CWB, mm) as a drought indicator differs largely within Germany and was calculated to estimate the available water supply. It is defined as the difference between the precipitation height and the amount of the ETP.

Adverse weather conditions

Moreover, we accounted the occurrence of adverse weather events in order to evaluate their impact on the yield potential. Due to limitations in the climate projection as daily values based on the available DWD data, we counted the frequency of those days with high precipitation events, those days with potential heat stress impact, and those days with negative CWB and calculated their cumulative numbers for each crop developmental phase and each individual site. We defined high precipitation events in two ways in order to account for all days that may have caused water logging and lodging even in short phases such as SBP or GP in the first place and in particular for those precipitation events that cause severe logging and lodging effects in particular during summer months. Thus, we considered those days with a minimum rainfall of 20 mm in 24 hours as reported and analysed in Gömann *et al.* (2015) and the number of days, which had more than 40 mm of daily rainfall as high rainfall events (Trnka *et al.* 2014; Mäkinen *et al.* 2018). We used 27°C as upper temperature threshold with considerable impact on yield losses due to sterilization of grains of wheat around anthesis (Tashiro & Wardlaw 1989; Mitchell *et al.* 1993), and 31°C as threshold for large detrimental effects around anthesis (Porter & Gawith 1999; Wheeler *et al.* 1996).

Site-specific characteristics

Climate conditions

In order to obtain additional site-specific information of each trial site, the long-term mean annual temperature, precipitation, and CWB were calculated using the HYRAS dataset based on the 30-year reference period 1961-1990 (Supporting Material Figure 18). Mean annual temperatures ranged from 7.8 to 10.6°C at the sites of this study. The average was at 8.9°C and the median at 8.8°C. Mean annual precipitation at the sites varied between 580 and 1110 mm. The average was 774 mm and the median 744 mm. As for the mean annual CWB, the minimum was 198 mm, the maximum 822 mm, the average 465 mm, and the median was at 431 mm.

Each site can be determined by the mean number of stress events during a specific growth phase. For example, based on the number of heat stress days during the generative phase – detected

over the entire observation period – the number of these stress events for each site varied between 1.6 and 3.6 days and was 2.4 days in average.

Soil type

Soil types differ in water and nutrient availability and thus have an impact on the yield potential. Therefore, the soil type was retrieved from the publications at the level of the soil type group according to the German soil classification system – KA5 (Ad-hoc-AG Boden 2005). If not available in the publication, soil type data was obtained from the soil type classification map of the Federal Institute for Geosciences and Natural Resources (BGR) in Germany (Düwel *et al.* 2007). Four soil type groups were identified for the experimental sites in this study: 8 loamy sands, 12 sandy loams, 13 loams, and 10 clayey silts. Locations with loamy soils (loam and sandy loam) are dominant within the dataset over the experimental years from 1958 until 2015, whereas silty soils (clayey silt) and sandy soils (loamy sand) were predominant in the early and mid-1980s.

Soil yield potential

The suitability of a site under agricultural land use and its estimated yield potential is an indicator for the annual productivity of grain yields. Thus, we retrieved soil yield potential for all sites in this study based on the Muencheberg Soil Quality Rating (MSQR) developed by the Leibniz Centre for Agricultural Landscape Research (ZALF) at a global scale (Mueller *et al.* 2010). In brief, this approach evaluates a set of soil describing properties, such as the substrate, rooting depth, topsoil structure, or soil compaction in combination with potential yield effecting hazardous factors that are critical for farming and limit the overall soil quality, such as drought risk, soil depth above solid rock, flooding, or extreme waterlogging regimes. The final scores range from about 0 to 102 points and are displayed on a map that shows the MSQR for cropland in Germany based on the land use stratified soil map of Germany at scale 1:1,000,000. The MSQR for the 43 sites in this study ranged from 31 to 99 points, with a median at 69 and a mean of 67.9 points. In order to divide the research area in relatively poor and relatively good soils, the data set was split at a soil yield potential of 70 points.

Statistical methods and models

General trend analysis – linear and segmented

In order to analyse the development of all obtained phenological, climatic, and agro-climatic time series, data were fitted with ordinary linear regression models (Equation 4) in the first place and depicted using the statistical software R (R Development Core Team 2008). Linear trends and point data were then analysed visually and when trend changes were obvious within the point data, the data was analysed again by segmented piecewise linear regressions (Equation 5) to obtain more

detailed information about these potential trend changes (Piepho & Ogutu 2003; Schabenberger & Pierce 2001).

$$E(y) = a + bx \quad (4)$$

$$E(y) = \begin{cases} a_1 + b_1x; & \text{if } x < x_0 \\ a_2 + b_2x; & \text{if } x > x_0 \end{cases} \quad (5)$$

where the parameters of the model are a_1 , a_2 , b_1 , b_2 and x_0 .

There is an implicit constraint that the regression lines must intersect at $x = x_0$. This can be done by removing one parameter and explicitly introduce x_0 as a parameter:

$$a_1 + b_1x_0 = a_2 + b_2x_0, \quad (6)$$

which can be transformed into:

$$a_2 = a_1 + b_1x_0 - b_2x_0 \quad (7)$$

and allows removing a_2 from the list of parameters to be estimated, leaving the parameters a_1 , b_1 , b_2 and x_0 .

Segmented plateau analysis for maximum yield and nitrogen development

To test whether the yield and nitrogen development result in any kind of levelling, data were plotted against year using linear regressions with an upper plateau (Equation 7) – graphically depicted as a rising line or curve followed by a plateau. The ‘linear plateau’ model corresponds to a special case of the segmentation approach with $b_2 = 0$.

The segmentation analysis is based on an iterative approach where a breakpoint value is estimated based on non-linear least squares (Mugge 2003, 2008). The initial parameters were derived from values of a pre-fitted ordinary linear model. The advantage of this type of fit is that it can estimate the year of change or transition to plateau. The significances of these trends were calculated with the t -test. Only those phenological and climatic changes with significant trends were chosen for the final discussion.

General decoupling - dissecting genetic from non-genetic sources

Here we explicitly point out that the dataset used for this analysis differs from the dataset used to investigate phenology and climate trends (Figure 6). A subset of years with experimental data, which include cultivar information, was established. Next, all data about the beginning of the phenological stages, the duration of phenological phases, and the agro-climatic variables were

attached for those experimental years where it was possible to obtain this information. However, this dataset faces certain limitations. First, the true phenology of the cultivars used in the fertilization trials may differ from the phenological information obtained from the DWD. Second, agro-climatic information was only available for those years where weather and phenological data was available and adverse weather events occurred. Moreover, effects of individual agro-climatic conditions are considered to occur only when they vary in their variability and error. It also needs to be considered that cultivars largely vary in occurrence, duration over time, and in location. Also, the applied N-levels vary between experiments, over time, and in location.

To overcome the uncertainty of such unbalanced datasets, we used well established statistical mixed-effect models, which take the large number of environmental and non-environmental co-variates into account. These models include a pre-determined number of independent factors treated as random effects. Moreover, to disentangle the main effects that influence the evolution of winter wheat yields and to quantify the impact of an individual agro-climatic factor, a varying number of fixed effects can be included in these models.

Grain yield is a function of genetic and non-genetic conditions and thus, a standard three-way model after Laidig *et al.* (2008) was established:

$$y_{ijk} = \mu + G_i + L_j + Y_k + LY_{jk} + GL_{ij} + GY_{ik} + GLY'_{ijk} \quad (8)$$

where y_{ijk} represents the mean yield of the i^{th} genotype in the j^{th} location and the k^{th} year, μ is the overall mean, G_i is the main effect of the i^{th} genotype, L_j is the main effect of the j^{th} location, Y_k is the main effect of the k^{th} year, LY_{jk} is the jk^{th} location×year interaction effect, GL_{ij} is the ij^{th} genotype×location interaction effect, GY_{ik} is the ik^{th} genotype×year interaction effect, GLY'_{ijk} is the residual of the ijk^{th} genotype×location×year interaction effect and error of the mean. As in Piepho *et al.* (2014), we assume that all effects except μ , G_i and Y_k are random and independent with constant variance, following a normal distribution. Thus, we integrated genetic and non-genetic time trends as fixed regression components into the model. G_i was then estimated as the following regression term based on the year of release:

$$G_i = \beta r_i + H_i \quad (9)$$

where β is the fixed regression coefficient for the genetic trend, r_i is the first year of testing (year of release) for the i^{th} cultivar, and H_i is the random deviation of G_i from the genetic trend line. If there was a linear non-genetic time trend, we modelled Y_k as:

$$Y_k = \gamma t_k + Z_k \quad (10)$$

where γ is the fixed regression coefficient for the non-genetic trend, t_k is the continuous covariate for the experimental year, and Z_k is a random residual. Both, β and γ quantify the genetic and non-genetic trends per year in the same units as y_{ijk} .

In this study, we made use of data from crops grown under optimum N-fertilization levels and full crop protection. Hence, changes in agronomic practices can be considered to play a minor role and the time effect predominantly represents the effect of climatic changes. To evaluate whether the overall climate change has to be accounted for as linear or non-linear regression terms in the mixed model, a pre-analysis was carried out, modelling the time effect firstly with a linear relationship and secondly with a quadratic relationship. The latter should account for the potential yield levelling. While the linear relationship was significant ($p < 0.001$) in the pre-test, the quadratic was not ($p = 0.69$). Hence, the time trend was included as a linear function and a potential yield levelling cannot be traced back to climate change only.

Specific decoupling – dissecting individual agro-climatic trends

We further investigated whether an agronomic variable has a specific impact on winter wheat yield development. While we assume that γ in equation (10) represents all climatic changes over time combined, we assume that Z_k in equation (10) neither represents the inter-year variability of a single agro-climatic variable appropriately nor does it account for the effect of a climatic factor at a specific location. Thus, in order to simultaneously model inter-year and inter-location variation due to climatic or agronomic variables, we modified the model by regressing LY_{jk} on these variables:

$$LY_{jk} = \alpha s_{jk} + C_{jk} \quad (11)$$

where α is the fixed regression coefficient for the respective climatic or agronomic covariate, s_{jk} is the specific value of the covariate for the k^{th} year and the j^{th} location, and C_{jk} is a random residual location×year interaction.

Crop growth and yields not merely depend on weather effects during the growing season, but also on the site and soil conditions, which, hence, should be considered more explicitly. To account for such disparities among the experimental sites, the variance estimates were additionally adjusted for their location attributes (L_j) yield potential and soil type, and each tested within in separate models as:

$$L_j = \delta u_j + S_j \quad (12)$$

where L_j is the main effect of the j^{th} location, δ is the fixed regression coefficient for the respective spatial attribute or site condition (e.g., yield potential), u_j is the specific value of the attribute for the j^{th} location, and S_j is the random deviation from the trend.

Estimating the intensity of individual agro-climatic variables on yield variation

For each independent variable assessed, the total variance, defined as the sum of variance components of all random effects, was estimated twice: once without and once with the agro-climatic variable included. The model without the factor is henceforth called M_{-x} and the model with the specific factor is called M_{+x} , where M is the model, x describes the specific factor, and “-“ and “+“ refer to the absence or presence of the factor, respectively. In both models, trend components in G_i , Y_k , and L_j were modelled using regression equations (9), (10), and (12), respectively. In M_{+x} , however, the spatio-temporal covariate s_{jk} was modelled additionally as per equation (11). The sum of all variance components estimated in M_{+x} ($Var_y(M_{+x})$) was subtracted from the corresponding sum estimated in M_{-x} and expressed as a percentage of that of M_{-x} ($Var_y(M_{-x})$) (Equation 13), describing the impact of a single climatic or agronomic factor on the overall yield development. This corresponds to the coefficient of determination (R^2) for generalized linear mixed models as introduced by Piepho (2019):

$$\%Var_y = \frac{Var_y(M_{-x}) - Var_y(M_{+x})}{Var_y(M_{-x})} \cdot 100 \quad (13)$$

In order to assess the impact of climatic or agronomic factors on yield development under different site-specific conditions, this procedure was repeated for subsets of two groups of soil type and two groups of soil yield potential. For this purpose, soils of sandy loam and loamy sand were combined and addressed as sandy soils, and loams and clayey silts were addressed as loamy soils. The threshold for the two groups of different yield potential was the median yield potential (70) across the study sites. For further analysis, the agro-climatic variables were also tested for interaction with the time effect.

Adjusting trends of agro-climatic covariates

To compare the slope for an agro-climatic variable (α) with the overall time trend (γ) and the genetic time trend (β), α was multiplied by the covariate’s slope in an ordinary regression on time over the entire observation period (b , from equation 4) to yield an adjustment climate trend:

$$\alpha_{adj} = \alpha \cdot b \quad (14)$$

Results

Yield development as a result of soil type and site-specific yield potential

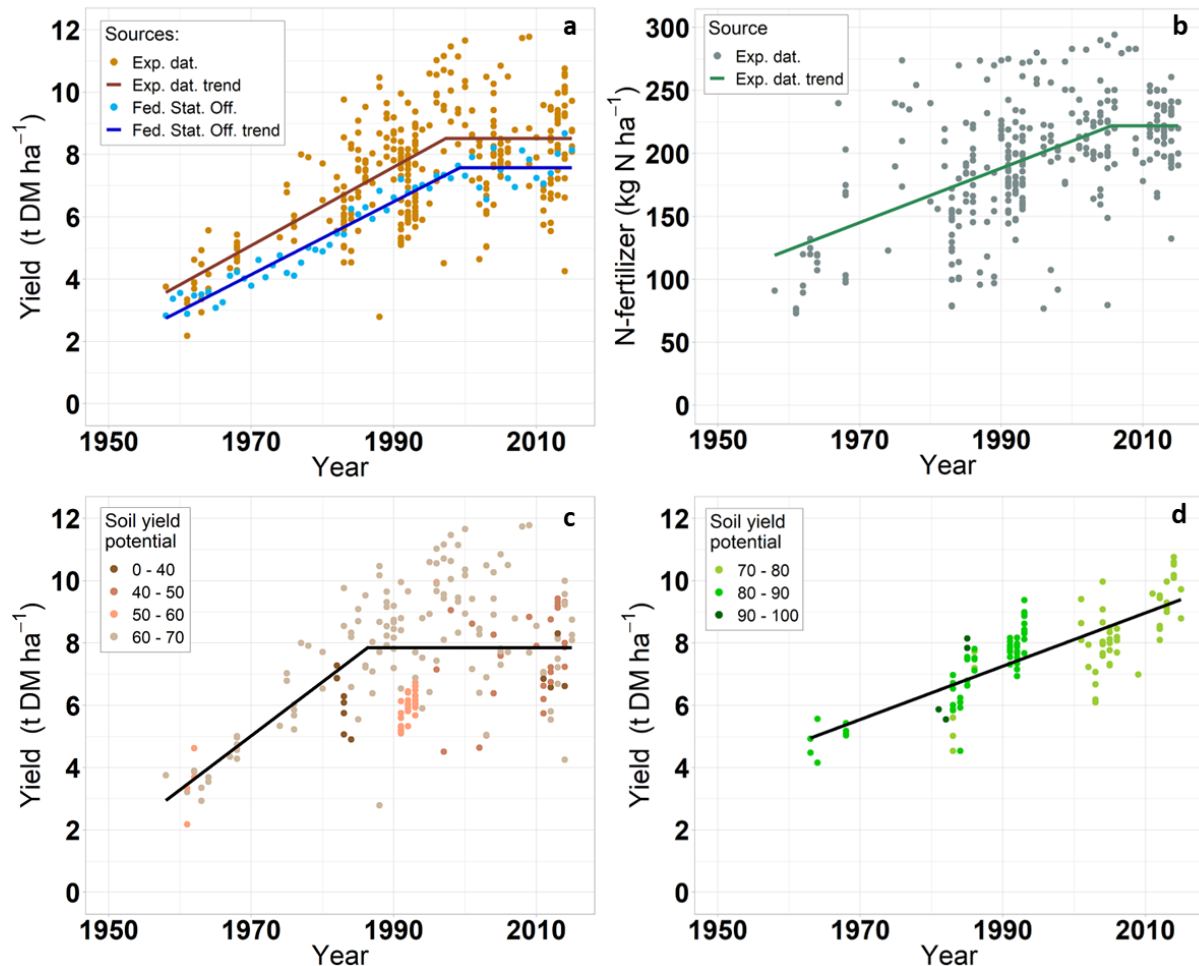


Figure 9: Grain yield development (as dry matter content) of winter wheat and nitrogen fertilization dosages across the study sites in Germany between 1949 and 2016. (a), Overall grain yield development. Data points refer to the derived experimental values (Exp. dat.) as described in Methods and to mean values of the Federal Statistical Office of Germany (Fed. Stat. Off.) The blue line visualizes the development of the official statistical data and the brown line shows the yield development of the experimental data. (b), Development of nitrogen fertilization dosages. (c), Yield development of sites with yield potential lower than 70 points. (d), Yield development of sites with a yield potential of more than 70 points. The yield potential classification of the sites is based on the Muencheberg Soil Quality Rating (Mueller et al. 2010) (MSQR, Methods)

Over all the trials analysed in this study, between 1958 and 1997 the annual yield of winter wheat increased on average by $0.12 \text{ t DM ha}^{-1} \text{ yr}^{-1}$ and reached a plateau at $8.35 \text{ t DM ha}^{-1}$ (Figure 9a, equation coefficients in Table 1). This corresponds to average wheat yields in Germany recorded by the Federal Statistical Office which also show increases starting in the late 1950s until the end of the 1990s. From around 1997 onwards, no further yield increase was observed in our trial data, which also corresponds with the official data and with other studies which point out a yield levelling

starting in the late 1990s (Brisson *et al.* 2010; Grassini *et al.* 2013). In parallel, the optimal nitrogen fertilizer dosage increased by about 2 kg N ha⁻¹ yr⁻¹ between 1958 and 2006 (Figure 9b) with no further increase after 2006.

At sites with relatively low yield potential (< 70 quality points, Methods), yield levelling occurred about a decade earlier compared to the average of all sites (Figure 9c), while for sites with relatively high yield potential no stagnation was revealed. Still, our data indicate that yield levelling occurred at sites with light soils (sandy loams and loamy sands) as well as at sites with heavy soils (clayey silts and loams) (Supporting Information Figure 15). The optimal nitrogen dosage showed a levelling for all soils and both yield potential groups (Supporting Information Figure 16a - d).

Table 1: Regression coefficients of winter wheat yield (t DM ha⁻¹) and nitrogen fertilization (kg N ha⁻¹) trends estimated by segmented regression line analysis and simple linear models (equation 4-7). Heavy soils refer to loams and clayey silts and light soils to sandy loams and loamy sands (Methods). Low yield potential soils are soils with MSQR below 70 points and high yield potential soils with MSQR above 70 points (Methods). SE describes the standard error of the fitted parameter.

Dependent variable	Subset	n	Term	Estimate	SE	t value	Sign.
Winter wheat yield	All experimental sites	328	Intercept	-231	0.12	-11.43	<0.001
			Trend	0.12	0.01	11.77	<0.001
			Breakpoint	1997.6	1.7	1179.9	<0.001
	Low yield potential	211	Intercept	-336.2	50.7	-6.6	<0.001
			Trend	0.17	0.03	6.75	<0.001
			Breakpoint	1986.3	2.3	846.5	<0.001
	High yield potential	117	Intercept	-163	12.5	-13	<0.001
			Trend	0.08	0.01	13.6	<0.001
			Breakpoint	1996.5	1.4	1350.9	<0.001
	Heavy soils	151	Intercept	-258.5	17.4	-14.9	<0.001
			Trend	1.34	0.01	15.24	<0.001
			Breakpoint	1996.5	1.4	1350.9	<0.001
	Light soils	177	Intercept	-396.3	104.3	-3.8	<0.001
			Trend	0.2	0.05	3.86	<0.001
			Breakpoint	1983	3.	601.4	<0.001
Federal Statistic Office	67	Intercept	-226.1	10.5	-21.6	<0.001	
		Trend	0.12	0.005	22.1	<0.001	
		Breakpoint	1999.3	1.41	1421.7	<0.001	

Nitrogen fertilization	All sites	328	Intercept	-4104.4	438.9	-9.4	<0.001
			Trend	2.16	0.22	9.78	<0.001
			Breakpoint	2005.6	3	667.4	<0.001
	Heavy soils	151	Intercept	-4235.5	441.6	-9.6	<0.001
			Trend	2.22	0.22	10	<0.001
			Breakpoint	2007.6	3.6	557.3	<0.001
	Light soils	177	Intercept	-3877.3	960.3	-4	<0.001
			Trend	2.04	0.48	4.24	<0.001
			Breakpoint	2002.3	4.7	429.1	<0.001
	Low yield potential	211	Intercept	-3815.7	632.9	-6	<0.001
			Trend	2.01	0.32	6.33	<0.001
			Breakpoint	2003.5	4.2	472.4	<0.001
	High yield potential	117	Intercept	-7144.1	825	-8.7	<0.001
			Trend	3.68	0.41	8.87	<0.001
			Breakpoint	1997.2	1.9	1025.6	<0.001

Earlier occurrence of wheat growth stages and shortened development phases except for stem elongation

Besides agronomic and soil factors, weather conditions during the whole growing season and the occurrence of severe weather events during sensitive crop growth phases significantly affected crop development and yields. Altogether, between 1951 and 1968 the sowing dates of winter wheat shifted to nearly 7 days later, while for the period 1969 until 2015 a shift towards earlier dates by 12.6 days is documented (Figure 10a, equation coefficients in Table 2). Yet, there was a strong geographical heterogeneity, and sowing tended to shift to earlier dates by up to 6 days per decade at North German sites, whereas South German sites showed inconsistent patterns of sowing dates (± 2 days per decade) during the same period (Supporting Information Figure 17). A similar pattern as for the overall trend in sowing was found for the dates of emergence ($r^2 = 0.88$ between sowing and emergence dates) and of heading ($r^2 = 0.34$ between sowing and heading dates). For both stages, the change from later dates towards earlier dates occurred around 1970. Harvest dates shifted to 26 days later between 1951 and 1961. Afterwards and until 2015, a shift towards earlier harvests by approximately 17 days occurred. Between 1961 and 2015, the onset of stem elongation changed by 24 days towards earlier dates and estimated hard dough occurred 21 days earlier in 2015 than in 1979. The growth duration of winter wheat was shortened by more than two weeks, which almost equally affected the vegetative and generative phase (Figure 5b). Within the vegetative phase, contrasting patterns were revealed for individual development stages. While the leaf development phase was shortened by 16 days between 1951 and 1974, the stem elongation phase was prolonged

by nearly two weeks (3.7 days per decade) between 1951 and 1987. Beyond 1974 and 1987, no further changes in the duration of leaf development and stem extension, respectively, were detected. Expressed in thermal duration (Methods), the vegetative phase of winter wheat was extended by 81 °Cd during the entire 55 years of observation time, whereas the generative phase was reduced by 72 °Cd (Figure 10c). The stem elongation phase was prolonged by 134 °Cd in the period from 1951 to 1999, whereas it was reduced by 85 °Cd between 1999 and 2006. From 1952 to 1979, the leaf development phase was reduced by 126 °Cd.

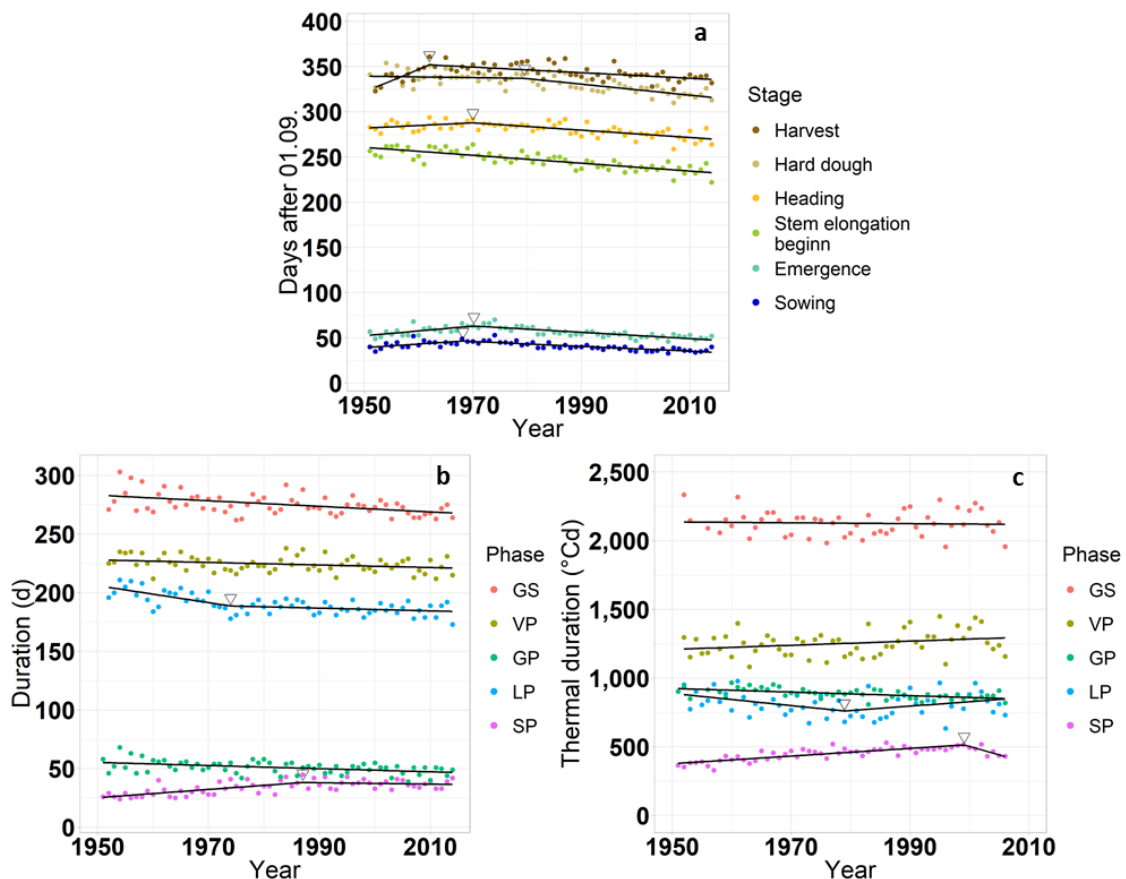


Figure 10: Estimated phenology trends of winter wheat across the study sites between 1951 and 2015. (a), Average days of sowing, harvest, and the actual crop phenological stages (emergence, begin of stem elongation, heading, and hard dough) after the 1st of September. Average duration (b) and thermal duration (c) of the entire growing season (GS) divided into the generative phase (GP) and vegetative phase (VP). The latter comprises the leaf development phase (LP) and the stem elongation phase (SP). Inverse triangles indicate trend changes.

Table 2: Regression coefficients of the linear and segmented regression analysis of the phenological beginning (days after Sep 1st) and duration (d) of winter wheat development

Stages and phases	Term	Estimates	SE	t value	P value
Sowing	Intercept	-743.6	245.1	-3.033	0.004
	Trend part 1	0.401	0.125	3.209	0.002
	Trend part 2	-0.668	0.129	-5.189	<0.001
	Breakpoint	1968.2	2.254	0	<0.001
Emergence	Intercept	-991.5	252.8	-3.923	<0.001
	Trend part 1	0.535	0.129	4.152	<0.001
	Trend part 2	-0.886	0.135	-6.568	<0.001
	Breakpoint	1970.2	2	0	<0.001
Stem elongation begin	Intercept	1113.4	75.9	14.676	<0.001
	Trend	-0.437	0.038	-11.426	<0.001
Heading	Intercept	-296.5	403.4	-0.735	0.465
	Trend part 1	0.297	0.206	1.442	0.155
	Trend part 2	-0.703	0.215	-3.265	0.002
	Breakpoint	1970	3.995	0	0.001
Hard dough	Intercept	500.9	295.7	1.694	0.095
	Trend part 1	-0.083	0.15	-0.55	0.584
	Trend part 2	-0.529	0.188	-2.807	0.007
	Breakpoint	1979.5	6.442	0	0.008
Harvest	Intercept	-4529.9	1232.9	-3.674	0.001
	Trend part 1	2.488	0.63	3.95	<0.001
	Trend part 2	-2.797	0.633	-4.419	<0.001
	Breakpoint	1962	1.489	0	<0.001
Growing Season	Intercept	746.5	106.8	6.99	<0.001
	Trend	-0.238	0.054	-4.411	<0.001
Leaf development	Intercept	1654.3	246.4	6.713	<0.001
	Trend part 1	-0.743	0.126	-5.916	<0.001
	Trend part 2	0.640	0.138	4.650	<0.001
	Breakpoint	1974	3.241	0	<0.001
Stem elongation	Intercept	-674.5	88.1	-7.656	<0.001
	Trend part 1	0.359	0.045	8.017	<0.001
	Trend part 2	-0.433	0.078	-5.555	<0.001
	Breakpoint	1987	3.178	0	<0.001
Vegetative phase	Intercept	438.8	85.3	5.147	<0.001
	Trend	-0.108	0.043	-2.513	0.015
Generative phase	Intercept	316.2	64.7	4.888	<0.001
	Trend	-0.134	0.033	-4.099	<0.001

Increasing temperatures during the vegetative growth period

Across the trial locations, the annual mean temperature increased on average by $0.024^{\circ}\text{C yr}^{-1}$ and was nearly 1.3°C higher in 2006 than in 1951 (Supporting Information Figure 18, equation coefficients in Table 3). The same trend was found for the mean annual minimum and maximum temperatures. The temperature increase was accompanied by an increase of the mean annual potential evapotranspiration by 1.6 mm yr^{-1} , summing up to 85 mm over the entire observation period of 55 years. However, mean annual precipitation and mean annual climatic water balance did not change significantly, even though the latter showed a negative trend indicating dryer conditions.

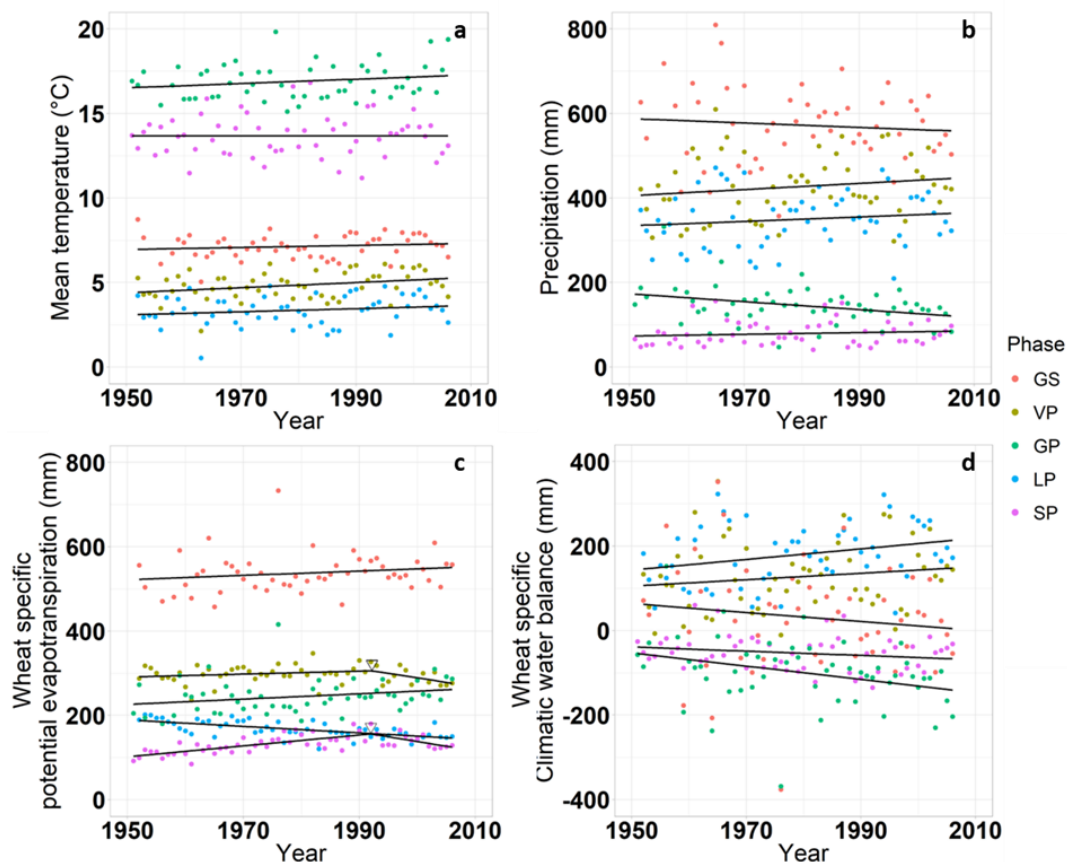


Figure 11: Climate trends within phenological growth phases of winter wheat across the study sites in Germany. Trends are shown for the growing season (GS), vegetative phase (VP), leaf development phase (LP), generative phase (GP), and stem elongation phase (SP). (a), Mean temperature between 1951 and 2014. (b), Precipitation between 1951 and 2014. (c), Wheat specific potential evapotranspiration between 1951 and 2006. (d), Wheat-specific climatic water balance between 1951 and 2006

Climate change became apparent not only by enhanced annual mean temperatures but also by higher mean temperatures during the vegetative phase of winter wheat (Figure 11a, equation coefficients in Table 3). Temperatures in this phase were approximately 0.8°C higher in 2006 than in 1951. The vegetative phase reflects in the pattern of a shortened total duration in days (Figure 10b), but also of a prolongation of the thermal duration (Figure 10c). The reduced duration of the

generative phase (both, in days and thermal) and a reduced amount of total precipitation during that phase by approximately 52 mm (Figure 11b) may have had negative effects on the overall grain-filling period and consequently on winter wheat yields. Moreover, a change was observed for the potential evapotranspiration during this phase (Figure 11c) as well as for the climatic water balance by 86 mm (Figure 11d). An increase of the potential evapotranspiration was additionally detected for the stem elongation phase from 1951 onwards before it started to decrease between around 1992 and 2006. By contrast, the potential evapotranspiration during the leaf development phase decreased constantly throughout the entire observation period. The vegetative phase apparently, was dominated by the course of evapotranspiration during the stem elongation phase. It is noteworthy that between 1998 and 2006 TD during stem elongation decreased by about 40 °Cd, and the trend of potential evapotranspiration turned from an increase to a decrease in 1992, which lasted until 2006.

Table 3 Regression coefficients for the linear and segmented trends of climatic factors during phenological phases of winter wheat. P values refer to the slope coefficient

Climate factor	Unit	Stages and phases	Period	Intercept	Trend	P value
Thermal duration	°Cd	Growing season	1952-2006	2735.9	-0.307	0.711
		Vegetative phase	1952-2006	-1742.5	1.504	0.045
		Generative phase	1951-2006	3485.8	-1.313	<0.001
		Leaf development	1952-1979	9999.9	-4.671	0.011
			1979-2006	-6214.4	3.522	0.099
		Stem elongation	1951-1999	-5055.1	2.786	<0.001
			1999-2006	24898.9	-12.198	0.013
Mean temperature	°C	Growing season	1952-2006	-4.8	0.006	0.342
		Vegetative phase	1952-2006	-25.2	0.015	0.024
		Generative phase	1951-2006	-8.4	0.013	0.166
		Leaf development	1952-2006	-14.9	0.009	0.218
		Stem elongation	1951-2006	13.5	0	0.992
		Calendar year	1951-2006	-39.1	0.024	<0.001
Maximum temperature	°C	Growing season	1952-2006	-7.2	0.009	0.175
		Vegetative phase	1952-2006	-21.5	0.015	0.023
		Generative phase	1951-2006	-13.5	0.018	0.14
		Leaf development	1952-2006	-8.4	0.008	0.309
		Stem elongation	1951-2006	16.8	0.001	0.931
		Calendar year	1951-2006	-37.3	0.025	<0.001

Minimum temperature	°C	Growing season	1952-2006	-10.9	0.007	0.316
		Vegetative phase	1952-2006	-35.6	0.019	0.013
		Generative phase	1951-2006	-0.3	0.006	0.347
		Leaf development	1952-2006	-29.5	0.015	0.078
		Stem elongation	1951-2006	8.1	0	0.998
		Calendar year	1951-2006	-43.3	0.024	<0.001
		Precipitation	mm	Growing season	1952-2006	1594.6
Vegetative phase	1952-2006			-1017.4	0.73	0.245
Generative phase	1951-2006			2000.3	-0.937	0.018
Leaf development	1952-2006			-683.6	0.522	0.347
Stem elongation	1951-2006			-320.7	0.202	0.393
Calendar year	1951-2006			-859.8	0.815	0.371
Potential evapotranspiration	mm			Growing season	1952-2006	-488.9
		Vegetative phase	1952-1992	-486.9	0.399	0.153
			1992-2006	4979	-2.345	0.041
		Generative phase	1951-2006	-1003.6	0.631	0.072
		Leaf development	1952-2006	1687.4	-0.768	<0.001
		Stem elongation	1951-1992	-2571.6	1.371	<0.001
			1992-2006	4678.5	-2.27	0.024
Calendar year	1951-2006	-4719.1	2.758	<0.001		
Climatic water balance	mm	Growing season	1952-2006	2131.8	-1.06	0.355
		Vegetative phase	1952-2006	-1377.4	0.76	0.277
		Generative phase	1951-2006	3003.9	-1.567	0.023
		Leaf development	1952-2006	-2301.4	1.254	0.034
		Stem elongation	1951-2006	935.1	-0.499	0.14
		Calendar year	1951-2006	3852.3	-1.939	0.2
		Global radiation sum	W m ⁻²	Growing season	1983-2015	-4151.6
Vegetative phase	1983-2015			-78.7	0.599	0.85
Generative phase	1983-2015			-4016.5	2.351	0.271
Leaf development	1983-2015			430.3	0.124	0.967
Stem elongation	1983-2015			-171.5	0.311	0.898
Calendar year	1951-2006			-19682.9	11.179	0.099

Climatic variation explained yield variability the most

Differentiating the results of the main influential factors on yield development from the specific agro-climatic effects, the general findings are discussed first and the individual climatic factors thereafter. The effect of the three main influential factors – ‘genotype’ (genetic variation over time), ‘location’ (covering all regional variation), and ‘time’ (comprising all changes along the timeline except those caused by altering genotypes) (Methods) – as well as their interactions highlight that the genotype effect explained about 4% of the variability of the yield development and therefore was comparatively low (Figure 12). The effect of the location on crop yield explained about 22% of the total variance. Nearly 17% of the variance was explained by the location×time interaction, whereas the genotype × time interaction and the genotype × location interaction either had no or a very low impact of about 1%. The three-way genotype × location × time interaction accounted for 5% of the total variance. However, the variability of the long-term yield development was predominantly explained by more than 50% of the total of the factors summarized as time effect.

Changes in agronomic practices only play a minor role since data from crops grown under optimum N-fertilization levels and full crop protection were considered. Thus, the time effect mainly represents climatic changes.

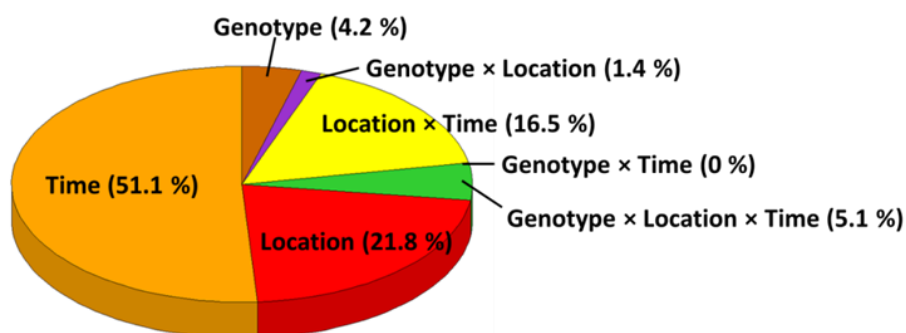


Figure 12: Proportions of variance explained by the main influential factors (genotype, location, and time) and their interactions in German long-term yield data. Results indicate a relative strong variance of all factors that changes along the timeline (time effect) except those caused by altering genotypes, which were relatively low. Moderate variabilities were only found for the location effect and the location × time interaction. Other interaction effects were rather low with no effect for the genotype × time interaction

Elevated temperatures, heat stress, and drought-affected yield development

In order to quantify the influence of an individual agro-climatic factor in terms of explained variance on yield development, we modified our model by including a fixed regression term for that particular agro-climatic variable (Methods). The estimated variances explain the importance of a

The trend of the agro-climatic factors on yield development (Table 5), however, may vary from their magnitude of the explained variance. As for the genetic and non-genetic (time) effects, the trends were positively related to yield development at all sites combined and increased in average by about $0.044 \text{ t ha}^{-1} \text{ yr}^{-1}$ and $0.049 \text{ t ha}^{-1} \text{ yr}^{-1}$, respectively. The individual agro-climatic variables, however, were mainly negatively associated with yield (except for the mean global radiation during the stem elongation phase). For instance, while the mean temperature during the generative phase ($^{\circ}\text{C}$) reduced yields by about $-0.278 \text{ t ha}^{-1} \text{ }^{\circ}\text{C}^{-1}$ temperature increase, the effect over time was comparatively low with $-0.004 \text{ t ha}^{-1} \text{ yr}^{-1}$.

Table 4 Estimated explained variance (%) of the agro-climatic variables (units in parentheses) on winter wheat yield development between 1958 and 2006 across the study sites in Germany. All explained variances are estimated after accounting for the genetic and non-genetic time trends. Low yield potential sites refer to sites with quality points between 0 and less than 70, while high yield potential sites refer to quality points between 70 and 100. (Methods)

Phenological phase or stage	Agro-climatic variable	Description	Sites					
			Explained variance (%)			n		
			All	Low yield potential	High yield potential	All	Low yield potential	High yield potential
Growing season	GS_HS27_n	Number of heat stress days with Tmax > 27°C	22	24.7	16.1	236	141	95
	GS_HS31_n	Number of heat stress days with Tmax > 31°C	13.1	15.3	22.3	236	141	95
	GS_HS27_Tm_n	Number of heat stress days with Tmean > 27°C	4.3	3.7	2.1	236	141	95
	GS_HS27_sum	Cumulative heat stress temperature with Tmax > 27°C (°C)	22.6	25.2	17.4	236	141	95
	GS_HS31_sum	Cumulative heat stress temperature with Tmax > 31°C (°C)	13.4	15.4	23.3	236	141	95
	GS_HS27_Tm_sum	Cumulative heat stress temperature with Tmean > 27°C (°C)	4.2	3.6	2.1	236	141	95
	GS_GR_mean	Daily global radiation means (W m ⁻² d ⁻¹)	-	-	7.4	-	-	87
	GS_ETPm	Daily potential evapotranspiration means (mm)	12.2	13.7	5.3	231	136	95
	GS_ETPs	Total potential evapotranspiration sum (mm)	11.1	15.8	3.2	231	136	95
	GS_CWBneg_n	Number of days with negative climatic water balance	2.4	1.8	-	236	141	-
	GS_CWBm	Daily climatic water balance mean (mm)	2.7	5.1	-	231	136	-
	GS_CWBs	Total climatic water balance sum (mm)	2.9	5.3	-	231	136	-
	GS_TD	Thermal duration (°Cd)	2.3	4.5	-	231	136	-
	GS	Duration (d)	6.3	8.7	-	233	138	-
Generative phase	GP_T_mean	Mean temperature (°C)	15.9	18.6	12	229	134	95
	GP_T_max	Maximum temperature (°C)	18	22.5	11.4	232	137	95
	GP_HS27_n	Number of heat stress days with Tmax > 27°C	24.8	28.8	15.5	236	141	95

	GP_HS31_n	Number of heat stress days with Tmax > 31°C	16.7	21	24.8	236	141	95
	GP_HS27_Tm_n	Number of heat stress days with Tmean > 27°C	4.3	3.7	2.1	236	141	95
	GP_HS27_sum	Cumulative heat stress temperature with Tmax > 27°C (°C)	25.5	29.5	17.1	236	141	95
	GP_HS31_sum	Cumulative heat stress temperature with Tmax > 31°C (°C)	16.9	21.1	25.7	236	141	95
	GP_HS27_Tm_sum	Cumulative heat stress temperature with Tmean > 27°C (°C)	4.2	3.6	2.1	236	141	95
	GP_GR_sum	Total global radiation sum (W m ⁻²)	-	1.2	4.7	-	108	87
	GP_ETPm	Daily potential evapotranspiration means (mm)	18.2	26.1	3.8	229	-	95
	GP_ETPs	Total potential evapotranspiration sum (mm)	11.1	16.4	6	229	-	95
	GP_CWBm	Daily climatic water balance mean (mm)	2.9	7.5	-	229	-	-
	GP_CWBs	Total climatic water balance sum (mm)	-	3.1	-	-	134	-
	GP_TD	Thermal duration (°Cd)	-	-	2.9	-	95	-
	GP	Duration (d)	4.3	11	-	232	137	-
Vegetative phase	VP_T_mean	Mean temperature (°C)	2	-	-	231	-	-
	VP_HR20_n	Number of days with precipitation > 20 mm (mm)	2.3	-	-	236	-	-
	VP_HR20_sum	Cumulative rainfall amounts of days with precipitation > 20mm (mm)	2.8	-	-	236	-	-
	VP_GR_mean	Daily global radiation means (W m ⁻²)	-	1.1	-	-	108	-
	VP_CWBneg_n	Number of days with negative climatic water balance	3.7	-	-	236	-	-
	VP_TD	Thermal duration (°Cd)	2.1	-	3.6	231	-	95
Leaf development phase	LP_T_mean	Mean temperature (°C)	3	-	-	231	-	-
	LP_GR_mean	Daily global radiation means (W m ⁻²)	5.6	2	30.4	195	108	87
	LP_GR_sum	Cumulative global radiation amount (W m ⁻²)	1.5	-	9.3	195	-	87
	LP_P_mean	Daily precipitation means (mm)	2.9	-	-	231	-	-

	LP_CWBm	Daily climatic water balance mean (mm)	3.1	-	-	231	-	-
	LP_CWBneg_n	Number of days with negative climatic water balance	3.3	4.3	-	236	141	-
	LP_TD	Thermal duration (°Cd)	2.7	-	-	231	-	-
	LP	Duration (d)	2.6	3.8	-	233	138	-
Stem elongation phase	SP_HS27_n	Number of heat stress days with Tmax > 27°C	-	-	1.6	-	-	95
	SP_HS27_sum	Cumulative heat stress temperature with Tmax > 27°C (°C)	-	-	1.8	-	-	59
	SP_GR_mean	Daily global radiation means (W m ⁻²)	3.9	-	6.9	196	-	87
	SP_P_mean	Daily precipitation means (mm)	-	-	2.5	-	-	95
	SP_P_sum	Total precipitation sum (mm)	3.3	-	5.5	231	-	95
	SP_HR20_n	Number of days with precipitation > 20 mm	3.3	-	-	236	-	-
	SP_HR20_sum	Cumulative rainfall amounts of days with precipitation > 20 mm	3.5	-	-	236	-	-
		SP_CWBm	Daily climatic water balance mean (mm)	-	-	2.7	-	-
	SP_CWBs	Total climatic water balance sum (mm)	-	-	6.1	-	-	95
Sowing	SD	Day of year	9.1	11.2	6.1	233	138	95
Emergence	ED	Day of year	9	6.6	5	233	138	95
Hard dough	HDD	Day of year	4.4	9.7	-	234	139	-
Harvest	HVD	Day of year	2.8	8.9	-	233	138	-

Table 5 Coefficient estimates of the fixed effects (genotype, time, and selected agro-climatic variables as found in Fig. 4) in the mixed-effect models on the yield development over time. SE denotes the standard error, DF the degree of freedom, n the number of observations, and p the significance of the estimates of each model. Values in parentheses describe the trend of the appropriately selected agro-climatic variable adjusted by its trend over time (Methods). Low yield potential sites refer to sites with quality points between 0 and less than 70, while high yield potential sites refer to quality points between 70 and 100. (Methods)

Sites	Model	n	Effect	Estimate	SE	DF	t value	p
All	1	229	Intercept	-70.674	17.689	53.5	-3.996	<0.001
			Genotype	0.042	0.009	52.6	4.658	<0.001
			Time	0.065	0.014	91.9	4.606	<0.001
			Mean temperature during the generative phase (°C)	-0.278 (-0.004)	0.09	36.2	-3.1	0.0037
	2	232	Intercept	-70.987	17.587	53.2	-4.036	<0.001
			Genotype	0.042	0.009	52.4	4.721	<0.001
			Time	0.064	0.014	97	4.617	<0.001
			Maximum temperature during the generative phase (°C)	-0.228 (-0.004)	0.068	44.9	-3.329	0.0017
	3	236	Intercept	-71.15	17.671	53.6	-4.026	<0.001
			Genotype	0.04	0.009	53.6	4.472	<0.001
			Time	0.066	0.014	99.4	4.793	<0.001
			Number of days with Tmax > 27°C during the generative phase	-0.098 (-0.0005)	0.021	66.2	-4.547	<0.001
	4	236	Intercept	-67.226	17.787	56.3	-3.78	<0.001
			Genotype	0.038	0.009	56.3	4.195	<0.001
			Time	0.063	0.014	93.8	4.437	<0.001
			Number of days with Tmax > 31°C during the generative phase	-0.291 (-0.001)	0.074	77.9	-3.92	<0.001
5	196	Intercept	-111.275	22.055	21.8	-5.045	<0.001	
		Genotype	0.06	0.011	21.7	5.412	<0.001	
		Time	0.065	0.027	51.9	2.44	0.0181	

		Global radiation mean during the growing season ($W m^{-2}$)	-0.027 (-0.0006)	0.024	78.2	-1.141	0.2572
6	195	Intercept	-111.901	22.138	21.6	-5.055	<0.001
		Genotype	0.061	0.011	21.6	5.409	<0.001
		Time	0.057	0.026	43.2	2.217	0.0319
		Global radiation mean during the leaf development phase ($W m^{-2}$)	-0.037 (0.0031)	0.022	64.1	-1.671	0.0996
7	196	Intercept	-107.707	22.308	21.5	-4.828	<0.001
		Genotype	0.057	0.011	21.5	5.11	<0.001
		Time	0.038	0.027	42.1	1.404	0.1678
		Global radiation mean during the stem elongation phase ($W m^{-2}$)	0.006 (0.002)	0.005	67.6	1.196	0.236
8	231	Intercept	-67.273	17.884	55.1	-3.762	<0.001
		Genotype	0.038	0.009	55	4.213	<0.001
		Time	0.062	0.015	95.2	4.164	<0.001
		Cumulative precipitation amount during the stem elongation phase (mm)	-0.003 (-0.006)	0.002	88.6	-1.326	0.1874
9	133	Intercept	-68.859	17.779	55.7	-3.873	<0.001
		Genotype	0.027	0.011	39.9	2.447	0.0189
		Time	0.063	0.018	89.2	3.443	<0.001
		Cumulative precipitation amount of days with precipitation > 20 mm during the vegetative phase (mm)	-0.013 (-0.0007)	0.005	54.3	-2.747	0.0081
10	229	Intercept	-72.312	17.656	54.3	-4.096	<0.001
		Genotype	0.04	0.009	52.9	4.44	<0.001
		Time	0.06	0.015	87.7	4.107	<0.001
		Mean potential evapotranspiration during the generative phase (mm)	-0.01 (-0.0063)	0.004	87.4	-2.325	0.0224
11	231	Intercept	-67.449	17.968	54.8	-3.754	<0.001
		Genotype	0.038	0.01	54.6	4.234	<0.001

			Time	0.062	0.015	92	4.14	<0.001	
			Climatic Water balance during the stem elongation phase (mm)	-0.06 (0.0299)	0.085	91	-0.704	0.4832	
Low yield potential	1	134	Intercept	-79.469	19.39	30.4	-4.098	<0.001	
			Genotype	0.0463	0.01	29.6	4.729	<0.001	
				Time	0.0638	0.018	71.2	3.489	<0.001
				Mean temperature during the generative phase (°C)	-0.31 (-0.0039)	0.119	31.8	-2.606	0.0138
	2	137	Intercept	-79.03	19.306	30.6	-4.094	0.0003	
			Genotype	0.0463	0.01	29.8	4.762	<0.001	
			Time	0.0609	0.018	79.9	3.48	<0.001	
				Maximum temperature during the generative phase (°C)	-0.261 (-0.0039)	0.091	37.8	-2.864	0.0068
	3	141	Intercept	-79.858	19.323	32.6	-4.133	<0.001	
			Genotype	0.044	0.01	32.6	4.546	<0.001	
			Time	0.061	0.017	83.4	3.579	<0.001	
			Number of days with Tmax > 27°C during the generative phase	-0.115 (-0.0055)	0.03	54.8	-3.846	<0.001	
	4	141	Intercept	-75.933	19.602	34.1	-3.874	<0.001	
			Genotype	0.042	0.01	34.1	4.257	<0.001	
Time			0.062	0.018	87.6	3.551	<0.001		
Number of days with Tmax > 31°C during the generative phase			-0.36 (-0.0017)	0.105	56.6	-3.44	0.0011		
5	109	Intercept	-140.762	19.185	8.6	-7.337	<0.001		
		Genotype	0.075	0.01	8.4	7.755	<0.001		
		Time	0.07	0.034	50.1	2.053	0.0454		
		Global radiation mean during the growing season (W m ⁻²)	-0.02 (-0.0001)	0.034	40.3	-0.588	0.5596		
6	108	Intercept	-142.203	19.19	8.4	-7.41	<0.001		

		Genotype	0.076	0.01	8.4	7.818	<0.001
		Time	0.059	0.035	49.9	1.708	0.0939
		Global radiation mean during the leaf development phase (W m ⁻²)	-0.04 (0.0003)	0.029	39.1	-1.377	0.1762
7	109	Intercept	-139.277	19.93	8.9	-6.988	<0.001
		Genotype	0.073	0.01	8.9	7.29	<0.001
		Time	0.03	0.035	50.9	0.856	0.3962
		Global radiation mean during the stem elongation phase (W m ⁻²)	0.01 (0.0036)	0.008	38.4	1.335	0.1896
8	141	Intercept	-76.159	19.703	33.1	-3.865	<0.001
		Genotype	0.042	0.01	33.1	4.245	<0.001
		Time	0.06	0.018	88.8	3.263	0.0016
		Cumulative precipitation amount during the stem elongation phase (mm)	-0.004 (-0.0037)	0.003	54.8	-1.6	0.1153
9	141	Intercept	-78.441	19.483	33	-4.026	<0.001
		Genotype	0.043	0.01	33	4.4	<0.001
		Time	0.059	0.018	88.3	3.216	0.0018
		Cumulative precipitation amount of days with precipitation > 20 mm during the vegetative phase (mm)	-0.006 (-0.0015)	0.003	60.2	-1.805	0.0762
10	134	Intercept	-80.651	19.487	31	-4.139	<0.001
		Genotype	0.045	0.01	30.9	4.612	<0.001
		Time	0.065	0.018	71	3.586	<0.001
		Mean potential evapotranspiration during the generative phase (mm)	-0.517 (-0.0116)	0.168	42.5	-3.077	0.0036
11	136	Intercept	-76.251	19.876	32.5	-3.836	<0.001
		Genotype	0.042	0.01	32.5	4.178	<0.001
		Time	0.059	0.019	78	3.127	0.0025
		Climatic Water balance during the stem elongation phase (mm)	-0.004 (0.0002)	0.003	48.1	-1.244	0.2197

High yield potential	1	134	Intercept	-79.469	19.39	30.4	-4.098	<0.001
			Genotype	0.0463	0.01	29.6	4.729	<0.001
			Time	0.0638	0.018	71.2	3.489	<0.001
			Mean temperature during the generative phase (°C)	-0.31 (-0.0039)	0.119	31.8	-2.606	0.0138
	2	137	Intercept	-79.03	19.306	30.6	-4.094	0.0003
			Genotype	0.0463	0.01	29.8	4.762	<0.001
			Time	0.0609	0.018	79.9	3.48	<0.001
			Maximum temperature during the generative phase (°C)	-0.261 (-0.0039)	0.091	37.8	-2.864	0.0068
	3	141	Intercept	-79.858	19.323	32.6	-4.133	<0.001
			Genotype	0.044	0.01	32.6	4.546	<0.001
			Time	0.061	0.017	83.4	3.579	<0.001
			Number of days with Tmax > 27°C during the generative phase	-0.115 (-0.0055)	0.03	54.8	-3.846	<0.001
	4	141	Intercept	-75.933	19.602	34.1	-3.874	<0.001
			Genotype	0.042	0.01	34.1	4.257	<0.001
			Time	0.062	0.018	87.6	3.551	<0.001
			Number of days with Tmax > 31°C during the generative phase	-0.36 (-0.0017)	0.105	56.6	-3.44	0.0011
5	109	Intercept	-140.762	19.185	8.6	-7.337	<0.001	
		Genotype	0.075	0.01	8.4	7.755	<0.001	
		Time	0.07	0.034	50.1	2.053	0.0454	
		Global radiation mean during the growing season (W m ⁻²)	-0.02 (-0.0001)	0.034	40.3	-0.588	0.5596	
6	108	Intercept	-142.203	19.19	8.4	-7.41	<0.001	
		Genotype	0.076	0.01	8.4	7.818	<0.001	
		Time	0.059	0.035	49.9	1.708	0.0939	

		Global radiation mean during the leaf development phase (W m^{-2})	-0.04 (0.0003)	0.029	39.1	-1.377	0.1762
7	109	Intercept	-139.277	19.93	8.9	-6.988	<0.001
		Genotype	0.073	0.01	8.9	7.29	<0.001
		Time	0.03	0.035	50.9	0.856	0.3962
		Global radiation mean during the stem elongation phase (W m^{-2})	0.01 (0.0036)	0.008	38.4	1.335	0.1896
8	141	Intercept	-76.159	19.703	33.1	-3.865	<0.001
		Genotype	0.042	0.01	33.1	4.245	<0.001
		Time	0.06	0.018	88.8	3.263	0.0016
		Cumulative precipitation amount during the stem elongation phase (mm)	-0.004 (-0.0037)	0.003	54.8	-1.6	0.1153
9	141	Intercept	-78.441	19.483	33	-4.026	<0.001
		Genotype	0.043	0.01	33	4.4	<0.001
		Time	0.059	0.018	88.3	3.216	0.0018
		Cumulative precipitation amount of days with precipitation > 20 mm during the vegetative phase (mm)	-0.006 (-0.0015)	0.003	60.2	-1.805	0.0762
10	134	Intercept	-80.651	19.487	31	-4.139	<0.001
		Genotype	0.045	0.01	30.9	4.612	<0.001
		Time	0.065	0.018	71	3.586	<0.001
		Mean potential evapotranspiration during the generative phase (mm)	-0.517 (-0.0116)	0.168	42.5	-3.077	0.0036
11	136	Intercept	-76.251	19.876	32.5	-3.836	<0.001
		Genotype	0.042	0.01	32.5	4.178	<0.001
		Time	0.059	0.019	78	3.127	0.0025
		Climatic Water balance during the stem elongation phase (mm)	-0.004 (0.0002)	0.003	48.1	-1.244	0.2197

Sites with relatively low yield potential were particularly affected by temperature and heat stress events.

After analysing the sensitivity of individual agro-climatic factors for the total of the sites represented, we separately examined those sites with relatively low (< 70 quality points) and relatively high (> 70 quality points) soil yield potential (Method). In comparison to the average of all locations, temperature-related effects were on average about one-sixth higher at sites with low yield potential (Figure 13, Table 4). There, the number of days with heat stress above 27°C during the generative phase explained nearly 30%, being the strongest effect of a single agro-climatic factor at the same time. Heat stress days above 31°C during the generative phase still explained up to 21%. The number of heat stress days above 31°C doubled within the total of the period considered (Supporting Information Figure 6). Moreover, while the effect of the mean temperature during the generative phase increased to as much as 19%, the effect of maximum temperatures during the generative phase was even more pronounced and explained nearly 23% of the yield variation. As a consequence, the effect of the mean evapotranspiration during the generative phase also increased by more than one third at sites with light soils to 26% in comparison to the total of the sites considered. Similar effects were found for soils classified as light soils, which are shown in Supporting Material Table 11.

Except for the effect of days with maximum temperatures above 31°C during the generative phase, temperature and heat stress effects were less pronounced at sites with higher yield potential (Figure 13). Here, the explained yield variance decreased to about 16% for the effect of days with maximum temperatures above 27°C during the generative phase. Yet, when stress events with maximum temperatures above 31°C occurred, the explained variance increased from 17% to 25%.

Regarding the exposure of wheat to heat stress events above 31°C during the generative phase along the overall time effect, sites with fewer heat stress events were less afflicted by high temperatures than sites with more stress events (Figure 14a). Winter wheat yields increased at sites of low yield potential and with an average of 1.6 heat stress days by 0.1 t DM ha⁻¹ yr⁻¹, while at sites with an average of 3.6 heat stress days yields increased by about 0.088 t DM ha⁻¹ yr⁻¹. At sites with high yield potential and exposed to 1.9 heat stress days during the generative phase, yields increased by about 0.072 t DM ha⁻¹ yr⁻¹ and by about 0.071 t DM ha⁻¹ yr⁻¹ at sites with 3.0 heat stress days (Figure 14b).

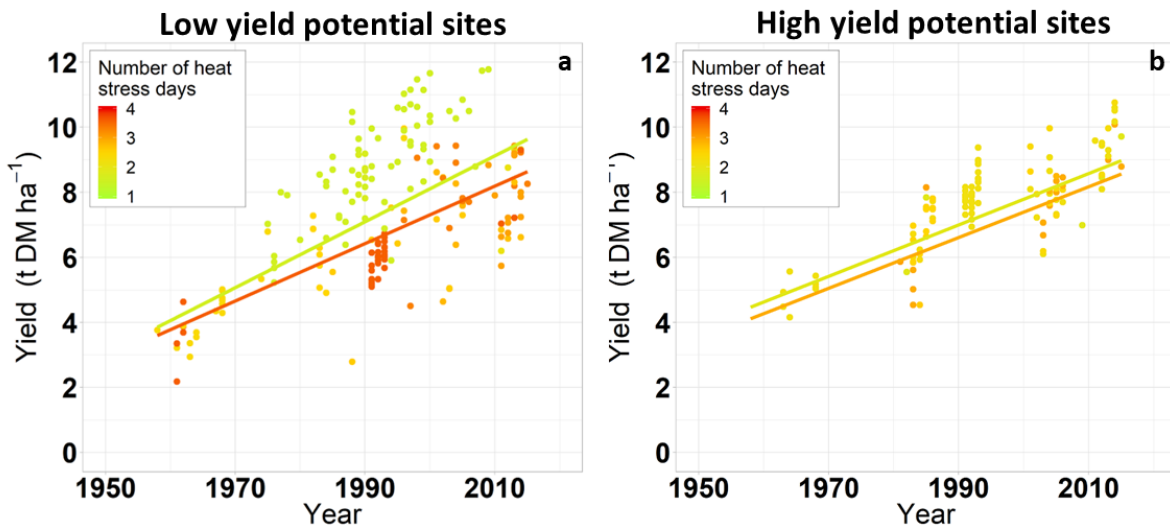


Figure 14: Grain yield evolution of winter wheat at sites with different heat stress conditions during the generative growth phase at sites with (a) low (0-70 quality points) and (b) high (70-100 quality points) yield potential (classified based on the Muncheberg Soil Quality Rating (Mueller *et al.* 2010) (MSQR, Methods). The different colours depict the number of heat stress days during generative phase for each single site-year (points) and trend (lines) at the sites with the lowest (green lines (a) & (b)) and highest (red line (a); orange line (b)) number of heat stress days.

Negative effects due to high rainfall events and water deficit

Interestingly, our data reveal that effects related to high precipitation events (defined as days with more than 20 mm precipitation) became relevant during the vegetative phase (Figure 13). Here, the total amount of precipitation through high rainfall events explained about 2.8% of the variance in winter wheat yields. The effect was strongest during the stem elongation phase (3.5%), which still is inferior to temperature-related effects. Nevertheless, waterlogging might become more likely due to high precipitation events, leading to oxygen deficiency or enhanced erosion processes, which causes nutrient losses accelerated by a reduced ground cover canopy in particular during the leaf development phase at sites with higher clay content (Nearing *et al.* 2005; Malik *et al.* 2002). The effect of the overall precipitation amount during the stem elongation phase was more than 1.5-fold stronger at sites of high yield potential (5.5%) as compared to all sites (3.3%). The magnitude of radiation effects increased at sites with higher yield potential, foremost during leaf development to up to 30%. The relatively large temperature and radiation effects are presumed to have resulted in an enhanced effect of the negative climatic water balance in particular during stem elongation. This effect was not evident when considering the total of all sites or sites with low yield potential only. All climate effects are found in a similar way in soils classified as heavy (Supporting Information Table 7).

Discussion

For interpreting the results of the statistical models used for time series analysis, several aspects need to be considered. Firstly, these models tend to include collinearity effects between predictor variables (e.g., temperature and precipitation) and hence results do not stack up automatically to 100% (Lobell & Burke 2010b). This means a single effect might be suppressed or intensified due to interdependencies or confounding effects with other variables. Moreover, they assume that past relationships will continue in future, even though, e.g., management systems may have evolved or changed completely, and they may have low signal-to-noise ratios in yield or weather records in many locations (Lobell & Burke 2010a).

In this meta-analysis, we found that many agro-climatic effects were negatively related to yield development except for the mean global radiation during stem elongation phase. We assume that the prolongation of the stem elongation phase was caused by breeding progress since the mean temperature during this phase did not change significantly and modelling revealed no effect. Moreover, the stem elongation phase is known to be critical for yield development and has been proposed as a target trait to improve yield and environmental adaptation of wheat in numerous studies (González *et al.* 2003; Kronenberg *et al.* 2017; Miralles *et al.* 2000). The prolongation of the stem elongation phase may, however, also have been due to advanced sowing, which may have been a consequence of changed climates prior to sowing dates (Johnen *et al.* 2012). The probability of a higher number of leaf primordia initiated between sowing and the double ridge stage is greater with earlier sowing and may lead to a delay of the appearance of the leaves that emerge until stem elongation and of the final flag leaf until heading (Johnen *et al.* 2012). However, the duration of the stem elongation phase did not change significantly beyond 1988 - nearly one decade before winter wheat yields, in general, started to level off (Figure 9a). Interestingly, the TD of the stem elongation phase showed an ongoing increase by approximately 40 °Cd between 1988 and 1997. This may indicate that in this period winter wheat continued to increase radiation uptake due to enhanced temperature and light use potential during stem elongation as well as due to increased nitrogen uptake from the continuous increase of fertilizer input (Loomis & Amthor 1999).

The values presented in Figure 12 reflect the explained variance of the main effects (genotype, location, time) and their interactions. The results show that the variability of the time effects explained the variance of the winter wheat yields over time and across the study sites the most, followed by the variability of the location effect. However, a lower explained variance of the genotype effect does not automatically mean that this factor has a lower influence on yield development. The slopes of the specific covariates used in the fixed regression part of the mixed-

effects model might, therefore, provide a more detailed assessment (Table 5). While most of the agro-climatic parameters had a negative impact on yield development, the effect of the genotype was always positive. However, the slopes of the agro-climatic covariates come in their own unit and in themselves have no time unit as the genetic and the overall time effect. Hence, an adjusted climate trend, which was obtained by multiplying the slope of the covariate with the time trend of this specific covariate, was used for comparison with the two temporal trends (Methods). We found that the trend of the genetic progress was, e.g., about one hundred times larger than the trend of the mean or maximum temperature during the generative phase at all study sites ($0.004 \text{ t ha}^{-1} \text{ yr}^{-1}$) – as well as at sites with lower or greater yield potential. Moreover, the results indicate a high-temperature variability between the years and over the locations in this study.

This study uses the agronomic yield maxima for each experimental year and site as achieved by optimal N-fertilization dosage (estimated from fertilizer dose – yield response functions, Methods) and optimal plant protection. In this way, the effect of variation of agronomic practices over time was minimized so that the overall time trend essentially reflects climatic effects (Figure 12 and Figure 13). In practice, however, optimal agronomic management is often not realized on the farmers' fields (Figure 9a). In practical farming, socio-economic aspects have an important influence on the intensity of agronomic inputs, for example the fact that since the late 1990s subsidies from the European Union have been paid based on production area instead on yield, or that export subsidies were reduced (Himanen et al. 2013, Reidsma et al. 2009). Nevertheless, we also assume that the optimal amount of N fertilizer is a result of decreasing prices of nitrogen, comparable to, e.g., decreasing prices of the crops and, additionally.

The increased potential evapotranspiration during stem elongation between 1951 and 1992 is very likely a result of the stem elongation phase prolongation rather than a climatic change response, as for mean temperature and precipitation no significant changes were detected, and mixed-model analysis revealed no effects due to potential evapotranspiration. This prolongation is probably also the explanation of the increased number of days with negative CWB until 1997. Resulting water limitations, accompanied by an increased number of heat stress days during stem elongation (Supporting Information Figure 6) may have enhanced irreversible plant damage associated with yield losses in particular on shallow soils and/or in dry regions before maturity was reached (Farooq *et al.* 2011; Semenov 2009).

Our data show that yield stagnation in German winter wheat occurred since the late 1990s for all sites combined, and since the late 1980s on soils with relatively low yield potential. Climate variation – spatial and temporal – explained most of the variability of the winter wheat yields

(> 50%), whereas genetic variation over time explained only 4%. Our results emphasize that except for heat stress days with more than 31°C, sites with higher yield potential were less prone to adverse weather effects than sites with lower yield potential. In general, elevated temperatures, heat stress during the generative phase, and drought stress during the stem elongation phase affected wheat development the most. Regarding the sole effect of the agro-climatic variables at all experimental sites combined, the mean temperature during the generative phase explained about 16% of the yield variability. Days with maximum temperatures above 27 or 31°C during the generative phase explained about 25% and 17%, respectively. With respect to the winter wheat yield development of the entire observation period (1958-2015), the mean temperature during the generative phase reduced yields by about 0.23 t ha⁻¹ in total. At sites with higher yield potential, relatively large radiation effect during the leaf development (30%) and negative precipitation effects during stem elongation (5.5%) are presumed to have resulted in an enhanced effect of the negative climatic water balance in particular during stem elongation. Hence, the response of yield productivity to past climatic conditions demonstrates the sensitivity of German wheat production to climatic variation and underlines the need of finding adaptation strategies for food production under expected on-going climate change.

The analysis shows that German wheat production is continuously adjusting to climatic changes, both with regard to the genetic adjustment (i.e., respective cultivar/variety selection choice) as well as management adjustment, especially shift of sowing times. However, In the light of continuous climatic changes in the future, further cropping systems adjustments might be required to support stable winter wheat production in Germany. As such, it might be necessary to employ additional measures such as irrigation, in particular at sites with light soils and high risk of drought induced yield losses. Furthermore, earlier sowing in combination with 'early' wheat genotypes might be suitable to escape drought stress.

Acknowledgment

The study was financially supported by the Germany Research Foundation – DFG (Grant number: Stu 127/19-3 and PI 377/20-1). Frank Schaarschmidt (Institute of Biostatistics, Leibniz University Hannover) gave support on the statistical analyses. We furthermore thank Friedrich Laidig (University of Hohenheim) for his statistical advice. The authors declare that there are no competing interests.

Author Contributions

All authors contributed to the content of the manuscript, discussed the results and commented on the manuscript. E.B. and L.B. collected the data. E.B. carried out the statistical analysis and wrote the major part of the manuscript.

Data Accessibility

All data and sources used in this study are available at Bonares Datenzentrum (<https://doi.org/10.20387/bonares-YG6F-K61B>). Supporting information is available (link to journal site). Reprints and permissions information is available online at (journal link). Correspondence and requests for material should be addressed to E.B. and H.S.

References

- Ad-hoc-AG Boden (Ed.) (2005) *Bodenkundliche Kartieranleitung - KA5*. Schweizerbart Science Publishers, Stuttgart, Germany.
- Alexander LV, Zhang X, Peterson TC et al. (2006) Global observed changes in daily climate extremes of temperature and precipitation. *Journal of Geophysical Research*, 111, 1403.
- Asseng S, Ewert F, Martre P et al. (2014) Rising temperatures reduce global wheat production. *Nature Climate Change*, 5, 143–147.
- Basso B, Ritchie JT, Cammarano D, Sartori L (2011) A strategic and tactical management approach to select optimal N fertilizer rates for wheat in a spatially variable field. *European Journal of Agronomy*, 35, 215–222.
- Bönecke E, Breitsameter L, Brüggemann N, Feike T, Kage H, Kersebaum K-C, Stützel H (2020): Dataset of winter wheat yields in Germany between 1958 and 2015 from N-fertilization experiments, Leibniz Centre for Agricultural Landscape Research (ZALF), <https://doi.org/10.20387/bonares-YG6F-K61B>
- Brisson N, Gate P, Gouache D, Charmet G, Oury F-X, Huard F (2010) Why are wheat yields stagnating in Europe? A comprehensive data analysis for France. *Field Crops Research*, 119, 201–212.
- Calderini DF, Slafer GA (1998) Changes in yield and yield stability in wheat during the 20th century. *Field Crops Research*, 57, 335–347.
- Chen C, Zhou GS, Pang YM (2015) Impacts of climate change on maize and winter wheat yields in China from 1961 to 2010 based on provincial data. *The Journal of Agricultural Science*, 153, 825–836.

- Delogu G, Cattivelli L, Pecchioni N, Falcis D de, Maggiore T, Stanca AM (1998) Uptake and agronomic efficiency of nitrogen in winter barley and winter wheat. *European Journal of Agronomy*, 9, 11–20.
- Düwel O, Siebner CS, Utermann, J., Krone, F. Bodenarten der Böden Deutschlands. Bericht über länderübergreifende Auswertungen von Punktinformationen im FISBo BGR, Hannover.
- Evans LT (1996) *Crop Evolution, Adaptation and Yield*. Cambridge University Press.
- Farooq M, Bramley H, Palta JA, Siddique KHM (2011) Heat Stress in Wheat during Reproductive and Grain-Filling Phases. *Critical Reviews in Plant Sciences*, 30, 491–507.
- Frich P, Alexander LV, Della-Marta P, Gleason B, Haylock M, Klein Tank AMG, Peterson T (2002) Observed coherent changes in climatic extremes during the second half of the twentieth century. *Climate Research*, 19, 193–212.
- Frick C, Steiner H, Mazurkiewicz A, Riediger U, Rauthe M, Reich T, Gratzki A (2014) Central European high-resolution gridded daily data sets (HYRAS). Mean temperature and relative humidity. *Meteorologische Zeitschrift*, 23, 15–32.
- Gömman H, Bender A, Bolte A et al. (2015) Agrarrelevante Extremwetterlagen und Möglichkeiten von Risikomanagementsystemen. Studie im Auftrag des Bundesministeriums für Ernährung und Landwirtschaft (BMEL). Johann Heinrich von Thünen-Institut, Braunschweig, Online-Ressource (XVIII, 289 S., 10481 KB).
- González FG, Slafer GA, Miralles DJ (2003) Floret development and spike growth as affected by photoperiod during stem elongation in wheat. *Field Crops Research*, 81, 29–38.
- Grassini P (2010) Distinguishing between yield advances and yield plateaus in historical crop production trends - Supplementary Information. In: *Fair Trade for Teachers*, p 60. Commonwealth Secretariat.
- Grassini P, Eskridge KM, Cassman KG (2013) Distinguishing between yield advances and yield plateaus in historical crop production trends. *Nature communications*, 4, 2918.
- Hafner S (2003) Trends in maize, rice, and wheat yields for 188 nations over the past 40 years. A prevalence of linear growth. *Agriculture, Ecosystems & Environment*, 97, 275–283.
- Haude W (1954) *Zur praktischen Bestimmung der aktuellen und potentiellen Evaporation und Evapotranspiration*. Schweinfurter Dr. und Verlag-Ges.
- Haylock, Hofstra N, Tank AKG, Klok EJ, Jones PD, New M (2008) A European daily high-resolution gridded data set of surface temperature and precipitation for 1950–2006. *Journal of Geophysical Research: Atmospheres*, 113.
- Himanen SJ, Hakala K, Kahiluoto H (2013) Crop responses to climate and socioeconomic change in northern regions. *Regional Environmental Change*, 13, 17–32.

- Huld T, Müller R, Gambardella A (2012) A new solar radiation database for estimating PV performance in Europe and Africa. *Solar Energy*, 86, 1803–1815.
- Johnen T, Boettcher U, Kage H (2012) A variable thermal time of the double ridge to flag leaf emergence phase improves the predictive quality of a CERES-Wheat type phenology model. *Computers and Electronics in Agriculture*, 89, 62–69.
- Kronenberg L, Yu K, Walter A, Hund A (2017) Monitoring the dynamics of wheat stem elongation. Genotypes differ at critical stages. *Euphytica*, 213, 69.
- Laidig F, Drobek T, Meyer U (2008) Genotypic and environmental variability of yield for cultivars from 30 different crops in German official variety trials. *Plant Breeding*, 127, 541–547. <http://onlinelibrary.wiley.com/doi/10.1111/j.1439-0523.2008.01564.x/full>.
- Laidig F, Piepho H-P, Drobek T, Meyer U (2014) Genetic and non-genetic long-term trends of 12 different crops in German official variety performance trials and on-farm yield trends. *Theoretical and Applied Genetics*, 127, 2599–2617.
- Laidig F, Piepho H-P, Rentel D, Drobek T, Meyer U, Huesken A (2017) Breeding progress, variation, and correlation of grain and quality traits in winter rye hybrid and population varieties and national on-farm progress in Germany over 26 years. *Theoretical and Applied Genetics*, 130, 981–998. <https://doi.org/10.1007/s00122-017-2865-9>.
- Lobell, D, Burke, M (Eds.) (2010a) *Climate Change and Food Security: Adapting Agriculture to a Warmer World*. Springer Netherlands, Dordrecht.
- Lobell DB, Burke MB (2010b) On the use of statistical models to predict crop yield responses to climate change. *Agricultural and Forest Meteorology*, 150, 1443–1452.
- Lobell DB, Field CB (2007) Global scale climate–crop yield relationships and the impacts of recent warming. *Environmental Research Letters*, 2, 14002.
- Lobell DB, Schlenker W, Costa-Roberts J (2011) Climate trends and global crop production since 1980. *Science (New York, N.Y.)*, 333, 616–620.
- Loomis RS, Amthor JS (1999) Yield Potential, Plant Assimilatory Capacity, and Metabolic Efficiencies. *Crop Science*, 39, 1584.
- Mackay I, Horwell A, Garner J, White J, McKee J, Philpott H (2011) Reanalyses of the historical series of UK variety trials to quantify the contributions of genetic and environmental factors to trends and variability in yield over time. *Theoretical and Applied Genetics*, 122, 225–238.
- Mäkinen H, Kaseva J, Trnka M et al. (2018) Sensitivity of European wheat to extreme weather. *Field Crops Research*, 222, 209–217.
- Malik AI, Colmer TD, Lambers H, Setter TL, Schortemeyer M (2002) Short-term waterlogging has long-term effects on the growth and physiology of wheat. *New Phytologist*, 153, 225–236.
- McMaster GS, Wilhelm W (1997) Growing degree-days: one equation, two interpretations.

- Meehl GA, Tebaldi C (2004) More Intense, More Frequent, and Longer Lasting Heat Waves in the 21st Century. *Science* (New York, N.Y.), 305, 994–997.
<http://science.sciencemag.org/content/sci/305/5686/994.full.pdf>.
- Meier U (1997) BBCH-Monograph. Growth stages of plants–Entwicklungsstadien von Pflanzen–Estadios de las plantas–Développement des Plantes. Berlin und Wien: Blackwell Wissenschaftsverlag, 622.
- Menzel A (2003) Plant Phenological Anomalies in Germany and their Relation to Air Temperature and NAO. *Climatic Change*, 57, 243–263.
- Miralles DJ, Richards RA, Slafer GA (2000) Duration of the stem elongation period influences the number of fertile florets in wheat and barley. *Functional Plant Biology*, 27, 931–940.
- Mitchell RAC, Mitchell VJ, Driscoll SP, Franklin J, Lawlor DW (1993) Effects of increased CO₂ concentration and temperature on growth and yield of winter wheat at two levels of nitrogen application. *Plant, Cell and Environment*, 16, 521–529.
- Moot DJ, Henderson AL, Porter JR, Semenov MA (1996) Temperature, CO₂ and the growth and development of wheat. Changes in the mean and variability of growing conditions. *Climatic Change*, 33, 351–368.
- Mueller L, Schindler U, Mirschel W et al. (2010) Assessing the productivity function of soils. A review. *Agronomy for Sustainable Development*, 30, 601–614. <https://doi.org/10.1051/agro/2009057>.
- Muggeo V (2003) Estimating regression models with unknown break-points. *Statistics in Medicine*, 22, 3055–3071.
- Muggeo V (2008) *Segmented*. An R package to fit regression models with broken-line relationships. *R news*, 8, 20–25.
- Nearing MA, Jetten V, Baffaut C et al. (2005) Modeling response of soil erosion and runoff to changes in precipitation and cover. *Catena*, 61, 131–154.
- Olesen JE, Børgesen CD, Elsgaard L et al. (2012) Changes in time of sowing, flowering and maturity of cereals in Europe under climate change. *Food additives & contaminants. Part A, Chemistry, analysis, control, exposure & risk assessment*, 29, 1527–1542.
- Piepho HP, Ogutu JO (2003) Inference for the break point in segmented regression with application to longitudinal data. *Biometrical Journal*, 45, 591–601.
- Piepho H-P, Laidig F, Drobek T, Meyer U (2014) Dissecting genetic and non-genetic sources of long-term yield trend in German official variety trials. *Theoretical and Applied Genetics*, 127, 1009–1018.
- Piepho H-P (2019) A coefficient of determination (R²) for generalized linear-mixed models. *Biometrical Journal*, 61, 860–872.

- Porter JR, Gawith M (1999) Temperatures and the growth and development of wheat: a review. *European Journal of Agronomy*, 10, 23–36.
- Porter JR, Semenov MA (2005) Crop responses to climatic variation. *Philosophical Transactions of the Royal Society of London. Series B, Biological Sciences*, 360, 2021–2035.
- R Development Core Team (2008). R: A language and environment for statistical computing. R Foundation for Statistical Computing, Vienna, Austria.
- Raun WR, Solie JB, Johnson GV, Stone ML, Mullen RW, Freeman KW, Thomason WE, Lukina EV (2002) Improving nitrogen use efficiency in cereal grain production with optical sensing and Vvariable rate application. *Agronomy Journal*, 94, 815.
- Rauthe M, Steiner H, Riediger U, Mazurkiewicz A, Gratzki A (2013) A Central European precipitation climatology – Part I. Generation and validation of a high-resolution gridded daily data set (HYRAS). *Meteorologische Zeitschrift*, 22, 235–256.
- Reidsma P, Oude Lansink A, Ewert F (2008) Economic impacts of climatic variability and subsidies on European agriculture and observed adaptation strategies. *Mitigation and Adaptation Strategies for Global Change*, 14, 35.
- Reyer CP, Leuzinger S, Rammig A et al. (2013) A plant's perspective of extremes. *Terrestrial plant responses to changing climatic variability. Global Change Biology*, 19, 75–89.
- Schabenberger O, Pierce FJ (2001) Contemporary statistical models for the plant and soil sciences. CRC Press.
- Schlenker W (2010) Crop responses to climate and weather: cross-section and panel models. In: *Climate Change and Food Security: Adapting Agriculture to a Warmer World* (eds Lobell D, Burke M), pp 99–108. Springer Netherlands, Dordrecht.
- Semenov MA (2009) Impacts of climate change on wheat in England and Wales. *Journal of the Royal Society, Interface*, 6, 343–350.
- Siebert S, Ewert F (2012) Spatio-temporal patterns of phenological development in Germany in relation to temperature and day length. *Agricultural and Forest Meteorology*, 152, 44–57.
- Slafer GA, Rawson HM (1994) Does temperature affect final numbers of primordia in wheat? *Field Crops Research*, 39, 111–117.
- Tashiro T, Wardlaw IFAN (1989) A comparison of the effect of high temperature on grain development in wheat and rice. *Annals of Botany*, 64, 59–65.
- Trnka M, Feng S, Semenov MA et al. (2019) Mitigation efforts will not fully alleviate the increase in water scarcity occurrence probability in wheat-producing areas. *Science Advances*, 5, eaau2406. <https://advances.sciencemag.org/content/advances/5/9/eaau2406.full.pdf>.

- Trnka M, Rötter RP, Ruiz-Ramos M, Kersebaum KC, Olesen JE, Žalud Z, Semenov MA (2014) Adverse weather conditions for European wheat production will become more frequent with climate change. *Nature Climate Change*, 4, 637–643.
- van Ittersum MK, Cassman KG, Grassini P, Wolf J, Titttonell P, Hochman Z (2013) Yield gap analysis with local to global relevance—A review. *Field Crops Research*, 143, 4–17.
- Wheeler TR, Hong TD, Ellis RH, Batts GR, Morison JIL, Hadley P (1996) The duration and rate of grain growth, and harvest index, of wheat (*Triticum aestivum* L.) in response to temperature and CO₂. *Journal of Experimental Botany*, 62, 623–630.
- Whitfield DM, Smith CJ (1992) Nitrogen uptake, water use, grain yield and protein content in wheat. *Field Crops Research*, 29, 1–14.
- Wiesmeier M, Hübner R, Kögel-Knabner I (2015) Stagnating crop yields. An overlooked risk for the carbon balance of agricultural soils? *The Science of the Total Environment*, 536, 1045–1051.
- Wollenweber B, Porter JR, Schellberg J (2003) Lack of interaction between extreme high-temperature events at vegetative and reproductive growth stages in wheat. *Journal of Agronomy and Crop Science*, 189, 142–150.
- Zadoks JC, Chang TT, Konzak CF (1974) A decimal code for the growth stages of cereals. *Weed Research*, 14, 415–421.

Supporting Material

Crop and drought parameters

The thermal duration (TD, °Cd) for each phenological phase was calculated after (McMaster & Wilhelm 1997):

$$TD = \sum_{d=1}^n \text{Max}(T_{\text{mean}_d} - T_{\text{base}}, 0) \quad (15)$$

with T_{mean_d} as the daily temperature mean (°C) summarized from 1 to n days (d) is, and 0 °C is used as base temperature T_{base} for winter wheat. The potential evapotranspiration (ETP, mm) above winter wheat crops was calculated using Haude 1954 as:

$$ETP = f_H \cdot e_s \cdot \left(1 - \frac{r}{100}\right) \quad (16)$$

With

$$e_s = 6.11 \cdot e^{\left(\frac{17.62 \cdot T}{243.12 + T}\right)} \quad (17)$$

where r is the relative air humidity (%) at 2 pm, e_s is the saturated vapour pressure of the air derived from the air temperature T at 2 pm, and f_H is the correction factor of the monthly transpiration of the corresponding crop in mm hPa d⁻¹ (winter wheat: March 0.19, April 0.26, Mai 0.34, June 0.38, July 0.34, August 0.22, September 0.21, October 0.20, November – February 0.18). Data on air temperature at 2 pm was substituted in this study by available long-term data sets on maximum air temperature. Correspondingly, 2 pm air humidity values can be substituted with minimum air humidity values. However, gridded long-term data on relative air humidity was only available for mean values - not minimum values. In order to avoid underestimation of the potential evapotranspiration through mean values, we derived correction factors to estimate the daily minimum air humidity from daily mean air humidity values. Therefore, daily minimum and mean air humidity values were obtained for each geographical areas of Germany (north, south, east, west, and central) from independent long-term data sets of hourly air humidity records available at the Climate Data Centre (CDC) of the DWD (<https://cdc.dwd.de/portal/201810240858/index.html>). Selected stations, their location and record duration can be found in Table 12 of the Supporting Information material. For the obtained daily minimum and mean values, saturation deficits were calculated and ordinary linear relationships with intercept forced through 0 % saturation deficit established (equation 18) on a monthly basis for each direction. The regression coefficients are shown in the Supporting Information Table 6.

$$E(y) = bx \quad (18)$$

To validate the estimations, other independent data sets within the same direction were chosen and the root mean square error (RMSE) between the observed and the predicted minimum air humidity values calculated:

$$RMSE = \sqrt{\frac{\sum_{i=1}^N (x_o - x_e)^2}{N}} \quad (19)$$

where x_o and x_e are the observed and estimated air humidity values, respectively, and N represents the sample size. The results of the RMSE are shown in Supporting Information Table 7.

Climatic water balance (CWB) is an indicator for the available water supply. It is defined as the difference between the precipitation height and the amount of the ETP (mm). CWB differs largely within Germany and was, hence, additionally calculated.

Table 6 Selected stations with hourly measured air humidity values

Direction	Station ID	Station name	Federal state	Latitude	Longitude	Elevation	Start date	End date	Usage
Central	2597	Kissingen, Bad	Bayern	50.2241	10.0792	282	01.01.1951	31.12.2018	Estimation
Central	2925	Leinefelde	Thüringen	51.3933	10.3123	356	01.01.1956	31.12.2018	Validation
East	3015	Lindenberg	Brandenburg	52.2085	14.118	98	01.01.1951	31.12.2018	Estimation
East	3552	Neuruppin	Brandenburg	52.9037	12.8072	38	01.01.1973	31.12.2018	Validation
North	4466	Schleswig	Schleswig-Holstein	54.5275	9.5487	43	01.01.1951	31.12.2018	Estimation
North	4745	Soltau	Niedersachsen	52.9604	9.793	75	01.01.1966	31.12.2018	Validation
South	4887	Stötten	Baden-Württemberg	48.6657	9.8646	734	01.01.1951	31.12.2018	Estimation
South	125	Altenstadt	Bayern	47.8342	10.8667	756	01.01.1971	31.12.2018	Validation
West	553	Bocholt	Nordrhein-Westfalen	51.838	6.6107	25	01.01.1951	31.12.1970	Estimation
West	554	Bocholt-Liedern	Nordrhein-Westfalen	51.8293	6.5365	23	01.01.1971	31.12.2005	Estimation
West	3023	Lingen	Niedersachsen	52.5181	7.3081	22	01.01.1951	20190209	Validation

Table 7 Regression coefficients of the relationship between the saturation deficit of the minimum and mean air humidity. Coefficients were estimated for each direction, month, and period as listed in Table 6 and the linear regression functions forced through 0% deficit (Methods). The root mean square error (RMSE) was calculated between observed and estimated minimum air humidity values

Orientation	Month	Coefficient	RMSE (%)
North	January	1.72	5.7
	February	1.77	7.7
	March	1.89	9
	April	1.84	10.1
	May	1.79	10
	June	1.82	9.1
	July	1.88	8.7
	August	1.98	9.3
	September	2.05	8
	October	2.02	8.4
	November	1.87	6.6
	December	1.77	5.3
South	January	1.68	8.8
	February	1.67	9.9
	March	1.59	10.7
	April	1.53	11
	May	1.57	9.7
	June	1.61	9
	July	1.57	8.8
	August	1.61	9.4
	September	1.71	9.4
	October	1.8	10
	November	1.79	9.8
	December	1.66	8.5
East	January	1.69	4.9
	February	1.79	6.7
	March	1.72	8.3
	April	1.6	9.2
	May	1.58	9
	June	1.61	8.1
	July	1.63	8.1
	August	1.66	8.6

	September	1.82	8
	October	1.89	7.9
	November	1.8	5.6
	December	1.7	4.5
West	January	1.61	6
	February	1.71	7.4
	March	1.75	9
	April	1.72	9.5
	May	1.7	9
	June	1.74	7.7
	July	1.8	7.8
	August	1.86	7.9
	September	2.01	7.4
	October	1.97	7.7
	November	1.77	6.5
	December	1.65	5.6
Central	January	1.69	5.1
	February	1.81	6.2
	March	1.82	7.6
	April	1.72	9.1
	May	1.77	8.7
	June	1.79	7.8
	July	1.82	8.2
	August	1.9	9.6
	September	2.12	9.1
	October	2.23	8.7
	November	1.86	5.6
	December	1.71	4.7

Yield and nitrogen fertilization development under site specific characteristics

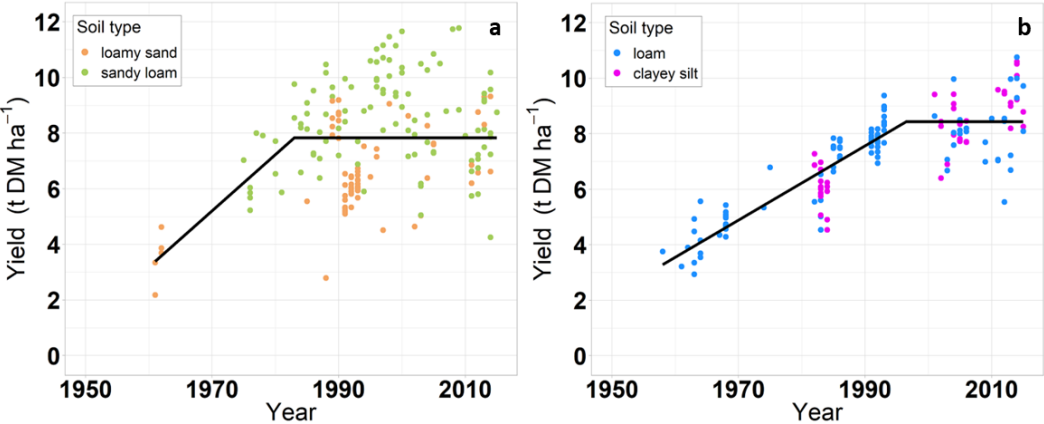


Figure 15: Grain yield development of winter wheat across the study sites in Germany between 1949 and 2016. Soil types are presented according to German soil classification(Ad-hoc-AG Boden 2005) (Method). a, Overall trend for soils classified as light soils (Methods). b, Overall trend for soils classified as heavy soils.

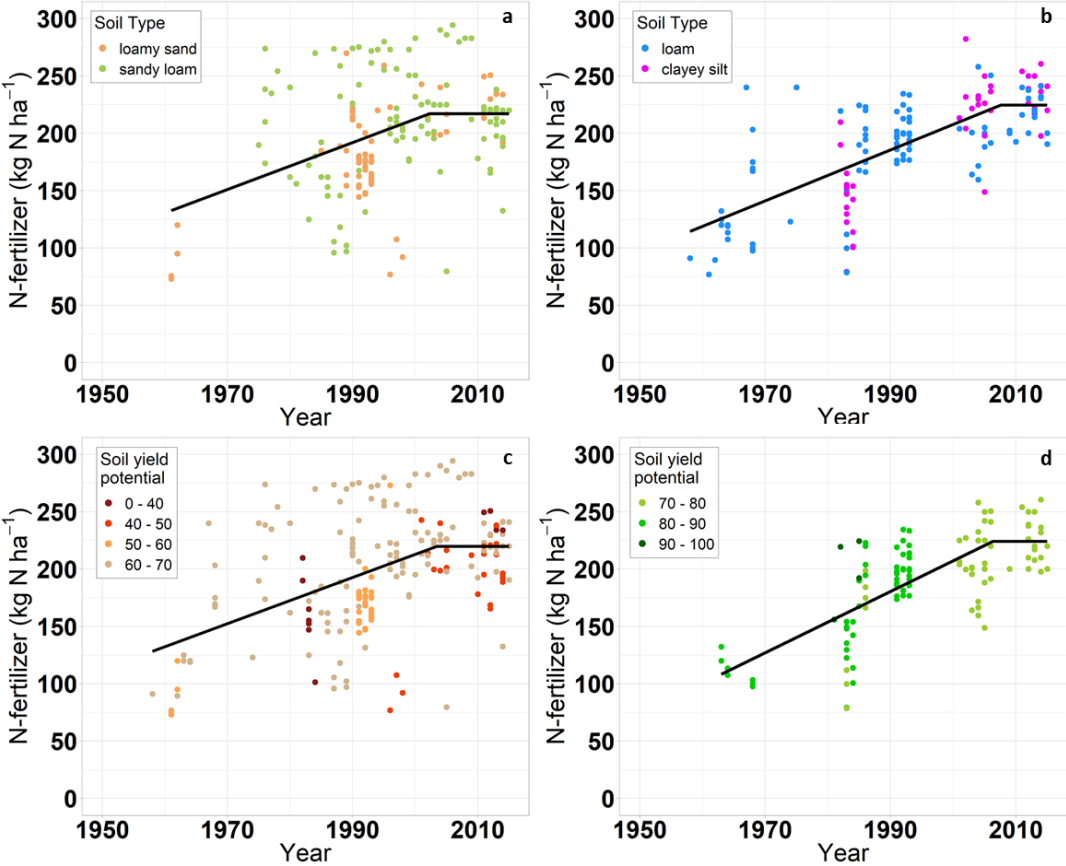


Figure 16: Fertilization development under different soil and site conditions across the study sites between 1958 and 2015. Soil types are presented according to German soil classification(Ad-hoc-AG Boden 2005) and the soil yield potential according to the Muencheberg Soil Quality Rating(Mueller et al. 2010) (MSQR, see Methods). The black trend lines refer to fitted functions. a, Overall trend for soils classified as light soils. b, Overall trend for soils classified as heavy soils. c, Trends for sites with relatively low soil yield potential. d, Trends for sites with relatively high soil yield potential

Phenology

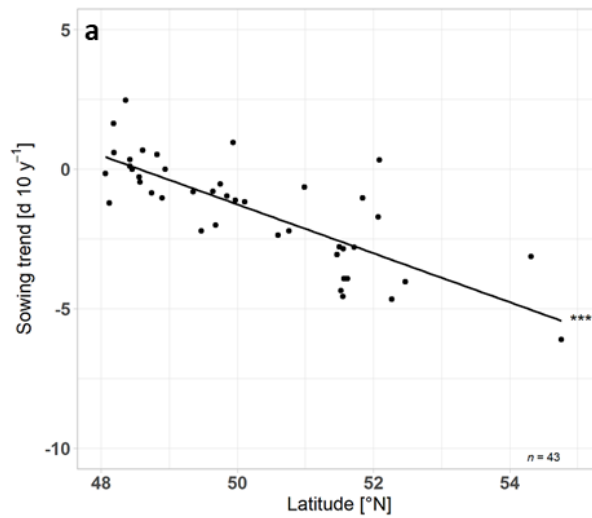


Figure 17: Sowing date trends across the study sites as decadal change and dependent on latitude for each site analysed in this study. Three asterisks define significance at the 0.1% level.

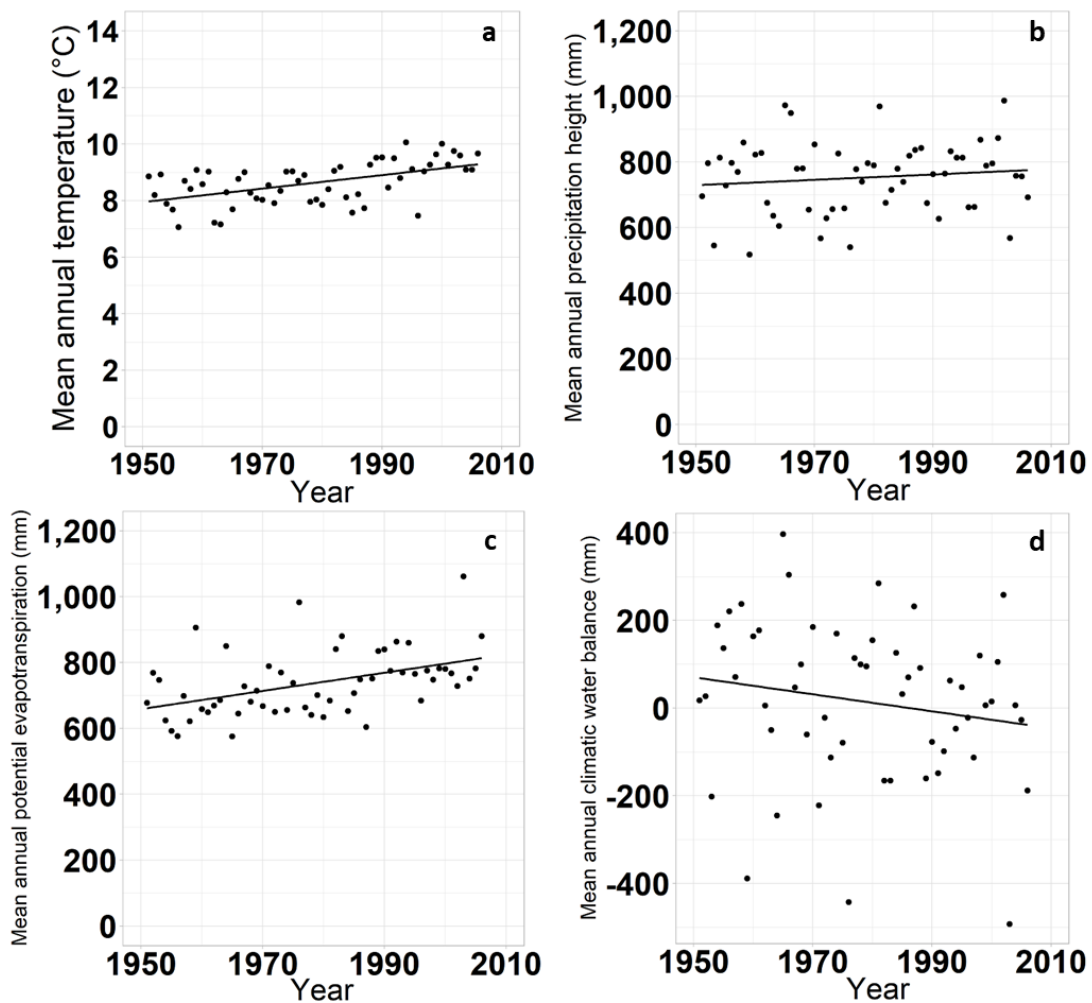


Figure 18: Climate trends across the study sites in Germany between 1951 and 2006. a, Mean annual temperature between. b, Mean annual precipitation height between. c, Mean annual potential evapotranspiration between. d, Mean annual climatic water balance between

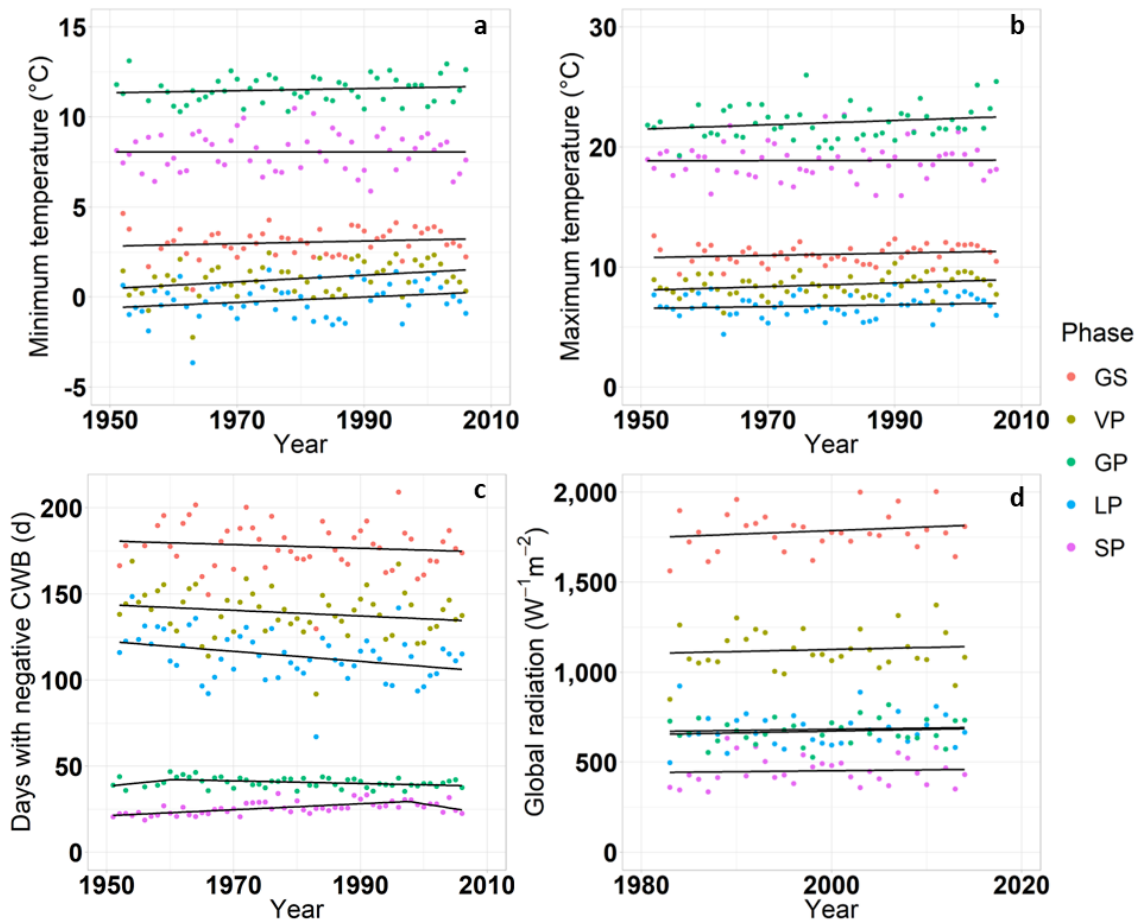


Figure 19: Development of adverse weather conditions during phenological phases of winter wheat across the study sites. Trends are shown for the growing season (GS), vegetative phase (VP), leaf development and tillering phase (LP), generative phase (GP), and stem elongation and booting phase (SBP). a, Maximum temperature between 1951 and 2006. b, minimum temperature between 1951 and 2006. c, Mean frequency of days with negative climatic water balance (CWB) between 1951 and 2006. d, Global radiation sum between 1983 and 2015

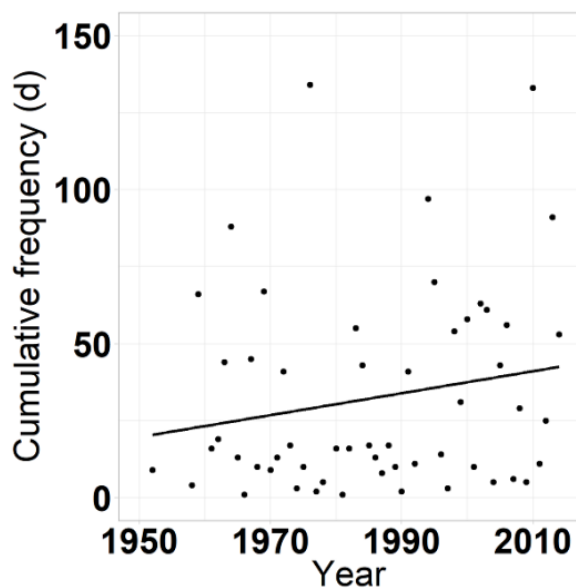


Figure 20: Development of occurring heat stress events (cumulative days with $T_{max} > 31\text{ }^{\circ}\text{C}$) during the stem elongation phase across all sites with a soil yield potential below 70 quality points

Variance analysis

Table 8 Estimated explained variance of the agro-climatic variables (units in parentheses) on winter wheat yield development between 1958 and 2006 across the study sites in Germany after removing the effect of soil yield potential or the soil type. All explained variances are estimated after already accounting for the genetic and non-genetic time trends

Phenological phase or stage	Agro-climatic variable	Description	n	Explained variance (%)	
				Removed soil effect	
				Soil yield potential	Soil type
Growing season	GS_HS27_n	Number of heat stress days with $T_{\max} > 27^{\circ}\text{C}$	236	21.3	21
	GS_HS31_n	Number of heat stress days with $T_{\max} > 31^{\circ}\text{C}$	236	12.3	11.5
	GS_HS27_Tm_n	Number of heat stress days with $T_{\text{mean}} > 27^{\circ}\text{C}$	236	3.8	2.5
	GS_HS27_sum	Cumulative heat stress temperature with $T_{\max} > 27^{\circ}\text{C}$ ($^{\circ}\text{C}$)	236	21.9	21.6
	GS_HS31_sum	Cumulative heat stress temperature with $T_{\max} > 31^{\circ}\text{C}$ ($^{\circ}\text{C}$)	236	12.6	11.8
	GS_HS27_Tm_sum	Cumulative heat stress temperature with $T_{\text{mean}} > 27^{\circ}\text{C}$ ($^{\circ}\text{C}$)	236	3.7	2.4
	GS_ETPm	Daily potential evapotranspiration means (mm)	231	11.5	10
	GS_ETPs	Total potential evapotranspiration sum (mm)	231	9.4	9.7
	GS_CWBneg_n	Number of days with negative climatic water balance	236	2.7	2.6
	GS_CWBm	Daily climatic water balance mean (mm)	231	2.4	-
	GS_CWBs	Total climatic water balance sum (mm)	231	2.6	-
	GS_TD	Thermal duration ($^{\circ}\text{C}\text{d}$)	231	2.1	6.3
	GS	Duration (d)	233	5.9	5
	Generative phase	GP_T_mean	Mean temperature ($^{\circ}\text{C}$)	229	15.8
GP_T_max		Maximum temperature ($^{\circ}\text{C}$)	232	17.4	16.8

	GP_HS27_n	Number of heat stress days with $T_{\max} > 27^{\circ}\text{C}$	236	25	23.9
	GP_HS31_n	Number of heat stress days with $T_{\max} > 31^{\circ}\text{C}$	236	16.2	14.4
	GP_HS27_Tm_n	Number of heat stress days with $T_{\text{mean}} > 27^{\circ}\text{C}$	236	3.8	2.5
	GP_HS27_sum	Cumulative heat stress temperature with $T_{\max} > 27^{\circ}\text{C}$ ($^{\circ}\text{C}$)	236	25.7	24.6
	GP_HS31_sum	Cumulative heat stress temperature with $T_{\max} > 31^{\circ}\text{C}$ ($^{\circ}\text{C}$)	236	16.4	14.6
	GP_HS27_Tm_sum	Cumulative heat stress temperature with $T_{\text{mean}} > 27^{\circ}\text{C}$ ($^{\circ}\text{C}$)	236	3.7	2.4
	GP_ETPm	Daily potential evapotranspiration means (mm)	229	18.5	15.2
	GP_ETPs	Total potential evapotranspiration sum (mm)	229	10.4	8.8
	GP_CWBm	Daily climatic water balance mean (mm)	229	2.7	-
	GP	Duration (d)	232	4.6	3.1
Vegetative phase	VP_T_mean	Mean temperature ($^{\circ}\text{C}$)	231	2	6.7
	VP_HR20_n	Number of days with precipitation > 20 mm (mm)	236	2.6	2.4
	VP_HR20_sum	Cumulative rainfall amount of days with precipitation > 20 mm (mm)	236	3.1	2.9
	VP_CWBneg_n	Number of days with negative climatic water balance	236	3.4	2.4
	VP_TD	Thermal duration ($^{\circ}\text{Cd}$)	231	1.8	6.3
Leaf development phase	LP_T_mean	Mean temperature ($^{\circ}\text{C}$)	231	2.5	9
	LP_GR_mean	Daily global radiation mean (W m^{-2})	195	6.3	8.7
	LP_GR_sum	Cumulative global radiation amount (W m^{-2})	195	1.9	3
	LP_P_mean	Daily precipitation means (mm)	231	3.2	-
	LP_CWBm	Daily climatic water balance mean (mm)	231	3.5	-
	LP_CWBneg_n	Number of days with negative climatic water balance	236	3.4	2.2
	LP_TD	Thermal duration ($^{\circ}\text{Cd}$)	231	1.8	7.2

	LP	Duration (d)	233	1.7	2.5
Stem elongation phase	SP_GR_mean	Daily global radiation means ($W m^{-2}$)	196	4.8	4.3
	SP_P_sum	Total precipitation sum (mm)	231	3.3	4.9
	SP_HR20_n	Number of days with precipitation > 20 mm	236	3.3	3.7
	GS_HR20_sum	Cumulative rainfall amount of days with precipitation > 20 mm	236	3.3	3.9
Sowing	SD	Day of year	233	8.7	7.6
Emergence	ED	Day of year	233	8.9	7.5
Hard dough	HDD	Day of year	234	5.2	2
Harvest	HVD	Day of year	233	2.8	-

Table 9 Estimated explained variance of the agro-climatic variables (units in parentheses) on winter wheat yield development between 1958 and 2006 across the study sites that are characterised through soil yield potential lower than 70 quality points and after removing the effect of soil yield potential or the soil type. All explained variances are estimated after accounting for the genetic and non-genetic time trends. Additionally, the effect of the soil type was removed in second model

Phenological phase or stage	Agro-climatic variable	Description	n	Explained variance (%)	
				Removed soil effect	
				Soil type	
Growing season	GS_HS27_n	Number of heat stress days with $T_{max} > 27^{\circ}C$	141	28.9	
	GS_HS31_n	Number of heat stress days with $T_{max} > 31^{\circ}C$	141	15.8	
	GS_HS27_Tm_n	Number of heat stress days with $T_{mean} > 27^{\circ}C$	141	-	
	GS_HS27_sum	Cumulative heat stress temperature with $T_{max} > 27^{\circ}C$ ($^{\circ}C$)	141	29.5	
	GS_HS31_sum	Cumulative heat stress temperature with $T_{max} > 31^{\circ}C$ ($^{\circ}C$)	141	15.7	
	GS_HS27_Tm_sum	Cumulative heat stress temperature with $T_{mean} > 27^{\circ}C$ ($^{\circ}C$)	141	-	
	GS_ETPm	Daily potential evapotranspiration mean ($mm d^{-1}$)	136	12.6	

	GS_ETPs	Total potential evapotranspiration sum (mm)	136	14.2
	GS_CWBm	Daily climatic water balance mean (mm d ⁻¹)	136	1.2
	GS_CWBs	Total climatic water balance sum (mm)	136	1.5
	GS_CWBneg_n	Number of days with negative climatic water balance	141	2.9
	GS_TD	Thermal duration (°Cd)	136	17.7
	GS	Duration (d)	138	6.7
Generative phase	GP_T_mean	Mean temperature (°C)	134	16.5
	GP_T_max	Max temperature mean (°C)	137	23.1
	GP_HS27_n	Number of heat stress days with T _{max} > 27°C	141	32.4
	GP_HS31_n	Number of heat stress days with T _{max} > 31°C	141	17.2
	GP_HS27_Tm_n	Number of heat stress days with T _{mean} > 27°C	141	-
	GP_HS27_sum	Cumulative heat stress temperature with T _{max} > 27°C (°C)	141	33.1
	GP_HS31_sum	Cumulative heat stress temperature with T _{max} > 31°C (°C)	141	17.3
	GS_HS27_Tm_sum	Cumulative heat stress temperature with T _{mean} > 27°C (°C)	141	-
	GP_GR_sum	Total global radiation sum (W m ⁻²)	108	
	GP_ETPm	Daily potential evapotranspiration mean (mm)	134	23
	GP_ETPs	Total potential evapotranspiration sum (mm)	134	13.5
	GP_CWBm	Daily climatic water balance mean (mm)	134	4.9
	GP_CWBs	Total climatic water balance sum (mm)	134	1.1
	GP	Duration (d)	137	9.1
Vegetative phase	VP_GR_mean	Daily global radiation mean (W m ⁻²)	108	3
	VP_CWBneg_n	Number of days with negative climatic water balance	141	3.3
	LP_GR_mean	Daily global radiation mean (W m ⁻²)	108	7.4

Leaf development phase	LP_CWBneg_n	Number of days with negative climatic water balance	141	2.8
	LP	Duration (d)	138	2.9
Sowing	SD	Day of year	138	7.1
Emergence	ED	Day of year	138	5.2
Hard dough	HDD	Day of year	139	3.3
Harvest	HVD	Day of year	138	2.5

Table 10 Estimated explained variance of the agro-climatic variables (units in parentheses) on winter wheat yield development between 1958 and 2006 across the study sites that are characterised through soil yield potential greater 70 quality points and after removing the effect of soil yield potential or the soil type. All explained variances are estimated after accounting for the genetic and non-genetic time trends. Additionally, the effect of the soil type was removed in second model

Phenological phase or stage	Agro-climatic variable	Description	n	Explained variance (%)
				Removed soil effect
				Soil type
Growing season	GS_HS27_n	Number of heat stress days with $T_{max} > 27^{\circ}\text{C}$	95	15.7
	GS_HS31_n	Number of heat stress days with $T_{max} > 31^{\circ}\text{C}$	95	27
	GP_HS27_Tm_n	Number of heat stress days with $T_{mean} > 27^{\circ}\text{C}$	95	9.8
	GS_HS27_sum	Cumulative heat stress temperature with $T_{max} > 27^{\circ}\text{C}$ ($^{\circ}\text{C}$)	95	17.2
	GS_HS31_sum	Cumulative heat stress temperature with $T_{max} > 31^{\circ}\text{C}$ ($^{\circ}\text{C}$)	95	28.4
	GS_HS27_Tm_sum	Cumulative heat stress temperature with $T_{mean} > 27^{\circ}\text{C}$ ($^{\circ}\text{C}$)	95	9.8
	GS_GR_mean	Daily global radiation means (W m^{-2})	87	4.6
	GS_ETPm	Daily potential evapotranspiration means (mm)	95	7.8
	GS_ETPs	Total potential evapotranspiration sum (mm)	95	9.7
Generative phase	GP_T_mean	Mean temperature ($^{\circ}\text{C}$)	95	14.8

	GP_T_max	Maximum temperature (°C)	95	12.6
	GP_HS27_n	Number of heat stress days with $T_{max} > 27^{\circ}\text{C}$	95	15
	GP_HS31_n	Number of heat stress days with $T_{max} > 31^{\circ}\text{C}$	95	30.2
	GP_HS27_Tm_n	Number of heat stress days with $T_{mean} > 27^{\circ}\text{C}$	95	9.8
	GP_HS27_sum	Cumulative heat stress temperature with $T_{max} > 27^{\circ}\text{C}$ (°C)	95	16.7
	GP_HS31_sum	Cumulative heat stress temperature with $T_{max} > 31^{\circ}\text{C}$ (°C)	95	31.6
	GP_HS27_Tm_sum	Cumulative heat stress temperature with $T_{mean} > 27^{\circ}\text{C}$ (°C)	95	9.8
	GP_GR_sum	Total global radiation sum (W m^{-2})	87	-
	GP_ETPm	Daily potential evapotranspiration mean (mm)	95	8.6
	GP_ETPs	Total potential evapotranspiration sum (mm)	95	7.1
	GP_TD	Thermal duration (°Cd)	95	-
Vegetative phase	VP_TD	Thermal duration (°Cd)	95	1.9
Leaf development phase	LP_GR_mean	Daily global radiation mean (W m^{-2})	87	23.6
	LP_GR_sum	Total global radiation sum (W m^{-2})	87	6.6
Stem elongation phase	SP_HS27_n	Number of heat stress days with $T_{max} > 27^{\circ}\text{C}$	95	1.9
	SP_HS27_sum	Cumulative heat stress temperature with $T_{max} > 27^{\circ}\text{C}$ (°C)	59	2
	SP_GR_mean	Daily global radiation mean (W m^{-2})	87	5
	SP_P_mean	Daily precipitation mean (mm)	95	2
	SP_P_sum	Total precipitation sum (mm)	95	6.3
	SP_CWBm	Daily climatic water balance mean (m)	95	1.9
	SP_CWBs	Total climatic water balance sum (mm)	95	4.1
Sowing	SD	Date (Day of year)	95	1.5
Emergence	ED	Date (Day of year)	95	17.2

Table 11 Estimated explained variance of the agro-climatic variables (units in parentheses) on winter wheat yield development between 1958 and 2006 across the study sites that are characterised through light soils. All explained variances are estimated after accounting for the genetic and non-genetic time trends. Additionally, the effect of the soil yield potential was removed in second model

Phenological phase or stage	Agro-climatic variable	Description	n	Explained variance (%)		
				Removed soil effect	Yield potential	
Growing season	GS_HS27_n	Number of heat stress days with $T_{\max} > 27^{\circ}\text{C}$	121	37	39.5	
	GS_HS31_n	Number of heat stress days with $T_{\max} > 31^{\circ}\text{C}$	121	15.4	14.9	
	GS_HS27_TM_n	Number of heat stress days with $T_{\text{mean}} > 27^{\circ}\text{C}$	121	2.9	1.2	
	GS_HS27_sum	Cumulative heat stress temperature with $T_{\max} > 27^{\circ}\text{C}$ ($^{\circ}\text{C}$)	107	35.9	36.2	
	GS_HS31_sum	Cumulative heat stress temperature with $T_{\max} > 31^{\circ}\text{C}$ ($^{\circ}\text{C}$)	53	11.1	8.7	
	GS_P_sum	Total precipitation sum (mm)	117	1.2		
	GS_HR40_n	Number of days with precipitation > 40 mm	121	1.6	1.8	
	GS_HR20_sum	Cumulative rainfall amount of days with precipitation > 20 mm	70		2.1	
	GS_CWBneg_n	Number of days with negative climatic water balance	121	4.3	5	
	GS_ETPm	Daily potential evapotranspiration mean (mm)	117	21.6	17.1	
	GS_ETPs	Total potential evapotranspiration sum (mm)	117	22.7	16.7	
	GS_CWBm	Daily climatic water balance mean (mm)	117	3		
	GS_CWBs	Total climatic water balance sum (mm)	117	4.2		
	GS_TD	Thermal duration ($^{\circ}\text{Cd}$)	117	5.4	8.7	
	GS	Duration (d)	119	23.5	25.5	
	Generative phase	GP_T_mean	Mean temperature ($^{\circ}\text{C}$)	115	27.7	25.1

	GP_T_max	Max temperature mean (°C)	118	34.3	34.7
	GP_HS27_n	Number of heat stress days with $T_{max} > 27^{\circ}\text{C}$	121	39.3	44.2
	GP_HS31_n	Number of heat stress days with $T_{max} > 31^{\circ}\text{C}$	121	21.4	22.8
	GP_HS27_Tm_n	Number of heat stress days with $T_{mean} > 27^{\circ}\text{C}$	121	2.9	1.2
	GP_HS27_sum	Cumulative heat stress temperature with $T_{max} > 27^{\circ}\text{C}$ (°C)	105	34.6	37.6
	GP_GR_sum	Total global radiation sum (W m^{-2})	105	2.8	4.1
	GP_ETPm	Daily potential evapotranspiration mean (mm)	115	32.7	31.5
	GP_ETPs	Total potential evapotranspiration sum (mm)	115	19.6	15.5
	GP_CWBm	Daily climatic water balance mean (mm)	115	3.5	1.4
	GP_CWBs	Total climatic water balance sum (mm)	115	1.9	
	GP_CWBneg_n	Number of days with negative climatic water balance	121	1.1	1.1
	GP_TD	Thermal duration (°Cd)	115		5.6
	GP	Duration (d)	118	14.7	20.4
Vegetative phase	VP_HS27_n	Number of heat stress days with $T_{max} > 27^{\circ}\text{C}$	121	6.5	3
	VP_HS31_n	Number of heat stress days with $T_{max} > 31^{\circ}\text{C}$	121	2.1	4.5
	VP_GR_mean	Daily global radiation mean (W m^{-2})	105	4.3	6.3
	VP_GR_sum	Total global radiation sum (W m^{-2})	105		3.7
	VP_HR20_n	Number of days with precipitation > 20 mm	121	1.5	2.9
	VP_CWBneg_n	Number of days with negative climatic water balance	121	6.9	5.6
	VP_ETPm	Daily potential evapotranspiration mean (mm)	116	7	4.3
	VP_ETPs	Total potential evapotranspiration sum (mm)	116	7.9	4.8
	VP_TD	Thermal duration (°Cd)	116	1.8	1.6
	VP	Duration (d)	118	5.8	4.5

Leaf development phase	LP_T_mean	Mean temperature (°C)	116		1.4
	LP_GR_mean	Daily global radiation mean (W m ⁻²)	105	4.3	3.6
	LP_GR_sum	Total global radiation sum (W m ⁻²)	105	1.2	
	LP_ETPm	Daily potential evapotranspiration mean (mm)	116	3.3	
	LP_ETPs	Total potential evapotranspiration sum (mm)	116	1.1	
	LP_CWBneg_n	Number of days with negative climatic water balance	121	6.1	4
	LP_TD	Thermal duration (°Cd)	116	3.8	5.5
	LP	Duration (d)	118	10.1	12.2
Stem elongation phase	SP_HS27_n	Number of heat stress days with T _{max} > 27°C	121	3.7	1.3
	SP_HS31_n	Number of heat stress days with T _{max} > 31°C	121	2.1	4.5
	SP_ETPs	Total potential evapotranspiration sum (mm)	116	1.4	3
	SP_CWBneg_n	Number of days with negative climatic water balance	121	2.2	4.1
	SP_TD	Thermal duration (°Cd)	116		1.7
	SP	Duration (d)	116		2.8
Sowing	SD	Date (Day of year)	118	17.2	20.9
Emergence	ED	Date (Day of year)	118	13.5	12.7
Stem elongation begin	SED	Date (Day of year)	119	2.8	5
Hard dough	HDD	Date (Day of year)	120	12.5	17.2
Harvest	HVD	Date (Day of year)	119	8.5	6.4

Table 12: Estimated explained variance (%) of the agro-climatic variables (units in parentheses) on winter wheat yield development between 1958 and 2006 across the study sites that are characterised through heavy soils. All explained variances are estimated after accounting for the genetic and non-genetic time trends. Additionally, the effect of the soil yield potential was removed in second model

Phenological phase or stage	Agro-climatic variable	Description	n	Explained variance (%)	
				Removed soil effect	Yield potential
Growing season	GS_HS27_n	Number of heat stress days with $T_{max} > 27^{\circ}\text{C}$	115	10.1	7.7
	GS_HS31_n	Number of heat stress days with $T_{max} > 31^{\circ}\text{C}$	115	22.1	20.5
	GS_HS27_Tm_n	Number of heat stress days with $T_{mean} > 27^{\circ}\text{C}$	115	2	2.5
	GS_HS27_sum	Cumulative heat stress temperature with $T_{max} > 27^{\circ}\text{C}$ ($^{\circ}\text{C}$)	114	10.8	8.4
	GS_HS31_sum	Cumulative heat stress temperature with $T_{max} > 31^{\circ}\text{C}$ ($^{\circ}\text{C}$)	61	28.7	26.9
	GS_GR_mean	Daily global radiation mean (W m^{-2})	90	1.7	
	GS_GR_sum	Total global radiation sum (W m^{-2})	90	2.6	1.8
	GS_HR20_sum	Cumulative rainfall amount of days with precipitation > 20 mm	97	29.2	27.9
	GS	Duration (d)	114		
Generative phase	GP_T_mean	Mean temperature ($^{\circ}\text{C}$)	114	3.9	3.9
	GP_T_max	Maximum temperature ($^{\circ}\text{C}$)	114	6.9	5.7
	GP_HS27_n	Number of heat stress days with $T_{max} > 27^{\circ}\text{C}$	115	13.6	11.6
	GP_HS31_n	Number of heat stress days with $T_{max} > 31^{\circ}\text{C}$	115	23.1	22.1
	GP_HS27_Tm_n	Number of heat stress days with $T_{mean} > 27^{\circ}\text{C}$	115	2	2.5
	GP_HS27_sum	Cumulative heat stress temperature with $T_{max} > 27^{\circ}\text{C}$ ($^{\circ}\text{C}$)	114	14.9	12.8
	GP_HS31_sum	Cumulative heat stress temperature with $T_{max} > 31^{\circ}\text{C}$ ($^{\circ}\text{C}$)	56	20.7	15.1

	GP_GR_sum	Total global radiation sum ($W\ m^{-2}$)	90	5.9	5.9
Vegetative phase	VP_HR20_sum	Cumulative rainfall amount of days with precipitation > 20 mm	84	40.3	42.4
	VP_ETPs	Total potential evapotranspiration sum (mm)	115		1.3
Leaf development phase	LP_GR_mean	Daily global radiation mean ($W\ m^{-2}$)	90	12.1	20
	LP_GR_sum	Total global radiation sum ($W\ m^{-2}$)	90	5	10.1
	LP_P_mean	Daily precipitation mean (mm)	115	4.4	7.4
	LP_P_sum	Total precipitation sum (mm)	115	2.8	3.5
	LP_HR20_n	Number of days with precipitation > 20 mm	115	2.4	1.6
	LP_CWBm	Daily climatic water balance mean (mm)	115	2.5	6.7
	LP_CWBs	Total climatic water balance sum (mm)	115	5.9	8.7
Stem elongation phase	SP_HS27_sum	Cumulative heat stress temperature with $T_{max} > 27^{\circ}C$ ($^{\circ}C$)	67		1.2
	SP_GR_mean	Daily global radiation mean ($W\ m^{-2}$)	90	12.8	18.5
	SP_GR_sum	Total global radiation sum ($W\ m^{-2}$)	90	4	11.7
	SP_P_mean	Daily precipitation mean (mm)	115	6.1	7.8
	SP_P_sum	Total precipitation sum (mm)	115	11.8	10.7
	SP_HR20_n	Number of days with precipitation > 20 mm	115	1.6	
	SP_ETPm	Daily potential evapotranspiration mean (mm)	115	5	5.1
	SP_ETPs	Total potential evapotranspiration sum (mm)	115		2.9
	SP_CWBm	Daily climatic water balance mean (mm)	115	8.1	9.7
	SP_CWBs	Total climatic water balance sum (mm)	115	15	16.9
Sowing	SD	Date (Day of year)	115	2.9	2.4
Emergence	ED	Date (Day of year)	115	6.8	7.5

Additional material

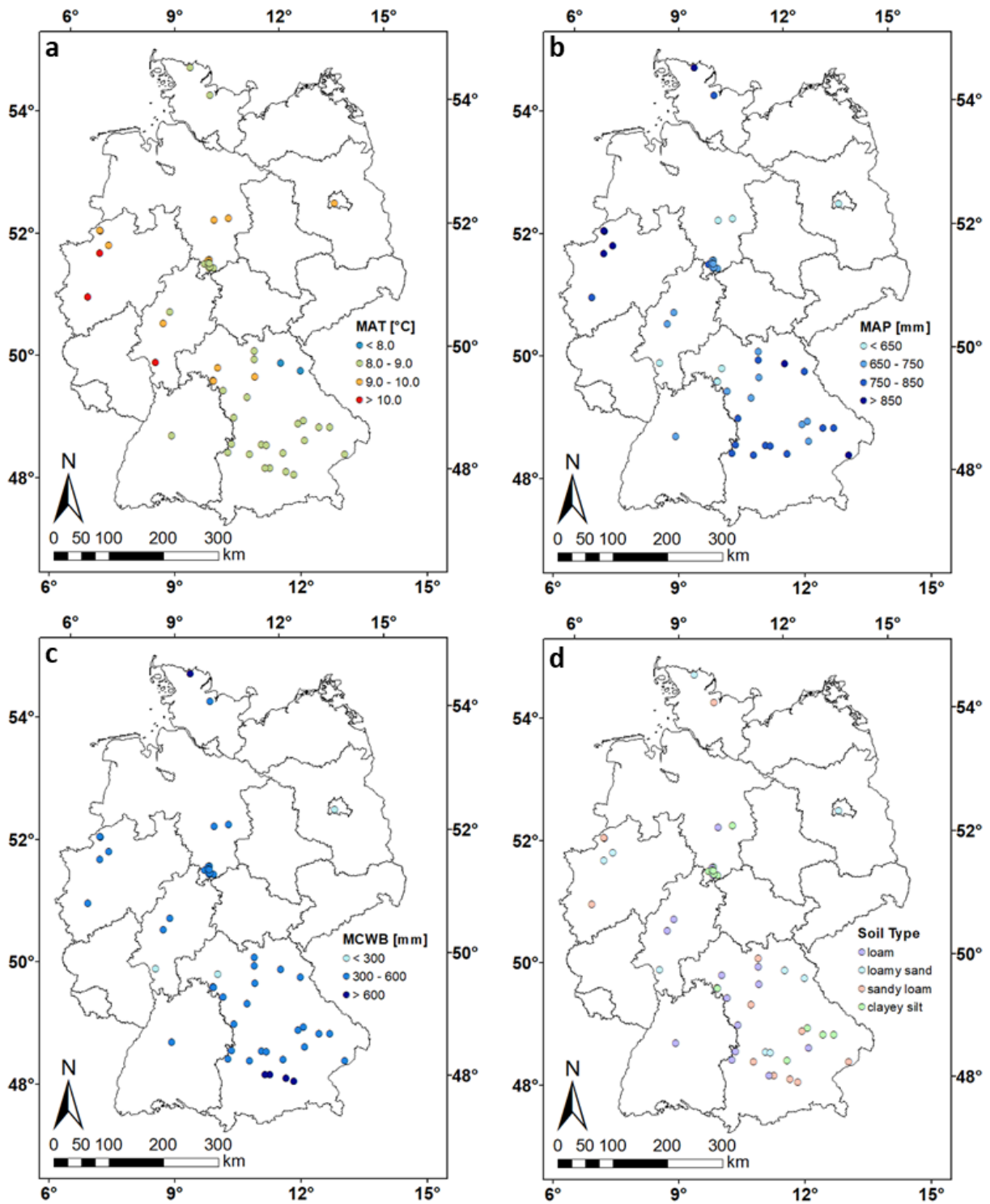


Figure 21: Spatial distribution of the locations in this study and their long term (1977-2006) climate and soil conditions. a, Mean annual temperature (MAT). b, Mean annual precipitation (MAP). c, Mean annual climatic water balance (MCWB). d, Soil types after reference (Ad-hoc-AG Boden 2005)

Determining the within-field yield variability from seasonally changing soil conditions

Eric Boenecke¹, Erika Lueck², Joerg Ruehlmann³, Ralf Gruending¹, Uwe Franko¹

¹Department for Soil Physics, Helmholtz Centre for Environmental Research – UFZ, 06120 Halle, Germany

²Institute of Earth and Environmental Science – Applied Geophysics, University of Potsdam, 14476 Potsdam, Germany

³Department of Plant Nutrition, Leibniz Institute of Vegetable and Ornamental Crops – IGZ, 14979 Grossbeeren, Germany

Abstract

Crop yield variations are strongly influenced by the spatial and temporal availabilities of water and nitrogen in the soil during the crop growth season. To estimate the quantities and distributions of water and nitrogen within a given soil, process-oriented soil models have often been used. These models require detailed information about the soil characteristics and profile architecture (e.g., soil depth, clay content, bulk density, field capacity and wilting point), but high-resolution information about these soil properties, both vertically and laterally, is difficult to obtain through conventional approaches. However, on-the-go electrical resistivity tomography (ERT) measurements of the soil and data inversion tools have recently improved the lateral resolutions of the vertically distributed measurable information. Using these techniques, nearly 19,000 virtual soil profiles with defined layer depths were successfully created for a 30 ha silty cropped soil over loamy and sandy substrates in Central Germany, which were used to initialise the CARbon and Nitrogen DYnamics (CANDY) model. The soil clay content was derived from the electrical resistivity (ER) and the collected soil samples using a simple linear regression approach (the mean R^2 of clay = 0.39). The additional required structural and hydrological properties were derived from pedotransfer functions. The modelling results, derived soil texture distributions and original ER data were compared with the spatial winter wheat yield distribution in a relatively dry year using regression and boundary line analysis. The yield variation was best explained by the simulated soil water content ($R^2 = 0.18$) during the grain filling and was additionally validated by the measured soil water content with a root mean square error (RMSE) of 7.5 Vol.%.

Keywords

Soil process modelling · Electrical Resistivity Tomography (ERT) · Soil water variability · Boundary line analysis

Introduction

Within-field variations in crop growth and productivity are caused by the spatial and temporal availabilities of water and nitrogen in the soil (Eghball et al. 2003; Shahandeh et al. 2005). Their distributions, however, depend on complex interactions between the spatial distributions of soil properties, weather conditions and field management (Batchelor et al. 2002; Machado et al. 2002). With regard to the soil, soil texture is one of the main factors influencing within-field variability that farmers have little control over (Godwin and Miller 2003). Similarly, several studies have shown yield variabilities between dry and wet years (Kaspar et al. 2004; Kravchenko et al. 2003). In contrast, yields are more easily controlled by field management, such as via tillage practices and crop rotation (Kravchenko et al. 2003; Berzsenyi et al. 2000; Varvel 2000).

To simulate the effects of field management and weather conditions on the soil water and nitrogen availabilities for a given soil type, process-oriented soil organic matter (SOM) models have been used numerous times (Stockmann et al. 2013). For instance, Smith et al. (1997) tested nine SOM models using long-term data sets from seven long-term experimental sites to predict long-term changes in the SOM. The advantages of these models are their relatively easy initialization, their relatively simple structure, their potential use for larger scales and time-steps (Smith et al. 1998). Furthermore, they can easily be linked to GIS software and used with relatively low computational intensities (Stockmann et al. 2013).

However, SOM models remain insufficiently considered in precision agriculture (PA) (Manzoni and Porporato 2009; Stoorvogel and Bouma 2005). Most of these models use a one-dimensional conceptual approach to describe the water and nitrogen movements within several profile layers (Smith et al. 1998; Vereecken et al. 2016). Thus, a detailed description of the profile architecture (e.g., layer thickness, soil texture, bulk density, water retention characteristic) is advantageous for initializing the models. This soil information is normally obtained from traditional general purpose soil maps. These maps depict soil type differences as relatively large polygon units or at small scales which appear inappropriate for PA (Robert 1993). For example, the classical soil survey map which was available for the field used in this study delineates only six soil unit classes arranged in 14 polygon units (Figure 26, left). These units are derived from representative soil profiles, or constant (but large) survey grids. However, such data can be affected by spatial uncertainties due to the soil variabilities between two measurement points (Pracilio et al. 2003; Wong and Asseng 2004, 2006).

To bridge this gap in soil information, a higher resolution is required. Therefore, Hartemink and Minasny (2014) and Viscarra Rossel et al. (2011) highlighted the potential of proximal soil sensing techniques. Vereecken et al. (2016), in particular, suggested linking the soil process models with modern spatial survey measurements to determine the seasonal changes in nutrient and water availability. Although there is an overall lack of explicit spatial SOM models that describe SOM dynamics precisely at the field scale, Kruger et al. (2013) linked site-specific variations (electromagnetic inductions) and detailed soil depth information (ground penetrating radar) with agro-ecosystem modelling. They investigated the suitability of the geophysics of the model results of grain maize biomass production. In another study by Wong et al. (2006), a crop-soil simulation model was upscaled based on high-resolution apparent soil electrical conductivity (ECa) maps to identify site-specific areas with the greatest financial and environmental risks in a Mediterranean environment.

Information about the soil properties can be retrieved using mobile systems for continuous (on-the-go) measurements from the surface, as well as direct-push-techniques and borehole systems (stop-and-go). Investigations have shown that the ECa and its reciprocal, the apparent electrical resistivity (ERa), are particularly useful as a proxy for the physical properties of soil with stable field patterns when used for PA (Adamchuk et al. 2004; Allred et al. 2008; Gebbers and Lück 2005; Grisso et al. 2009; Vitharana et al. 2008). ERa is largely dependent on the particle size distribution, which affects the soil moisture content as a result of pore size differences, and on the soil salinity, which is related to smaller particles, such as clay and fine silt (Brevik et al. 2006; Corwin and Lesch 2003; Fukue et al. 1999; Samouelian et al. 2005). The studied soil volume and soil depth depend on the individual sensor specifications (Allred et al. 2008; Gebbers and Lück 2005). Sensitivity functions are used to characterize the depth of the investigation, as well as the maximum depth of exploration with the sensor used. The depths of investigation characteristic (DIC) functions identify the contribution from a thin layer to the measured signal for the specific sensor. Thus, the depth of the investigation can be defined unambiguously as the depth of the maximum response due to a horizontal thin layer within a half space (Roy and Apparao 1971). The 70 % cumulative response is used to estimate the depth of exploration (McNeill 1980). Commercially available instruments, such as the EM38 (McNeill 1980; Rhoades et al. 1989), the Dualem system (Dualem 2005), the VERIS-3100 device (Lund et al. 1999) and the ARP system (Dabas et al. 1994), have their characteristic depths of investigation. The DIC is either determined by the geometry of the electrodes for the direct current devices (Roy and Apparao 1971) or by the coil spacing for the induction method (McNeill 1980; Saey et al. 2009) and their signal frequencies (Schamper et al. 2012).

Because of the fixed specifications of these systems, they are mainly used to image lateral changes of the electrical soil properties and, therefore, only identify trends of a vertical nature. However, relatively new on-the-go multi-sensor systems have been developed to map the soil ERa variations from the surface for both the lateral and vertical direction (Lueck and Ruehlmann 2013; Pan et al. 2014). The Geophilus system used in the former study combines a rolling electrode system with an electronic power supply and measurement device (Lueck and Ruehlmann 2013). With this advanced sensor system, the electrical data can be continuously recorded with a significantly higher lateral resolution of a few meters and for a larger exploration depth of approximately 1.5 m (Lueck and Ruehlmann 2013). The primary data includes information about the entire soil volume from the soil surface down to the depth of exploration, weighted by the sensitivity function of the sensor. The inverted ERa data, however, provides information about certain layers within the soil profile and can be found by applying numerical inversion tools (Loke and Barker 1995; Pellerin and Wannamaker 2005; Samouelian et al. 2005). Various examples of detecting the vertical structure of the soils using non-invasive methods are given by Besson et al. (2004), Saey et al. (2015) and Tabbagh et al. (2000).

Additionally, SOM models require information about the soil water retention characteristics (field capacity, wilting point) and structural soil characteristics (bulk density, pore volume, particle density). Pedotransfer functions (PTF's) are the recommended tools for deriving these parameters for soil models (Vereecken et al. 2016). They close the gap between the scarce direct soil measurements and the soil data that is required for the application of high-resolution soil models (McBratney et al. 2002; Vereecken et al. 2016; Wosten et al. 2001).

The objective of this study was to (i) combine soil process knowledge with high resolution and well distributed geophysical measurements and (ii) compare the simulated spatial soil water variability with the within-field crop yield patterns in a semi-arid loess soil area. Simulations of the soil water distribution were done using the soil process model CARbon and Nitrogen DYnamics (CANDY). To obtain the required inherent soil parameters for the model, the soil texture was derived from inverted ERa data, and additional structural and hydrological properties were derived from pedotransfer functions. To evaluate the model results, the georeferenced winter wheat yield monitor data from 2011 was compared with the modelled spatial soil water content, derived soil texture distribution and the basic layer-specific ER data. The comparison was done for a relevant farming grid of 36 x 36 m using regression and boundary line analysis. Furthermore, the simulated soil water content was validated by the measured soil water content using the root mean square error (RMSE).

Materials and Methods

Study area

The study was conducted on a 30 ha field (51°40'30" N, 12°00'09" E) located in Central Germany, east of the Harz Mountains and 20 km north of the city Halle (Saale). This area is part of the European loess belt, which stretches from Western Europe (France, Belgium) to the Eastern European (Ukraine, Russia) lowlands (Haase et al. 2007). The topography of the study region is undulating, and the selected field has a flat terrain in the north-east (88.4 m a.s.l), sloping gently into a depression in the south-west (84.1 m a.s.l) (Figure 24, left).

The soil types in this area are generally classified as Chernozem and Cambisol by the FAO classification system. They were formed from Holocene aeolian deposits (carbonate loess) over fluvioglacial deposits and morainic material from the Middle Pleistocene period (Saale ice age) (Knoth 1992; Eissmann 1994). Thus, topsoil conditions are considered homogeneous, and soil variability is supposed to occur in the subsoil.

The daily resolution weather data (air temperature, precipitation, sunshine duration) were provided by the nearest agrometeorological stations of the German Weather Service (DWD) within a 30 km radius at the research site. The prevailing climatic condition is temperate, with a mean annual temperature of 9.7°C and a mean annual precipitation of 533 mm (1981–2010). Thus, the amount of water within the rooting zone of the soil is one of the limiting factors for crop growth in this area. The annual precipitation in the relatively dry year 2011 was 40 mm below the long-term annual average. The amounts of precipitation in March, April and May (crop growth season) in 2011 were 27.7 mm, 12.8 mm and 40.9 mm below the mean monthly amounts of precipitation, respectively (Figure 22).

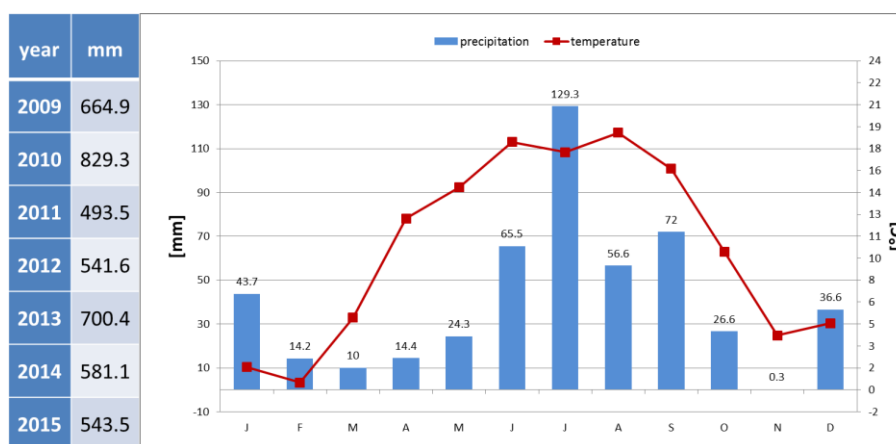


Figure 22: Left: annual precipitation sums of the modelling period (2009-2015); right: monthly average temperature and precipitation sum in 2011

Cultivation represents the conventional farming practices of this area. The management data were provided by the farmer for the period 2009 to 2015 and thus are a limiting factor for the modelling period. The crop rotation included canola (*Brassica napus*) in 2009 and 2014, winter wheat (*Triticum aestivum*) in 2010, 2011, 2013 and 2015, and grain maize (*Zea mays*) in 2012. The canola yields were 4.1 t ha^{-1} and 4.8 t ha^{-1} , respectively, and the winter wheat yields ranged from 5.2 to 8.2 t ha^{-1} (mean = 7.1 t ha^{-1}). In 2012, 10.5 t ha^{-1} of corn were produced. The applied mineral fertilizers were urea, urea ammonium nitrate and calcium ammonium nitrate. The average amount of applied N per annum was approximately 160 kg ha^{-1} for the canola and winter wheat crops and 115 kg ha^{-1} for the corn crops. No irrigation occurred.

Electrical conductivity mapping and data inversion

At the study site, the relatively new Geophilus system, developed by Lueck and Ruehlmann (2013), was used. This mobile device was developed to record not only lateral but also vertical ER changes, making it possible to conduct imaging of both the lateral heterogeneity and stratification. The version used is based on equatorial dipole-dipole arrays consisting of one transmitter dipole and five pairs of potential electrodes. A sketch and a photo of the electrode configuration can be found in Figure 23.

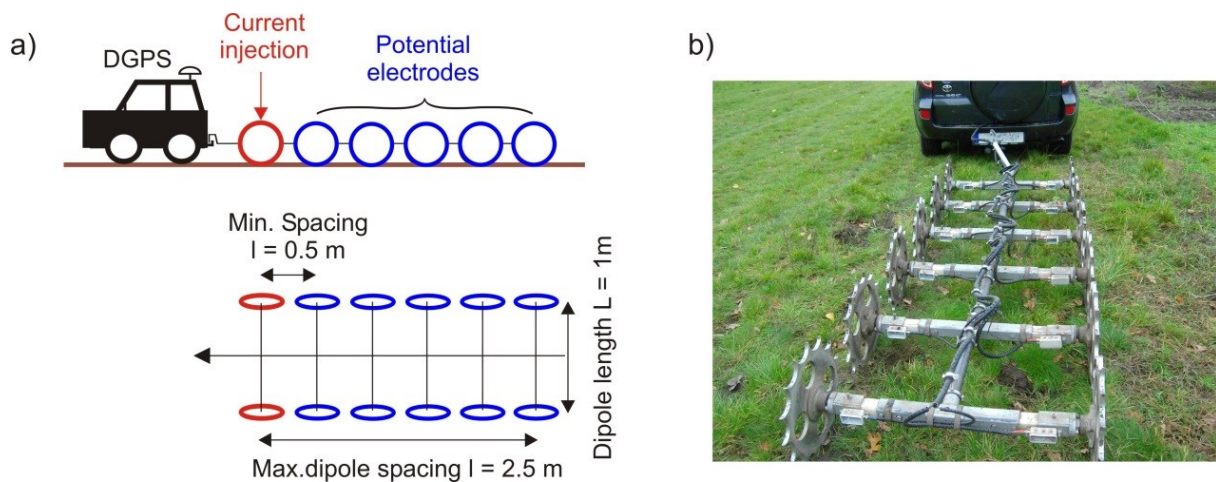


Figure 23: Sketch (a) and photo (b) of the Geophilus system. The electrodes are arranged as an equatorial dipole-dipole-array with a dipole length of 1 m. The dipole spacing ranges from 0.5 to 2.5 m

The dipole length of all dipoles was 1 m. The dipole spacing ranged from 0.5 to 2.5 m (representing channels 1 to 5) with increments of 0.5 m. Increasing dipole spacing results in increasing depths of investigation. The data for the first dipole distance are mostly focused on the uppermost soil (depth of maximum response is approximately 0.25 m). With greater dipole distances, the signal reaches greater depths but with more flattened peaks of maximum sensitivity.

The data from the last dipole, with a spacing of 2.5 m, reaches a depth of 1.5 m. The electronic measurements were carried out with the instrument 'rabbit' (produced by Radic-Research, Berlin, Germany) which is optimized for quasi continuous data acquisition (Radic 2014). The Geophilus data were geo-referenced with an accuracy of ± 0.1 m (dGPS).

The Geophilus field campaign was conducted in August 2014 (Figure 24, right). Good soil conditions with respect to the galvanic coupling between the soil and electrodes resulted in a high signal-to-noise ratio. The galvanic contact for the mobile resistivity measurements is influenced not only by the soil moisture but also by the character of the surface. Wet soil resulted in a better contact than dry soil, and soft and smooth surfaces resulted in a better contact than rough or hard surfaces. All electrical measurements were performed at the surface. The ERA was calculated using the injected current, the measured voltages of the five pairs of electrodes and the configuration factor of the equatorial dipole-dipole electrode array. Using a low-frequency electrical current, the apparent resistivity was calculated and stored in its complex form for both the absolute value and the phase angle. Digital stacking reduces the noise and enables the noise itself to be quantified by considering the standard deviation for each data point. For further data processing, all data were stored in a simple ASCII-format. An estimated standard deviation of less than 10 % is relatively rare for dynamic measurements but was reached for nearly all channels (channel 1-4). Only the last channel was found to be noisier, with a standard deviation of 16 % for the amplitudes of resistivity. The inline point spacing is restricted by the sampling rate of the instrument and the driving velocity and was approximately 2.5 m. The cross-line point spacing was 12 m. The data processing included a correction for the offset between the GPS and electrodes, an elimination of outliers and a near neighbour gridding with a unique grid spacing of 6 m using a triangle-based linear interpolation.

The apparent resistivity measured at the surface can be regarded as the spatial mean of the true resistivity of the individual layers weighted by the sensitivity function of the corresponding horizontal dipole-dipole array. The transformation of the apparent resistivities into the true specific resistivities of the soil layers is carried out using data inversion (Menke 2012). Starting with the measured data, the model parameters, in the form of a resistivity model, are estimated. Using this estimated spatial parameter distribution; synthetic data are modelled and compared with the observed data. The parameter distribution fits the data well if the differences between the measured and the modelled data are small. For these data processing steps, the commercial tool RES2DINV by Loke and Barker (1996) was used. Only the 2-dimensional inversion was considered because the crossline sampling is usually greater than the footprint of the electrode array used. The large number of data points (more than 30000) caused them to be split into smaller datasets. Therefore, the data of each line (approximately 1000 data points) were inverted separately and then were later

combined. The thickness of the grid cells in the model discretization was adapted to the unit dipole spacing of 0.5 m and the resulting depth resolution. Starting with a thickness of 0.25 m for the first layer, the thickness of every deeper layer increased by 10 %. The sensitivity function of a lateral dipole-dipole array, with a dipole length of 1 m, results in a depth of exploration of approximately 1.5 m (Lueck and Ruehlmann 2013). In spite of the discretization of the model, less than five layers can be expected for a Geophilus dataset (composed of several grid cells with similar resistivities). The discretisation of the model for the inversion process, with respect to the electrode spacing, led to block depths of 0.12 m, 0.26 m, 0.41 m, 0.58 m, 0.76 m, 0.96 m, 1.19 m, 1.43 m and 1.70 m with a 4 x 4 m resolution, producing a total of 18763 georeferenced data points. Additionally, the topographic conditions were also detected from the measurements of the Geophilus (Figure 24, left).

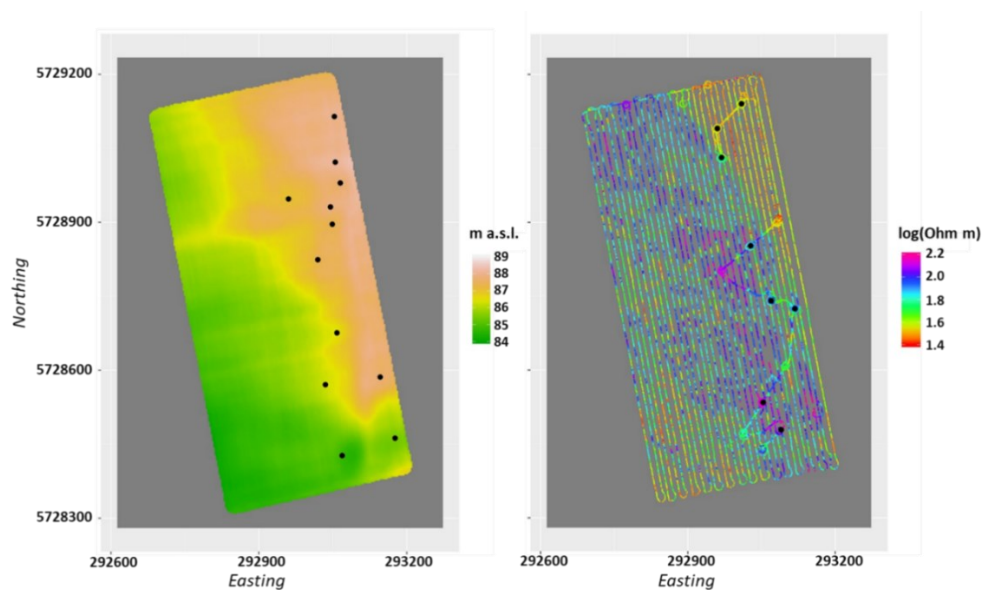


Figure 24: Sampling points in the study field taken in 2012 based on the topographic features (left, elevation map measured by the Geophilus system) and the sampling points taken in 2014 based on the min-max range of the Geophilus ERA recordings (here, channel 4 on a logarithmic scale) (right)

Soil sampling and laboratory analyses

To assess the relationship between the true specific resistivity and soil texture, a total of 92 soil texture samples were used from 20 soil profiles (Figure 24). The profiles were sampled in two measurement campaigns, down to a maximum depth of 2 m using a hydraulic-driven soil tube with a core diameter of 80 mm. Twelve sampling points were chosen for their topographic conditions and were sampled in October 2012 (Figure 24, left), and eight locations were selected within the max-min range of the already available ERA maps (based on previous measurements by the same Geophilus system) and were sampled in August 2014 during the Geophilus measurements (Figure 24, right). The samples were taken after the pedo-genetically horizon differences or determined substrate changes and soil profiles were described according to the German soil survey guidelines (Ad-hoc AG Boden

2005). All sampling locations were georeferenced using a global positioning system (GPS) receiver with a positional accuracy of 2 to 3 m. During the second measurement campaign, another 35 samples were taken at the same eight locations in order to assess the gravimetric water content.

The samples were stored in plastic bags, air-dried and pre-treated in accordance with ISO 11277. The particle size distribution (PSD) for the clay (< 2 µm) and silt fractions (2 – 63 µm) were analysed following the Köhn pipette method after separating the sand fraction (63 – 2000 µm) and the coarse material (> 2000 µm). The analyses were carried out using the Sedimat 4-12 analyser (UGT, Müncheberg, Germany). A pooled sample of 25 augerings were taken within a radius of 3 m, down to 0.3 m soil depths at each location, in order to measure the organic carbon (OC) content (%) used to initialise the model. At the study site, the upper 0.3 m were free of inorganic carbon; thus, the total carbon (TC) was determined in accordance with DIN ISO 10694 by dry combustion after homogenization and grinding of the fine soil particles and was measured for OC content. The soil samples were analysed using a gas-phase chromatograph, the vario EL cube (Elementar, Hanau, Germany). The water content was calculated by the difference of the fresh soil weight and the weight of the dry soil sample. Samples were oven dried at 105°C for 48 h.

Soil texture assignment and soil classification

To obtain the spatial soil texture distribution, an ordinary least square regression was carried out between each measured fine soil fraction and the measured ER at the sampling points. To overcome the disparity of the different depths of the pedo-genetic horizons and ER layers, the fine soil fractions were summarized by a weighted arithmetic mean with respect to the inverted ERa block depths. The ER data were averaged within a 7 m radius at the sampling points. The two soil fractions with the strongest Pearson's correlation coefficients (r) were taken to derive their contents for each data point as a dataset of continuous data after

$$y = a + b\rho \quad (20)$$

where y is the soil fraction of either clay, silt or sand (in %), ρ is the resistivity (in Ohm m) and a and b are the two regression coefficients to be estimated. The complementary third soil fraction was calculated by subtracting the two derived soil fractions from 100 %. Additionally, the allocated particle size distribution (PSD) of each data point was located within the German soil texture triangle of the German soil survey guidance to determine the soil texture class (Ad-hoc AG Boden 2005). This was done in order to compare the inferred soil texture in this study with that of the classical soil maps. For every layer, a cross validation was carried out to determine the mean residual standard error.

Inferring required soil properties

The bulk density, particle density, pore volume, field capacity and permanent wilting point were inferred from the pedotransfer functions (PTFs) to create the complete soil profiles used to initialise CANDY. The bulk density (in g cm^{-3}) was calculated following the approach of the standardized bulk density derived by Ruehlmann and Korschens (2009); the particle density (in g cm^{-3}) was calculated following the work of Ruhlmann et al. (2006); the pore volume (in %) was based on the relationship between the bulk density and particle density. The hydrological characteristics field capacity and permanent wilting point were calculated following the pedotransfer functions of Rawls and Brakensiek (1985), according to the water retention model of Brooks and Corey (1964).

Soil profile assembling and soil modelling

To produce an appropriate soil texture map of the individual soil profiles that would prove to be suitable input for the simulation model, all layers were assembled using the geographic coordinates of each data point taken from the ERa stratification and are henceforth addressed as virtual soil profiles. Within the chosen field, 18,763 profiles with a 4 x 4 m resolution (~30 ha) were produced for the continuous dataset. For the categorical soil class distribution, a total of 502 dissimilar profiles were constructed. Maps of each layer were produced to help visualize the geographic differences.

To quantify the spatial soil water content at certain times of the crop growth period, the agroecosystem model CARbon Nitrogen DYnamics (CANDY) was used in this study (Franko et al. 1995). The database driven soil model simulates downward and upward flows using a one-dimensional approach for individual soil profiles. Following the capacity concept, the vertical water fluxes start at the soil surface when precipitation enters the soil profile until an infiltration surplus occurs; following this, the water flux is modelled as surface runoff. The drainage from one horizon to another occurs when the actual water content of each horizon is greater than the water content of the field capacity. A full mathematical description of the model can be found in Franko et al. (1995) and Franko et al. (2015).

Data analysis

To validate the soil texture distribution, a leave-one-out cross correlation approach was performed for each layer and soil fraction. To evaluate the results, the simulated water content, derived soil texture distribution and original ER data were compared with the yield data from 2011 using boundary line analysis. As suggested by Lark (1997) and applied by Shatar and McBratney

(2004), the use of boundary line analysis (or quantile regression analysis) supports site-specific interpretations of yield response to a single factor, even though the yield is affected by multiple factors. The boundary line represents the maximum value of the response variables attained at different values of the independent variable (Koenker 2005). The boundary line regression fits a non-parametric regression line in the 0.95 quantile of the independent variable by grouping the independent variable into discrete classes and averaging the maximum-yields of each class. All variables were aggregated for comparison on a 36 x 36 m grid relevant to farming, and scatter plot graphs were constructed for the interpretation of these data. Additionally, quadratic models were applied between the variables and the yields to estimate and compare the coefficients of determination (R^2). Furthermore, the root mean square error (RMSE) between the observed (October 2014) and predicted soil moisture values was calculated as follows:

$$RMSE = \sqrt{\frac{\sum_{i=1}^N (\theta_o - \theta_e)^2}{N}} \quad (21)$$

where θ_o and θ_e are the observed and estimated soil moisture values, respectively, and N represents the sample size. All data processing and analysis were conducted using the open source statistical software R version 3.3.1 (R Core Team 2016).

Results and discussion

Soil properties

The soil of the pedo-genetic horizons (A and B horizons) is considered to be solum developed from loess substrate, although a loess layer was not found at each profile. The greatest variability occurred in the lowermost substrate layer, with an alternating morainic and fluvioglacial parent material, including various sizes of banks and lenses of sand and gravel. The data analysis (Figure 25) indicated that the soil textures of the pedological horizons and the loess layers are dominated by clayey silts (classes: Lu, Ut4), which is typical for soils developed from the loess in this area (Altermann et al. 2005). A few horizons were detected as loamy silts (classes: Uls, Ut2, Ut3), and some colluvial horizons were detected as loam (Ls3, Ls4) and loamy sand (Sl2). The overall silt content for the solum and the loess layers ranged from 20 to 79 %, the clay content ranged from 7 to 30 % and the sand content ranged from 7 to 73 % (Table 13). The fluvioglacial deposits and morainic materials were dominated by pure sands and loamy sands (classes: Ss, St2, Su2, Sl2, Sl3), containing between 52 and 97 % sand, between 3 and 39 % silt and between 0 and 12% clay. A minimal number of sandy loams and loams were found (classes: Sl4, Ls3, Ls4, Slu). Two samples of the subsoil were determined to be silt soils (classes: Uls, Us), with silt contents of 52 % and 77 %.

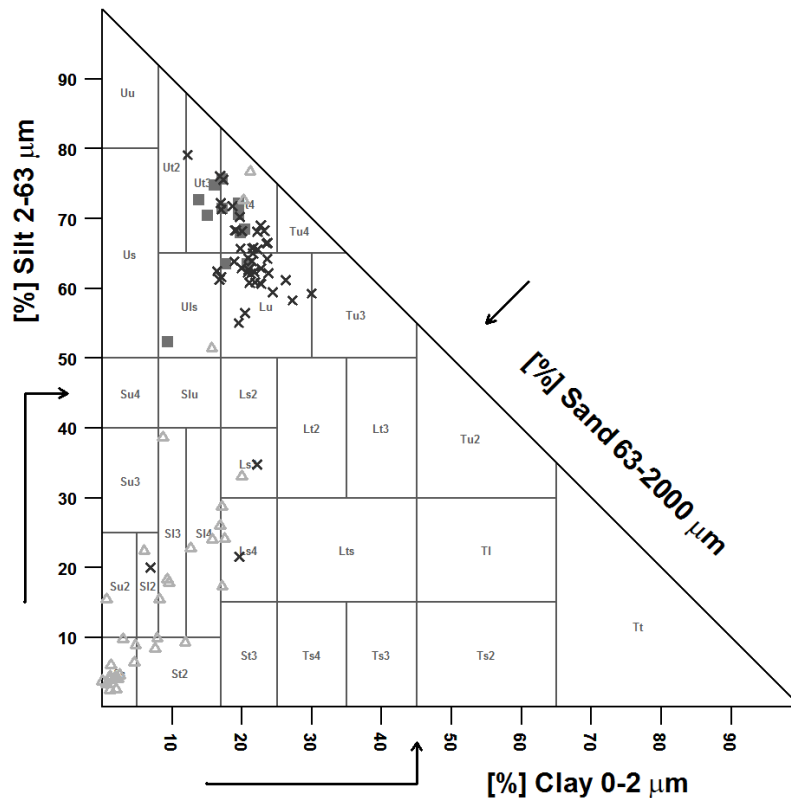


Figure 25: Soil texture distribution of the upper soil horizons (crosses), the intermediate loess layer (squares) and the lowermost substrate (triangles) following the German soil classification system (Ad-hoc AG Boden 2005)

The percentage of the coefficient of variation (CV%) for the sand fraction showed the highest variability in the solum layer (71 %) and lowest variation in the lowermost substrate (27.2 %). CV% for the clay and silt fractions of the solum and the loess layers were relatively low at <20 % clay content, and <18 % silt content. However, both fractions showed contrasting variabilities within the morainic and fluvioglacial material, which had CV% of 82.8 % and 101.1 %, respectively. The organic carbon (OC) content in the topsoil was within the expected range of the study site and varied between 1.03 and 1.48 % (CV% = 9.9 %).

As measured in the soil core samples, the overall thickness of the solum (A and B horizons) varied between 0.44 and 0.91 m (mean = 0.61 m, SD = 0.12 m). The sandy material started between 0.51 and 1.04 m (mean = 0.71 m, SD = 0.15 m) below the surface, and the thickness of the loess layer ranged from 0 to 0.27 m and was found between 0.57 and 1.04 m depths (mean = 0.77, SD = 0.13 m) (Table 13).

Table 13: Descriptive statistics of the sample data from the study site, where OC is the organic carbon content, SD is the standard deviation, CV%, is the percentage of coefficient of variation and the sample size is n.

Parameter	Horizon*	Substrate	n	Min	Max	Mean	SD	CV%
Clay (%)	A	Solum	20	18.9	29.9	22.2	2.8	12.7
Silt (%)	A	Solum	20	55	68.3	62.0	2.9	4.7
Sand (%)	A	Solum	20	10.8	25.4	15.8	3	19.1
Clay (%)	B	Solum	28	20	23.7	19.5	3.8	19.5
Silt (%)	B	Solum	28	20	79.1	62.8	14.2	22.7
Sand (%)	B	Solum	28	7	73.1	17.6	15.6	88.2
Clay (%)	C1	Loess	12	9.3	20.7	17.2	3.3	19.2
Silt (%)	C1	Loess	12	52.4	75.7	68.6	6.4	9.3
Sand (%)	C1	Loess	12	7.2	38.3	14.2	8.3	58.5
Clay (%)	C2	Morainic/Fluvioglacial	32	0	21.2	8.4	7.0	82.8
Silt (%)	C2	Morainic/Fluvioglacial	32	2.5	76.8	18.7	18.9	101.1
Sand (%)	C2	Morainic/Fluvioglacial	32	2.0	96.4	75.3	20.5	27.2
OC (%)	A	Solum (0 – 0.3 m)	20	1.03	1.48	1.33	0.13	9.9

* Mean horizon depth in m: A = 0.33, B = 0.58, C1 = 0.75, C2 = 1.39

Relationships between ER and particle-size fractions

The overall variation of ER was best explained by the clay ($R^2 = 0.39$, $\sigma = 4.1$) and sand ($R^2 = 0.33$, $\sigma = 16.4$) and most poorly explained by the silt ($R^2 = 0.25$, $\sigma = 13.9$). Table 14 shows the regression parameters, the mean residual standard error (σ) and the coefficient of determination (R^2) for the clay and sand fractions. Except for the upper 0.26 m, R^2 was relatively large within the layers (clay ≥ 0.41 , sand ≥ 0.32). The largest R^2 occurred in the clay at two depths (0.41-0.58 m and at 1.43-1.7 m) and the sand at 0.41-0.58 m. The lowest R^2 occurred in the upper 0-0.26 m soil depth (clay ≤ 0.04 and sand ≤ 0.19). The Pearson's correlation coefficient (r) for clay was negatively correlated with the clay (mean = -0.59) and positively correlated with the sand (mean = 0.56) for all layers.

Most studies predict the soil texture distributions from the ECa rather than the ER of the distinct layers (Rodriguez-Perez et al. 2011; Terron et al. 2011). Thus, it is difficult to compare the values derived in this study with those from other published studies. Progress in predicting the layer-specific soil textures is mentioned in Piikki et al. (2015), Saey et al. (2009) and Vitharana et al. (2006). The last found a strong correlation ($r = 0.83$) between the ECa and clay content at 0.5-0.8 m and a weaker correlation ($r = 0.40$) at 0-0.4 m. Their prediction was based on ECa measurements from different sensor systems. However, the moderate correlations found in this study were expected, because ER is simultaneously influenced by multiple factors (e.g., temperature or soil water salinity).

Table 14 Regression parameters (intercept and factor), the mean residual standard error (σ) after cross validation and the coefficient of determination (R^2) of the linear model between the variable ER (Ohm m), used as a proxy, and the clay and sand contents at each depth.

Depth (m)	Variable (%)	Intercept	Factor	σ	R^2	p-value
0-0.12	Clay	26.6	-0.13	2.83	0.04	0.43
0-0.12	Sand	5.5	0.30	2.84	0.16	0.09
0.12-0.26	Clay	26.7	-0.13	2.75	0.04	0.39
0.12-0.26	Sand	5.2	0.31	2.77	0.19	0.05
0.26-0.41	Clay	31.6	-0.29	2.46	0.41	0.00
0.26-0.41	Sand	-27.2	1.18	10	0.41	0.00
0.41-0.58	Clay	29.9	-0.25	3.63	0.54	0.00
0.41-0.58	Sand	-23.2	0.99	15.61	0.49	0.00
0.58-0.76	Clay	23	-0.12	4.65	0.48	0.00
0.58-0.76	Sand	4.1	0.5	25.39	0.34	0.01
0.76-0.96	Clay	16.1	-0.08	4.88	0.46	0.00
0.76-0.96	Sand	38.6	0.28	23.08	0.33	0.01
0.96-1.19	Clay	15.2	-0.07	5.26	0.49	0.00
0.96-1.19	Sand	49.9	0.24	22.35	0.35	0.01
1.19-1.43	Clay	15.2	-0.07	5.14	0.51	0.00
1.19-1.43	Sand	51	0.22	22.68	0.34	0.01
1.43-1.7	Clay	15.4	-0.07	4.99	0.54	0.00
1.43-1.7	Sand	50.7	0.21	22.52	0.35	0.01

Spatial soil texture distribution

Due to the higher resolution of the multichannel mapping system, Geophilus, and the subsequent stratification, the soil class maps produced show soil class variabilities with greater vertical and lateral resolutions compared to classical soil maps (Figure 26). **Fehler! Verweisquelle konnte nicht gefunden werden.** shows the detected soil texture classes (STC) derived from the German soil classification, their appropriate class meanings for the clay, silt and sand contents and their areal representations (ha) for each inverted ERa layer depth. As expected, the texture variability of the field becomes evident in the subsoil, whereas the first 0.26 m of the topsoil (mainly A-horizon) is characterized by a single soil class (Lu) over the 30 ha field (**Fehler! Verweisquelle konnte nicht gefunden werden.**). The soil at 0.26-0.41 m depths is still dominated by the clayey silts (28.8 ha, Lu and Ut4), yet areas of loamy and sandy substrates are already visible. Between 0.41 m and 0.76 m, the soil class variability is the largest. At this soil depth, the soil texture distribution ranged from areas with high sand content but low clay and silt contents (pure sand - Ss: 92.5 %, 2.5 %, and 5 %,

respectively) to areas with high clay and silt contents but low sand content (silty clays - Tu4: 28.5 %, 57.5 %, and 3 %, respectively). Clayey silts (Lu, Ut4) occupied ~9-21 ha, loamy silts (Uls) occupied ~4-5 ha, sandy loams (Slu) occupied ~3-8 ha and loamy sands (Sl3) occupied ~0-4 ha. Smaller areas (≤ 1 ha) are occupied by silty clays (Tu4), loamy sands (Sl4, Sl2, and Su2), pure sands (Ss) and silty sands (Su3). The patterns of the sandy structures form a visible wide-ranging NW-SE band across the field (Figure 24, right). The north-eastern part of the field is composed of a relatively homogeneous block of sandy morainic material, showing similar profiles with relatively small vertical changes. Between 0 and 0.96 m of the profiles consist of clayey silts (Ut4, Lu4) and below 0.96 m they consist of loamy sands (Sl3). In a study carried out by Vitharana et al. (2008), similar homogeneous topsoil over heterogeneous subsoils were identified for comparable soils in Belgium. The soils in their study were also developed on aeolian loess deposited over undulating Tertiary sandy or clayey substrates.

Table 15: Estimated soil texture classes (German soil classification system), the class mean values for the clay, silt and sand contents and their areal distributions (ha) within each layer

Soil texture class	Clay (%)	Silt (%)	Sand (%)	Texture class representation (ha) per soil depth (m)																
				0-0.12	0.12-0.26	0.26-0.41	0.41-0.58	0.58-0.76	0.76-0.96	0.96-1.19	1.19-1.43	1.43-1.7								
clayey silt (Lu)	23.5	57.5	19	30	30	19	13.04	9.42												
clayey silt (Ut4)	21	72	7				9.8	7.6												
silty clay (Tu4)	28.5	68.5	3				0.03	0.16												
loamy silt (Uls)	12.5	57.5	30				0.07	4.22	5.02											
sandy loam (Slu)	12.5	45	42.5				0.96	3.46	8.25	0.05										
loamy sand (Sl3)	10	25	65				0.03	1.24	4.24	12.04	10.76	9.85	8.93							
loamy sand (Sl4)	14.5	25	60.5				0.11		0.57	8.0	5.23	5.61	6.38							
loamy sand (Sl2)	6.5	17.5	76						1.04	4.95	5.43	5.19	4.89							
loamy sand (Su2)	2.5	17.5	80					0.12	0.56	2.16	1.5	1.56	1.62							
sand (Ss)	2.5	5	92.5						0.56	2.8	7.09	7.81	8.2							
silty sand (Su3)	4	32.5	63.5					0.16	0.34											

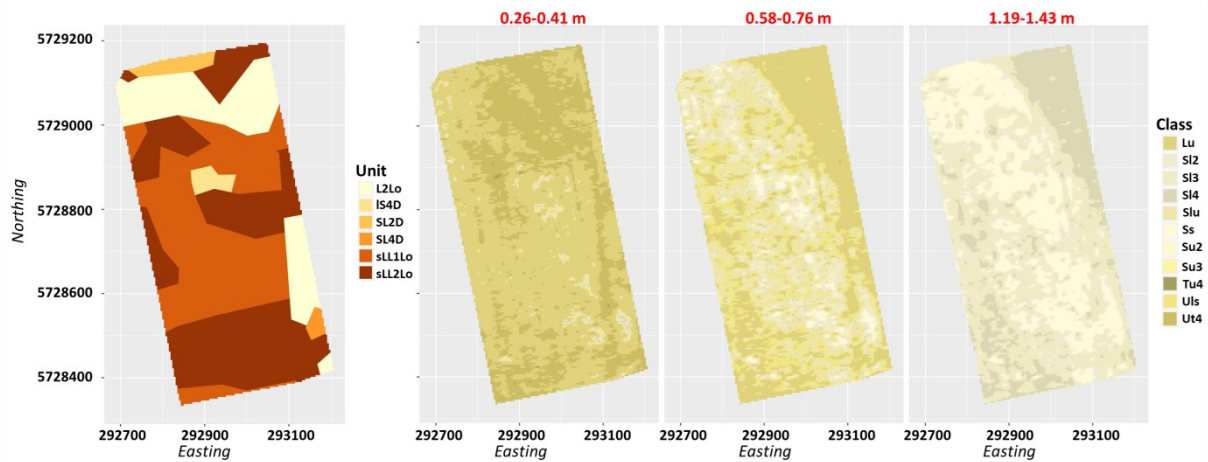


Figure 26: Comparison of the soil texture heterogeneities of the selected study field from the German soil survey map, with the soil units representing the soil texture values from a representative soil profile and averaged values of a 50 x 50 m survey grid at a 1 m soil depth (left), and the soil texture class distribution map derived from the linear regression model at a 4 x 4 m resolution for the different soil depths (right) according to the German soil classification system (Ad-hoc AG Boden 2005)

Modelled soil water variability

The spatial soil water dynamics were calculated by the soil model. To evaluate the model results and to explain the yield variability under water stress, the winter wheat production of the relatively dry year of 2011 was chosen. The winter wheat yield distribution is shown as the averaged values in Figure 27 and varied between 1.1 and 7.9 t ha⁻¹ (mean = 5.1 t ha⁻¹, SD = 1.25 t ha⁻¹) (Figure 27, left). The overall yield amount was ~2 t ha⁻¹ below the average winter wheat productivity (7.1 t ha⁻¹) between 2008 and 2015. With regard to the modelling results, no impact on the within-field yield variation was found for the soil water at 0-0.3 m ($R^2 < 0.01$) at any time in the vegetation period. However, with increasing soil depths, the importance of the subsoil becomes evident. Considering the soil water content at 0-1 m for the period between the 1st and the 10th of June 2011, the yield variability was explained with $R^2 < 0.14$, but was better explained ($R^2 = 0.18$) by the distribution of the overall soil water content (0-1.7 m) (Figure 28). The distribution of the latter is shown in Figure 27 (right). The beginning of June is known as the grain filling period, and the yield quality and quantity is sensitive to the water availability. At this time, the roots of the cereal crops are already fully developed; the leaf cover grade is at its maximum, and the daily demand for water is at its highest. The overall soil water content for this period ranged from between 265 and 443 mm (mean = 370 mm, SD = 43 mm). In comparison, the yield variability was explained by the clay content with $R^2 = 0.17$ and by the original ER with $R^2 = 0.15$. The RMSE between the measured and simulated soil water contents was 7.52 Vol.%.

The spatial patterns of the calculated water content agree with the distributions of the fluvioglacial deposits and the morainic materials found underground. The driest areas were found in the profiles with sandy subsoil (clay content below 5 % and silt content below 10 %). Areas with morainic and more clayey materials proved to have more soil water.

Figure 28 shows the estimated yields in relation to the soil water content and the corresponding regression and boundary lines (with the latter as a measure for the maximum attainable yields). Both lines correspond to an optimal curve for the water dependency of arable crop yields. The boundary line was fitted at the 0.95 quantile of the soil moisture data using a bandwidth of 35 data points to estimate the non-parametric regression smoothing. The attainable yields increased with increasing soil water contents and reached a maximum of approximately 7 t ha^{-1} for soil water contents between 350 and 420 mm. The yields decreased when the soil water content exceeded 420 mm. Generally, the yield variance indicates that other environmental conditions influenced crop growth and productivity (e.g., agronomic effects, plant diseases or pathogen infestations). However, the estimated trends of the regression and the boundary line basically confirm the well-known relationship between water supply and plant yield.

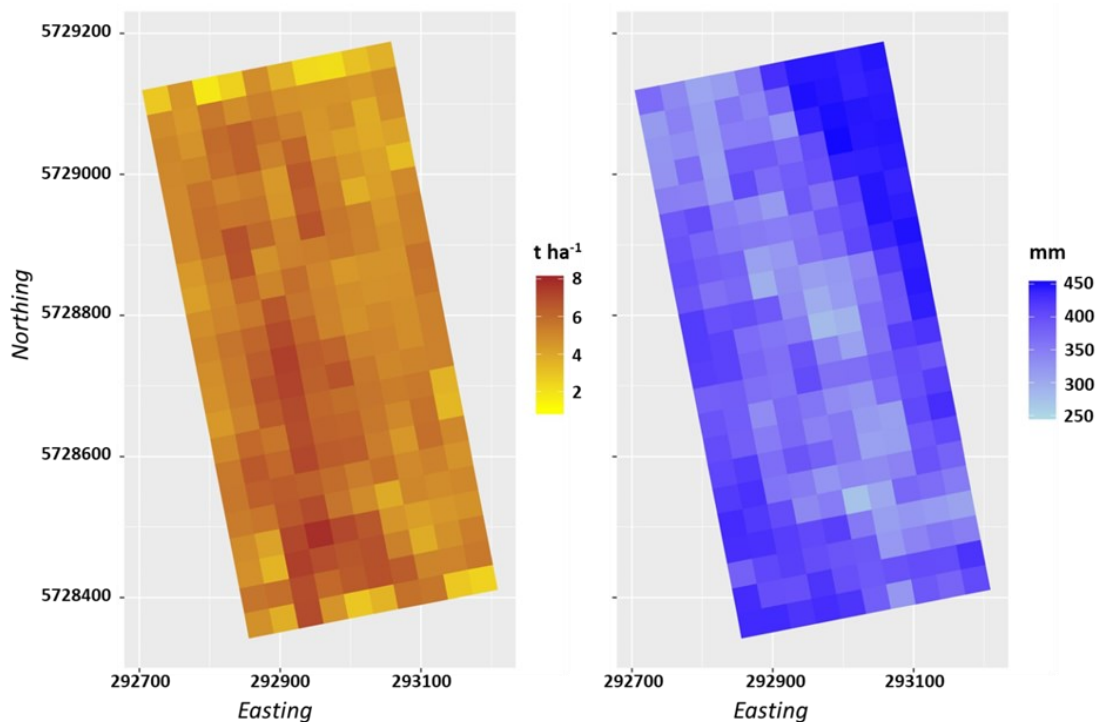


Figure 27: Winter wheat yield variability in 2011 (left) and the calculated soil water content at 0-1.7 m soil depths from 01.06.-10.06.2011 (right) with a 36 x 36 m resolution

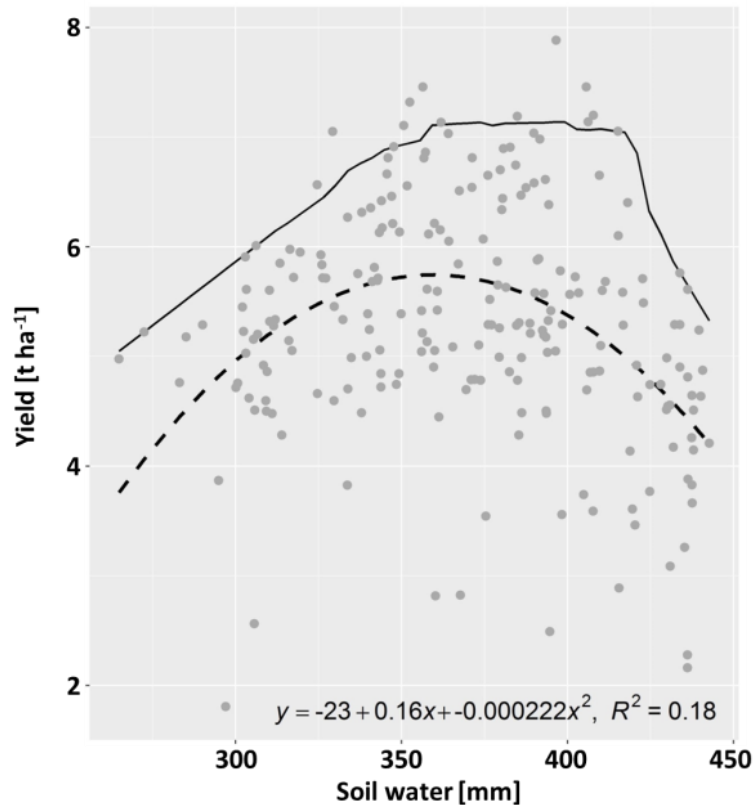


Figure 28: Winter wheat yields and the corresponding regression (dashed) and boundary lines (solid) in relation to the soil water content (0-1.7 m). The formula and R^2 for the regression function are shown.

Models with a spatially complex framework require numerous input data and parameters and are subject to many sources of uncertainty, including errors in measurement, inadequate sampling resolutions, positional uncertainties and uncertainties in model specifications (Heuvelink et al. 2007). The quantification of uncertainties (particularly in terms of their evaluation or validation) is still a major problem, yet there are still opportunities to use models for predictive or prospective purposes. The error may not be easy to quantify in practice, particularly for some environmental factors or data related to anthropogenic activities.

Conclusion

The combination of SOM models with spatial ERa data can support the optimization of farm management strategies. Based on the inverted ERa data, soil texture samples and pedotransfer functions, this study successfully produced high resolution spatial soil input data for soil process-oriented modelling. To evaluate the model results, regression and boundary line analysis was able to interpret the site-specific yield productivity. This study found that the spatial soil water distribution that includes the subsoil during grain filling was the most responsible for the variations in crop yield.

For areas with generally homogeneous topsoil, as is common in the Chernozem areas, this method can be used to detect heterogeneous structures in the subsoil. This highlights the importance of stratification by data inversion of the multichannel ERT. Furthermore, modelling the spatial soil water content during the crop growth season at different soil depths may help to improve decision systems in PA.

This study's approach demonstrates the main steps of how to get from the basic input data for the ideal spatial modelling outputs:

1. Allocating soil textures at individual layers based on linear regression.
2. Deriving structural soil properties (bulk density, particle density and pore volume) and water retention characteristics (field capacity and wilting point) from the pedotransfer functions.
3. Constructing virtual soil profiles by database-driven layer stacking.
4. Modelling spatial soil dynamic properties.

The procedure can be easily implemented for appropriate PA strategies and, although untested, it might be applicable in other fields and be able to contribute to improve crop production.

Acknowledgements

This research project was funded by the German Federal Office for Agriculture and Food (*Bundesanstalt für Landwirtschaft und Ernährung – BLE*), Project No. 2815410210. Special thanks go to soil specialist Marco Knötig from AgroSat, Baasdorf, Germany, for supporting the field operations.

References

- Ad-hoc AG Boden (2005). *Bodenkundliche Kartieranleitung* (5ed.). Stuttgart, Germany: Schweitzerbart.
- Adamchuk, V. I., Hummel, J. W., Morgan, M. T., & Upadhyaya, S. K. (2004). On-the-go soil sensors for precision agriculture. *Computers and Electronics in Agriculture*, 44(1), 71-91, doi:10.1016/j.compag.2004.03.002.
- Allred, B. J., Daniels, J. J., & Ehsani, M. R. (2008). *Handbook of Agricultural Geophysics*. New York, USA: CRC Press.
- Altermann, M., Rinklebe, J., Merbach, I., Korschens, M., Langer, U., & Hofmann, B. (2005). Chernozem - Soil of the Year 2005. *Journal of Plant Nutrition and Soil Science*, 168(6), 725-740, doi:10.1002/jpln.200521814.

- Batchelor, W. D., Basso, B., & Paz, J. O. (2002). Examples of strategies to analyze spatial and temporal yield variability using crop models. *European Journal of Agronomy*, 18(1-2), 141-158, doi:Pii S1161-0301(02)00101-6 Doi 10.1016/S1161-0301(02)00101-6.
- Berzsenyi, Z., Győrffy, B., & Lap, D. (2000). Effect of crop rotation and fertilisation on maize and wheat yields and yield stability in a long-term experiment. *European Journal of Agronomy*, 13(2-3), 225-244, doi:http://dx.doi.org/10.1016/S1161-0301(00)00076-9.
- Besson, A., Cousin, I., Samouelian, A., Boizard, H., & Richard, G. (2004). Structural heterogeneity of the soil tilled layer as characterized by 2D electrical resistivity surveying. *Soil & Tillage Research*, 79(2), 239-249, doi:10.1016/j.still.2004.07.012.
- Brevik, E. C., Fenton, T. E., & Lazari, A. (2006). Soil electrical conductivity as a function of soil water content and implications for soil mapping. *Precision Agriculture*, 7(6), 393-404, doi:10.1007/s11119-006-9021-x.
- Brooks, R. H., & Corey, A. T. (1964). Hydraulic properties of porous media. In *Hydrological Paper* (Vol. 3). Fort Collins, CO, USA: Colorado State University.
- Corwin, D. L., & Lesch, S. M. (2003). Application of soil electrical conductivity to precision agriculture: Theory, principles, and guidelines. *Agronomy Journal*, 95(3), 455-471, doi:10.2134/agronj2003.4550.
- Dabas, M., Decriaud, J. P., Ducomet, G., Hesse, A., Mounir, A., & Tabbagh, A. (1994). Continuous recording of resistivity with towed arrays for systematic mapping of buried structures at shallow depths. *Revue d'Archéométrie*, 18, 13-17.
- Dualem (2005). DUALEM-1S and DUALEM-2S User's Manual. Milton, Ontario, Canada: Dualem, Inc.
- Eghball, B., Schepers, J. S., Negahban, M., & Schlemmer, M. R. (2003). Spatial and Temporal Variability of Soil Nitrate and Corn Yield Joint contribution of the USDA-ARS and the Univ. of Nebraska Agric. Res. Div., Lincoln, NE, as paper no. 13618. *Agronomy Journal*, 95(2), 339-346, doi:10.2134/agronj2003.3390.
- Eissmann, L. (1994). Grundzüge der Quartärgeologie Mitteldeutschlands - Sachsen, Sachsen-Anhalt, Südbrandenburg, Thüringen (Features of the Quaternary Geology of Central Germany - Saxonia, Saxonia-Anhalt, South Brandenburg, Thuringia). In L. Eissmann, & T. Litt (Eds.), *Das Quartär Mitteldeutschlands - Ein Leitfaden und Exkursionsführer (The Quaternary in Central Germany - A guideline and excursion guide)*, DEUQUA-Tagung in Leipzig 1994, 7, 55-135. Altenburg, Germany: Altenburger Naturwissenschaftliche Forschung.
- Franke, U., Oelschlagel, B., & Schenk, S. (1995). Simulation of Temperature, Water and Nitrogen Dynamics Using the Model Candy. *Ecological Modelling*, 81(1-3), 213-222, doi:Doi 10.1016/0304-3800(94)00172-E.

- Fukue, M., Minato, T., Horibe, H., & Taya, N. (1999). The micro-structures of clay given by resistivity measurements. *Engineering Geology*, 54(1-2), 43-53, doi:Doi 10.1016/S0013-7952(99)00060-5.
- Gebbers, R., & Lück, E. (2005). Comparison of geoelectrical methods for soil mapping. *Precision Agriculture*, 5, 473-479.
- Godwin, R. J., & Miller, P. C. H. (2003). A review of the technologies for mapping within-field variability. *Biosystems Engineering*, 84(4), 393-407, doi:10.1016/S1537-5110(02)00283-0.
- Grisso, R., Alley, M., Holshouser, D., & Thomason, W. (2009). Precision Farming Tools: Soil Electrical Conductivity. *Virginia Cooperative Extension*, Richmond, USA.
- Haase, D., Fink, J., Haase, G., Ruske, R., Pecs, M., Richter, H., et al. (2007). Loess in Europe - its spatial distribution based on a European Loess Map, scale 1 : 2,500,000. *Quaternary Science Reviews*, 26(9-10), 1301-1312, doi:10.1016/j.quascirev.2007.02.003.
- Hartemink, A. E., & Minasny, B. (2014). Towards digital soil morphometrics. *Geoderma*, 230(0), 305-317, doi:10.1016/j.geoderma.2014.03.008.
- Heuvelink, G. B. M., Brown, J. D., & van Loon, E. E. (2007). A probabilistic framework for representing and simulating uncertain environmental variables. *International Journal of Geographical Information Science*, 21(5), 497-513, doi:10.1080/13658810601063951.
- Kaspar, T. C., Pulido, D. J., Fenton, T. E., Colvin, T. S., Karlen, D. L., Jaynes, D. B., et al. (2004). Relationship of Corn and Soybean Yield to Soil and Terrain Properties. *Agronomy Journal*, 96(3), 700-709, doi:10.2134/agronj2004.0700.
- Knoth, W. (1992). Geological Overview Map of Sachsen-Anhalt 1:400 000. Halle (Saale), Germany: Geologisches Landesamt Sachsen-Anhalt.
- Koenker, R. (2005). *Quantile regression* (Vol. 38). New York, USA: Cambridge university press.
- Kravchenko, A. N., Thelen, K. D., Bullock, D. G., & Miller, N. R. (2003). Relationship among crop grain yield, topography, and soil electrical conductivity studied with cross-correlograms. *Agronomy Journal*, 95(5), 1132-1139, doi:10.2134/agronj2003.1132.
- Kruger, J., Franko, U., Fank, J., Stelzl, E., Dietrich, P., Pohle, M., et al. (2013). Linking Geophysics and Soil Function Modeling-An Application Study for Biomass Production. *Vadose Zone Journal*, 12(4), 1-13, doi:10.2136/vzj2013.01.0015.
- Lark, R. M. (1997). An empirical method for describing the joint effects of environmental and other variables on crop yield. *Annals of Applied Biology*, 131(1), 141-159, doi:DOI 10.1111/j.1744-7348.1997.tb05402.x.
- Loke, M. H., & Barker, R. D. (1995). Least-squares deconvolution of apparent resistivity pseudosections. *GEOPHYSICS*, 60(6), 1682-1690, doi:10.1190/1.1443900.

- Loke, M. H., & Barker, R. D. (1996). Rapid least-squares inversion of apparent resistivity pseudosections by a quasi-Newton method. *Geophysical Prospecting*, *44*(1), 131-152, doi:DOI 10.1111/j.1365-2478.1996.tb00142.x.
- Lueck, E., & Ruehlmann, J. (2013). Resistivity mapping with GEOPHILUS ELECTRICUS - Information about lateral and vertical soil heterogeneity. *Geoderma*, *199*(0), 2-11, doi:10.1016/j.geoderma.2012.11.009.
- Lund, E., Christy, C., & Drummond, P. (1999). Practical applications of soil electrical conductivity mapping. *Precision Agriculture*, *99*, 771-779.
- Machado, S., Bynum, E. D., Archer, T. L., Lascano, R. J., Wilson, L. T., Bordovsky, J., et al. (2002). Spatial and Temporal Variability of Corn Growth and Grain Yield. *Crop Science*, *42*(5), 1564-1576, doi:10.2135/cropsci2002.1564.
- Manzoni, S., & Porporato, A. (2009). Soil carbon and nitrogen mineralization: Theory and models across scales. *Soil Biology & Biochemistry*, *41*(7), 1355-1379, doi:10.1016/j.soilbio.2009.02.031.
- McBratney, A. B., Minasny, B., Cattle, S. R., & Vervoort, R. W. (2002). From pedotransfer functions to soil inference systems. *Geoderma*, *109*(1-2), 41-73, doi:Pii S0016-7061(02)00139-8
- McNeill, J. (1980). Electromagnetic terrain conductivity measurement at low induction numbers. Geonics Limited, Ontario, Canada.
- Menke, W. (2012). *Geophysical data analysis: Discrete inverse theory: MATLAB edition* (Vol. 45). Oxford, UK: Academic press.
- Pan, L., Adamchuk, V. I., Prasher, S., Gebbers, R., Taylor, R. S., & Dabas, M. (2014). Vertical Soil Profiling Using a Galvanic Contact Resistivity Scanning Approach. *Sensors*, *14*(7), 13243-13255, doi:10.3390/s140713243.
- Pellerin, L., & Wannamaker, P. E. (2005). Multi-dimensional electromagnetic modeling and inversion with application to near-surface earth investigations. *Computers and Electronics in Agriculture*, *46*(1-3), 71-102, doi:10.1016/j.compag.2004.11.017.
- Piikki, K., Wetterlind, J., Soderstrom, M., & Stenberg, B. (2015). Three-dimensional digital soil mapping of agricultural fields by integration of multiple proximal sensor data obtained from different sensing methods. *Precision Agriculture*, *16*(1), 29-45, doi:10.1007/s11119-014-9381-6.
- Pracilio, G., Asseng, S., Cook, S. E., Hodgson, G., Wong, M. T. F., Adams, M. L., et al. (2003). Estimating spatially variable deep drainage across a central-eastern wheatbelt catchment, Western Australia. *Australian Journal of Agricultural Research*, *54*(8), 789-802, doi:10.1071/Ar02084.
- R Core Team (2016). A language and environment for statistical computing. Vienna, Austria: R Foundation for Statistical Computing.

- Radic, T. (2014). SIP Rabbit - for precision agriculture measurements. http://www.radic-research.de/Flyer_Rabbit_171114.pdf: Last accessed [15.12.2017]
- Rawls, W. J., & Brakensiek, D. L. 1985. Prediction of soil water properties for hydrologic modeling. In *Watershed management in the eighties, 1985* (pp. 293-299). St Joseph, USA, American Society Agricultural Engineers.
- Rhoades, J. D., Manteghi, N. A., Shouse, P. J., & Alves, W. J. (1989). Soil Electrical-Conductivity and Soil-Salinity - New Formulations and Calibrations. *Soil Science Society of America Journal*, 53(2), 433-439, doi:10.2136/sssaj1989.03615995005300020020x.
- Robert, P. (1993). Characterization of soil conditions at the field level for soil specific management. *Geoderma*, 60(1), 57-72, doi:[http://dx.doi.org/10.1016/0016-7061\(93\)90018-G](http://dx.doi.org/10.1016/0016-7061(93)90018-G).
- Rodriguez-Perez, J. R., Plant, R. E., Lambert, J. J., & Smart, D. R. (2011). Using apparent soil electrical conductivity (ECa) to characterize vineyard soils of high clay content. *Precision Agriculture*, 12(6), 775-794, doi:10.1007/s11119-011-9220-y.
- Roy, A., & Apparao, A. (1971). Depth of Investigation in Direct Current Methods. *GEOPHYSICS*, 36(5), 943-959, doi:Doi 10.1190/1.1440226.
- Ruehlmann, J., & Korschens, M. (2009). Calculating the Effect of Soil Organic Matter Concentration on Soil Bulk Density. *Soil Science Society of America Journal*, 73(3), 876-885, doi:10.2136/sssaj2007.0149.
- Rühlmann, J., Körschens, M., & Graefe, J. (2006). A new approach to calculate the particle density of soils considering properties of the soil organic matter and the mineral matrix. *Geoderma*, 130(3-4), 272-283, doi:10.1016/j.geoderma.2005.01.024.
- Saey, T., De Smedt, P., Delefortrie, S., de Vijver, E. V., & Van Meirvenne, M. (2015). Comparing one- and two-dimensional EMI conductivity inverse modeling procedures for characterizing a two-layered soil. *Geoderma*, 241, 12-23, doi:10.1016/j.geoderma.2014.10.020.
- Saey, T., Simpson, D., Vermeersch, H., Cockx, L., & Van Meirvenne, M. (2009). Comparing the EM38DD and DUALEM-21S Sensors for Depth-to-Clay Mapping. *Soil Science Society of America Journal*, 73(1), 7-12, doi:10.2136/sssaj2008.0079.
- Samouelian, A., Cousin, I., Tabbagh, A., Bruand, A., & Richard, G. (2005). Electrical resistivity survey in soil science: a review. *Soil & Tillage Research*, 83(2), 173-193, doi:10.1016/j.still.2004.10.004.
- Schamper, C., Rejiba, F., & Guerin, R. (2012). 1D single-site and laterally constrained inversion of multifrequency and multicomponent ground-based electromagnetic induction data - Application to the investigation of a near-surface clayey overburden. *GEOPHYSICS*, 77(4), Wb19-Wb35, doi:10.1190/Geo2011-0358.1.

- Shahandeh, H., Wright, A. L., Hons, F. M., & Lascano, R. J. (2005). Spatial and Temporal Variation of Soil Nitrogen Parameters Related to Soil Texture and Corn Yield. *Agronomy Journal*, 97(3), 772-782, doi:10.2134/agronj2004.0287.
- Shatar, T. M., & McBratney, A. B. (2004). Boundary-line analysis of field-scale yield response to soil properties. *Journal of Agricultural Science*, 142(5), 553-560, doi:10.1017/S0021859604004642.
- Smith, P., Andren, O., Brussaard, L., Dangerfield, M., Ekschmitt, K., Lavelle, P., et al. (1998). Soil biota and global change at the ecosystem level: describing soil biota in mathematical models. *Global Change Biology*, 4(7), 773-784, doi:DOI 10.1046/j.1365-2486.1998.00193.x.
- Smith, P., Smith, J. U., Powlson, D. S., McGill, W. B., Arah, J. R. M., Chertov, O. G., et al. (1997). A comparison of the performance of nine soil organic matter models using datasets from seven long-term experiments. *Geoderma*, 81(1-2), 153-225, doi:Doi 10.1016/S0016-7061(97)00087-6.
- Stockmann, U., Adams, M. A., Crawford, J. W., Field, D. J., Henakaarchchi, N., Jenkins, M., et al. (2013). The knowns, known unknowns and unknowns of sequestration of soil organic carbon. *Agriculture Ecosystems & Environment*, 164(0), 80-99, doi:10.1016/j.agee.2012.10.001.
- Stoorvogel, J., & Bouma, J. 2005. Precision agriculture: The solution to control nutrient emissions. In J. V. Stafford (Ed.), *Proceedings of 5th European Conference on Precision Agriculture*, pp. 47-55. Wageningen, Netherlands: Wageningen Academic Publishers.
- Tabbagh, A., Dabas, M., Hesse, A., & Panissod, C. (2000). Soil resistivity: a non-invasive tool to map soil structure horizonation. *Geoderma*, 97(3-4), 393-404, doi:Doi 10.1016/S0016-7061(00)00047-1.
- Terron, J. M., da Silva, J. R. M., Moral, F. J., & Garcia-Ferrer, A. (2011). Soil apparent electrical conductivity and geographically weighted regression for mapping soil. *Precision Agriculture*, 12(5), 750-761, doi:10.1007/s11119-011-9218-5.
- Varvel, G. E. (2000). Crop Rotation and Nitrogen Effects on Normalized Grain Yields in a Long-Term Study Joint contribution of USDA-ARS and the Nebraska Agric. Res. Div., Journal Ser. no. 12880. *Agronomy Journal*, 92(5), 938-941, doi:10.2134/agronj2000.925938x.
- Vereecken, H., Schnepf, A., Hopmans, J. W., Javaux, M., Or, D., Roose, D. O. T., et al. (2016). Modeling Soil Processes: Review, Key Challenges, and New Perspectives. *Vadose Zone Journal*, 15(5), 1-57, doi:10.2136/vzj2015.09.0131.
- Viscarra Rossel, R. A., Adamchuk, V. I., Sudduth, K. A., McKenzie, N. J., & Lobsey, C. (2011). Proximal soil sensing: an effective approach for soil measurements in space and time. In *Advances of Agronomy*, 113, 237-282. Amsterdam, Netherlands: Academic Press.

- Vitharana, U. W. A., Van Meirvenne, M., Cockx, L., & Bourgeois, J. (2006). Identifying potential management zones in a layered soil using several sources of ancillary information. *Soil Use and Management*, 22(4), 405-413, doi:10.1111/j.1475-2743.2006.00052.x.
- Vitharana, U. W. A., Van Meirvenne, M., Simpson, D., Cockx, L., & De Baerdemaeker, J. (2008). Key soil and topographic properties to delineate potential management classes for precision agriculture in the European loess area. *Geoderma*, 143(1-2), 206-215, doi:10.1016/j.geoderma.2007.11.003.
- Wong, M. T. F., & Asseng, S. 2004. Fluctuations in spatial variability of wheat yield. In *Proceedings of 4th International Crop Science Congress*. Brisbane, Australia:
http://www.regional.org.au/au/asa/2004/poster/1/4/1158_wongmt.htm: Last accessed [15.12.2017]
- Wong, M. T. F., & Asseng, S. (2006). Determining the causes of spatial and temporal variability of wheat yields at sub-field scale using a new method of upscaling a crop model. *Plant and Soil*, 283(1-2), 203-215, doi:10.1007/s11104-006-0012-5.
- Wong, M. T. F., Asseng, S., & Zhang, H. (2006). A flexible approach to managing variability in grain yield and nitrate leaching at within-field to farm scales. [journal article]. *Precision Agriculture*, 7(6), 405-417, doi:10.1007/s11119-006-9023-8.
- Wosten, J. H. M., Pachepsky, Y. A., & Rawls, W. J. (2001). Pedotransfer functions: bridging the gap between available basic soil data and missing soil hydraulic characteristics. *Journal of Hydrology*, 251(3-4), 123-150, doi:Doi 10.1016/S0022-1694(01)00464-4.

Part II – Site variable nutrient management

Guidelines for precise lime management based on high-resolution soil pH, texture and SOM maps generated from proximal soil sensing data

Eric Bönecke¹, Swen Meyer¹, Sebastian Vogel², Ingmar Schröter³, Robin Gebbers², Charlotte Kling⁴, Eckart Kramer³, Katrin Lück⁵, Anne Nagel³, Golo Philipp⁶, Felix Gerlach⁵, Stefan Palme⁴, Dirk Scheibe⁷, Karin Zieger⁸, Jörg Rühlmann¹

¹ Leibniz-Institute of Vegetable and Ornamental Crops, Theodor-Echtermeyer-Weg 1, 14947, Grossbeeren, Germany

² Leibniz Institute for Agricultural Engineering and Bioeconomy (ATB), Engineering for Plant Production, Max-Eyth-Allee 100, 14469, Potsdam, Germany

³ Eberswalde University for Sustainable Development, Landscape Management and Nature Conservation, Schicklerstraße 5, 16225, Eberswalde, Germany

⁴ Gut Wilmersdorf GbR, Wilmersdorfer Str. 23, 16278, Angermünde OT Wilmersdorf, Germany

⁵ Land- und Forstwirtschaft Komturei Lietzen GmbH & Co KG, Lietzen Nord 38, 15306, Lietzen, Germany

⁶ Landwirtschaft Petra Philipp, Berliner Str. 36B, 15234, Frankfurt/O. OT Booßen, Germany

⁷ LAB Landwirtschaftliche Beratung Der Agrarverbände Brandenburg GmbH, Eberswalder Str. 84H, 15374, Müncheberg, Germany

⁸ iXmap Service GmbH & Co. KG, Peter-Henlein-Str. 5, 93128, Regenstauf, Germany

Abstract

Soil acidification is caused by natural pedogenetic processes and anthropogenic impacts but can be counteracted by regular lime application. Although sensors and applicators for variable-rate liming (VRL) exist, there are no established strategies for using these tools or helping to implement VRL in practice. Therefore, this study aimed to provide guidelines for site-specific liming based on proximal soil sensing. First, high-resolution soil maps of the liming-relevant indicators (pH, soil texture and soil organic matter content) were generated using on-the-go sensors. The soil acidity was predicted by two ion-selective antimony electrodes ($RMSE_{pH}$: 0.37); the soil texture was predicted by a combination of apparent electrical resistivity measurements and natural soil-borne gamma emissions ($RMSE_{clay}$: 0.046 kg kg^{-1}); and the soil organic matter (SOM) status was predicted by a combination of red (660 nm) and near-infrared (NIR, 970 nm) optical reflection measurements ($RMSE_{SOM}$: 6.4 g kg^{-1}). Second, to address the high within-field soil variability (pH varied by 2.9 units, clay content by 0.44 kg kg^{-1} and SOM by 5.5 g kg^{-1}), a well-established empirical lime recommendation algorithm that represents the best management practices for liming in Germany was adapted, and the lime requirements (LRs) were determined. The generated workflow was applied to a 25.6 ha test field in north-eastern Germany, and the variable LR was compared to the conventional uniform LR. The comparison showed that under the uniform liming approach, 63% of the field would be over-fertilized by approximately 12 t of lime, 6% would receive approximately 6 t too little lime and 31% would still be adequately limed.

Keywords

Variable rate soil liming · Soil texture · Soil pH · Soil organic matter · Soil sensing · Site specific soil management

Introduction

The productivity of agricultural soils is highly controlled by their acidity and buffering capacity. Soil acidity results from the release of H^+ from dissolved and solid acids to form H_3O^+ ions in the soil solution and is measured as pH. Soil acidity is a key factor in soil fertility that concurrently influences several yield-relevant soil properties, such as:

- i. nutrient availability (particularly P) and pollutant mobility (especially Al, Mn, Cd) (Dahiya and Singh 1982; Goulding and Blake 1998; Gray et al. 2006),
- ii. nutrient utilization and use efficiency (particularly N) (Ahmad et al. 2016; Edmeades et al. 1986),
- iii. biological activity (Cheng et al. 2013; Ekenler and Tabatabai 2003; Larink and Joschko 2014; Stöven and Schnug 2005),
- iv. soil humus content and type (Briedis et al. 2012; Haynes and Naidu 1998; Paradelo et al. 2015),
- v. soil structure, porosity and aggregate stability (aeration, water availability, root growth) (Fiedler and Bergmann 1955; Hartge 1959; Schachtschabel and Hartge 1958), and
- vi. water infiltration, water storage and soil erosion (Ahn et al. 2013; Cuisinier et al. 2011; Horsnell 1984).

For these reasons, farmers strive to obtain and maintain an optimal soil pH to improve crop growth in their fields (Tunney et al. 2010). As soil acidification is a pedogenetic process in humid climates, more protons (H^+ ions) are added or liberated by precipitation and internal soil processes over time than the soil is able to neutralize (Fujii et al. 2012; Blume et al. 2016). The physico-chemical processes that are relevant to acidification include the dissociation of carbonic acids, the atmospheric deposition of acidic gases and/or acidic precipitation, microbial respiration and/or root exudates, oxidation reactions and the formation of organic acids and anthropogenic activities, e.g., fertilization, or the removal of alkalis by harvesting crops (Holland et al. 2018; Goulding 2016). Hence, in soils that do not contain geogenic carbonates, farmers need to apply lime to their fields to maintain soil fertility.

However, even in countries with intensive agricultural production, such as Germany, the soil pH of agricultural fields is often not within the optimum range. According to a recent national soil pH survey by Jacobs et al. (2018) in Germany, only 35% of the arable soils and 24% of the grassland soils were in the optimum range, whereas the pH of approximately 42% of the mineral soils under arable farming and 57% of the grassland soils was too low. Apparently, lime management on farms in

Germany is not sufficient. One reason is that most farmers do not manage soil heterogeneity at the field scale. They try to avoid (i) the additional effort required for soil sampling, (ii) the uncertainties concerning the interpretation of soil information and fertilization decision making and, (iii) the problems related to the availability and use of appropriate fertilizer application technology.

Since crops vary in their tolerance to soil acidity, the optimum pH at which maximum yields are achieved ranges between 5.3 and 6.6 (Goulding 2016). Below this range, yields of crops with high lime demand may decrease by approximately 20-40% (Holland et al. 2018; Kerschberger 1996; Kerschberger and Marks 2007; Manna et al. 2007). Hence, the main goal of liming is to reduce the total acidity of a specified soil volume (e.g., the plough layer) by increasing the pH value to a target value that is optimal for crop growth (Sims 1996). In contrast, pH values that are too high may also have negative effects on nutrient availability and reduce crop yields by 5-10% (von Wulffen et al. 2008). To determine the lime requirement (LR) of a soil to achieve its target pH value, several practical techniques have been developed. The most commonly used LR tests are as follows:

- i. soil-lime incubations involving increasing rates of liming material applied to a fixed quantity of soil, equilibration for a certain duration and deriving a lime-response curve from the pH changes,
- ii. soil-base titrations with the titration of a soil suspension with a basic solution (e.g., $\text{Ca}(\text{OH})_2$ or NaOH) (McLean 1978; Alley and Zelazny 1987) and pH measurement after a certain equilibration time, followed by the conversion of the added basic solution into a lime requirement,
- iii. soil-buffer equilibration (the most widespread approach in the USA), adding a chemical buffer solution to a soil sample, allowing them to equilibrate and measuring the buffer pH decrease to assess the amount of soil acidity to be neutralized by liming (McLean 1978), and
- iv. estimates based on algorithms developed in empirical studies that use soil pH and other soil properties such as soil texture, soil organic matter, soil type or CEC as indicators of the soil carbon buffer capacity; this method is mainly used in the UK and Germany.

In this study, an empirical algorithm (LR test type iv, above) was used as a standard and adapted to precision farming by including mappings from proximal soil sensors. The empirical algorithm was developed by the Association of German Agricultural Investigation and Research Institutions (VDLUFA) and has been established as the best management practice for liming in Germany (von Wulffen et al. 2008). The procedure is based on 30 years of fertilization trials studying the correlation between soil pH and agricultural yield, brought into a simplified management structure (Kerschberger 1996; Kerschberger et al. 2000; Kerschberger and Marks 2007). The

approach involves two steps: (i) a soil sampling of one mixed soil sample that is composed of several sub-samples from either the whole field or from sub-plots of 3-5 ha of assumed soil homogeneity and (ii) a look-up table system that defines the target pH value for the management unit from the analysed soil texture, soil organic matter (SOM) content and the current pH value (Methods). However, the VDLUFA guidelines for liming are limited because they are based on relatively rough classifications of soil texture and SOM into five and four classes, respectively. However, the algorithms that are needed in the context of the present-day requirements of precision farming should be continuous and stepless.

Furthermore, site-specific and variable-rate liming (VRL), which is a precondition for optimizing soil acidity management, requires soil data at a very fine spatial scale (von Cossel et al. 2019). High-resolution maps can therefore help to assess internal field variations in soil properties and reduce the decision uncertainty caused by this unknown spatial variation (Schellberg et al. 2008; Zhang et al. 2016). Various soil proximal sensors are available that can provide information on relevant input parameters for lime requirement calculations, including geo-electrical and gamma-ray sensors for soil texture, optical sensors for organic matter content and ion-selective pH electrodes for pH values (Adamchuk et al. 2018; Gebbers 2018).

Most sensors do not measure the soil property of interest directly but provide readings from a proxy that can be related to the soil property of interest by analysing reference soil samples and establishing statistical models. Sensors for measuring electrical resistivity (ERa) and its reciprocal, bulk electrical conductivity (ECa), are commonly used for mapping soil properties that are affected by soil texture, water content and bulk density as well as by mineralogy, porosity, salinity, temperature and organic matter (Corwin and Lesch 2005). The natural variation in total γ -activity in soils is mainly related to the decay of K, U and Th isotopes. Since K is usually associated with clay minerals, γ -activity is a good indicator of clay content and soil texture. Compared to the spatial variations in ERa (ECa), the spatial variation in soil moisture has little effect on γ -activity. Thus, a multiple-sensor approach combining electrical and γ measurements can improve the determination of soil properties (Castrignano et al. 2012; Mahmood et al. 2013). Optical sensors that obtain visible and near-infrared (Vis-NIR) spectra can provide information on soil properties such as the clay, iron oxide, SOM content and carbon mineralogy (Rossel and Chen 2011), and electrochemical sensors that use ion-selective membranes can detect the activity of ions such as hydrogen, potassium or nitrate (Gebbers and Adamchuk 2010; Adamchuk and Viscarra Rossel 2011).

However, the successful adoption of these systems in practice is often hindered by the lack of knowledge on (i) how the sensors work and how reliable they are, (ii) how the sensor data should be

calibrated, and (iii) how the sensor data should be further processed to produce site-specific liming recommendations that are in line with best management practices. These questions are related to the scientific foundations of measurement principles, soil buffering, technical possibilities and restrictions, and socio-economic aspects, including cost efficiency and official regulations.

Moreover, only a few studies have compared VRL with conventional approaches (Borgelt et al. 1994; Zaman et al. 2003; Bianchini and Mallarino 2002). For North American soils, Borgelt et al. (1994) found that mean liming rates would have resulted in over-fertilization of 9 to 12% and under-fertilization of 37 to 41%, whereas Bianchini and Mallarino (2002) found that much less lime (56-61%) needed to be applied with the VRL approach. In a similar study in the UK, Zaman et al. (2003) found that 35% of the tested field required more than the average liming rate, 56% required less and only 9% was adequately limed. However, none of these studies used high-resolution soil maps based on proximal soil sensing. This kind of sensor-based approach was explored by Kuang et al. 2014, 2015. They used on-the-go visible and near infrared (vis-NIR) spectroscopy sensors and two statistical methods (artificial neuronal networks and partial least square regression) to generate high-resolution SOC, pH and clay content maps as inputs for VRL on two fields in Denmark. For one of these fields, Kuang et al. 2014 compared sensor based VRL with uniform liming and observed increase in spring barley yields under VRL. However, Kuang et al. 2014 used a high number of soil reference samples (132 samples on 18 ha) and the proximal soil sensing system was operating at a slow speed of 2 km/h. This might not be accepted for practical farm management. Lime recommendations were calculated by an algorithm from the “Danish Centre for Food and Agriculture”, but no bibliographical references or other details were provided.

With practical application in mind, the overarching objective of this paper is to provide guidelines/a protocol for deriving high-resolution lime recommendation maps from the following mobile proximal soil sensor systems: pH electrode, electrical conductivity, gamma ray and optical dual wavelength systems. The specific objectives were (i) to test different proximal soil sensors and sensor combinations to predict the target parameters of soil pH, texture and soil organic matter (SOM) content, (ii) to apply an adapted and currently well-accepted lime recommendation algorithm to the demands of site-specific acidity management and (iii) to compare the results of the novel *variable*-rate liming approach with a *uniform*-rate liming strategy developed with the conventional protocol.

Materials and Methods

Workflow for producing the variable lime requirement maps

To produce the variable lime requirement maps, extensive guidelines were established, including the proximal soil sensing as well as the whole data processing method, from generating maps of soil pH, texture and SOM to the calculation of the precise lime demand to the aggregation of the data to potential working widths (Figure 29). All data processing and statistical analyses were carried out in the free R software environment for statistical computing and graphics (version 3.6.1) (R Core Team 2018).

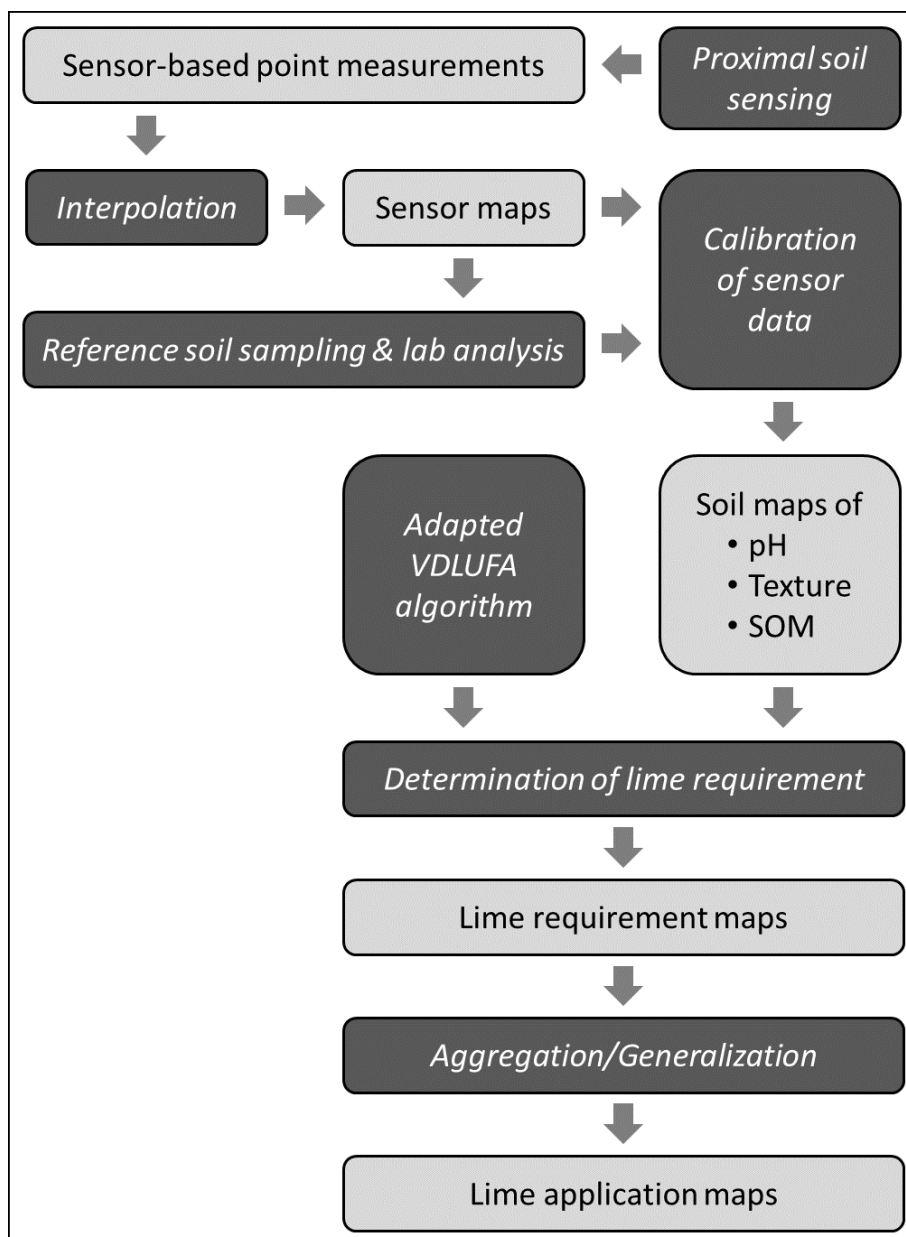


Figure 29: Flow chart visualizing the workflow from the proximal soil sensing to the calculation of the final lime requirement/application maps

Applied on-the-go sensors for generating high-resolution maps of pH, texture and SOM

In this study, the non-commercially available Geophilus measurement system (Lück and Rühlmann 2013) and the commercially available Veris MSP (VERIS Technologies, Salinas, KS, USA) (Figure 30) to generate high-resolution soil ancillary data and subsequent predictions of the parameters soil pH, texture and SOM.

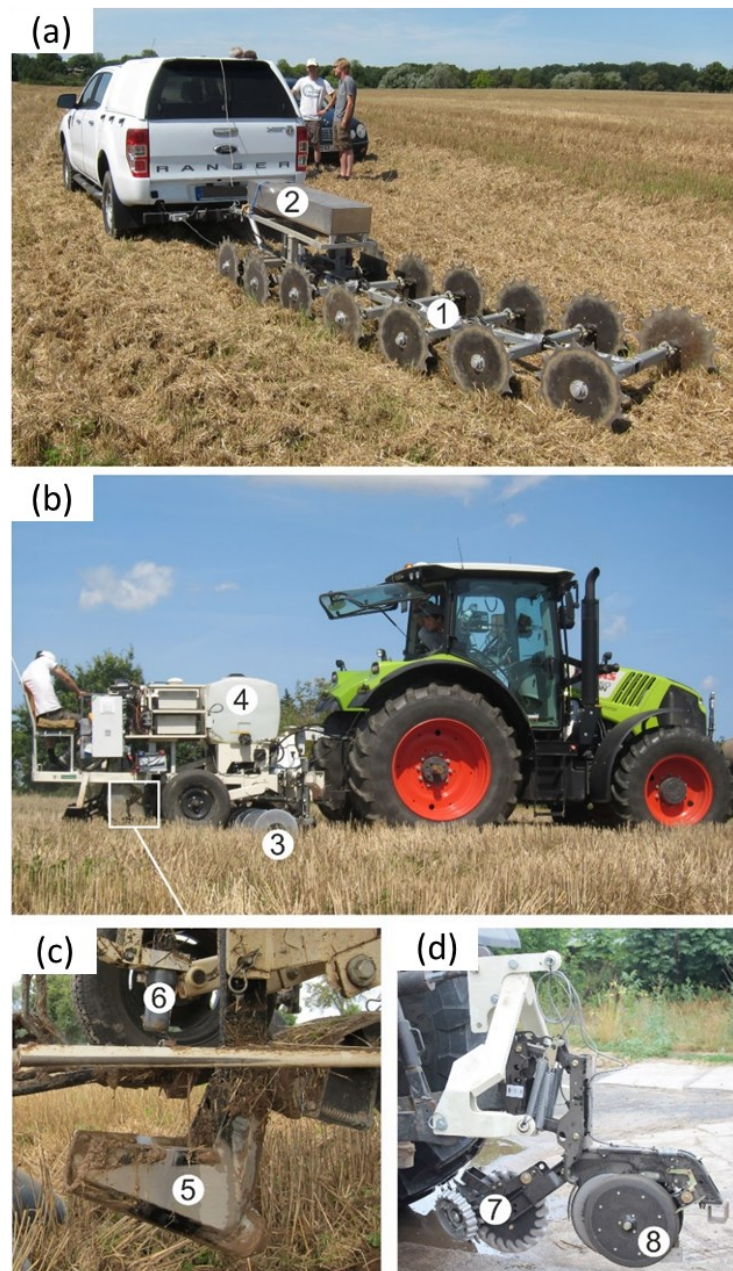


Figure 30: Applied soil sensing platforms: (a) The non-commercially available Geophilus system with 7 rolling electrode pairs (1) and a γ probe (2), (b) the commercially available Veris mobile sensor platform (Veris MSP) by VERIS Technologies with the ERA instrument (3), (c) the Soil pH ManagerTM (water tank (4), soil sampler (5) and pH electrodes (6)) and (d) the OpticMapper (opening coulter (7) and optical module between depth-sensing side wheels (8))

Geophilus measurement system

The Geophilus system is merely built for scientific purposes and includes a multi-depth electrical resistivity sensor and a gamma ray sensor (Lück and Rühlmann 2013) (Figure 30a). The Geophilus system consists of seven pairs of rolling electrodes. One pair directs an electrical current into the soil, and the other six pairs measure the voltage drop. Electrical resistivity (ERa) is explored at six depth levels, from the soil surface to a depth of investigation of 1.5 m. The γ -sensor measures the soil-borne γ -radiation activity as the total counts per second (cps) in approximately the upper 0.3 m soil layer. The system logs the sensor values each second along with the co-ordinates tracked with a differential Global Navigation Satellite System (dGNSS). When mapping with a typical speed of 10 km/h, the sampling interval is approximately 3 m. When the distance between the tracks is 18 m (Figure 31a), approximately 200 data points are measured per hectare.

The Geophilus system enables the fusion of sensor data to produce additional information. Because the γ -radiation is less sensitive to soil moisture than the ERa readings, the ratio between the γ -activity and the ERa of the array with the smallest electrode spacing (investigation depth: 0-0.25 m) represents the influence of the soil water on the ERa readings. This ratio is expressed as the dimensionless soil water index (SWI):

$$SWI = \frac{\gamma}{ERa} \cdot 100 \quad (22)$$

where SWI increases with increasing soil moisture.

Veris multisensor platform

Currently, there is only one commercially available automated on-the-go pH sensor system. The Soil pH Manager™ is part of the Veris MSP (Figure 30b and c) and was developed based on the work of Adamchuk et al. (1999), and described and applied by Lund et al. (2005) and Schirrmann et al. (2011a, b).

Soil pH Manager

The pH value was measured on-the-go by two ion selective antimony electrodes on naturally moist soil material. While driving across the field, a sampler was lowered into the soil to approximately 0.12 m depth, and the soil flowed through the sampler's orifice. When the soil sampler was raised out of the soil, the soil inside the sampler was pressed against the two ion-selective antimony electrodes. Measurements were recorded if they were sufficiently stable within a maximum time of 20 s. A logger recorded the raw potential data along with the dGNSS co-ordinates. Additionally, an online conversion of the voltage data into pH values was conducted based on a preceding calibration with pH 4 and 7 standard solutions. After each measurement, the sampler was

pushed into the soil again, and the old soil sample was replaced by new material that entered the sampler trough. In the meantime, the pH electrodes were cleaned with tap water from two spray nozzles to prepare them for the next measurement cycle. Typically, pH values were recorded every 10-12 s. Geographic co-ordinates were recorded when the sampler shank was raised out of the soil. This sensor can be operated at an approximate speed of 7.5 km/h. With measurements taken every 10 s and a track distance of 12 m, approximately 30 measurements per hectare can be obtained (Figure 31b). After calibration, the estimated total error of the soil pH maps is less than 0.3 pH (Adamchuk and Lund 2008). In addition, ERa is measured by the sensor platform at a rate of 1 Hz with a galvanic coupled resistivity instrument using six parallel rolling coulter electrodes. This electrode configuration provided readings from two depths with a median depth of exploration of 0.12 and 0.37 m, and the data are expressed as the apparent electrical conductivity (ECa) (Gebbers et al. 2009).

OpticMapper

The soil organic matter (SOM) content was estimated using data generated from the OpticMapper (Veris Technologies, Salinas, KS, USA) (Figure 30d). It is an on-the-go optical soil sensor that basically consists of a single photodiode and two light sources (LED) that enable reflectance measurements at 660 nm (red) and 940 nm (near-infrared NIR), each with a bandwidth of 20 nm. According to Kweon et al. (2013) and Kweon and Maxton (2013), absorption at these two wavelengths is particularly sensitive to organic matter content. At the front, the OpticMapper has an opening coulter that cuts crop residues. The optical module is mounted on the bottom of a furrow 'shoe' between two side wheels that control the sensing depth. The wear plate is pressed against the bottom of the furrow approximately 0.04 m below the soil surface with a consistent pressure to provide a self-cleaning function. Light is emitted alternately from the two LEDs and passes through a sapphire window onto the soil. The reflected light is captured by a photodiode, and the light intensity is stored in dimensionless values. The digital reflectance data and GNSS co-ordinates are recorded at a rate of 1 Hz. At a speed of 10-12 km/h and 12 m track distance, an average of 260 reflection data points per hectare can be collected (Figure 31c).

Test field

The selected test field is part of the farm Komturei Lietzen (KL) and is located approximately 40 km east of Berlin (Germany) in the eastern North German Plain (5831100N, 450100E; UTM ETRS89 33N). While the Geophilus system and the Soil pH Manager were applied in April 2018, the OpticMapper campaign was conducted in August 2018. Records were taken along the field's working tracks. This driving path caused fewer errors than driving against the actual working tracks and addressing their spatial irregularities.

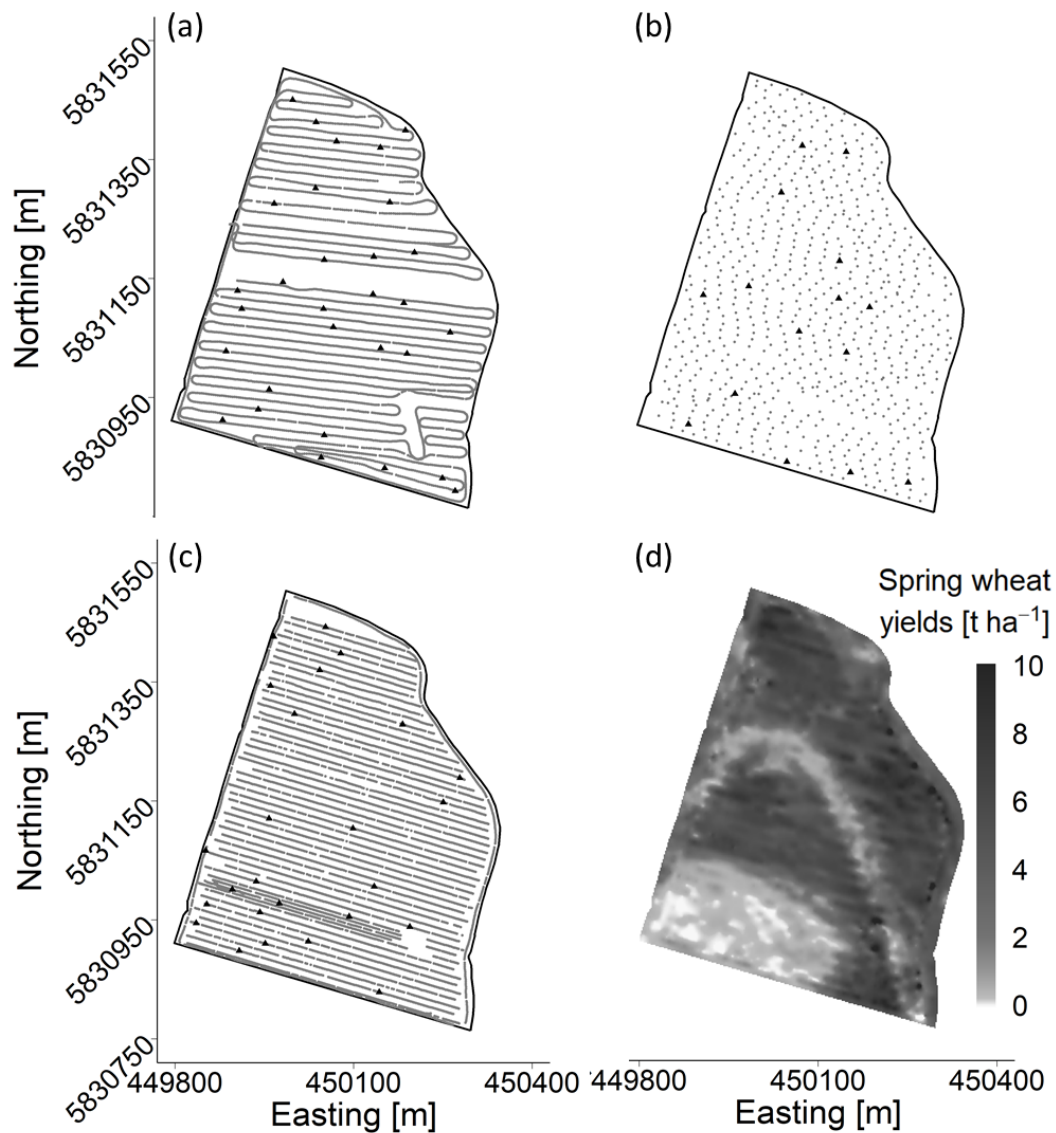


Figure 31: Spatial resolution of the proximal soil sensor measurements of the Geophilus system (a), the Soil pH Manager (b) and the OpticMapper (c) and the sampled soil reference points (black triangles) and yield pattern (d) in the test field (KL60)

The soils at the agricultural study site developed on morainic landscapes shaped by the Pleistocene glaciation processes as well as by fluvial processes in the river valley of the *Oder* River (Krbetschek et al. 2008). The patterns of spring wheat yield from 2018 therefore reflect the natural geological conditions of the current test field (Figure 31d). In accordance with the German soil classification system KA5 (Eckelmann et al. 2005), the soil textures at the study site range from pure sand (class: Ss) to loamy sands (classes: St2, Su2, Sl2 and Sl3) and loams (classes: Lt2, Ls2, Ls3 and Ls4). Hence, the soil cover is highly heterogeneous at the test site and in the selected field (field 60 of KL, henceforth called *KL60*) and is therefore a good example for demonstrating the potential of proximal soil sensing for site-specific lime management. Climatically, the test site is located in the transition zone of the humid oceanic and dry continental climates. The annual mean temperature is 9 °C, and the total mean annual precipitation is 550 mm.

Interpolation of the point-based sensor data

Data cleaning and pre-processing

Before data interpolation, the raw sensor data were observed visually in advance (e.g., for points with strong deviations from the surrounding observations), and obvious measurement errors were removed if necessary. These errors may occur due to insufficient sensor connectivity to the soil or recording issues related to the handling of the sensor platforms. For example, the OpticMapper still records measurements while the sensor shoe is being lifted out of the soil. Thus, records from residual soil –for example, those taken while driving from one tracking line to the next at the end of the field – were removed from the overall data set. To avoid errors in building the covariance matrices used in kriging, observations that shared identical spatial locations were identified, and duplicates were removed in advance.

Variography

The theoretical semivariogram models were fitted as global variograms to the empirical semivariograms, which provided the spatial weighting function for the subsequent kriging interpolation. The empirical semivariogram calculations were performed by selecting robust variogram estimates to prevent effects from extreme outliers (Cressie 1993). The theoretical variograms were additionally fitted with localized cut-offs to meet the criteria of obtaining good fits at distances smaller than the whole plot. Furthermore, the model fitting was performed by weighted least squares approximation (fit method 7 in *gstat*), dividing the number of pairs in one bin by the square of the bin's metric distance (Pebesma 2004). After an initial fit of the semivariogram model, a leave-one-out cross-validation procedure was applied (Webster and Oliver 2007) using the initial semivariogram model to predict the values by ordinary kriging at each measurement location after excluding the sample value at that particular point.

Interpolation

Two geostatistical methods were applied: The Geophilus' point-based sensor data were interpolated using the geostatistical method of ordinary kriging, and block kriging was applied for the soil pH and OpticMapper data (R package '*gstat*'; Pebesma (2004)). The smoothing procedure block kriging eliminates spatial outliers that show a strong deviation from the surrounding observations. Block kriging produces averaged values within a predefined neighbourhood (block) around the prediction location (Olea 2012). To maintain an appropriate ratio between the prediction of real spatial micro-patterns and the elimination of erroneous sensor measurements, different block sizes were tested, and a suitable block size of 20 x 20 m with low root mean square error (RMSE) values

was chosen. This block size allows for inclusion of measurements along one track and measurements from neighbouring tracks.

Due to the sensor high measurement intervals and the consequent high spatial resolution, two criteria (whichever applies first) were established to reduce the number of neighbouring points in the ordinary kriging procedure to considerably reduce the computation time: (i) the maximum distance from the prediction location was set to 100 m and (ii) the maximum number of nearest observations was set to 100. To facilitate automation of the applied processes, this localized kriging approach allows the computation time to be reduced and avoids the complexity of filtering model variograms for local prediction models (Hengl 2009). The final raster data sets created had a spatial resolution of 2 x 2 m for each parameter and were clipped to the boundary of the field.

More advanced geostatistical methods could have been used (e.g., kriging with local variograms, external drift kriging or modelling of spatial anisotropy). However, the geostatistical methods were restricted to simple methods here to keep the focus on the main topic of this research, which is the complete workflow of sensor-based site-specific liming. Moreover, considering their feasibility under practical conditions, geostatistical modelling efforts should be reasonable regarding the extent to which interpolation errors can be minimized. For experts, it would be easy to integrate more advanced geostatistical methods. However, in addition to being time intensive, more advanced methods introduce some problems (e.g., overfitting). Furthermore, ordinary kriging with a large amount of data is relatively robust according to Webster and Oliver (2007) and Goovaerts (1997). That is, kriging results will not differ substantially regardless of the variogram modelling and kriging approaches.

Reference soil sampling

Reference soil sampling locations were selected based on the proximal soil sensor data (sensor-guided sampling). To relate the sensor data to the target parameters, 30 reference soil samples were taken from the field for soil texture analysis, 15 for pH and 25 for SOM at locations that met the following three criteria (Adamchuk et al. 2011):

- i. The targeted samples cover the entire range of the sensor data (feature space):
From the sensor data, high and low values were selected using the 30% and 70% quantiles. This was in order to have the calibration model be based on a wide range of values.
- ii. The location is spatially homogeneous:
To avoid the sampling of outliers or erroneous sensor measurements, high and low values should be clustered within a radius of 30 m around the reference sampling point.

- iii. The samples are well distributed throughout the area of investigation: Conditioned Latin hypercube sampling by Minasny and McBratney (2006) (using R package 'clhs'; Roudier (2011)) was applied to spread the sampling points evenly over the field by maximizing the distance between them. This was done by means of stratified sampling using x and y co-ordinates and the consecutive point ID of the sensor measurements.

Soil samples were taken along the soil sensing trajectory. At each reference sampling point, five subsamples were taken with an auger from 0 to 0.3 m depth within a radius of 0.5 m. The bulked samples were oven-dried at 75°C and sieved to less than 2 mm in the laboratory. The pH value was measured in 10 g of soil and 25 ml of 0.01 M CaCl₂ solution according to DIN ISO 10390 with a glass electrode after 60 min. The particle size distribution of the < 2 mm fraction was determined according to the German standard for soil science (DIN ISO 11277) by wet sieving and sedimentation after the removal of organic matter with H₂O₂ and dispersion by 0.2 N Na₄P₂O₇. The soil organic carbon (SOC) was analysed by elementary analysis using the dry combustion method (DIN ISO 10694) after removing the inorganic carbon with hydrochloric acid. To calculate the amount of SOM, the SOC was multiplied by 1.72 (Peverill et al. 1999).

Spatial prediction of soil texture, pH and SOM

To construct relationship models between the sensor data and the lab-analysed soil properties, the interpolated on-the-go sensor data were extracted at the reference sampling locations. Calibrating the interpolated sensor data (particularly the pH data) resulted in better models (lower RMSE, higher R²) than the models developed by calibrating the sensor point data first and interpolating afterwards because pre-processing and interpolation removes some noise from the sensor data.

Since the calibration of the pH sensor data is solely related to the lab-analysed pH values, a univariate linear regression (ULR) model was generated. The predictions of the three soil texture fractions and SOM, on the other hand, were based on the Geophilus (ERa, γ, DEM, SWI) and OpticMapper (Red, IR) data, respectively. Hence, multi-variate linear regression (MLR) models were applied as:

$$z = b_0 + b_1X_1 + b_2X_2 + \dots + b_nX_n + \epsilon \quad (23)$$

where z is the dependent variable at the i th site; X_1, X_2, \dots, X_n are the ancillary data measured at the same site; $b_0, b_1, b_2, \dots, b_n$ are the $n + 1$ regression coefficients; and ϵ is the random error. Before MLR modelling was applied, the interpolated sensor data were checked for their predictive power. If Pearson's correlation coefficient (R) of two variables was found to be larger than 0.65, the

variable that correlated best with the target soil property was chosen. Based on the reduced data set of independent variables, a backward stepwise selection (R package 'caret'; Kuhn et al. (2019)) was conducted to find the best set of predictive variables for the MLR model. To assess the accuracy of the MLR models, a k-fold cross-validation was applied one hundred times with $k = 3$ for SOM and $k = 4$ for the soil texture prediction. The accuracy of each model was determined using the root mean square error (RMSE) and the coefficient of determination (R^2).

Here, clay, silt and sand were considered as fractions summing to 100% or 1 kg kg^{-1} and having non-negative values (De Gruijter et al. 1997). Hence, when the soil fractions are estimated individually from MLR models, compositional data rules apply to the predicted values (Huang et al. 2014; Muzzamal et al. 2018). To meet these requirements, an additive log-ratio (ALR) transformation was performed (R package 'compositions'; van den Boogaart and Tolosana-Delgado (2008)) following the approaches of Chayes (1960) and Aitchison (1982). In ALR, no fraction is interpreted as isolated from the others. The two advantages of this approach are (i) the removal of closure effects and (ii) the production of suitable data for classical statistical analysis, such as MLR, because the transformed values may be closer to a normal distribution than the untransformed data through perturbation (Odeh et al. 2003).

Determination of variable lime requirements (CaO amounts)

In this study, an empirical lime requirement algorithm was utilized and was adapted to the needs of high-resolution soil data. The conventional VDLUFA approach consists of a look-up table system that allows farmers in Germany to very easily determine the lime requirement (LR) as the amount of CaO that needs to be applied to adjust the soil pH value towards the optimum level and maintain that level until the next fertilization cycle (von Wulffen et al. 2008). This approach defines five pH/lime supply classes for five mineral soil texture classes (Table 16) and for a peat soil class as well as four SOM classes ($\leq 4 \text{ g kg}^{-1}$, $4.1\text{...}8 \text{ g kg}^{-1}$, $8.1\text{...}15 \text{ g kg}^{-1}$, $15.1\text{...}30 \text{ g kg}^{-1}$) for arable land. The current pH values in classes A and B are further subdivided into small 1/10 pH unit steps.

Table 16: Soil pH and lime requirement from the VDLUFA guidelines (von Wulffen et al. 2008)

pH class/lime supply	Description	Lime requirement
A – very low	<u>Conditions:</u> Significant impairment of soil structure and nutrient availability, very high lime requirement, significant yield losses in almost all crops up to complete yield loss, greatly increased plant availability of heavy metals in the soil. <u>Action:</u> Liming takes precedence over other fertilization measures regardless of the crop.	Recovery liming
B – low	<u>Conditions:</u> Still sub-optimal conditions for soil structure and nutrient availability, high lime requirement, mostly still significant yield losses in lime-demanding crops, increased plant availability of heavy metals in the soil. <u>Action:</u> Within the crop rotation, preferential liming for lime-demanding crops.	Build-up liming
C – optimal	<u>Conditions:</u> Optimal conditions for soil structure and nutrient availability, low lime requirement, hardly or no additional yield through liming. <u>Action:</u> Within the crop rotation, liming for lime-demanding crops.	Maintenance liming
D – high	<u>Conditions:</u> Soil pH status is higher than intended, no lime requirement. <u>Action:</u> No lime application	No liming
E – very high	<u>Conditions:</u> The soil pH status is much higher than intended and can negatively affect nutrient availability as well as crop yield and quality. <u>Action:</u> No liming or use of fertilizers that, as a result of physio-chemical or chemical reactions, acidify the soil.	No liming and no use of fertilizers that react physio-chemically to alkaline conditions

Table 17: Content ranges (kg kg⁻¹) of the VDLUFA soil texture groups

VDLUFA soil group (SG)	Clay	Silt	Sand
Sand (1)	0-0.05	0-0.25	0.7-1
Weak loamy sand (2)	0-0.17	0-0.5	0.42-0.95
Strong loamy sand (3)	0.08-0.25	0-0.5	0.33-0.83
Sandy to silty loam (4)	0-0.35	0-1	0-0.75
Clayey loam to clay (5)	0.25-1	0-0.75	0-0.65

This rough soil texture and SOM classification system contrasts with the sensitivity and density of the information mapped with mobile on-field sensor systems. Thus, the conventional VDLUFA approach was improved by deriving a continuous or ‘stepless’ algorithm, i.e., using real values for the three soil properties instead of classified integer values. The adaptation is briefly summarized here.

First, a central value was defined for each VDLUFA soil group (SG) and SOM class. For the soil groups, the mean clay contents were considered according to the KA5 classes that are assigned to the particular VDLUFA soil groups in kg kg^{-1} : SG1: 0.025, SG2: 0.085, SG3: 0.165, SG4: 0.175 and SG5: 0.625. For the SOM classes, the median values 2, 6, 11.5 and 22.5 were set as references in g kg^{-1} . Second, the pH values of the corresponding five lime supply levels A – E (Table 17) were related to both the five clay contents and the four SOM contents as reported above. Third, non-linear regressions were used to calculate the functional relationships that allow the estimation of the respective lime supply level (A – E) for any combination of clay and SOM content. Finally, the lime fertilization recommendation can be calculated depending on the difference between the current and the target pH (lime supply level C, Table 17) as well as the actual clay and SOM content.

Data aggregation and evaluation of the variable lime requirements

Because accurate GNSS receivers and auto-guidance systems are available at reasonable prices, controlled trafficking has gained much popularity and can almost be seen as an integral part of precision agriculture in practice. Consequently, prescription maps for liming should consider the fixed tramlines and working widths used in controlled trafficking. The results were therefore not only shown for the potentially highest resolution of 2 x 2 m but were also aggregated for possible lime spreader working widths of 18 x 18 m and 36 x 36 m for management purposes.

To evaluate the novel VRL approach, the lime amounts from the generalized *variable* LR maps were compared with possible LRs from a *uniform* liming strategy, and each management unit (e.g., 18 x 18 m) was determined to be either *under-*, *adequately* or *over-*fertilized by the uniform liming approach. Therefore, the pH range for each management unit was computed by subtracting or adding the pH RMSE from each modelled pH value. Afterwards, these pH ranges were used to calculate CaO threshold values for over- and under-fertilization using the stepless algorithm described above. For simplicity, the estimates are based on the error (RMSE) of the derived pH map only, as pH has been determined to be the most important soil property for LR estimation in the investigated soils (Vogel et al. 2020).

The uniform lime demand was determined from the VDLUFA look-up table system using the average pH, SOM and soil texture values for the corresponding SOM and soil texture groups as derived from the sensor-based soil maps of the test field. To account for the coarse classification system of the conventional VDLUFA approach, the uniform estimated LR based on the known soil texture group was additionally compared to estimated LRs based on other potentially selectable soil texture groups.

Results and discussion

Geostatistics

The empirical semivariograms and the fitted models for all on-the-go sensor data formed the basis for the interpolation of the sensor point measurements by ordinary kriging (Figure 32). The selected semivariogram models and the derived variogram parameters sill, nugget and range are summarized in Table 18. The nugget indicates that the sensor data show no or very low spatial micro-variance and random error in their measurements. The spatial correlation structure of the sensor data on the test field can be best characterized by circular (γ , elevation, pH, ECa), exponential (Red, IR) and Gaussian (ERa) models. Cut-offs were set at a distance when a first local maxima is reached or became slightly visible. Due to the exponential character of the fitted semivariogram model for the OpticMapper sensor data, the sill, i.e., the limit of spatial correlation, is reached at rather low ranges of 55 (Infrared) and 60 m (Red), indicating very high spatial variability in that optical soil characteristic. The remaining sensor data showed slightly lower spatial variability with higher ranges of 170 (ERa) to 316 m (pH).

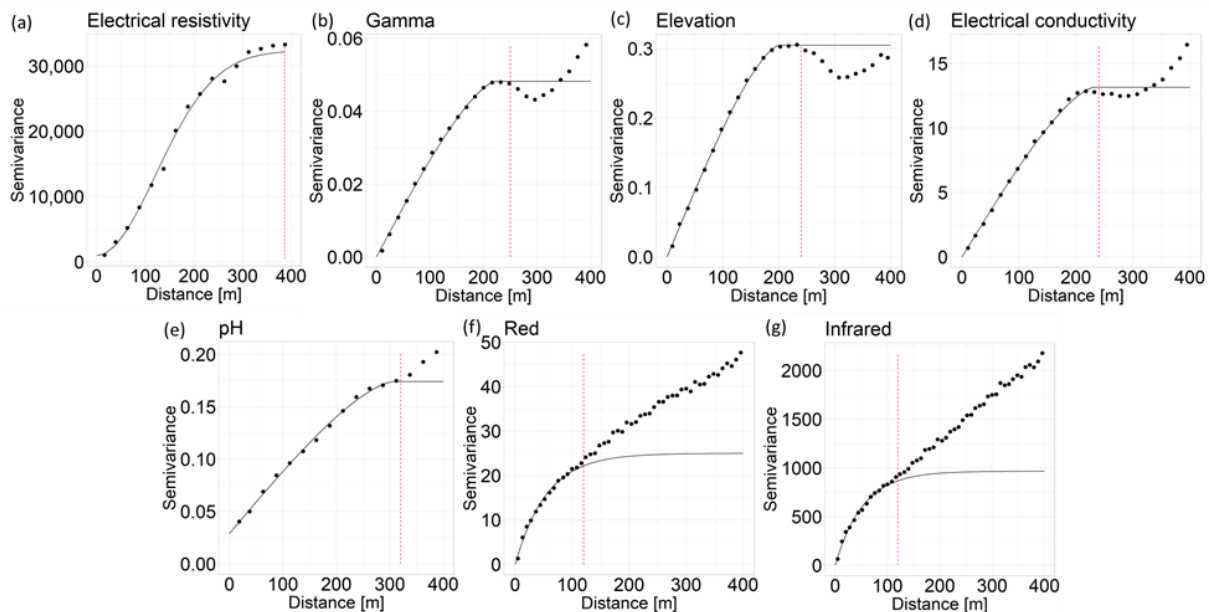


Figure 32: Semivariogram analysis of the sensor point data for ordinary kriging analysis of the field KL60: Electrical resistivity (a), Gamma (b), Elevation (c), Electrical conductivity (d), pH (e), Red (f) and Infrared (g) (Model parameters found in Table 18). Dashed lines (red) represent the spatial separation distance up to which point pairs are included in the semivariance estimates

Table 18: Parameters of the semivariogram models of the on-the-go sensor data

Parameter	M	Cut-off, m	Sill	N	Range, m
Electrical resistivity	G	380	32362.72	9	171.2
Gamma	C	250	0.05	0	211.7
Elevation	C	240	0.3	0	198.1
Electrical conductivity	C	240	13.15	0	231.9
pH sensor	C	320	0.15	0	306.2
Red	E	120	24.97	0	54.9
Infrared	E	120	965.59	0	52.2

Regionalized sensor data

The interpolated mapping results are shown in Figure 33. They have a spatial resolution of 2 m and show distinct spatial patterns. The colour scales (and displayed value ranges) of the ERa, ECa and γ data as well as those for the SWI indicate the moisture and/or textural condition at the specific location. For example, for ERa, while values of < 100 Ohm m indicate areas with high soil moisture and/or higher clay content, values of > 150 Ohm m represent the driest and/or most sandy areas (Figure 33). Since both ERa and soil γ are strongly related to soil texture, the low-resistivity areas correspond well to the high γ -activity areas, and vice versa. Differences between the patterns in the two maps can be explained by the different soil moisture sensitivities of the two sensors, as shown in the SWI map, with lower values indicating dryer areas and higher values indicating wetter areas. ERa and ECa represent the same content, as they are reciprocal values, and the scales and colours are arranged accordingly to provide similar interpretations. Lower values of ECa (< 3 mS m⁻¹) indicate dryer and more sandy areas, and higher ECa values (> 6 mS m⁻¹) indicate higher soil moisture and clay contents. The OpticMapper sensor data are characterised by a large cluster of high red and IR values (dimensionless) in the southern and south-western parts of the field. Lower values can be found in the immediate surroundings to the north and to the east as well as in the northernmost part of the field. The spatial patterns of the IR map show more contrasts than those of the red map, whereas the IR/red ratio map shows patterns that are almost identical to the IR patterns. The sensor pH values in field KL60 show four different zones. The northern part of the field is characterized by the highest pH values. To the southeast, there are intermediate pH values and, farther to the south, the pH increases slightly. In the southernmost part of the field, however, the pH values reach their minimum.

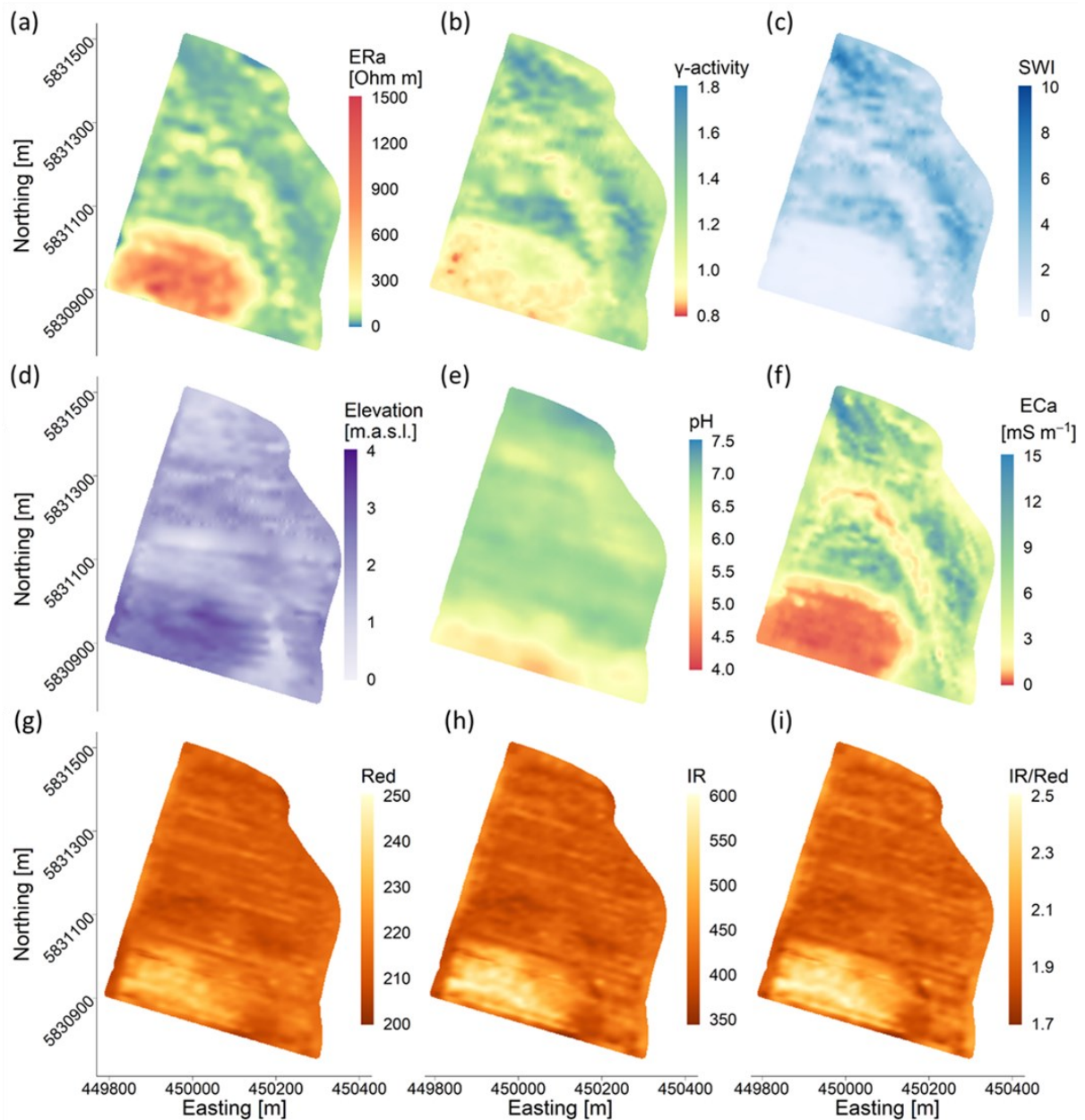


Figure 33: Mapping results from the sensors available in this study: (a) electrical resistivity (ERa, first channel of the Geophilus system, 0-0.25 m), (b) γ -activity (0-0.3 m), (c) calculated soil moisture index, SWI (dimensionless), (d) digital elevation model, (e) pH, (f) electrical conductivity (ECa-shallow of the Veris MSP; median depth 0.12 m), (g) red (dimensionless, from the Optic mapper of the Veris MSP), (h) infrared (IR, dimensionless) and (i) IR/Red ratio (dimensionless)

Calibration of the sensor data

The sensor-based spatial prediction models for pH, soil texture and SOM were calibrated and validated using the lab analysed soil samples selected based on the sensor maps. The descriptive statistics for the reference soil samples are summarized in Table 19.

Table 19: Overview of the laboratory results for the soil properties measured in this study

Parameter	n	Min	Max	Mean	Median	SD
pH	15	4.3	6.6	6	6.4	0.8
SOC (g kg ⁻¹)	25	5.8	29.1	15.4	16.2	8
Clay (kg kg ⁻¹)	30	0.012	0.461	0.191	0.175	0.128
Silt (kg kg ⁻¹)	30	0.022	0.289	0.134	0.11	0.088
Sand (kg kg ⁻¹)	30	0.301	0.961	0.675	0.716	0.21

The prediction performance of the univariate linear regression model for pH was very good, with an R^2 of 0.91 and an RMSE of 0.37 (Table 20). The calibrated pH values are lower than the field-measured sensor pH values (Figure 34). This occurred for the following three reasons:

- i. The field pH was measured with antimony electrodes instead of with the glass electrodes that are standard in the laboratory.
- ii. The field pH was measured in tap water, which has a neutral to slightly alkaline pH value, whereas the lab analysis was performed with 0.01 M CaCl₂ solution. Due to the exchange processes of Al³⁺ by Ca²⁺ at the surface of soil colloids, the pH measured in salt solution is generally lower by 0.6 (± 0.2) pH units. Furthermore, in salt solution, there is no suspension effect to balance the diffusion potential between the pH electrode and the soil solution (Blume et al. 2016).
- iii. The exposure time between the soil and the solution in which the pH value is measured is a maximum of 20 s (Lund et al. 2005) in the field compared to 60 min during the laboratory procedure. During that time, many more protons can be emitted and measured by the pH electrode.

MLR models were used to regionalize the SOM content and soil texture with the sensor data. After testing the proxy variables for independence, the SOM content was predicted using the covariates IR, SWI and ECa. These and the lab-analysed SOC results multiplied by 1.72 were used to calibrate the sensor data. The prediction performance is shown in Figure 34, showing that the RMSE for SOM was 6.4 g kg⁻¹ with a range of approximately 55 g kg⁻¹.

After analysing ERa, γ , SWI and elevation for interdependence, only γ and ERa were used as independent variables for predicting the soil texture fractions of sand and clay in the combined MLR and ALR approach. The soil texture prediction results are shown in Figure 34c-e. The good

performance of the models is reflected by, e.g., the prediction of the clay and sand fraction; 87 and 88% of the variability could be explained, and the corresponding RMSE values were 0.046 kg kg⁻¹ and 0.072 kg kg⁻¹, respectively. Due to the log-ratio transformation of the two predictors, the sand and clay fractions, the prediction of the silt fraction was poor, with an RMSE of 0.039 kg kg⁻¹.

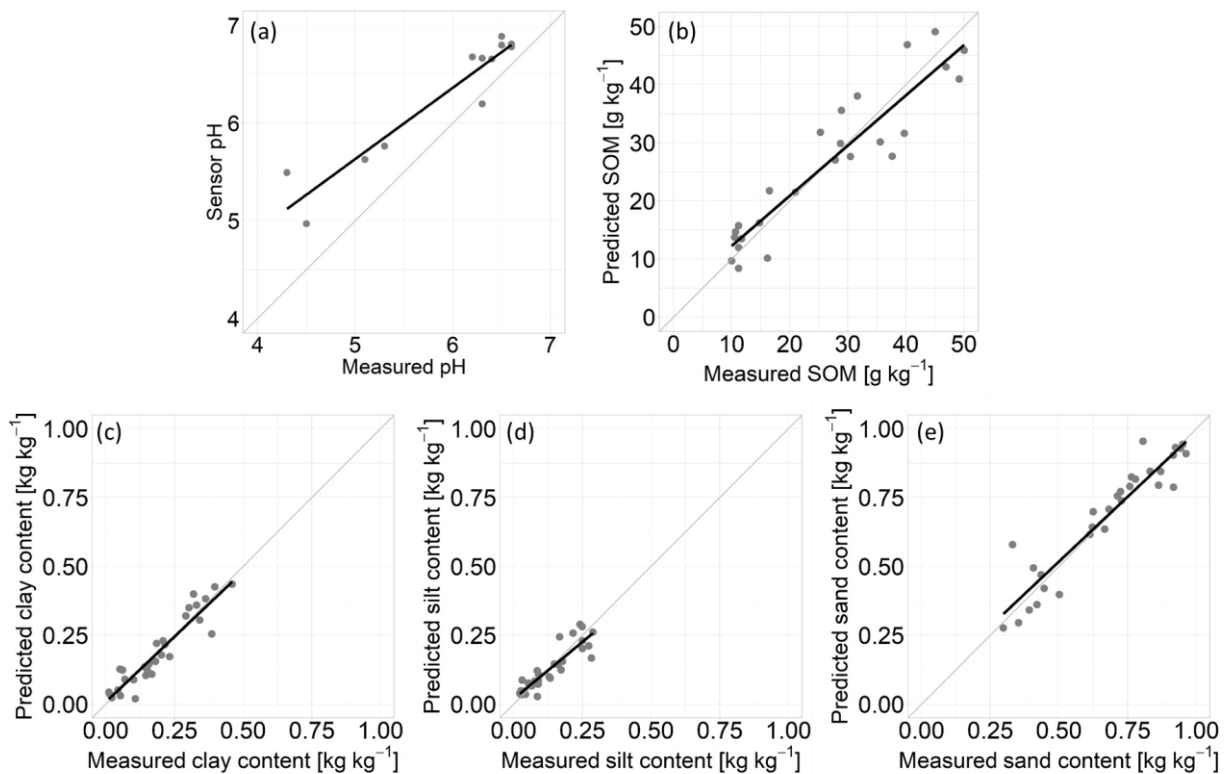


Figure 34: Calibration model qualities for the predicted soil parameters pH (a), soil organic matter (SOM) (b), clay (c), silt (d) and sand (e)

Generated soil maps

The soil maps of the pH, clay and SOM in KL60 are the basis for the calculation of the site-specific lime requirement of the field following the VDLUFA guidelines for liming in Germany. The descriptive statistics for the predicted soil properties can be found in Table 20.

Regarding the soil texture, derived regression models were applied to the interpolated Geophilus raster data sets, and the soil texture fractions were predicted for the entire field (Figure 35). Sand is the dominant soil texture fraction, followed by the clay fraction and a comparatively low mean silt content. However, the sand and clay fraction values have relatively large ranges of 0.7 kg kg⁻¹ and 0.44 kg kg⁻¹, respectively, whereas the silt fraction values have a comparatively low range of 0.26 kg kg⁻¹. Larger portions of sand were found in the more elevated areas to the south, the south-western part of the field and near the eastern and north-eastern borders. A more linear sandy zone stretches out from the southeast to the northwest in the centre of the field. This might have been

formed by streams as part of the (post-) Palaeozoic glacial landscapes, which are well known for their high soil and sediment variability (Krbetschek et al. 2008). Glacial, periglacial and interglacial processes created a mosaic of landforms and unconsolidated sediments that vary over short distances. Clayey areas dominate the lower elevated flanks along the sandy areas from the southeast to the northwest, indicating lower water drainage. The silt fraction in this field shows less pronounced variation than the sand and clay fractions.

Table 20: Validation results and descriptive statistics for the predicted soil properties from the (uni- and multi-variate) linear models

Parameter	Min	Max	Mean	Median	SD	CV%	R ²	RMSE	Model
Clay (kg kg ⁻¹)	0.01	0.45	0.17	0.17	0.1	57.9	0.87	0.046	ALR-MLR
Silt (kg kg ⁻¹)	0.03	0.29	0.12	0.11	0.06	51.9	0.79	0.039	ALR-MLR
Sand (kg kg ⁻¹)	0.26	0.96	0.71	0.72	0.16	23	0.88	0.072	ALR-MLR
pH	4.2	7.1	5.7*	6.4	5.2*	8.9	0.91	0.37	LM
SOM (g kg ⁻¹)	6.6	62.1	30	30.2	10.5	34.9	0.82	6.4	MLR

SOM: soil organic matter, SD: standard deviation, CV%: percentage of coefficient of variation, R²: coefficient of determination, RMSE: root mean square error, ULR: univariate linear regression, MLR: multi-variate linear regression and ALR: additive log-ratio model

* calculated with exponentiated data

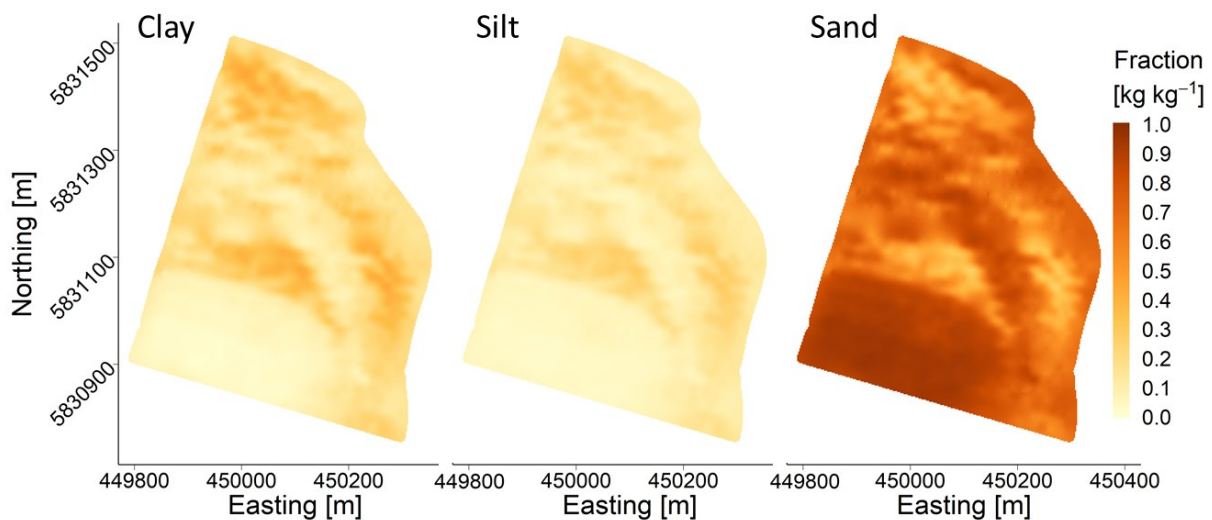


Figure 35: Predicted clay content (left), silt content (middle) and sand content (right) from the Geophilus sensor platform

The classified soil texture map (Figure 36a) shows that the classes, according to the German soil classification system KA5, cover a relatively wide range from pure sand (Ss) to slightly loamy sand (St2), highly loamy sand (Sl4), medium clayey sand (St3), highly sandy loam (Ls4) and clayey sandy loam (Lts). The distribution of the classes corresponds well to the findings of the clay, silt and sand

distribution and provides some clarification. An area of approximately 4 ha is covered by pure sand only in the southern part of the field. Slightly loamy sand (St2) covers a total area of approximately 7 ha. The classes Sl4 and Ls4 are only visible in tiny patches of less than 5 ha combined. They occur as transition areas to clayey sandy loam (Lts, which covers three larger areas of approximately 5.5 ha in the centre, the west and the north of the field) and very slightly loamy sand (St2, which covers approximately 7.7 ha in total). The KA5 soil classification was chosen to avoid the insufficient spatial resolution of the VDLUFA soil texture classification system.

In other studies, Boenecke et al. (2018) and Meyer et al. (2019) used data from the Geophilus system to successfully generate predictive soil texture maps of the clay, silt and sand fractions of the topsoil for practical purposes. Meyer et al. (2019) achieved the best prediction results by deriving the soil texture of the topsoil using the gamma mapping results and by calculating the dimensionless relationship between the gamma and electrical resistivity mapping results.

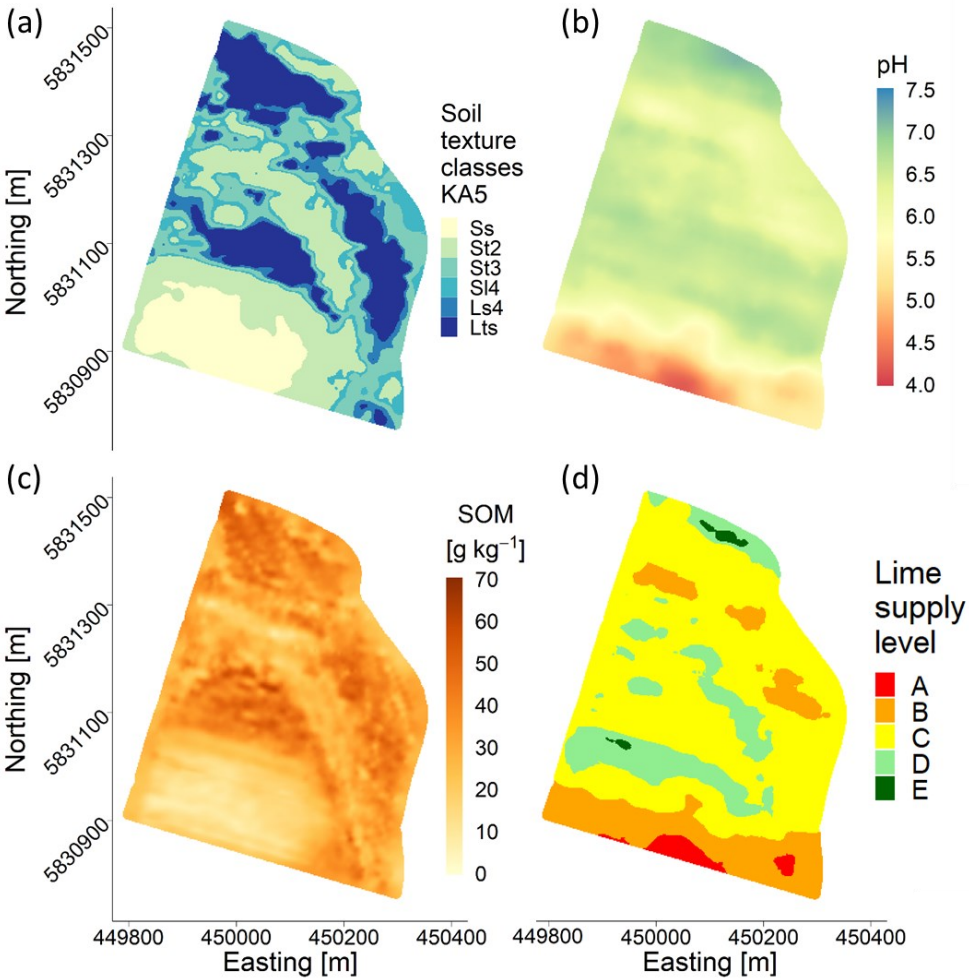


Figure 36: Geophilus mapped soil texture classes (derived from the German KA5 soil texture classification (Eckelmann et al. 2005)) Ss: pure sand; St2: slightly loamy sand; St3: medium clayey sand; Sl4: highly sandy loam; Ls4: highly sandy loam; Lts: clayey sandy loam (a), the MSP-mapped pH values (b) and SOM content (c) and the lime supply level at 2 x 2 m resolution

The calibrated pH values in field KL60 ranged between 4.2 and 7.1 (Figure 36b) with a median of 6.4. Since the pH calibration is based on a univariate linear regression model, the spatial patterns of the calibrated data were identical to the sensor data and indicated four different zones of soil acidity. The error of the pH measurements was 0.07 pH units larger than that determined by Adamchuk and Lund (2008). It is striking that the lowest pH values were found in the sandy regions of the field, which also showed the lowest amounts of SOM. In contrast, pH values were highest in the loamy parts of the field that had higher SOM contents.

The field KL60 is characterized by low SOM content, showing a mean of 30 g kg⁻¹, a range of 55.5 g kg⁻¹ and a standard deviation of 10.5 g kg⁻¹. The spatial patterns of the SOM map show many similarities to those of the soil texture map (Figure 36c). The slightly elevated sandy hilltops in the southern and central parts of the field are characterized by lower amounts of SOM. In contrast, higher amounts can be found in the lower-lying areas, coinciding with a loamy soil texture and higher pH values.

In a study by Kuang et al. (2015), artificial neuronal network (ANN) and partial least square regression (PLSR) were used for the calibration of a visible and near infrared (vis-NIR) sensor data to generate high-resolution maps of pH, SOC and clay. Using a high number of soil reference samples for their two test fields (n = 132 and n = 80), calibration with ANN outperformed the PLSR method. For example, the root mean square error (RMSE) for the ANN calibrated sensor data was 12.5 g kg⁻¹ for SOC, 0.12 for pH and 0.0096 kg kg⁻¹ for the clay content (PLSR: 14.8 g kg⁻¹ for SOC, 0.13 for pH, 0.0105 kg kg⁻¹ for clay content).

Regarding the lime supply status of KL60, approximately 20% of the field requires recovery or build-up liming (levels A and B), and 16.5% requires no liming at all (levels D and E). Nearly two-thirds of the field is within the optimal lime supply range (level C) and only requires maintenance liming (Figure 36d). By decreasing the resolution to management conform units, the areal percentages did not change considerably (Table 21).

Table 21: Areal percentages of the VDLUFA lime supply levels (A, B, C, D, E, description in Table 1) at the spatial resolutions of potential lime spreader working widths (18 x 18 m and 36 x 36)

Resolution (m)	A	B	C	D	E
2 x 2	2.1	18.2	63.2	15.8	0.7
18 x 18	2.4	17.8	64.9	14.3	0.6
36 x 36	2.2	18.5	64.3	15	-

Determined lime requirements and data aggregation

The high-resolution LR map (expressed in t CaO ha⁻¹) was used to generate a prescription map for liming whose spatial resolution was adapted to the working width of a lime spreader (Figure 37). For that, the CaO data were resampled to an 18 x 18 m raster grid and aligned to the appropriate management direction of the field (Figure 37b). For spreaders with larger working widths, e.g., 36 x 36, the creation of maps with larger raster widths leads to information losses and increasingly over- or under-limed portions of the field (Figure 37c). The map shows that the total LR of field KL60 is rather low. Nevertheless, relatively high spatial variability exists that can only be well explained by the combination of all three soil maps: pH, soil texture and SOM (Table 22). The 2 x 2 m resolution map shows that CaO values had a range of more than 7 t ha⁻¹, with some areas requiring no lime at all and some areas showing very high demand. Low lime requirements were identified in the northern and central parts of the field where pH values are high, SOM content is low and the soil texture is dominated by sand. In contrast, the higher lime requirements in the northern central areas are particularly caused by the loamy soil textures that increase the target pH value according to the VDLUFA guidelines for liming. As mentioned above, this is because soils with a higher clay content require more lime to stabilize their soil structure. Furthermore, clayey soils can be prone to aluminium toxicity, which can be counteracted by liming (Schilling 2000; Blume et al. 2016). The highest lime requirements on field KL60 can be seen in the south and southeast. These areas coincide with the lowest pH values and sandy soil textures.

The aggregation of the 2 x 2 m resolution map to management units of 18 x 18 m and 36 x 36 m revealed that the maximum LRs decreased by approximately 6% and 13%, respectively. The cumulative LR amounts increased by 11% and 25%, respectively.

Table 22: Summary statistics for the final lime requirements at the three different map resolutions

Resolution (m)	Min	Max	Mean	Median	SD	CV%	Cumulative (t)
2 x 2	0	7.4	1.03	0.8	1.17	113.9	28.4
18 x 18	0	6.97	1.06	0.8	1.21	113.9	31.5
36 x 36	0	6.51	1.11	0.8	1.27	114.2	35.4

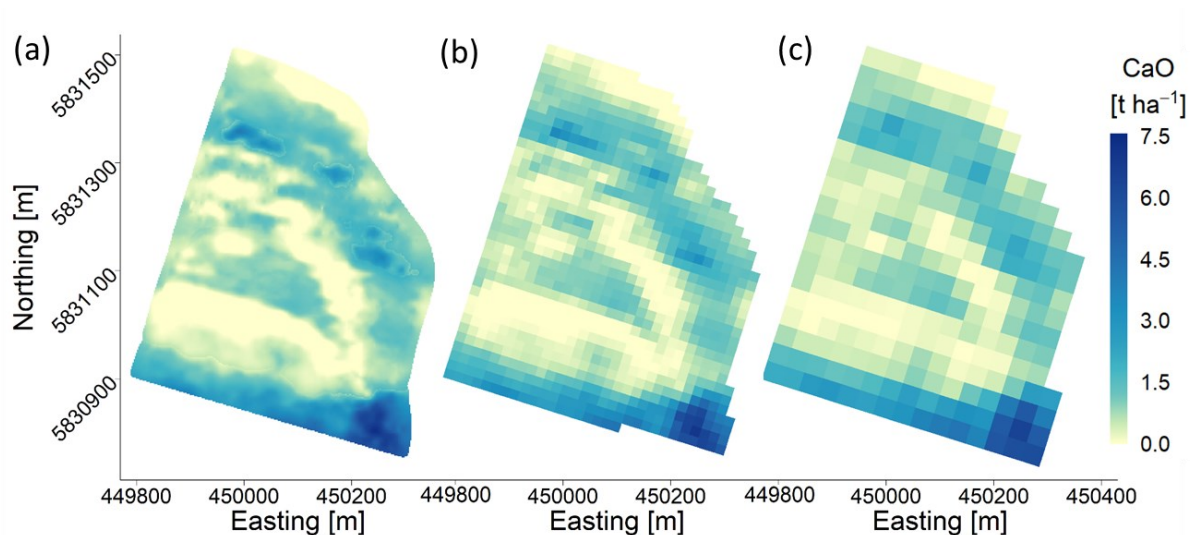


Figure 37: Final CaO requirements calculated at 2 x 2 m resolution (a) and aggregated for potential lime spreader working widths of 18 x 18 m (b) and 36 x 36 m (c) aligned in the management direction

Evaluation and comparison of the variable-rate lime requirements

The variable liming results were compared with a uniform liming approach in which the lime demands were determined following the conventional VDLUFA guidelines. Assuming that the sensor based LR map most closely reflects the actual LR conditions in the field, uniform liming would result in certain areas of the field being under-, adequately or over-fertilized (Table 23, Figure 38). According to the mean values for the clay, silt and sand fractions in the test field (Table 20), VDLUFA soil texture group 2 (Table 17) would be most suitable for assessing the LR in the uniform fertilization strategy. The errors and uncertainties of the conventional approach can hardly be quantified. While the pH and SOM content can be more easily assessed by laboratory analysis, the texture values are often measured by quick on-field methods in conventional farming practices. However, this method is highly prone to error (Stocker and Walthert 2013) and may lead to the potential selection of adjacent soil groups (e.g., in this study, soil group 1 or 3). Moreover, these errors and variances are usually not considered in practice. Within this study, the uncertainties of the conventional approach were therefore expressed by comparing the lime demands of the potentially selectable soil groups as per the VDLUFA soil classification system (Table 17).

It also needs to be emphasized that a soil mapping process is also not free from error. A digital soil map is the outcome of several consecutive steps that are associated with uncertainties. These steps include soil sampling, laboratory analysis and final digital soil mapping (comprising sensor data interpolation and parameter calibration). Uncertainties can be caused by several factors, such as the measurement methods and tools as well as the natural variability of the soil. For example, even high-resolution surveys suffer from the fact that a field cannot be measured at each individual point. Such

uncertainties are discussed widely in the literature (Brendan et al. 2017; Piiki and Söderström 2019). Due to the complexity of error propagation, only a few studies have tried to compare the impacts of sources of errors to optimize the soil mapping process (Mueller et al. 2004; Gebbers and De Bruin 2010). Gebbers and De Bruin (2010) have shown how the relevance of factor uncertainties (e.g., sampling design and interval, positioning error, regionalisation method) can be quantified by global sensitivity analyses of a stochastic simulation model of the soil mapping process. They found that uncertainties due to the sampling density, the spatial variation of soil properties and the prediction method had the greatest influence on the results. Compared to the errors of these factors, the error of the soil chemical analysis had little impact when it was increased from 0 to 20%. Hence, the accuracy of the entire soil mapping process can most efficiently be improved by increasing the sampling density (e.g., by using mobile sensor platforms), while improving the precision of chemical and physical laboratory analyses has a smaller effect.

Regarding the estimates of the uniform LR map based on VDLUFA soil group 2 (SG2), 1.1 t CaO ha⁻¹ should be applied according to the VDLUFA look-up scheme. The total CaO demand based on this soil group is only approximately 1 t different from the total lime demand of the variable LR map (Table 23). While this difference is relatively low, a uniform LR determination using soil group 1 or 3 would lead to nearly half the CaO demand or an almost three times higher CaO demand, respectively, than the total LR determined by the variable approach. While approximately one-third of the field would be adequately fertilized using SG2 for lime demand determination, the adequately fertilized area would increase to approximately half of the field with SG1 and decrease to less than 10% with SG3 (Figure 38). In contrast, nearly two-thirds of the field would be over-fertilized by approximately 12 t CaO with SG2, and slightly more than 10% would be under-fertilized. With SG1, in comparison, only one-third of the field would be over-fertilized, and 11% would be under-fertilized. Interestingly, by choosing SG3, the over-fertilized areas of the field would increase to more than 90% of the field, and a total of approximately 55 t too much CaO would be applied to the field. Making up less than 1% of the area, the under-fertilized areas might be neglected. Although SG4 and SG5 would most likely not be chosen in this example, the over-fertilized areas would increase by merely 5% and 7%, respectively, in comparison to those under SG3. However, the determined CaO amounts would therefore double or triple.

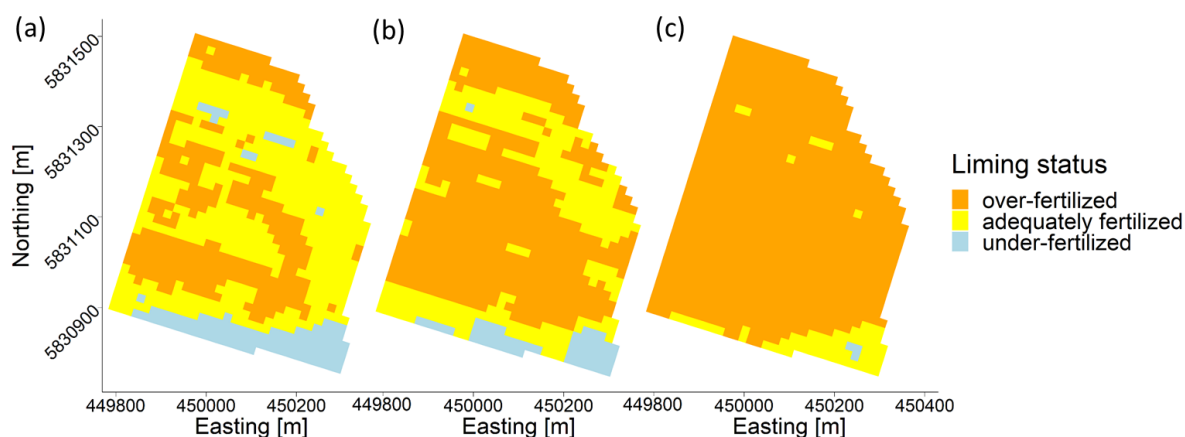


Figure 38: Distribution of the over-, adequately and under-fertilized areas with uniform LRs (estimates for soil groups 1 (a), 2 (b) and 3 (c) in the VDLUFA classification) compared with the example estimated variable LR for 18 x 18 m management units

Table 23: Comparison between the variable and uniform liming approach for all possible VDLUFA soil groups with data aggregation to 18 x 18 m

Soil group*	VDLUFA target CaO amount**	Total CaO amount		Adequately fertilized area		Over-fertilized area		Under-fertilized area	
		Uniform approach	Variable approach	%	t	%	t	%	t
	t ha ⁻¹	t	t	%	t	%	t	%	t
1	0.6	17.8	31.5	53.4	-7.4	34.2	4.6	12.3	-11.1
2	1.1	32.7	31.5	31.1	-4.5	61.5	12.3	7.4	-7.2
3	2.9	86.2	31.5	8.7	-3.3	91.1	57.9	0.2	-0.2
4	4.7	139.6	31.5	4.1	-0.9	95.9	108.9	0	0
5	6.7	199.1	31.5	0.9	0	99.1	167.4	0	0

* Content ranges of clay, silt and sand are shown in Table 2

** as per humus class 1 ($\leq 4 \text{ g kg}^{-1}$) and a mean pH value of 5.7

Only a few studies have compared variable-rate LR approaches with uniform LR approaches based on mean values. In North America, Borgelt et al. (1994), for example, compared variable lime rates with a uniform mean liming approach as well as with LRs estimated by a soil-buffer and a rule-based method. The latter was based on the parameters crop type, soil pH and soil texture. They produced variable-rate liming maps using geostatistical analysis and soil samples taken from a modified soil sampling design. Although the 8.8 ha test field in their study was less heterogeneous than that in this study, showing only two soil texture classes compared to KL60 (5 main groups, 6 subclasses), the mean liming rates would have resulted in over-fertilization of 9 to 12% and under-fertilization of 37 to 41% of the field. Overall, the uniform (mean-based) liming approach would have resulted in an 8 to 28% lower total lime application. In another study by Zaman et al. (2003) from the UK, 35% of the tested field required more lime under the variable approach than the average

amount, 56% less and 9% of the field was adequately limed. The field, however, had low ranges of sand (mean = 0.5 kg kg⁻¹, range = 0.1 kg kg⁻¹), silt (0.24 kg kg⁻¹, 0.11 kg kg⁻¹) and clay (0.26 kg kg⁻¹, 0.11 kg kg⁻¹) contents, and the LRs were estimated based on pH only. In two fields in North America, Bianchini and Mallarino (2002) found that 56-61% less lime needed to be applied under a variable lime rate approach based on a very dense sampling grid than under uniform application.

Determination of variable LR in all these studies was, however, based on regular sampling grids for soil texture and pH and none of these studies used spatial interpolation methods or high-resolution soil maps based on proximal soil sensing. In a study by Kuang et al. (2014), conducted on an 18 ha field in Denmark, variable liming rates were derived from high resolution mapping with a Vis-NIR spectrometer system and a recommendation algorithm from the Danish Centre for Food and Agriculture (DCA). They found that the VRL consumed the largest amount of lime (37 t) for the entire field, while the uniform treatment required just 25.3 t for entire field. However, for variable lime management the yield of spring barley of 7.57 t ha⁻¹ was slightly but significantly better than the yield of 7.51 t ha⁻¹ under uniform lime management.

Outlook

The success of lime applications based on this approach is currently being studied in field trials at different study sites and will be verified within the project period by repeated sensor campaigns with the multi-sensor platform and yield measurements. Moreover, the fusion of the sensor data within the project will be tested to enhance the predictability of the required soil parameters for liming. The financial aspects of this approach have not been addressed so far. It is evident that the costs to calibrate the sensors through soil sampling and soil analysis should be as low as possible. The number of reference samples taken in this study was relatively high. Part of the ongoing research is to reduce the number of reference samples to a maximum of 5 to 10 per field for pH, soil texture and SOC together while keeping prediction accuracy at a sufficient level. On the other hand, the economic and environmental value of precise liming must be highlighted. This value will only be perceived in the long term, and the adoption of precision liming will likely be supported by the relevant authorities. Farmers, advisors and service providers need training and accessible software tools to obtain the full benefits of existing soil mapping systems.

Conclusions

The present study presents a developed procedure that allows the easy and semi-automated generation of topsoil pH, texture and soil organic matter maps based on proximal soil sensing. This can be used for soil acidity management practices that respect the natural soil variability at a high

level of detail and improve the currently available best practices as described above. Moreover, this study provides guidelines for implementation in practice and, for scientists and advisors, information for the comparison and further development of approaches to variable-rate liming.

It was shown that high-resolution soil maps of pH, soil texture and soil organic matter could be generated through sensor-based digital soil mapping using two multi-sensor platforms and semi-automated (geo-)statistical methods. These soil maps exhibited small-scale spatial patterns and spatial interrelations between the target variables. More elevated parts of the field are characterized by a sandy soil texture, low amounts of SOM and low pH values. Zones at low elevations, which most likely developed from fluvial processes, are characterized by loamy soil textures, higher SOM contents and higher pH values.

Based on the high-resolution soil maps, a lime requirement map at 2 x 2 m spatial resolution was calculated following an adapted approach to the conventional VDLUFA guidelines for liming in Germany. However, to generate a lime prescription map that can be processed by a currently available lime spreader as used in the present study, the spatial resolution needed to be changed to 18 x 18 m. Given the high resolution of input data that proximal soil sensors can provide, the lack of precision in the currently available lime applicators is probably a bottleneck for the improvement of soil acidity management.

The combined average soil map error was used as a threshold value for identifying *over*, *adequately* and *under*-limed areas, and the LRs of the *precision* and the *uniform* liming approaches were compared. The results showed that 59% of the field would be over-fertilized by approximately 12 t of lime, 24% would receive approximately 10 t too little lime and merely 17% would be adequately limed with the uniform approach.

Acknowledgements

This work was conducted as part of the project 'pH-BB: precision liming in Brandenburg' (<http://ph-bb.com>). The project is part of the agricultural European Innovation Partnership program (EIP-AGRI) to improve agricultural productivity and sustainability (Project No.: 204016000014/80168341). The program is funded by the European Agricultural Fund for Rural Development of the European Commission and by the Ministry of Rural Development, Environment and Agriculture of the state of Brandenburg in Germany.

References

- Adamchuk, V.A., Ji, W., Viscarra Rossel, R., Gebbers, R., & Trembley, N. (2018). Proximal soil and plant sensing. In: Shannon, K., Sudduth, K., Clay, D. (Eds.): Precision farming basics (pp. 119-140). Madison, WI, USA: American Society of Agronomy.
- Adamchuk, V., & Lund, E. D. 2008. On-the-go mapping of soil pH using antimony electrodes. Paper Number: 083995 St Joseph, MI, USA: American Society of Agricultural and Biological Engineers
- Adamchuk, V., Morgan, M., & Ess, D. (1999). An automated sampling system for measuring soil pH. *Transactions of the ASAE*, 42(4), 885.
- Adamchuk, V., Rossel, R. A. V., Marx, D. B., & Samal, A. K. (2011). Using targeted sampling to process multivariate soil sensing data. *Geoderma*, 163(1-2), 63-73.
- Adamchuk, V., & Viscarra Rossel, R. (2011). Precision agriculture: proximal soil sensing. In Gliński, J., Horabik, J., & Lipiec, J. (Eds.) *Encyclopedia of Agrophysics* (pp. 650–656)., New York, USA: Springer.
- Ahmad, W., Dijkstra, F. A., Dalal, R. C., & Singh, B. (2016). Soil warming and liming impacts on the recovery of 15N in an acidic soil under soybean cropping. *Journal of Plant Nutrition and Soil Science*, 179(2), 193-197.
- Ahn, S., Doerr, S. H., Douglas, P., Bryant, R., Hamlett, C. A., McHale, G., et al. (2013). Effects of hydrophobicity on splash erosion of model soil particles by a single water drop impact. *Earth Surface Processes and Landforms*, 38(11), 1225-1233.
- Aitchison, J. (1982). The statistical analysis of compositional data. *Journal of the Royal Statistical Society: Series B (Methodological)*, 44(2), 139-160.
- Alley, M., & Zelazny, L. (1987). Soil Acidity: Soil pH and Lime Needs. In *Soil testing: Sampling, correlation, calibration, and interpretation* (Vol. 21, pp. 65-72). Madison, WI, USA: Soil Science Society of America.
- Bianchini, A. A., & Mallarino, A.P. (2002). Soil-sampling alternatives and variable-rate liming for a soybean–corn rotation. *Agronomy Journal*, 94(6), 1355-1366.
- Blume, H.-P., Brümmer, G. W., Horn, R., Kandeler, E., Kögel-Knabner, I., Kretschmar, R., et al. (2016). *Scheffer/Schachtschabel: Lehrbuch der Bodenkunde (Textbook of soil science)*. Berlin Heidelberg, Germany: Springer-Verlag.
- Boenecke, E., Lueck, E., Ruehlmann, J., Gruending, R., & Franko, U. (2018). Determining the within-field yield variability from seasonally changing soil conditions. *Precision Agriculture*, 19(4), 750-769.
- Borgelt, S., Searcy, S., Stout, B., & Mulla, D. (1994). Spatially variable liming rates: a method for determination. *Transactions of the ASAE*, 37(5), 1499-1507.

- Briedis, C., de Moraes Sá, J. C., Caires, E. F., de Fátima Navarro, J., Inagaki, T. M., Boer, A., et al. (2012). Soil organic matter pools and carbon-protection mechanisms in aggregate classes influenced by surface liming in a no-till system. *Geoderma*, 170, 80-88.
- Brendan P., Malone, B. P., Styc, Q., Minasny, B., McBratney, A. B. (2017). Digital soil mapping of soil carbon at the farm scale: A spatial downscaling approach in consideration of measured and uncertain data. *Geoderma*, 290, 91-99.
- Castrignano, A., Wong, M., Stelluti, M., De Benedetto, D., & Sollitto, D. (2012). Use of EMI, gamma-ray emission and GPS height as multi-sensor data for soil characterisation. *Geoderma*, 175, 78-89.
- Chayes, F. (1960). On correlation between variables of constant sum. *Journal of Geophysical research*, 65(12), 4185-4193.
- Cheng, L., Cord-Ruwisch, R., & Shahin, M. A. (2013). Cementation of sand soil by microbially induced calcite precipitation at various degrees of saturation. *Canadian Geotechnical Journal*, 50(1), 81-90.
- Corwin, D., & Lesch, S. (2005). Apparent soil electrical conductivity measurements in agriculture. *Computers and Electronics in Agriculture*, 46(1-3), 11-43.
- Cressie, N. A. (1993). Spatial prediction in a multivariate setting. In *Multivariate Environmental Statistics* (Vol. 6, pp. 99-108). Amsterdam, Netherlands: Elsevier.
- Cuisinier, O., Auriol, J.-C., Le Borgne, T., & Deneele, D. (2011). Microstructure and hydraulic conductivity of a compacted lime-treated soil. *Engineering Geology*, 123(3), 187-193.
- Dahiya, S., & Singh, R. (1982). Effect of soil application of CaCO₃ and Fe on dry matter yield and nutrient uptake in oats (*Avena sativa*). *Plant and Soil*, 65(1), 79-86.
- De Gruijter, J., Walvoort, D., & Van Gams, P. (1997). Continuous soil maps—a fuzzy set approach to bridge the gap between aggregation levels of process and distribution models. *Geoderma*, 77(2-4), 169-195.
- Eckelmann, W., Sponagel, H., & Grottenthaler, W. (2005). *Bodenkundliche Kartieranleitung*.-5. verbesserte und erweiterte-Auflage (Pedological Mapping Guidelines. 5th Improved and Extended Edition). Stuttgart, Germany: Schweizerbart Science Publishers.
- Edmeades, D., Rys, G., Smart, C., & Wheeler, D. (1986). Effect of lime on soil nitrogen uptake by a ryegrass-white clover pasture. *New Zealand Journal of Agricultural Research*, 29(1), 49-53.
- Ekenler, M., & Tabatabai, M. (2003). Effects of liming and tillage systems on microbial biomass and glycosidases in soils. *Biology and Fertility of Soils*, 39(1), 51-61.
- Fiedler, H., & Bergmann, W. (1955). Die Wirkung verschiedener Bodenstruktur-Verbesserungsmittel (The effect of various soil structure improvers). *Angewandte Chemie*, 67(22), 699-704.
- Fujii, K., Funakawa, S., & Kosaki, T. (2012). Soil Acidification. *Pedologist*, 55(3), 415-425.

- Gebbers, R. (2018). Proximal soil sensing and monitoring techniques. In Stafford, J. (Ed.): Precision agriculture for sustainability (pp. 29-78). Cambridge, UK: Burleigh Dodds Scientific Publishing.
- Gebbers, R., & Adamchuk, V. I. (2010). Precision agriculture and food security. *Science*, 327(5967), 828-831.
- Gebbers, R., De Bruin, S. (2010). Application of geostatistical simulation in precision agriculture. In Oliver, M. A. *Geostatistical applications for precision agriculture* (pp. 269-303). Dordrecht, Netherlands: Springer.
- Gebbers, R., Lück, E., Dabas, M., & Domsch, H. (2009). Comparison of instruments for geoelectrical soil mapping at the field scale. *Near Surface Geophysics*, 7(3), 179-190.
- Goovaerts, P. (1997). *Geostatistics for natural resources evaluation*. New York, NY, USA: Oxford University Press.
- Goulding, K. W. (2016). Soil acidification and the importance of liming agricultural soils with particular reference to the United Kingdom. *Soil Use and Management*, 32(3), 390-399.
- Goulding, K. W., & Blake, L. (1998). Land use, liming and the mobilization of potentially toxic metals. *Agriculture, Ecosystems & Environment*, 67(2-3), 135-144.
- Gray, C., Dunham, S., Dennis, P., Zhao, F., & McGrath, S. (2006). Field evaluation of in situ remediation of a heavy metal contaminated soil using lime and red-mud. *Environmental Pollution*, 142(3), 530-539.
- Hartge, K. (1959). Ursachen der Verbesserung der Strukturstabilität von Böden durch die Kalkung (Causes of the improvement of the structural stability of soils through liming). *Zeitschrift für Pflanzenernährung, Düngung, Bodenkunde (Journal of Plant Nutrition, Fertilization, Soil Science)*, 85(3), 214-227.
- Haynes, R. J., & Naidu, R. (1998). Influence of lime, fertilizer and manure applications on soil organic matter content and soil physical conditions: a review. *Nutrient Cycling in Agroecosystems*, 51(2), 123-137.
- Hengl, T. (2009). A practical guide to geostatistical mapping (Vol. 52). Amsterdam, The Netherlands: University of Amsterdam.
- Holland, J., Bennett, A., Newton, A., White, P., McKenzie, B., George, T., et al. (2018). Liming impacts on soils, crops and biodiversity in the UK: a review. *Science of the Total Environment*, 610, 316-332.
- Horsnell, L. (1984). Effect of soil moisture on the response of subterranean clover to lime. *Plant and Soil*, 81(2), 295-297.
- Huang, J., Subasinghe, R., & Triantafyllis, J. (2014). Mapping particle-size fractions as a composition using additive log-ratio transformation and ancillary data. *Soil Science Society of America Journal*, 78(6), 1967-1976.

- Jacobs, A., Flessa, H., Don, A., Heidkamp, A., Prietz, R., Dechow, R., et al. (2018). Landwirtschaftlich genutzte Böden in Deutschland: Ergebnisse der Bodenzustandserhebung (Agricultural soils in Germany: results of the soil condition survey). *Thünen Report* (Vol. 64, pp. 316). Braunschweig, Germany: Johann Heinrich von Thünen-Institut.
- Kerschberger, M. 1996. Ermittlung optimaler Bodenreaktion auf dem Ackerland (Vortrag) - Sekundärrohstoffe im Stoffkreislauf der Landwirtschaft und weitere Beiträge aus den öffentlichen Sitzungen (Determination of optimal soil reaction on the arable land - secondary raw materials in the material cycle of agriculture and further contributions from the public meetings). In *VDLUFA-Standpunkt* (Vol. 44, pp. 591-594). Darmstadt, Germany: VDLUFA-Verlag.
- Kerschberger, M., Deller, B., Hege, U., Heyn, J., Kape, H., Krause, O., et al. (2000). Bestimmung des Kalkbedarfs von Acker- und Grünlandböden (Determination of the lime requirement of arable and grassland soils). In *VDLUFA-Standpunkt*. Darmstadt, Germany: VDLUFA-Verlag.
- Kerschberger, M., & Marks, G. (2007). Einstellung und Erhaltung eines standorttypischen optimalen pH-Wertes im Boden--Grundvoraussetzung für eine effektive und umweltverträgliche Pflanzenproduktion (Setting and maintaining a site-specific optimum pH value in the soil - a basic requirement for effective and environmentally compatible plant production). *Berichte über Landwirtschaft (Reports on agriculture)*, 85(1), 56-77.
- Krbetschek, M. R., Degering, D., & Alexowsky, W. (2008). Infrared radiofluorescence ages (IR-RF) of Lower Saalian sediments from Central and Eastern Germany. *Zeitschrift der Deutschen Gesellschaft für Geowissenschaften (ZDGG) (Journal of the German Society for Earth Sciences)*, 159, 133-140.
- Kuang, B., Tekin, Y., Waine, T., & Mouazen, A. M. (2014). Variable rate lime application based on on-line visible and near infrared (vis-NIR) spectroscopy measurement of soil properties in a Danish field. *Proceedings International Conference of Agricultural Engineering*. Zurich, Switzerland, 06-10.07.2014.
- Kuang, B., Tekin, Y., & Mouazen, A. M. (2015). Comparison between artificial neural network and partial least squares for on-line visible and near infrared spectroscopy measurement of soil organic carbon, pH and clay content. *Soil and Tillage Research*, 146, 243-252.
- Kuhn, M., Williams, C. K., Engelhardt, A., Cooper, T., Mayer, Z., Ziem, A., et al. (2019). caret: Classification and Regression Training. R package version 6.0-84. Retrieved 20.07.2019 from URL <https://CRAN.R-project.org/package=caret>.
- Kweon, G., Lund, E., & Maxton, C. (2013). Soil organic matter and cation-exchange capacity sensing with on-the-go electrical conductivity and optical sensors. *Geoderma*, 199, 80-89.

- Kweon, G., & Maxton, C. (2013). Soil organic matter sensing with an on-the-go optical sensor. *Biosystems Engineering*, 115(1), 66-81.
- Larink, O., & Joschko, M. (2014). Einfluss der Standort-und Bodeneigenschaften auf die Bodenfauna (Influence of site and soil properties on soil fauna). In *Handbuch der Bodenkunde (Textbook of soil science)* (pp. 1-44). Müncheberg, Germany: Wiley-VCH.
- Lück, E., & Rühlmann, J. (2013). Resistivity mapping with GEOPHILUS ELECTRICUS—Information about lateral and vertical soil heterogeneity. *Geoderma*, 199, 2-11.
- Lund, E., Adamchuk, V., Collings, K., Drummond, P., & Christy, C. (2005). Development of soil pH and lime requirement maps using on-the-go soil sensors. *Precision Agriculture*, 5, 457-464.
- Mahmood, H., Hoogmoed, W., & van Henten, E. (2013). Proximal gamma-ray spectroscopy to predict soil properties using windows and full-spectrum analysis methods. *Sensors*, 13(12), 16263-16280.
- Manna, M., Swarup, A., Wanjari, R., Mishra, B., & Shahi, D. (2007). Long-term fertilization, manure and liming effects on soil organic matter and crop yields. *Soil and Tillage Research*, 94(2), 397-409.
- McLean, E. (1978). Principles underlying the practice of determining lime requirements of acid soils by use of buffer methods. *Communications in Soil Science and Plant Analysis*, 9(8), 699-715.
- Meyer, S., Kling, C., Vogel, S., Schröter, I., Nagel, A., Kramer, E., et al. (2019). Creating soil texture maps for precision liming using electrical resistivity and gamma ray mapping. In Stafford, J. V. (Ed.) *Precision Agriculture'19 Proceedings of the 12th European Conference on Precision Agriculture Wageningen* (pp. 92). Wageningen, The Netherlands: Wageningen Academic Publishers.
- Minasny, B., & McBratney, A. B. (2006). A conditioned Latin hypercube method for sampling in the presence of ancillary information. *Computers & Geosciences*, 32(9), 1378-1388.
- Mueller, T., Pusuluri, N., Mathias, K., Cornelius, P., & Barnhisel, R. (2004). Site-specific soil fertility management. *Soil Science Society of America Journal*, 68(6), 2031-2041.
- Muzzamal, M., Huang, J., Nielson, R., Sefton, M., & Triantafilis, J. (2018). Mapping soil particle-size fractions using additive log-ratio (ALR) and isometric log-ratio (ILR) transformations and proximally sensed ancillary data. *Clays and Clay Minerals*, 66(1), 9-27.
- Odeh, I. O., Todd, A. J., & Triantafilis, J. (2003). Spatial prediction of soil particle-size fractions as compositional data. *Soil Science*, 168(7), 501-515.
- Olea, R. A. (2012). *Geostatistics for engineers and earth scientists*. New York, NY, USA: Springer Science & Business Media, LLC.
- Paradelo, R., Virto, I., & Chenu, C. (2015). Net effect of liming on soil organic carbon stocks: a review. *Agriculture, Ecosystems & Environment*, 202, 98-107.

- Pebesma, E. J. (2004). Multivariable geostatistics in S: the gstat package. *Computers & Geosciences*, 30(7), 683-691.
- Peverill, K., Sparrow, L., & Reuter, D. (1999). *Soil analysis: an interpretation manual*. Collingwood, Australia: CSIRO publishing.
- Piiki, K., & Söderström, M. (2019). Digital soil mapping of arable land in Sweden – Validation of performance at multiple scales. *Geoderma*, 352, 342-350.
- R Core Team (2018). R: A language and environment for statistical computing. R Foundation for Statistical Computing, Vienna, Austria. 2012. URL <http://www.R-project.org>.
- Rossel, R. V., & Chen, C. (2011). Digitally mapping the information content of visible–near infrared spectra of surficial Australian soils. *Remote Sensing of Environment*, 115(6), 1443-1455.
- Roudier, P. (2011). clhs: a R package for conditioned Latin hypercube sampling. software. Retrieved 25.08.2019 from URL <https://github.com/pierreroudier/clhs/>.
- Schachtschabel, P., & Hartge, K. (1958). Die Verbesserung der Strukturstabilität von Ackerböden durch eine Kalkung (The improvement of the structural stability of arable soils by liming). *Zeitschrift für Pflanzenernährung, Düngung, Bodenkunde (Journal of Plant Nutrition, Fertilization, Soil Science)*, 83(3), 193-202.
- Schellberg, J., Hill, M. J., Gerhards, R., Rothmund, M., & Braun, M. (2008). Precision agriculture on grassland: Applications, perspectives and constraints. *European Journal of Agronomy*, 29(2-3), 59-71.
- Schilling, G. (2000). *Pflanzenernährung und Düngung: 164 Tabellen (Plant nutrition and fertilization: 164 tables)*. Stuttgart, Germany: Verlag Eugen Ulmer.
- Schirrmann, M., Gebbers, R., Kramer, E., & Seidel, J. (2011a). Evaluation of soil sensor fusion for mapping macronutrients and soil pH. In *The Second Global Workshop on Proximal Soil Sensing* (pp. 48-51). Montreal, Canada: McGill University press.
- Schirrmann, M., Gebbers, R., Kramer, E., & Seidel, J. (2011b). Soil pH mapping with an on-the-go sensor. *Sensors*, 11(1), 573-598.
- Sims, J. T. (1996). *Lime requirement (Methods of Soil Analysis Part 3: Chemical Methods)*. Madison, WI, USA: Soil Science Society of America, Inc. & American Society of Agronomy Inc.
- Stocker, N., & Walthert, L. (2013). Böden und Wasserhaushalt von Wäldern und Waldstandorten der Schweiz unter heutigem und zukünftigem Klima (BOWA-CH) - Datengrundlage und Datenharmonisierung. (Soils and water balance of forests and forest locations in Switzerland under current and future climates - Data basis and data harmonization) *Projektinterner Bericht (Internal project report)*, Zurich, Switzerland: ETH-Zurich.
- Stöven, K., & Schnug, E. (2005). Kalkung und Bodenleben (Liming and Soil Life). In Haneklaus, S., Rietz, R.-M., Rogasik, & J. Schroetter, S. (Ed.) *Recent advances in agricultural chemistry, Special*

- Issue 286*. Braunschweig, Germany: Bundesforschungsanstalt für Landwirtschaft (FAL) (Federal Research Center for Agriculture).
- Tunney, H., Sikora, F., Kissel, D., Wolf, A., Sonon, L., & Goulding, K. (2010). A comparison of lime requirements by five methods on grassland mineral soils in Ireland. *Soil Use and Management*, *26*(2), 126-132.
- van den Boogaart, K. G., & Tolosana-Delgado, R. (2008). "Compositions": a unified R package to analyze compositional data. *Computers & Geosciences*, *34*(4), 320-338.
- Vogel, S., Bönecke, E., Kling, C., Kramer, E., Lück, K., Nagel, A., et al. 2020. Base neutralizing capacity of agricultural soils in a quaternary landscape of north-east germany and its relationship to best management practices in lime requirement determination. *Agronomy*, *10*, 877.
- von Cossel, M., Druecker, H., & Hartung, E. (2019). Low-input estimation of site-specific lime demand based on apparent soil electrical conductivity and in situ determined topsoil pH. *Sensors*, *19*(23), 5280.
- von Wulffen, U., Roschke, M., & Kape, H.-E. (2008). Richtwerte für die Untersuchung und Beratung sowie zur fachlichen Umsetzung der Düngeverordnung (DüV): gemeinsame Hinweise der Länder Brandenburg, Mecklenburg-Vorpommern und Sachsen-Anhalt (veröffentlicht durch das Land Brandenburg) (Guide values for the examination and advice as well as for the professional implementation of the Fertilizer Ordinance (DüV): joint information from the states of Brandenburg, Mecklenburg-Western Pomerania and Saxony-Anhalt (published by the state of Brandenburg). Güterfelde, Germany: Landesamt für Verbraucherschutz & Landwirtschaft und Flurneuordnung (LVLf).
- Webster, R., & Oliver, M. A. (2007). *Geostatistics for Environmental Scientists*. Chichester, West Sussex, UK: John Wiley & Sons, Ltd.
- Zaman, Q., Shiel, R., & Schumann, A. (2003). Variable lime application based on within-field variation in soil pH. *Pakistan Journal of Agricultural Sciences*, *40*(1-2).
- Zhang, Y., Xiao, Y., Zhuang, Z., Zhou, L., Liu, F., & He, Y. (2016). Development of a near ground remote sensing system. *Sensors*, *16*(5), 648.

Thesis synthesis

General discussion

This thesis was split into two main parts. Within Part I of this thesis, the influence of weather changes at sites of different soil types and yield potential in Germany and the impact of the soil heterogeneity on field scale on the wheat yield variability was investigated. As the specific objectives of first study in Part I were to determine the magnitude of the effects of relevant agro-climatic changes on the long-term winter wheat yield development in Germany and to detect whether sites divided into classes of lower and higher yield potential (and different soil types) were affected differently, the developed hypothesis can be discussed as followed:

Detrimental weather conditions as e.g., increasing temperatures and drought during the growing season influenced the variation of German winter wheat yields and its yield productivity level significantly since the late 1950s. These effects were mainly negatively. Sites of lower yield potential and of sandy soils already had an incipient yield levelling in the mid to late 1980s showing annual variations of yield between 4-12 t ha⁻¹. These sites were in particular negatively influenced by detrimental weather conditions, e.g., e.g., number of heat stress days above 27°C during the generative phase with up to 30% impact. Contrary, at sites with higher yield potential, winter wheat yields have been constantly increasing over time. However, indications of yield levelling are also seen on sites of loamy to clayey soils for the last years. The analysis additionally revealed a shift of 13- and 17-days towards earlier in the year during the observation period for sowing and harvesting dates, respectively.

The overall results of this study showed that the effects of time and location explained the variance of the winter wheat yields the most. However, a lower explained variance of the genotype effect does not automatically mean that this factor has a lower influence on yield development. With unfavourable environmental conditions becoming more prevalent, breeding programs in high-yielding countries started to focus on crop varieties that are tolerant and resilient to abiotic stresses like heat and drought (Tester and Langridge, 2010; Witcombe et al., 2007). However, the climate resilience of European wheat is unknown as Kahiluoto et al., 2019 pointed out for the response diversity of wheat across European countries. Response diversity in breeding programs for crops refers to the intentional incorporation of genetic variations into cultivated plants to enhance their adaptability and resilience to changing environmental conditions and stresses (Elmqvist et al., 2003). By introducing a diverse range of genetic traits, such as disease resistance, drought tolerance, and nutrient efficiency, breeding programs can ensure that crops respond effectively to different

challenges. This diversity helps reduce the risk of widespread crop failures and increases the overall stability of agricultural systems. Moreover, response diversity allows farmers to select and cultivate crop varieties best suited to their specific local conditions, contributing to sustainable and productive agriculture. However, on a controversial note, Kahiluoto et al., 2019 indicate that current breeding programs and cultivar selection practices do not adequately prepare for climatic uncertainty. For instance, response diversity "hotspots" were found in Slovakia, while a response diversity was missing in Czechia, Germany, and for durum wheat in southern Europe. Hence, the search for heat and drought-tolerant crop varieties should be accompanied by sustainable management practices since breeding alone can't cover for agricultural intensification (Shah and Wu, 2019).

As the specific research goals of the second study in Part I were to detect the small-scale soil structures on a chernozem soil developed on loess and over old-morainic substrates and to model the soil water dynamics and to determine and evaluate the time when the water availability effected the winter wheat yield variability the most, the hypothesis can be discussed as the followed:

It was found that the small-scale yield variability was noticeably influenced by the amount of available water within the whole rooting zone during the grain filling phase in a comparatively dry year. The coefficient of determination (R^2) increased from <0.01 to 0.14 and 0.18 when the winter wheat yield variability of the chosen year was correlated with the amount of available water within 0-30 cm, 0-100 cm and 0-170 cm, respectively. Attained yields had a maximum of approximately 7 t ha^{-1} for available soil water contents between 350 and 420 mm. Below 350 mm, the maximum winter wheat yields decreased down to around 5 t ha^{-1} at 250 mm available soil water.

This study successfully showed the application of a process-oriented model to analyse the plant-soil interactions over a given period, i.e., to support the understanding of the crops or soils sensitivity to different weather patterns in a given area (e.g., yield reduction due to drought) (Heinen, 2023). However, the level of detail necessary to actually simulate processes directly correlates with the quantity of data required, i.e., modelling at a high spatial resolution, the measuring the soil properties for each single point and profile would be to time-intensive and financially highly demanding (Ørum et al., 2017; Pedersen and Lind, 2017). Therefore, it was shown in this study how mobile multi-sensor systems and data inversion made it possible to map the soil structure variability horizontally and laterally (Pan et al., 2014; Sharma and Verma, 2015).

Moreover, as the soil's physical properties are influenced by various physical, chemical, and biological factors, it is possible to establish empirical relationships for their prediction via so called pedotransfer-functions (PTFs) (Bouma, 1989). PTFs refer to the conversion of available data that are

relatively time- and cost-effective to measure into the required soil information with function for specific soil attributes (McBratney et al., 2002).

To initialize mechanistic models, they require information about the starting situation of the modelling period, foremost the water content, carbon, and nitrogen concentration, which often is difficult to achieve (Boote et al., 1996; Palosuo et al., 2011). In this study, the initialisation was done by starting the model two years in advance to have the state variables in concordance with the ambient weather conditions and the actual field management. It needs to be noted that the majority of the agro-ecosystem models do not consider lateral fluxes, but rather work one-dimensional along a single profile. For precision farming purposes they can be applied to spatially variable conditions, simulating multiple soil columns in parallel at the field and regional scale as also shown by e.g., (Kersebaum and Wallor, 2023; Witing et al., 2023).

In Part II of this thesis discussed the guidelines of a decision system for a sustainable fertilization at a yield variable site. As yield variability was already seen at sites of a higher yield potential and of relatively low soil heterogeneity, the annual variation of yields is even higher at sites of lower yield potential and greater soil heterogeneity making them more prone to higher yield variation and high risk of drought induced yield losses.

The specific objectives of the study in Part II were the creation of precise maps of the soil parameters pH, soil organic matter and texture derived from different proximal soil sensors and the adaptation of an existing but insufficient fertilization algorithms to the requirements of these modern sensor technologies. As this was done to show how small-scale soil property differences can be considered - exemplarily for liming - in a fertilization decision support system at sites with high yield variability to maintain or improve the soil's fertility and consequently crop productivity, the hypothesis can be discussed as followed:

As the soil pH can be influenced by internal soil processes resulting from natural processes (such as precipitation) or human activities (such as fertilization), liming has been recognized as a central management tool for centuries to address soil acidification and improve soil fertility (Dodgshon, 1978; Holland et al., 2018). The lime recommendation assessment based on this studies' sensor and decision support combination showed the best performance under the highest possible resolution of the underlying soil parameter maps. The sensor calibration with lab analysed reference soils showed a greater distinction of five-soil group differentiation after reclassification of the derived clay, silt and sand fractions, while conventional soil assessment maps only determined three out of the five soil groups. If lime recommendations are based on wrong field uniform soil texture allocations, 63% of the selected field would be over-fertilized by approximately 12 t of lime, 6%

would receive approximately 6 t too little lime and only 31% would be adequately limed. Hence, high-resolution soil maps exhibited the small-scale spatial patterns and spatial interrelations between the target variables and therefore suit as input data to determine fertilizer recommendations as required for a sustainable agriculture.

The solution of the last study in this thesis is therefore in line with several farming practices that have been identified sustainable regarding the nutrient and water management (Shah and Wu, 2019). The overall goal of these environmental adapted management strategies is to maintain a balanced nutrient input and output in the system, which involves matching the quantity of inputs to the crop's demand and synchronizing the timing of nutrient applications with crop growth stages, while improving, maintaining or enhancing the crop productivity and reduce degradation of the soil (Shah and Wu, 2019; Stagnari et al., 2019). Although not discussed in this study, other precision management techniques, such as the precise application of water or organic and mineral nitrogen fertilizers as well as other general management strategies, such as intercropping or various soil tillage methods (e.g., no-till, minimum tillage, strip tillage, ridge tillage, or mulch tillage) enhances crop productivity while preserving soil resources and protecting the environment (Reddy, 2016; Stagnari et al., 2019). These techniques also enable farmers to improve management strategies to the actual field conditions by combining traditional approaches with modern techniques that are environment friendly.

The use of smart farming technology and practices may therefore improve the agricultural productivity, has positive side effects on the environment, and is both accessible and effective for producers (Das V. et al., 2019; Lioutas et al., 2021).

Result summary

The overarching goal of this thesis was to investigate of the influence of weather changes and soil heterogeneity on the yield variability of winter wheat on field scale and between different sites and regions in Germany as well as to develop a decision system for a sustainable fertilization at a yield variable site. The following summary of the thesis can be made:

In the first study, this thesis showed that the variability of German winter wheat yields and its yield productivity level was influenced negatively by increasing temperatures and drought during the growing season over the last decades. Interestingly, it can also be seen that the influence of increasing temperatures had less of an impact on wheat at locations with higher yield potential. Contrary, the cultivation of wheat on sites with lower yield potential appears to be more vulnerable to climatic changes. This was made evident by a meta-analysis in which weather and wheat yield data

were collected over several decades at many locations of different site characteristics and by using statistical mixed models to separate the various yield influencing factors.

The second study revealed that the winter wheat yield variability is significantly influenced by the amount of water available over the whole soil profile during the grain filling phase. This effect is particularly pronounced in years with below-average precipitation. The main cause is related to the soil texture and structure – as differences in water retention and hydraulic conductivity between the loess layer and the underlying old moraine material determined the seasonal dynamics and availability of the soil water. Soil physical characteristics derived from calibration of interpolated electrical resistivity mapping with soil texture from selected point references and from pedotransfer functions enabled the usage of high-resolution soil maps. Based on these maps and with available weather data as well as the cultivation history of a field, a process model reproduced the water and nutrient dynamics could be modelled over several years of a crop rotation.

Finally, the last study showed exemplary for liming, as this is an easy to determine and cost-effective approach to maintain or improve the soil fertility, which itself is an indicator for the crop productivity, a prescription for small-scale and site-adapted fertilization could be developed at a site of high yield variation due to the underlying young moraine and fluvial substrates of which the soil developed. By using soil sensors, the heterogeneous soil structure was made visible and by using an adapted fertilization algorithm, the fertilization requirement was calculated in a dynamic way as it fits the high resolution of sensor-based soil maps. Conventional approaches (e.g., finger test, class-based fertilizer demand derivation), on the other hand, show high unreliability in fertilizer demand calculation and are more prone to misapplication.

Overall conclusions

As the influence of weather and climatic changes and the soil variability on the variation of winter wheat yields could be shown at different temporal and spatial scales in this thesis, the following conclusions can be drawn:

The analysis showed that German wheat production is continuously adjusting to climatic changes, both with regard to the genetic adjustment (i.e., respective cultivar/variety selection choice) as well as management adjustment, especially shift of sowing times. This underlines the need of continuing finding adaptation strategies for food production under expected ongoing climate change to support a stable wheat yield production in Germany. As such, it might be necessary to employ additional measures such as irrigation, in particular at sites prone to higher yield variability and high risk of drought induced yield losses. Furthermore, earlier sowing in combination with 'early'

wheat genotypes might be suitable to escape drought stress. As the yield increment of wheat slowed down in recent years, but the need of food for a growing world population is necessary, while at the same time taking environmental protection into account, an intensification of agriculture is necessary but from a sustainable point of view.

Knowing the subsoil structure is particularly relevant in years of lower precipitation for areas with relatively homogeneous top soils as can be found for chernozem soils developed over loess. The structure of the soil over the whole profile should be therefore correctly represented. Coupling soil physical information of higher resolution with a process model can help to assess the effects of water shortage on the crop yields and therefore meaningfully improve the derivation of management decisions compared to the conventional data basis (e.g., low resolution soil maps).

The availability of high-resolution soil maps also exhibits a small-scale fertilization, as they provide the spatial patterns and interrelations between the target soil parameters that are necessary to calculate fertilizer requirements. The approach of a precise field management becomes necessary for a sustainable agriculture that desires to keep the crop production level high while the land use pressure still increases. The example of the precision liming should be transferred to other nutrients. However, given the high resolution of input data that proximal soil sensors can provide, the lack of precision in the currently available fertilizer machineries is probably a bottleneck for the improvement of soil management. Moreover, adopting precision agriculture strategies requires socio-economical investments to implement the initial high costs for equipment and the necessary expert support due to the complexities of the systems.

Overall, the studies in this thesis illustrate that soil and climate influences crop yields. Climatic factors such as solar radiation, temperature, or precipitation imposes limitations on crop growth as does a variable soil structure, which influences the soil water availability in dry years even at sites with higher yield potential. It can be concluded that in particular the conventional crop production should still continue to be intensified, but from a sustainable point of view accounting for the within-field soil heterogeneity and the ambient weather conditions to avoid environmental contamination. Therefore, soil and weather information of appropriate resolution combined with optimised agronomic decision rules may reduce agriculturally induced environmental problems, mitigate the effects of climatic changes on crop production and significantly stabilise or improve yield levels for different site and soil characteristics. Besides the adoption of integrated farming approaches, which mainly aim to enhance nitrogen utilization, sustainable farming practices such as precision agriculture, improved nutrient management by minimizing the environmental pollution and keep the detrimental effects within the planetary boundaries (de Vries et al., 2013; Springmann et al., 2018).

Outlook

As stated above, the demand for an intensified but sustainable crop and soil management, the determination of the crop and soil adapted nutrient demand should be expanded to other nutrients in particular nitrogen to match the necessary supply in time and space (Goulding et al., 2008; Spiertz, 2009). N-losses should be minimised in systems where yields and soil stocks are achieved with nutrient inputs approximately equal to harvested exports and adjusted to the specific agro-ecological conditions such as land availability, soil fertility, water resources, weather patterns, labour requirements and markets (Drinkwater and Snapp, 2007; Spiertz, 2009). This challenge may be solved by combining all available technological innovations including remote and proximal sensing, the application of artificial intelligence or the genetic adaptation of new variety crops (Fountas et al., 2020; Tsiropoulos et al., 2017). On the crop level, remote sensing technologies have the potential to provide repetitive information on crop status throughout the vegetation period at different scales and for different crop factors (Shanmugapriya et al., 2019; Weiss et al., 2020). This should not only fit for a single crop but for a crop rotation as an integrated system to achieve a higher agronomic nutrient-use efficiencies by reducing environmental impacts and enhancing food quality, while maintaining acceptable yields (Spiertz and Ewert, 2009).

References

- Adamchuk, V.I., Allred, B., Doolittle, J., Grote, K., Rossel, R., Ditzler, C., West, L., 2015. Tools for proximal soil sensing. *Soil Surv. Staff Ditzler C West LEds Soil Surv. Man. Nat. Resour. Conserv. Serv. US Dep. Agric. Handb.* 18.
- Akaka, J., García-Gallego, A., Georgantzis, N., Rahn, C., Tisserand, J.-C., 2023. Development and Adoption of Model-Based Practices in Precision Agriculture, in: Cammarano, D., van Evert, F.K., Kempenaar, C. (Eds.), *Precision Agriculture: Modelling, Progress in Precision Agriculture*. Springer International Publishing, Cham, pp. 75–102. https://doi.org/10.1007/978-3-031-15258-0_4
- Aksoy, E., Gregor, M., Schröder, C., Löhnertz, M., Louwagie, G., 2017. Assessing and analysing the impact of land take pressures on arable land. *Solid Earth* 8, 683–695. <https://doi.org/10.5194/se-8-683-2017>
- Almekinders, C.J.M., Fresco, L.O., Struik, P.C., 1995. The need to study and manage variation in agro-ecosystems. *Neth. J. Agric. Sci.* 43, 127–142. <https://doi.org/10.18174/njas.v43i2.572>
- Aplin, P., 2004. Remote sensing: land cover. *Prog. Phys. Geogr.* 28, 283–293.
- Asseng, S., Cammarano, D., Basso, B., Chung, U., Alderman, P.D., Sonder, K., Reynolds, M., Lobell, D.B., 2017. Hot spots of wheat yield decline with rising temperatures. *Glob. Change Biol.* 23, 2464–2472. <https://doi.org/10.1111/gcb.13530>

- Asseng, S., Ewert, F., Martre, P., Rötter, R.P., Lobell, D.B., Cammarano, D., Kimball, B.A., Ottman, M.J., Wall, G.W., White, J.W., Reynolds, M.P., Alderman, P.D., Prasad, P.V.V., Aggarwal, P.K., Anothai, J., Basso, B., Biernath, C., Challinor, A.J., De Sanctis, G., Doltra, J., Fereres, E., Garcia-Vila, M., Gayler, S., Hoogenboom, G., Hunt, L.A., Izaurralde, R.C., Jabloun, M., Jones, C.D., Kersebaum, K.C., Koehler, A.-K., Müller, C., Naresh Kumar, S., Nendel, C., O'Leary, G., Olesen, J.E., Palosuo, T., Priesack, E., Eyshi Rezaei, E., Ruane, A.C., Semenov, M.A., Shcherbak, I., Stöckle, C., Stratonovitch, P., Streck, T., Supit, I., Tao, F., Thorburn, P.J., Waha, K., Wang, E., Wallach, D., Wolf, J., Zhao, Z., Zhu, Y., 2015. Rising temperatures reduce global wheat production. *Nat. Clim. Change* 5, 143–147. <https://doi.org/10.1038/nclimate2470>
- Aziz, T., Maqsood, M.A., Kanwal, S., Hussain, S., Ahmad, H.R., Sabir, M., 2015. Fertilizers and Environment: Issues and Challenges, in: Hakeem, K.R. (Ed.), *Crop Production and Global Environmental Issues*. Springer International Publishing, Cham, pp. 575–598. https://doi.org/10.1007/978-3-319-23162-4_21
- Balmford, A., Green, Rhys.E., Scharlemann, J.P.W., 2005. Sparing land for nature: exploring the potential impact of changes in agricultural yield on the area needed for crop production. *Glob. Change Biol.* 11, 1594–1605. <https://doi.org/10.1111/j.1365-2486.2005.001035.x>
- Bechmann, M., Stålnacke, P., Kværnø, S., Eggstad, H.O., Øygarden, L., 2009. Integrated tool for risk assessment in agricultural management of soil erosion and losses of phosphorus and nitrogen. *Sci. Total Environ.* 407, 749–759. <https://doi.org/10.1016/j.scitotenv.2008.09.016>
- Bergstrom, J.C., Taylor, L.O., 2006. Using meta-analysis for benefits transfer: Theory and practice. *Ecol. Econ., Environmental Benefits Transfer: Methods, Applications and New Directions* 60, 351–360. <https://doi.org/10.1016/j.ecolecon.2006.06.015>
- Bieling, C., Plieninger, T., Schaich, H., 2013. Patterns and causes of land change: Empirical results and conceptual considerations derived from a case study in the Swabian Alb, Germany. *Land Use Policy* 35, 192–203. <https://doi.org/10.1016/j.landusepol.2013.05.012>
- Blanchy, G., Bragato, G., Di Bene, C., Jarvis, N., Larsbo, M., Meurer, K., Garré, S., 2023. Soil and crop management practices and the water regulation functions of soils: a qualitative synthesis of meta-analyses relevant to European agriculture. *SOIL* 9, 1–20. <https://doi.org/10.5194/soil-9-1-2023>
- Blum, A., Jordan, W.R., 1985. Breeding crop varieties for stress environments. *Crit. Rev. Plant Sci.* 2, 199–238. <https://doi.org/10.1080/07352688509382196>
- Boote, K.J., Jones, J.W., Pickering, N.B., 1996. Potential uses and limitations of crop models. *Agron. J.* 88, 704–716.
- Bordoloi, R., Das, B., Yam, G., Pandey, P.K., Tripathi, O.P., 2019. Modeling of Water Holding Capacity Using Readily Available Soil Characteristics. *Agric. Res.* 8, 347–355. <https://doi.org/10.1007/s40003-018-0376-9>
- Bouma, J., 1989. Using Soil Survey Data for Quantitative Land Evaluation, in: Stewart, B.A. (Ed.), *Advances in Soil Science: Volume 9, Advances in Soil Science*. Springer US, New York, NY, pp. 177–213. https://doi.org/10.1007/978-1-4612-3532-3_4
- Bouman, B.A.M., Van Keulen, H., Van Laar, H.H., Rabbinge, R., 1996. The 'School of de Wit' crop growth simulation models: a pedigree and historical overview. *Agric. Syst.* 52, 171–198.
- Brady, N.C., Weil, R.R., 2008. *The Nature and Properties of Soils*. Pearson Prentice Hall.

- Brisson, N., Gate, P., Gouache, D., Charmet, G., Oury, F.-X., Huard, F., 2010. Why are wheat yields stagnating in Europe? A comprehensive data analysis for France. *Field Crops Res.* 119, 201–212. <https://doi.org/10.1016/j.fcr.2010.07.012>
- Brocca, L., Melone, F., Moramarco, T., Morbidelli, R., 2010. Spatial-temporal variability of soil moisture and its estimation across scales. *Water Resour. Res.* 46.
- Calderini, D.F., Slafer, G.A., 1998. Changes in yield and yield stability in wheat during the 20th century. *Field Crops Res.* 57, 335–347. [https://doi.org/10.1016/S0378-4290\(98\)00080-X](https://doi.org/10.1016/S0378-4290(98)00080-X)
- Cammarano, D., Van Evert, F.K., Kempenaar, C. (Eds.), 2023. *Precision Agriculture: Modelling, Progress in Precision Agriculture*. Springer International Publishing, Cham. <https://doi.org/10.1007/978-3-031-15258-0>
- Ceglar, A., Toreti, A., Lecerf, R., Van der Velde, M., Dentener, F., 2016. Impact of meteorological drivers on regional inter-annual crop yield variability in France. *Agric. For. Meteorol.* 216, 58–67.
- Challinor, A.J., Watson, J., Lobell, D.B., Howden, S.M., Smith, D.R., Chhetri, N., 2014. A meta-analysis of crop yield under climate change and adaptation. *Nat. Clim. Change* 4, 287–291. <https://doi.org/10.1038/nclimate2153>
- Chen, C., van Groenigen, K.J., Yang, H., Hungate, B.A., Yang, B., Tian, Y., Chen, J., Dong, W., Huang, S., Deng, A., Jiang, Y., Zhang, W., 2020. Global warming and shifts in cropping systems together reduce China's rice production. *Glob. Food Secur.* 24, 100359. <https://doi.org/10.1016/j.gfs.2020.100359>
- Cheng, M., McCarl, B., Fei, C., 2022. Climate Change and Livestock Production: A Literature Review. *Atmosphere* 13, 140. <https://doi.org/10.3390/atmos13010140>
- Cochran, W.G., 1939. Long-Term Agricultural Experiments. *Suppl. J. R. Stat. Soc.* 6, 104–148. <https://doi.org/10.2307/2983686>
- Curtis, T., Halford, N.G., 2014. Food security: the challenge of increasing wheat yield and the importance of not compromising food safety. *Ann. Appl. Biol.* 164, 354–372. <https://doi.org/10.1111/aab.12108>
- Das V., J., Sharma, S., Kaushik, A., 2019. Views of Irish Farmers on Smart Farming Technologies: An Observational Study. *AgriEngineering* 1, 164–187. <https://doi.org/10.3390/agriengineering1020013>
- Day, K.J., Hutchings, M.J., John, E.A., 2003. The effects of spatial pattern of nutrient supply on yield, structure and mortality in plant populations. *J. Ecol.* 91, 541–553. <https://doi.org/10.1046/j.1365-2745.2003.00799.x>
- de Vries, W., Kros, J., Kroeze, C., Seitzinger, S.P., 2013. Assessing planetary and regional nitrogen boundaries related to food security and adverse environmental impacts. *Curr. Opin. Environ. Sustain., Open issue* 5, 392–402. <https://doi.org/10.1016/j.cosust.2013.07.004>
- DESTATIS, 2019. *Statistisches Jahrbuch 2019 (eng.: Statistical Year Book 2019)*. Statistisches Bundesamt.
- Dodgshon, R.A., 1978. Land improvement in Scottish farming: marl and lime in Roxburghshire and Berwickshire in the eighteenth century. *Agric. Hist. Rev.* 26, 1–14.

- Doran, J.W., Parkin, T.B., 1994. Defining and Assessing Soil Quality, in: *Defining Soil Quality for a Sustainable Environment*. John Wiley & Sons, Ltd, pp. 1–21.
<https://doi.org/10.2136/sssaspecpub35.c1>
- Drinkwater, L.E., Snapp, S.S., 2007. Nutrients in Agroecosystems: Rethinking the Management Paradigm, in: Sparks, D.L. (Ed.), *Advances in Agronomy*. Academic Press, pp. 163–186.
[https://doi.org/10.1016/S0065-2113\(04\)92003-2](https://doi.org/10.1016/S0065-2113(04)92003-2)
- Dungait, J.A., Cardenas, L.M., Blackwell, M.S., Wu, L., Withers, P.J., Chadwick, D.R., Bol, R., Murray, P.J., Macdonald, A.J., Whitmore, A.P., 2012. Advances in the understanding of nutrient dynamics and management in UK agriculture. *Sci. Total Environ.* 434, 39–50.
- Elliott, J., Müller, C., Deryng, D., Chryssanthacopoulos, J., Boote, K.J., Büchner, M., Foster, I., Glotter, M., Heinke, J., Iizumi, T., 2015. The global gridded crop model intercomparison: data and modeling protocols for phase 1 (v1. 0). *Geosci. Model Dev.* 8, 261–277.
- Elmqvist, T., Folke, C., Nyström, M., Peterson, G., Bengtsson, J., Walker, B., Norberg, J., 2003. Response diversity, ecosystem change, and resilience. *Front. Ecol. Environ.* 1, 488–494.
- EUROSTAT, 2023. Land cover statistics [WWW Document]. URL https://ec.europa.eu/eurostat/statistics-explained/index.php?title=Land_cover_statistics (accessed 10.1.23).
- Evans, A., 2009. *The feeding of the nine billion: global food security for the 21st century*, A Chatham House report. Chatham House.
- Evenson, R.E., Gollin, D., 2003. Assessing the Impact of the Green Revolution, 1960 to 2000. *Science* 300, 758–762. <https://doi.org/10.1126/science.1078710>
- Ewert, F., van Ittersum, M.K., Heckeley, T., Therond, O., Bezlepkina, I., Andersen, E., 2011. Scale changes and model linking methods for integrated assessment of agri-environmental systems. *Agric. Ecosyst. Environ.* 142, 6–17.
- FAO [WWW Document], 2023. URL <https://www.fao.org/faostat/en/#data/QCL> (accessed 10.1.23).
- Finger, R., 2012. Nitrogen use and the effects of nitrogen taxation under consideration of production and price risks. *Agric. Syst.* 107, 13–20. <https://doi.org/10.1016/j.agsy.2011.12.001>
- Fischer, R.A. (Tony), Edmeades, G.O., 2010. Breeding and Cereal Yield Progress. *Crop Sci.* 50, S-85-S-98. <https://doi.org/10.2135/cropsci2009.10.0564>
- Fisher, R.A., Russell, E.J., 1925. III. The influence of rainfall on the yield of wheat at Rothamsted. *Philos. Trans. R. Soc. Lond. Ser. B Contain. Pap. Biol. Character* 213, 89–142.
<https://doi.org/10.1098/rstb.1925.0003>
- Foley, J.A., Ramankutty, N., Brauman, K.A., Cassidy, E.S., Gerber, J.S., Johnston, M., Mueller, N.D., O’Connell, C., Ray, D.K., West, P.C., Balzer, C., Bennett, E.M., Carpenter, S.R., Hill, J., Monfreda, C., Polasky, S., Rockström, J., Sheehan, J., Siebert, S., Tilman, D., Zaks, D.P.M., 2011. Solutions for a cultivated planet. *Nature* 478, 337–342.
<https://doi.org/10.1038/nature10452>
- Follett, R.F., Hatfield, J.L., 2001. Nitrogen in the Environment: Sources, Problems, and Management. *Sci. World J.* 1, 920–926. <https://doi.org/10.1100/tsw.2001.269>

- Fountas, S., Espejo-Garcia, B., Kasimati, A., Mylonas, N., Darra, N., 2020. The future of digital agriculture: technologies and opportunities. *IT Prof.* 22, 24–28.
- Garnett, T., Appleby, M.C., Balmford, A., Bateman, I.J., Benton, T.G., Bloomer, P., Burlingame, B., Dawkins, M., Dolan, L., Fraser, D., Herrero, M., Hoffmann, I., Smith, P., Thornton, P.K., Toulmin, C., Vermeulen, S.J., Godfray, H.C.J., 2013. Sustainable Intensification in Agriculture: Premises and Policies. *Science* 341, 33–34. <https://doi.org/10.1126/science.1234485>
- Gervois, S., Ciais, P., de Noblet-Ducoudré, N., Brisson, N., Vuichard, N., Viovy, N., 2008. Carbon and water balance of European croplands throughout the 20th century. *Glob. Biogeochem. Cycles* 22. <https://doi.org/10.1029/2007GB003018>
- Glæsner, N., Helming, K., De Vries, W., 2014. Do Current European Policies Prevent Soil Threats and Support Soil Functions? *Sustainability* 6, 9538–9563. <https://doi.org/10.3390/su6129538>
- Goddard, L., Aitchellouche, Y., Baethgen, W., Dettinger, M., Graham, R., Hayman, P., Kadi, M., Martínez, R., Meinke, H., 2010. Providing seasonal-to-interannual climate information for risk management and decision-making. *Procedia Environ. Sci.* 1, 81–101.
- Godfray, H.C.J., Beddington, J.R., Crute, I.R., Haddad, L., Lawrence, D., Muir, J.F., Pretty, J., Robinson, S., Thomas, S.M., Toulmin, C., 2010. Food security: the challenge of feeding 9 billion people. *Science* 327, 812–818. <https://doi.org/10.1126/science.1185383>
- Godwin, R.J., Miller, P.C.H., 2003. A Review of the Technologies for Mapping Within-field Variability. *Biosyst. Eng., Precision Agriculture - Managing Soil and Crop Variability for Cereals* 84, 393–407. [https://doi.org/10.1016/S1537-5110\(02\)00283-0](https://doi.org/10.1016/S1537-5110(02)00283-0)
- Gömann, H., Weingarten, P., 2018. Landnutzungswandel. *Handwörterbuch Stadt- Raumentwickl.*
- Gomiero, T., Pimentel, D., Paoletti, M.G., 2011. Is There a Need for a More Sustainable Agriculture? *Crit. Rev. Plant Sci.* 30, 6–23. <https://doi.org/10.1080/07352689.2011.553515>
- Goovaerts, P., 1999. Geostatistics in soil science: state-of-the-art and perspectives. *Geoderma* 89, 1–45. [https://doi.org/10.1016/S0016-7061\(98\)00078-0](https://doi.org/10.1016/S0016-7061(98)00078-0)
- Goulding, K., Jarvis, S., Whitmore, A., 2008. Optimizing nutrient management for farm systems. *Philos. Trans. R. Soc. B Biol. Sci.* 363, 667–680.
- Graham, I.D., Logan, J., 2004. Translating Research - Innovations in Knowledge Transfer and Continuity of Care. *Can. J. Nurs. Res. Arch.* 89–104.
- Grass, I., Loos, J., Baensch, S., Batáry, P., Librán-Embíd, F., Ficiciyan, A., Klaus, F., Riechers, M., Rosa, J., Tiede, J., Udy, K., Westphal, C., Wurz, A., Tschardtke, T., 2019. Land-sharing/-sparing connectivity landscapes for ecosystem services and biodiversity conservation. *People Nat.* 1, 262–272. <https://doi.org/10.1002/pan3.21>
- Grosz, B., Dechow, R., Gebbert, S., Hoffmann, H., Zhao, G., Constantin, J., Raynal, H., Wallach, D., Coucheney, E., Lewan, E., 2017. The implication of input data aggregation on up-scaling soil organic carbon changes. *Environ. Model. Softw.* 96, 361–377.
- Hall, D.G.M., Reeve, M.J., Thomasson, A.J., Wright, V.F., 1977. Water retention porosity and density of field soils.
- Hartkamp, A.D., White, J.W., Hoogenboom, G., 1999. Interfacing geographic information systems with agronomic modeling: a review. *Agron. J.* 91, 761–772.

- Havlin, J., Heiniger, R., 2020. Soil Fertility Management for Better Crop Production. *Agronomy* 10, 1349. <https://doi.org/10.3390/agronomy10091349>
- He, D., Oliver, Y., Rab, A., Fisher, P., Armstrong, R., Kitching, M., Wang, E., 2022. Plant available water capacity (PAWC) of soils predicted from crop yields better reflects within-field soil physicochemical variations. *Geoderma* 422, 115958. <https://doi.org/10.1016/j.geoderma.2022.115958>
- Heinen, M., 2023. Modelling Soil Water Dynamics, in: Cammarano, D., van Evert, F.K., Kempenaar, C. (Eds.), *Precision Agriculture: Modelling, Progress in Precision Agriculture*. Springer International Publishing, Cham, pp. 129–152. https://doi.org/10.1007/978-3-031-15258-0_6
- Hodges, S.C., 2010. Soil fertility basics.
- Hoffmann, H., Zhao, G., Asseng, S., Bindi, M., Biernath, C., Constantin, J., Coucheney, E., Dechow, R., Doro, L., Eckersten, H., 2016. Impact of spatial soil and climate input data aggregation on regional yield simulations. *PLoS One* 11, e0151782.
- Hoffmann, M.P., Haakana, M., Asseng, S., Höhn, J.G., Palosuo, T., Ruiz-Ramos, M., Fronzek, S., Ewert, F., Gaiser, T., Kassie, B.T., 2018. How does inter-annual variability of attainable yield affect the magnitude of yield gaps for wheat and maize? An analysis at ten sites. *Agric. Syst.* 159, 199–208.
- Holland, J.E., Bennett, A.E., Newton, A.C., White, P.J., McKenzie, B.M., George, T.S., Pakeman, R.J., Bailey, J.S., Fornara, D.A., Hayes, R.C., 2018. Liming impacts on soils, crops and biodiversity in the UK: A review. *Sci. Total Environ.* 610, 316–332.
- Jaynes, D.B., Colvin, T.S., 1997. Spatiotemporal Variability of Corn and Soybean Yield. *Agron. J.* 89, 30–37. <https://doi.org/10.2134/agronj1997.00021962008900010005x>
- Jones, J.W., Antle, J.M., Basso, B., Boote, K.J., Conant, R.T., Foster, I., Godfray, H.C.J., Herrero, M., Howitt, R.E., Janssen, S., Keating, B.A., Munoz-Carpena, R., Porter, C.H., Rosenzweig, C., Wheeler, T.R., 2017. Brief history of agricultural systems modeling. *Agric. Syst.* 155, 240–254. <https://doi.org/10.1016/j.agsy.2016.05.014>
- Ju, X.T., Kou, C.L., Christie, P., Dou, Z.X., Zhang, F.S., 2007. Changes in the soil environment from excessive application of fertilizers and manures to two contrasting intensive cropping systems on the North China Plain. *Environ. Pollut.* 145, 497–506. <https://doi.org/10.1016/j.envpol.2006.04.017>
- Kabat, P., Hutjes, R.W.A., Feddes, R.A., 1997. The scaling characteristics of soil parameters: From plot scale heterogeneity to subgrid parameterization. *J. Hydrol.* 190, 363–396.
- Kahiluoto, H., Kaseva, J., Balek, J., Olesen, J.E., Ruiz-Ramos, M., Gobin, A., Kersebaum, K.C., Takáč, J., Ruget, F., Ferrise, R., 2019. Decline in climate resilience of European wheat. *Proc. Natl. Acad. Sci.* 116, 123–128.
- Kang, Y., Khan, S., Ma, X., 2009. Climate change impacts on crop yield, crop water productivity and food security – A review. *Prog. Nat. Sci.* 19, 1665–1674. <https://doi.org/10.1016/j.pnsc.2009.08.001>
- Kanianska, R., 2016. Agriculture and Its Impact on Land-Use, Environment, and Ecosystem Services, in: *Landscape Ecology - The Influences of Land Use and Anthropogenic Impacts of Landscape Creation*. IntechOpen. <https://doi.org/10.5772/63719>

- Kersebaum, K.C., Boote, K.J., Jorgenson, J.S., Nendel, C., Bindi, M., Frühauf, C., Gaiser, T., Hoogenboom, G., Kollas, C., Olesen, J.E., 2015. Analysis and classification of data sets for calibration and validation of agro-ecosystem models. *Environ. Model. Softw.* 72, 402–417.
- Kersebaum, K.C., Nendel, C., 2014. Site-specific impacts of climate change on wheat production across regions of Germany using different CO₂ response functions. *Eur. J. Agron., Land, Climate and Resources* 2020. *Decision Support for Agriculture under Climate Change* 52, 22–32. <https://doi.org/10.1016/j.eja.2013.04.005>
- Kersebaum, K.C., Wallor, E., 2023. Process-Based Modelling of Soil–Crop Interactions for Site-Specific Decision Support in Crop Management, in: *Precision Agriculture: Modelling*. Springer, pp. 25–47.
- Kirchmann, H., Eskilsson, J., 2010. Low manganese (Mn) and copper (Cu) concentrations in cereals explained yield losses after lime application to soil. *Acta Agric. Scand. Sect. B-Soil Plant Sci.* 60, 569–572.
- Kuhnert, M., Yeluripati, J., Smith, P., Hoffmann, H., Van Oijen, M., Constantin, J., Coucheney, E., Dechow, R., Eckersten, H., Gaiser, T., 2017. Impact analysis of climate data aggregation at different spatial scales on simulated net primary productivity for croplands. *Eur. J. Agron.* 88, 41–52.
- Kutter, T., Tiemann, S., Siebert, R., Fountas, S., 2011. The role of communication and co-operation in the adoption of precision farming. *Precis. Agric.* 12, 2–17. <https://doi.org/10.1007/s11119-009-9150-0>
- Lambers, H., Oliveira, R.S., 2019. *Plant Physiological Ecology*. Springer International Publishing, Cham. <https://doi.org/10.1007/978-3-030-29639-1>
- Lindblom, J., Lundström, C., Ljung, M., Jonsson, A., 2017. Promoting sustainable intensification in precision agriculture: review of decision support systems development and strategies. *Precis. Agric.* 18, 309–331. <https://doi.org/10.1007/s11119-016-9491-4>
- Lioutas, E.D., Charatsari, C., De Rosa, M., 2021. Digitalization of agriculture: A way to solve the food problem or a trolley dilemma? *Technol. Soc.* 67, 101744. <https://doi.org/10.1016/j.techsoc.2021.101744>
- Lobell, D.B., Burke, M.B., 2010. On the use of statistical models to predict crop yield responses to climate change. *Agric. For. Meteorol.* 150, 1443–1452. <https://doi.org/10.1016/j.agrformet.2010.07.008>
- Lobell, D.B., Ortiz-Monasterio, J.I., 2007. Impacts of Day Versus Night Temperatures on Spring Wheat Yields: A Comparison of Empirical and CERES Model Predictions in Three Locations. *Agron. J.* 99, 469–477. <https://doi.org/10.2134/agronj2006.0209>
- Louwagie, G., Gay, S.H., Sammeth, F., Ratering, T., 2011. The potential of European Union policies to address soil degradation in agriculture. *Land Degrad. Dev.* 22, 5–17. <https://doi.org/10.1002/ldr.1028>
- Mahler, R.L., McDole, R.E., 1987. Effect of soil pH on crop yield in northern idaho 1. *Agron. J.* 79, 751–755.
- Matzner, E., Borken, W., 2008. Do freeze-thaw events enhance C and N losses from soils of different ecosystems? A review. *Eur. J. Soil Sci.* 59, 274–284.

- McBratney, A.B., Minasny, B., Cattle, S.R., Vervoort, R.W., 2002. From pedotransfer functions to soil inference systems. *Geoderma* 109, 41–73.
- McKenzie, F.C., Williams, J., 2015. Sustainable food production: constraints, challenges and choices by 2050. *Food Secur.* 7, 221–233. <https://doi.org/10.1007/s12571-015-0441-1>
- McLaren, J.S., 2000. The importance of genomics to the future of crop production. *Pest Manag. Sci.* 56, 573–579. [https://doi.org/10.1002/1526-4998\(200007\)56:7<573::AID-PS184>3.0.CO;2-D](https://doi.org/10.1002/1526-4998(200007)56:7<573::AID-PS184>3.0.CO;2-D)
- Meurer, K., Barron, J., Chenu, C., Coucheney, E., Fielding, M., Hallett, P., Herrmann, A.M., Keller, T., Koestel, J., Larsbo, M., Lewan, E., Or, D., Parsons, D., Parvin, N., Taylor, A., Vereecken, H., Jarvis, N., 2020. A framework for modelling soil structure dynamics induced by biological activity. *Glob. Change Biol.* 26, 5382–5403. <https://doi.org/10.1111/gcb.15289>
- Meurer, K.H.E., Chenu, C., Coucheney, E., Herrmann, A.M., Keller, T., Kätterer, T., Nimblad Svensson, D., Jarvis, N., 2020. Modelling dynamic interactions between soil structure and the storage and turnover of soil organic matter. *Biogeosciences* 17, 5025–5042. <https://doi.org/10.5194/bg-17-5025-2020>
- Mirschel, W., Schultz, A., Wenkel, K.O., Wieland, R., Poluektov, R.A., 2004. Crop growth modelling on different spatial scales—A wide spectrum of approaches. *Arch. Agron. Soil Sci.* 50, 329–343.
- Moll, R.H., Kamprath, E.J., Jackson, W.A., 1982. Analysis and Interpretation of Factors Which Contribute to Efficiency of Nitrogen Utilization1. *Agron. J.* 74, 562–564. <https://doi.org/10.2134/agronj1982.000219622007400030037x>
- Mosier, A.R., 2001. Exchange of gaseous nitrogen compounds between agricultural systems and the atmosphere. *Plant Soil* 228, 17–27. <https://doi.org/10.1023/A:1004821205442>
- Mulders, M.A., 1987. Remote sensing in soil science. Elsevier.
- Neina, D., 2019. The role of soil pH in plant nutrition and soil remediation. *Appl. Environ. Soil Sci.* 2019, 1–9.
- Niedertscheider, M., Kuemmerle, T., Müller, D., Erb, K.-H., 2014. Exploring the effects of drastic institutional and socio-economic changes on land system dynamics in Germany between 1883 and 2007. *Glob. Environ. Change Hum. Policy Dimens.* 28, 98–108. <https://doi.org/10.1016/j.gloenvcha.2014.06.006>
- Nowak, B., 2021. Precision Agriculture: Where do We Stand? A Review of the Adoption of Precision Agriculture Technologies on Field Crops Farms in Developed Countries. *Agric. Res.* 10, 515–522. <https://doi.org/10.1007/s40003-021-00539-x>
- O. Chung, S., A. Sudduth, K., T. Drummond, S., 2002. Determining yield monitoring system delay time with geostatistical and data segmentation approaches. *Trans. ASAE* 45, 915. <https://doi.org/10.13031/2013.9938>
- Oerke, E.-C., 2006. Crop losses to pests. *J. Agric. Sci.* 144, 31–43. <https://doi.org/10.1017/S0021859605005708>
- Oliver, M.A., Webster, R., 1989. A geostatistical basis for spatial weighting in multivariate classification. *Math. Geol.* 21, 15–35. <https://doi.org/10.1007/BF00897238>
- Ørum, J.E., Kudsk, P., Jensen, P.K., 2017. Economics of Site-Specific and Variable-Dose Herbicide Application, in: Pedersen, S.M., Lind, K.M. (Eds.), *Precision Agriculture: Technology and*

- Economic Perspectives, Progress in Precision Agriculture. Springer International Publishing, Cham, pp. 93–110. https://doi.org/10.1007/978-3-319-68715-5_4
- Paleari, S., 2017. Is the European Union protecting soil? A critical analysis of Community environmental policy and law. *Land Use Policy* 64, 163–173. <https://doi.org/10.1016/j.landusepol.2017.02.007>
- Palosuo, T., Kersebaum, K.C., Angulo, C., Hlavinka, P., Moriondo, M., Olesen, J.E., Patil, R.H., Ruget, F., Rumbaur, C., Takáč, J., 2011. Simulation of winter wheat yield and its variability in different climates of Europe: A comparison of eight crop growth models. *Eur. J. Agron.* 35, 103–114.
- Pan, L., Adamchuk, V.I., Prasher, S., Gebbers, R., Taylor, R.S., Dabas, M., 2014. Vertical soil profiling using a galvanic contact resistivity scanning approach. *Sensors* 14, 13243–13255.
- Pasquel, D., Roux, S., Richetti, J., Cammarano, D., Tisseyre, B., Taylor, J.A., 2022. A review of methods to evaluate crop model performance at multiple and changing spatial scales. *Precis. Agric.* 23, 1489–1513. <https://doi.org/10.1007/s11119-022-09885-4>
- Pedersen, S. M., Lind, K. M., 2017. Precision Agriculture – From Mapping to Site-Specific Application, in: Pedersen, Søren Marcus, Lind, Kim Martin (Eds.), *Precision Agriculture: Technology and Economic Perspectives, Progress in Precision Agriculture*. Springer International Publishing, Cham, pp. 1–20. https://doi.org/10.1007/978-3-319-68715-5_1
- Pellegrini, P., Fernández, R.J., 2018. Crop intensification, land use, and on-farm energy-use efficiency during the worldwide spread of the green revolution. *Proc. Natl. Acad. Sci. U. S. A.* 115, 2335–2340. <https://doi.org/10.1073/pnas.1717072115>
- Peng, S., Huang, J., Sheehy, J.E., Laza, R.C., Visperas, R.M., Zhong, X., Centeno, G.S., Khush, G.S., Cassman, K.G., 2004. Rice yields decline with higher night temperature from global warming. *Proc. Natl. Acad. Sci.* 101, 9971–9975. <https://doi.org/10.1073/pnas.0403720101>
- Petersen, R.G., 1994. *Agricultural Field Experiments: Design and Analysis*. CRC Press.
- Phalan, B., Balmford, A., Green, R.E., Scharlemann, J.P.W., 2011. Minimising the harm to biodiversity of producing more food globally. *Food Policy, The challenge of global food sustainability* 36, S62–S71. <https://doi.org/10.1016/j.foodpol.2010.11.008>
- Philibert, A., Loyce, C., Makowski, D., 2012. Assessment of the quality of meta-analysis in agronomy. *Agric. Ecosyst. Environ.* 148, 72–82. <https://doi.org/10.1016/j.agee.2011.12.003>
- Pierce, F.J., Nowak, P., 1999. Aspects of Precision Agriculture, in: Sparks, D.L. (Ed.), *Advances in Agronomy*. Academic Press, pp. 1–85. [https://doi.org/10.1016/S0065-2113\(08\)60513-1](https://doi.org/10.1016/S0065-2113(08)60513-1)
- Pinstrup-Andersen, P., 2000. The future world food situation and the role of plant diseases. *Can. J. Plant Pathol.* 22, 321–331. <https://doi.org/10.1080/07060660009500451>
- Porter, J.R., Semenov, M.A., 2005. Crop responses to climatic variation. *Philos. Trans. R. Soc. B Biol. Sci.* 360, 2021–2035. <https://doi.org/10.1098/rstb.2005.1752>
- Portmann, R., Beyerle, U., Davin, E., Fischer, E.M., De Hertog, S., Schemm, S., 2022. Global forestation and deforestation affect remote climate via adjusted atmosphere and ocean circulation. *Nat. Commun.* 13, 5569. <https://doi.org/10.1038/s41467-022-33279-9>
- Potapov, P., Hansen, M.C., Pickens, A., Hernandez-Serna, A., Tyukavina, A., Turubanova, S., Zalles, V., Li, X., Khan, A., Stolle, F., Harris, N., Song, X.-P., Baggett, A., Kommareddy, I., Kommareddy,

- A., 2022. The Global 2000-2020 Land Cover and Land Use Change Dataset Derived From the Landsat Archive: First Results. *Front. Remote Sens.* 3.
- Pretty, J., 2007. Agricultural sustainability: concepts, principles and evidence. *Philos. Trans. R. Soc. B Biol. Sci.* 363, 447–465. <https://doi.org/10.1098/rstb.2007.2163>
- Quinton, J.N., Govers, G., Van Oost, K., Bardgett, R.D., 2010. The impact of agricultural soil erosion on biogeochemical cycling. *Nat. Geosci.* 3, 311–314. <https://doi.org/10.1038/ngeo838>
- Rajsic, P., Weersink, A., 2008. Do farmers waste fertilizer? A comparison of ex post optimal nitrogen rates and ex ante recommendations by model, site and year. *Agric. Syst.* 97, 56–67. <https://doi.org/10.1016/j.agsy.2007.12.001>
- Rashmi, I., Karthika, K.S., Roy, T., Shinoji, K.C., Kumawat, A., Kala, S., Pal, R., 2022. Soil Erosion and Sediments: A Source of Contamination and Impact on Agriculture Productivity, in: Naeem, M., Bremont, J.F.J., Ansari, A.A., Gill, S.S. (Eds.), *Agrochemicals in Soil and Environment: Impacts and Remediation*. Springer Nature, Singapore, pp. 313–345. https://doi.org/10.1007/978-981-16-9310-6_14
- Reddy, P.P., 2016. *Sustainable Intensification of Crop Production*. Springer, Singapore. <https://doi.org/10.1007/978-981-10-2702-4>
- Reichardt, M., Jürgens, C., Klöble, U., Hüter, J., Moser, K., 2009. Dissemination of precision farming in Germany: acceptance, adoption, obstacles, knowledge transfer and training activities. *Precis. Agric.* 10, 525–545. <https://doi.org/10.1007/s11119-009-9112-6>
- Reijnders, L., 2003. Policies influencing cleaner production: the role of prices and regulation. *J. Clean. Prod.* 11, 333–338. [https://doi.org/10.1016/S0959-6526\(02\)00027-6](https://doi.org/10.1016/S0959-6526(02)00027-6)
- Robson, A., 2012. *Soil acidity and plant growth*. Elsevier.
- Rockström, J., Steffen, W., Noone, K., Persson, Å., Chapin, F.S., Lambin, E., Lenton, T.M., Scheffer, M., Folke, C., Schellnhuber, H.J., Nykvist, B., de Wit, C.A., Hughes, T., van der Leeuw, S., Rodhe, H., Sörlin, S., Snyder, P.K., Costanza, R., Svedin, U., Falkenmark, M., Karlberg, L., Corell, R.W., Fabry, V.J., Hansen, J., Walker, B., Liverman, D., Richardson, K., Crutzen, P., Foley, J., 2009. Planetary Boundaries: Exploring the Safe Operating Space for Humanity. *Ecol. Soc.* 14.
- Rogers, E.M., 2010. *Diffusion of Innovations*, 4th Edition. Simon and Schuster.
- Sarkar, D., Meena, V.S., Haldar, A., Rakshit, A., 2017. Site-Specific Nutrient Management (SSNM): A Unique Approach Towards Maintaining Soil Health, in: Rakshit, A., Abhilash, P.C., Singh, H.B., Ghosh, S. (Eds.), *Adaptive Soil Management : From Theory to Practices*. Springer, Singapore, pp. 69–88. https://doi.org/10.1007/978-981-10-3638-5_3
- Schiefer, J., Lair, G.J., Blum, W.E.H., 2016. Potential and limits of land and soil for sustainable intensification of European agriculture. *Agric. Ecosyst. Environ.* 230, 283–293. <https://doi.org/10.1016/j.agee.2016.06.021>
- Shah, F., Wu, W., 2019. Soil and crop management strategies to ensure higher crop productivity within sustainable environments. *Sustainability* 11, 1485.
- Shanmugapriya, P., Rathika, S., Ramesh, T., Janaki, P., 2019. Applications of remote sensing in agriculture-A Review. *Int J Curr Microbiol Appl Sci* 8, 2270–2283.

- Sharma, S., Verma, G.K., 2015. Inversion of Electrical Resistivity Data: A Review. *Int. J. Comput. Syst. Eng.* 9, 400–406.
- Sheehy, J.E., Mitchell, P.L., Ferrer, A.B., 2006. Decline in rice grain yields with temperature: Models and correlations can give different estimates. *Field Crops Res.* 98, 151–156. <https://doi.org/10.1016/j.fcr.2006.01.001>
- Shepherd, M., Chambers, B., 2007. Managing nitrogen on the farm: the devil is in the detail. *J. Sci. Food Agric.* 87, 558–568. <https://doi.org/10.1002/jsfa.2775>
- Shiferaw, B., Smale, M., Braun, H.-J., Duveiller, E., Reynolds, M., Muricho, G., 2013. Crops that feed the world 10. Past successes and future challenges to the role played by wheat in global food security. *Food Secur.* 5, 291–317. <https://doi.org/10.1007/s12571-013-0263-y>
- Shukla, P.R., Skea, J., Calvo Buendia, E., Masson-Delmotte, V., Pörtner, H.O., Roberts, D.C., Zhai, P., Slade, R., Connors, S., Van Diemen, R., 2019. IPCC, 2019: Climate Change and Land: an IPCC special report on climate change, desertification, land degradation, sustainable land management, food security, and greenhouse gas fluxes in terrestrial ecosystems.
- Silva, C.B., do Vale, S.M.L.R., Pinto, F.A.C., Müller, C.A.S., Moura, A.D., 2007. The economic feasibility of precision agriculture in Mato Grosso do Sul State, Brazil: a case study. *Precis. Agric.* 8, 255–265. <https://doi.org/10.1007/s11119-007-9040-2>
- Smith, P., House, J.I., Bustamante, M., Sobocká, J., Harper, R., Pan, G., West, P.C., Clark, J.M., Adhya, T., Rumpel, C., Paustian, K., Kuikman, P., Cotrufo, M.F., Elliott, J.A., McDowell, R., Griffiths, R.I., Asakawa, S., Bondeau, A., Jain, A.K., Meersmans, J., Pugh, T.A.M., 2016. Global change pressures on soils from land use and management. *Glob. Change Biol.* 22, 1008–1028. <https://doi.org/10.1111/gcb.13068>
- Spiertz, J.H.J., 2009. Nitrogen, Sustainable Agriculture and Food Security: A Review, in: Lichtfouse, E., Navarrete, M., Debaeke, P., Véronique, S., Alberola, C. (Eds.), *Sustainable Agriculture*. Springer Netherlands, Dordrecht, pp. 635–651. https://doi.org/10.1007/978-90-481-2666-8_39
- Spiertz, J.H.J., Ewert, F., 2009. Crop production and resource use to meet the growing demand for food, feed and fuel: opportunities and constraints. *NJAS Wagening. J. Life Sci.* 56, 281–300. [https://doi.org/10.1016/S1573-5214\(09\)80001-8](https://doi.org/10.1016/S1573-5214(09)80001-8)
- Springmann, M., Clark, M., Mason-D’Croz, D., Wiebe, K., BDIRSKY, B.L., Lassaletta, L., de Vries, W., Vermeulen, S.J., Herrero, M., Carlson, K.M., Jonell, M., Troell, M., DeClerck, F., Gordon, L.J., Zurayk, R., Scarborough, P., Rayner, M., Loken, B., Fanzo, J., Godfray, H.C.J., Tilman, D., Rockström, J., Willett, W., 2018. Options for keeping the food system within environmental limits. *Nature* 562, 519–525. <https://doi.org/10.1038/s41586-018-0594-0>
- Stafford, J.V., 2000. Implementing Precision Agriculture in the 21st Century. *J. Agric. Eng. Res.* 76, 267–275. <https://doi.org/10.1006/jaer.2000.0577>
- Stagnari, F., Galieni, A., D’Egidio, S., Pagnani, G., Pisante, M., 2019. Sustainable Soil Management, in: Farooq, M., Pisante, M. (Eds.), *Innovations in Sustainable Agriculture*. Springer International Publishing, Cham, pp. 105–131. https://doi.org/10.1007/978-3-030-23169-9_5
- Stoate, C., Báldi, A., Beja, P., Boatman, N.D., Herzog, I., van Doorn, A., de Snoo, G.R., Rakosy, L., Ramwell, C., 2009. Ecological impacts of early 21st century agricultural change in Europe – A review. *J. Environ. Manage.* 91, 22–46. <https://doi.org/10.1016/j.jenvman.2009.07.005>

- Stockmann, U., Adams, M.A., Crawford, J.W., Field, D.J., Henakaarchchi, N., Jenkins, M., Minasny, B., McBratney, A.B., De Courcelles, V. de R., Singh, K., 2013. The knowns, known unknowns and unknowns of sequestration of soil organic carbon. *Agric. Ecosyst. Environ.* 164, 80–99.
- Sundström, J.F., Albiñ, A., Boqvist, S., Ljungvall, K., Marstorp, H., Martiin, C., Nyberg, K., Vågsholm, I., Yuen, J., Magnusson, U., 2014. Future threats to agricultural food production posed by environmental degradation, climate change, and animal and plant diseases – a risk analysis in three economic and climate settings. *Food Secur.* 6, 201–215.
<https://doi.org/10.1007/s12571-014-0331-y>
- Supit, I., van Diepen, C.A., de Wit, A.J.W., Kabat, P., Baruth, B., Ludwig, F., 2010. Recent changes in the climatic yield potential of various crops in Europe. *Agric. Syst.* 103, 683–694.
<https://doi.org/10.1016/j.agsy.2010.08.009>
- Sylvester-Bradley, R., Lord, E., Sparkes, D. I., Scott, R. k., Wiltshire, J. j. j., Orson, J., 1999. An analysis of the potential of precision farming in Northern Europe. *Soil Use Manag.* 15, 1–8.
<https://doi.org/10.1111/j.1475-2743.1999.tb00054.x>
- Takács-György, K., 2008. Economic Aspects of Chemical Reduction on Farming: Role of Precision Farming – Will the Production Structure Change? *Cereal Res. Commun.* 36, 519–522.
- Tamirat, T.W., Pedersen, S.M., Lind, K.M., 2018. Farm and operator characteristics affecting adoption of precision agriculture in Denmark and Germany. *Acta Agric. Scand. Sect. B — Soil Plant Sci.* 68, 349–357. <https://doi.org/10.1080/09064710.2017.1402949>
- Tester, M., Langridge, P., 2010. Breeding Technologies to Increase Crop Production in a Changing World. *Science* 327, 818–822. <https://doi.org/10.1126/science.1183700>
- Teuling, A.J., Troch, P.A., 2005. Improved understanding of soil moisture variability dynamics. *Geophys. Res. Lett.* 32. <https://doi.org/10.1029/2004GL021935>
- Tilman, D., 1999. Global environmental impacts of agricultural expansion: The need for sustainable and efficient practices. *Proc. Natl. Acad. Sci.* 96, 5995–6000.
<https://doi.org/10.1073/pnas.96.11.5995>
- Trnka, M., Feng, S., Semenov, M.A., Olesen, J.E., Kersebaum, K.C., Rötter, R.P., Semerádová, D., Klem, K., Huang, W., Ruiz-Ramos, M., Hlavinka, P., Meitner, J., Balek, J., Havlík, P., Büntgen, U., 2019. Mitigation efforts will not fully alleviate the increase in water scarcity occurrence probability in wheat-producing areas. *Sci. Adv.* 5, eaau2406.
<https://doi.org/10.1126/sciadv.aau2406>
- Trnka, M., Rötter, R.P., Ruiz-Ramos, M., Kersebaum, K.C., Olesen, J.E., Žalud, Z., Semenov, M.A., 2014. Adverse weather conditions for European wheat production will become more frequent with climate change. *Nat. Clim. Change* 4, 637–643.
<https://doi.org/10.1038/nclimate2242>
- Tsiropoulos, Z., Carli, G., Pignatti, E., Fountas, S., 2017. Future Perspectives of Farm Management Information Systems, in: Pedersen, S.M., Lind, K.M. (Eds.), *Precision Agriculture: Technology and Economic Perspectives*, Progress in Precision Agriculture. Springer International Publishing, Cham, pp. 181–200. https://doi.org/10.1007/978-3-319-68715-5_9
- Turmel, M.-S., Speratti, A., Baudron, F., Verhulst, N., Govaerts, B., 2015. Crop residue management and soil health: A systems analysis. *Agric. Syst., Biomass use trade-offs in cereal cropping*

- systems:Lessons and implications from the developing world 134, 6–16.
<https://doi.org/10.1016/j.agsy.2014.05.009>
- United Nations, D. of E. and S.A., Population Division, 2019. World Population Prospects 2019 Highlights.
- Veldkamp, A., Kok, K., De Koning, G.H.J., Schoorl, J.M., Sonneveld, M.P.W., Verburg, P.H., 2001. Multi-scale system approaches in agronomic research at the landscape level. *Soil Tillage Res., LANDSCAPE RESEARCH-EXPLORING ECOSYSTEM PROCESSES AND THEIR* 58, 129–140.
[https://doi.org/10.1016/S0167-1987\(00\)00163-X](https://doi.org/10.1016/S0167-1987(00)00163-X)
- Vergni, L., Todisco, F., 2011. Spatio-temporal variability of precipitation, temperature and agricultural drought indices in Central Italy. *Agric. For. Meteorol.* 151, 301–313.
- Vetterlein, D., Doussan, C., 2016. Root age distribution: how does it matter in plant processes? A focus on water uptake. *Plant Soil* 407, 145–160.
- Villoria, N.B., 2019. Technology Spillovers and Land Use Change: Empirical Evidence from Global Agriculture. *Am. J. Agric. Econ.* 101, 870–893. <https://doi.org/10.1093/ajae/aay088>
- Viscarra Rossel, R., McBratney, A., Minasny, B., 2010. Proximal Soil Sensing. Springer Science+Business Media B.V.
- Vogel, H.-J., Eberhardt, E., Franko, U., Lang, B., Ließ, M., Weller, U., Wiesmeier, M., Wollschläger, U., 2019. Quantitative Evaluation of Soil Functions: Potential and State. *Front. Environ. Sci.* 7.
- Von Blottnitz, H., Rabl, A., Boiadjiev, D., Taylor, T., Arnold, S., 2006. Damage costs of nitrogen fertilizer in Europe and their internalization. *J. Environ. Plan. Manag.* 49, 413–433.
<https://doi.org/10.1080/09640560600601587>
- Wallach, D., Makowski, D., Jones, J.W., Brun, F., 2018. Working with dynamic crop models. Academic Press-Elsevier.
- Wang, J., Vanga, S.K., Saxena, R., Orsat, V., Raghavan, V., 2018. Effect of Climate Change on the Yield of Cereal Crops: A Review. *Climate* 6, 41. <https://doi.org/10.3390/cli6020041>
- Wang, R., Zhang, J., Cai, C., Wang, S., 2023. Mechanism of nitrogen loss driven by soil and water erosion in water source areas. *J. For. Res.* 34, 1985–1995. <https://doi.org/10.1007/s11676-023-01640-3>
- Warrick, A.W., Gardner, W.R., 1983. Crop yield as affected by spatial variations of soil and irrigation. *Water Resour. Res.* 19, 181–186. <https://doi.org/10.1029/WR019i001p00181>
- Webber, H., Ewert, F., Olesen, J.E., Müller, C., Fronzek, S., Ruane, A.C., Bourgault, M., Martre, P., Ababaei, B., Bindi, M., Ferrise, R., Finger, R., Fodor, N., Gabaldón-Leal, C., Gaiser, T., Jabloun, M., Kersebaum, K.-C., Lizaso, J.I., Lorite, I.J., Manceau, L., Moriondo, M., Nendel, C., Rodríguez, A., Ruiz-Ramos, M., Semenov, M.A., Siebert, S., Stella, T., Stratonovitch, P., Trombi, G., Wallach, D., 2018. Diverging importance of drought stress for maize and winter wheat in Europe. *Nat. Commun.* 9, 4249. <https://doi.org/10.1038/s41467-018-06525-2>
- Webster, R., 2007. Digital Soil Mapping: An Introductory Perspective - Edited by P. Lagacherie, A. B. McBratney & M. Voltz. *Eur. J. Soil Sci.* 58, 1217–1218. https://doi.org/10.1111/j.1365-2389.2007.00943_6.x

- Weiss, M., Jacob, F., Duveiller, G., 2020. Remote sensing for agricultural applications: A meta-review. *Remote Sens. Environ.* 236, 111402.
- White, J.W., Hoogenboom, G., 2010. Crop Response to Climate: Ecophysiological Models, in: Lobell, D., Burke, M. (Eds.), *Climate Change and Food Security: Adapting Agriculture to a Warmer World*, Advances in Global Change Research. Springer Netherlands, Dordrecht, pp. 59–83. https://doi.org/10.1007/978-90-481-2953-9_4
- Wiesmeier, M., Urbanski, L., Hobbey, E., Lang, B., von Lützw, M., Marin-Spiotta, E., van Wesemael, B., Rabot, E., Ließ, M., Garcia-Franco, N., 2019. Soil organic carbon storage as a key function of soils-A review of drivers and indicators at various scales. *Geoderma* 333, 149–162.
- Witcombe, J. r, Hollington, P. a, Howarth, C. j, Reader, S., Steele, K. a, 2007. Breeding for abiotic stresses for sustainable agriculture. *Philos. Trans. R. Soc. B Biol. Sci.* 363, 703–716. <https://doi.org/10.1098/rstb.2007.2179>
- Witing, F., Volk, M., Franko, U., 2023. Modeling Soil Organic Carbon Dynamics of Arable Land across Scales: A Simplified Assessment of Alternative Management Practices on the Level of Administrative Units. *Agronomy* 13, 1159.
- Witt, C., Dobermann, A., 2004. Toward a decision support system for site-specific nutrient management. *Increasing Product. Intensive Rice Syst. Site Rice Syst. Site-Specif. Nutr. Manag.* 359.
- Yang, R.-C., 2010. Towards understanding and use of mixed-model analysis of agricultural experiments. *Can. J. Plant Sci.* 90, 605–627. <https://doi.org/10.4141/CJPS10049>
- Ye, X., Zhang, Q., Viney, N.R., 2011. The effect of soil data resolution on hydrological processes modelling in a large humid watershed. *Hydrol. Process.* 25, 130–140.
- Young, O., 2006. Vertical Interplay among Scale-dependent Environmental and Resource Regimes. *Ecol. Soc.* 11.
- Zhang, N., Wang, M., Wang, N., 2002. Precision agriculture—a worldwide overview. *Comput. Electron. Agric.* 36, 113–132. [https://doi.org/10.1016/S0168-1699\(02\)00096-0](https://doi.org/10.1016/S0168-1699(02)00096-0)
- Zhang, X., Davidson, E.A., Mauzerall, D.L., Searchinger, T.D., Dumas, P., Shen, Y., 2015. Managing nitrogen for sustainable development. *Nature* 528, 51–59. <https://doi.org/10.1038/nature15743>
- Zribi, M., Baghdadi, N., Nolin, M., 2011. Remote sensing of soil, *Applied and Environmental Soil Science*. Hindawi.

Affidavit

I hereby declare under penalty of perjury that this dissertation – entitled ‘Variation of wheat yields as a consequence of soil and meteorological variability’ – has been composed by myself and describes my own work. Work done in collaboration with others have been specified within the text and the Acknowledgements. All references and verbatim extracts have been quoted, and all sources of information have been specifically acknowledged. I used only the sources mentioned and included all the citations correctly both in word or content. This thesis in whole has not been accepted in any previous application for a degree at this or any other university.

Hiermit erkläre ich unter Eid, dass diese Dissertation mit dem Titel "Variation of wheat yields as a consequence of soil and meteorological variability" (Deu: „Variation der Weizenerträge als Folge von bodenkundlichen und meteorologischen Schwankungen“) von mir selbst verfasst wurde und meine eigene Arbeit darstellt. Arbeiten, die in Zusammenarbeit mit anderen durchgeführt wurden, sind im Text und in den Danksagungen angegeben. Alle Referenzen und wörtlichen Auszüge wurden zitiert, und alle Informationsquellen wurden ausdrücklich genannt. Diese Arbeit wurde in ihrer Gesamtheit bei keiner früheren Bewerbung um einen Abschluss an dieser oder einer anderen Universität angenommen.

Halle (Saale), the 06.10.2023

.....

Curriculum Vitae

Name Eric Bönecke

Research Experience

Since 06/2019	Research Associate @Research Group HORTSYS: Horticultural Systems of the Future - Leibniz Institute of Vegetable and Ornamental Crops (IGZ) , Grossbeeren, Germany
Since 01/2023	<ul style="list-style-type: none"> • Research Project: "Site-differentiated and optimized nutrient management in arable farming - TONIA" (EIP-AGRI)
01/2022 - 12/2022	<ul style="list-style-type: none"> • Research Project: „Georeferenced and sensor-based data management systems for site-specific irrigation and fertilization of field-grown vegetables - GeoSenSys“ (BLE)
06/2019 - 09/2022	<ul style="list-style-type: none"> • Research Project: „ Precise liming in Brandenburg - pH-BB“ (EIP-AGRI)
06/2017 - 05/2019	Research Associate @Department of Systems Modeling, Institute of Horticultural Production Systems, Leibniz University Hanover , Hanover, Germany
06/2017 - 05/2019	<ul style="list-style-type: none"> • Research Project: „Data meta-evaluation on crop productivity development“ (DFG)
01/2013 - 05/2017	Research Associate @ Department for Soil System Science, Helmholtz Centre for Environmental Research (UFZ) , Halle (Saale), Germany
04/2016 - 08/2016	<ul style="list-style-type: none"> • Research Project: „Carbon sequestration, biodiversity and social structures in Southern Amazonia, Brazil - CarBioCial“ (BMBF)
01/2013 - 03/2016	<ul style="list-style-type: none"> • Research Project: „Site-adapted N-management based on site-specific soil processing“ (BLE)
03/2014	<ul style="list-style-type: none"> • Geophysical field practical course @ Department of Monitoring and Exploration Technologies, Helmholtz Centre for Environmental Research (UFZ), Leipzig
02/2010 - 06/2011	<ul style="list-style-type: none"> • Student assistant @ Commonwealth Scientific and Industrial Research Organisation (CSIRO), Darwin, Australia - Research project to write the diploma (master) thesis

Education

2004 – 2012	<ul style="list-style-type: none"> • Diploma Geography (major subjects: Soil Science and Geology) – Martin-Luther-University Halle-Wittenberg, Halle (Saale), Germany and Commonwealth Scientific and Industrial Research Organisation - CSIRO, Darwin, Australia
2003	<ul style="list-style-type: none"> • High School – Goethe Gymnasium, Weissenfels, Germany

Memberships

Since 2017	<ul style="list-style-type: none"> • German Society for Crop Science e.V. - GPW
Since 2013	<ul style="list-style-type: none"> • German Soil Science Society - DBG

Publications (peer-reviewed)

- Muhirwa, F., Shen, L., Elshkaki, A., Chiaka, J.C., Zhong, S., **Bönecke, E.**, Hirwa, H., Seka, A.M., Habiyakare, T., Tuyishimire, A. and Harerimana, B., 2023. Alert in the dynamics of water-energy-food production in African countries from a nexus perspective. *Resources, Conservation and Recycling*, 194, p.106990. [\[CrossRef\]](#)
- Koura, B. I., **Boenecke, E.**, Lohrberg, F., Dossa, L. H., 2023: "Urban Agricultural Heritage in Benin: The Role of Traditional Coconut-Cattle Systems in Cotonou". *Urban Agricultural Heritage*, edited by Frank Lohrberg, Katharina Christenn, Axel Timpe and Ayça Sancar, Berlin, Boston: Birkhäuser, 2023, pp. 98-104. [\[CrossRef\]](#)
- Horf, M., **Bönecke, E.**, Gebbers, R., Kling, C., Kramer, E., Rühlmann, J., Schröter, I., Schwanghart, W., Vogel, S., 2022: Utility of visible and near-infrared spectroscopy to predict base neutralizing capacity and lime requirement of quaternary soils. *Precision Agriculture*. [\[CrossRef\]](#)
- Vogel, S., **Bönecke, E.**, Kling, C., Kramer, E., Lück, K., Philipp, G., Rühlmann, J., Schröter, I., Gebbers, R., 2022: Direct prediction of site-specific lime requirement of arable fields using the base neutralizing capacity and a multi-sensor platform for on-the-go soil mapping. *Precision Agriculture*, 23, 127-149. [\[CrossRef\]](#)
- Carauta, M., Troost, C., Guzman-Bustamante, I., Hampf, A., Libera, A., Meurer, K., **Bönecke, E.**, Franko, U., Rodrigues, R. and Berger, T., 2021: Climate-related land use policies in Brazil: How much has been achieved with economic incentives in agriculture? *Land Use Policy*, 109, 105618. [\[CrossRef\]](#)
- Ruehlmann, J., **Bönecke, E.** and Meyer, S., 2021: Predicting the Lime Demand of Arable Soils from pH Value, Soil Texture and Soil Organic Matter Content. *Agronomy*, 11(4), 785. [\[CrossRef\]](#)
- Bönecke, E.**, Meyer, S., Vogel, S., Schröter, I., Gebbers, R., Kling, C., Kramer, E., Lück, K., Nagel, A., Philipp, G. and Gerlach, F., Palme, S., Scheibe, D., Zieger, K., Rühlmann, J., 2021: Guidelines for precise lime management based on high-resolution soil pH, texture and SOM maps generated from proximal soil sensing data. *Precision Agriculture*, 22(2), 493-523. [\[CrossRef\]](#)
- Hadasch, S., Laidig, F., Macholdt, J., **Bönecke, E.** and Piepho, H.P., 2020: Trends in mean performance and stability of winter wheat and winter rye yields in a long-term series of variety trials. *Field Crops Research*, 252, 107792. [\[CrossRef\]](#)
- Vogel, S., **Bönecke, E.**, Kling, C., Kramer, E., Lück, K., Nagel, A., Philipp, G., Rühlmann, J., Schröter, I. and Gebbers, R., 2020: Base neutralizing capacity of agricultural soils in a quaternary landscape of north-east Germany and its relationship to best management practices in lime requirement determination. *Agronomy*, 10(6), 877. [\[CrossRef\]](#)
- Bönecke, E.**, Breitsameter, L., Brüggemann, N., Chen, T.W., Feike, T., Kage, H., Kersebaum, K.C., Piepho, H.P. and Stützel, H., 2020: Decoupling of impact factors reveals the response of German winter wheat yields to climatic changes. *Global change biology*, 26(6), 3601-3626. [\[CrossRef\]](#)
- Meurer, K., **Boenecke, E.**, Franko, U., 2019: Evaluating emissions of nitrous oxide from cropland soils under different rotations in Mato Grosso, Brazil: A scenario simulation study. *Pedosphere*, 29(4), 432-443. [\[CrossRef\]](#)
- Boenecke, E.**, Lueck, E., Ruehlmann, J., Gruending, R. and Franko, U., 2018: Determining the within-field yield variability from seasonally changing soil conditions. *Precision Agriculture*, 19(4), 750-769. [\[CrossRef\]](#)

Data set publications (peer-reviewed)

- Bönecke, E.**, Schröter, I., Vogel, S., Rühlmann, J., Meyer, S., Gebbers, R., Kling, C., Philipp, G., Lück, K., Schubert, T., Scheibe, D., Kramer, E., 2023: Reference soil samples (pH, soil texture, SOC, TC, TN, P, K, Mg) from the project "pH-BB: Precision liming in Brandenburg" - data set 2 (farm 2), Bonares Data Centre.
- Bönecke, E.**, Schröter, I., Vogel, S., Rühlmann, J., Meyer, S., Gebbers, R., Kling, C., Philipp, G., Lück, K., Schubert, T., Scheibe, D., Kramer, E., 2023: Reference soil samples (pH, soil texture, SOC, TC, TN, P, K, Mg) from the project "pH-BB: Precision liming in Brandenburg" - data set 1 (farm 1), Bonares Data Centre.
- Bönecke, E.**, Breitsamter, L., Brueggemann, N., Chen, T.-W., Feike, T., Kage, H., Kersebaum, K.-C., Piepho, H.-P., Stuetzel, H., 2019: Winter wheat yield meta-dataset from N-fertilization experiments in Germany between 1958 and 2015, Bonares Data Centre.
- Vogel, S., **Bönecke, E.**, Kling, C., Kramer, E., Lück, K., Nagel, A., Philipp, G., Rühlmann, J., Schröter, I., 2020: Base neutralizing capacity from agricultural fields in the quaternary landscape of North-East Germany, Bonares Data Centre.

Publications (non-peer-reviewed)

- Bönecke, E.**; Schröter, I.; Meyer, S.; Kling, C.; Vogel, S.; Post, S.; Kramer, E.; Rühlmann, J.: Yield and texture-based management zones in a heterogeneous old morainic landscape, 14th ECPA 2023, Bologna, Italy, 02-06 Jul 2023 (conference contribution) [[CrossRef](#)]
- Bönecke, E.**, Sorge, S., Vogel, S., Schröter, I., Liftenegger, A., Kramer, E., Rühlmann, J.: Comparison of three liming management strategies on crop yields and economic indicators, Annual Assembly of the GPW, Berlin, Germany, 04-06 Sep 2023. (conference contribution) [[CrossRef](#)]
- Bönecke, E.**; The impact of agriculture on the environment and potential solutions, Online lecture series - Aspects of the Anthropocene, University of Vienna (colloquia abstract), Austria [[CrossRef](#)]
- Bönecke, E.**, Meyer, S., Rühlmann, J.: Praxisblatt: Bestimmung der Bodenart mittels mobiler Bodensensoren (eng.: Practice bulletin: Determination of the soil texture using mobile soil sensors), LBV-Info. Nov 2022. (practical journal)
- Bönecke, E.**, Meyer, S., Vogel, S., Schröter, I., Gebbers, R., Kling, C., Kramer, E., Lück, K., Nagel, A., Philipp, G. and Gerlach, F., Palme, S., Scheibe, D., Zieger, K., Rühlmann, J.: Präzise Kalkung In Brandenburg – pH-BB (eng.: Precision Liming in Brandeburg). (practical bulletins) [[CrossRef](#)]
- Rühlmann, J., **Bönecke, E.**: Mit Sensoren in den Boden geschaut. Gemüse, Jul 2022. (farmers journal) [[CrossRef](#)]
- Kling, C.; Vogel, S.; **Bönecke, E.**; Kramer, E.; Lück, K.; Nagel, A.; Philipp, G.; Rühlmann, J.; Schröter, I.; (2022): Standortangepasst Kalken! Aber wie? Darum lohnen sich Sensorkartierungen zur präzisen Kalkausbringung für Ihren Betrieb! Bauernzeitung Brandenburg (eng.: Liming adapted to the site! But how? That's why sensor mapping for precise lime application is worthwhile for your farm! Brandenburg Farmers' Newspaper). (practical journal) [[CrossRef](#)]
- Bönecke, E.**, Leseberg, C., Stützel H.: Factors influencing the yield development of winter wheat in Germany over the past 25 years, Annual Assembly of the GPW 2021, Rostock, Germany, 28-30 Sep 2021 (conference contribution) [[CrossRef](#)]

Publications continuation (non-peer-reviewed)

- Vogel, S., **Bönecke, E.**, Kling, C., Kramer, E., Lück, K., Nagel, A., Philipp, G., Rühlmann, J., Schröter, I., Gebbers, R., 2020: Praxisnah geforscht - EIP Projekt: pH-BB Präzise Kalkung in Brandenburg Bauernzeitung Brandenburg (eng.: Precision Liming in Brandeburg, Brandenburg Farmers' Newspaper), (18), S.24ff., (practical journal) [\[CrossRef\]](#)
- Vogel, S.; Lück, K.; Gebbers, R.; Rühlmann, J.; Scheibe, D.; Kling, C.; **Bönecke, E.**; Schröter, I.; Philipp, G.; Nagel, A.; Zieger, K.; Meyer, S.; Gerlach, F.; Palme, S.; Kramer, E., 2019: Kalkdüngung - aber bitte präzise. Landwirtschaft ohne Pflug (eng.: Lime fertilization - but please be precise. Farming without a plow), 48-53
- Hadasch, S., Laidig, F., Macholdt, J., **Bönecke, E.** and Piepho, H.P., 2020: Zunahme an genetischer Variabilität bei Winterweizen und Winterroggen (eng.: Increase in genetic variability in winter wheat and winter rye), Research Gate. [\[CrossRef\]](#)
- Franko, U., Oelschlägel, B., **Bönecke, E.**, Prays, N., Meurer, K., Schenk, S., Puhlmann, M., Kuka, K., Thiel, E., Mallast, J. (2015): CANDY Manual. Description of Background. Helmholtz-Centre for Environmental Research – UFZ. [\[CrossRef\]](#)
- Franko, U., Oelschlägel, B., **Bönecke, E.**, Prays, N., Meurer, K., Schenk, S., Puhlmann, M., Kuka, K., Thiel, E., Mallast, J. (2015): CANDY Technical Issues & Handling. Description of Usage. Helmholtz-Centre for Environmental Research – UFZ. [\[CrossRef\]](#)
- Franko, U., Oelschlägel, B.; **Bönecke, E.**, Prays, N., Meurer, K., Schenk, S., Puhlmann, M., Kuka, K., Thiel, E., Mallast, J. (2015): CANDY Database organisation. Description of Background. Helmholtz-Centre for Environmental Research – UFZ. [\[CrossRef\]](#)
- Oelschlägel, B., Franko,U., **Bönecke, E.**, Meurer, K., Prays, N., Witing, F. (2015): Optimizer. Description of Usage. Helmholtz-Centre for Environmental Research – UFZ. [\[CrossRef\]](#)